

https://dspace.org/

Optimisation of lipid production, harvesting processes and the mass culture of isochrysis galbana U4 for biodiesel production

Roopnarain, Ashira

2014-07-21
http://hdl.handle.net/10539/14945

Downloaded from a DSpace repository. https://dspace.org/

OPTIMISATION OF LIPID PRODUCTION, HARVESTING PROCESSES AND THE MASS CULTURE OF *ISOCHRYSIS GALBANA* U4 FOR BIODIESEL PRODUCTION

Ashira Roopnarain

A thesis submitted to the Faculty of Science, University of the Witwatersrand, in fulfillment of the requirements for the degree of Doctor of Philosophy

Johannesburg, 2014

DECLARATION

I declare that this thesis is my own, unaided work. It is being submitted for the Degree of Doctor of Philosophy at the University of the Witwatersrand, Johannesburg. It has not been submitted before for any other degree or examination at any other University.



15th day of May, 2014

Ashira Roopnarain **Date**

ABSTRACT

Due to the numerous disadvantages associated with the use of fossil fuels, focus has been drawn on the environmentally friendly, renewable and carbon-neutral alternative, algal-based biofuels. Many microalgal species have been studied due to their ability to produce significant lipid yields which may be converted to biodiesel. In the present study three microalgal species were screened and a model organism that produced maximal lipid yields, had the greatest lipid productivity and showed potential to be used on a large scale basis, was selected. The selected species was identified, using both morphological and molecular methods, as *Isochrysis galbana* U4. Nitrogen (N) limitation and depletion studies showed that an internal N reservoir determines cell growth and eventual lipid accumulation in *I. galbana* when the external N reserves are deplete. Intracellular N depletion was associated with a decrease in the pyrenoid size and chlorophyll content, a breakdown of the chloroplast and the production of large lipid bodies which is advantageous in terms of lipid sequestration for biodiesel production. Cost reduction approaches for the mass culture of *I. galbana* were investigated. Factors that were proven to reduce costs, without altering the final lipid yield, included the use of urea as a N source and the supply of lower phosphorus (P) levels since this species is capable of growing optimally with as little as 0.25 ppm P. Furthermore, *I. galbana* cells demonstrated spontaneous flocculating abilities when cultured for prolonged periods. This is advantageous in the cost reductions of downstream harvesting processes. Both, 7 L and 16 L photobioreactors (PBR) were tested. Culture upscale resulted in the concomitant decrease in algal growth rate which was attributed to the limitations on the carbon dioxide and light supply in scaled up systems. Hence, it is suggested that multiple smaller units be used in an industrial setup. Overall, *I. galbana* is a promising candidate for biodiesel production, due to its ability to produce large amounts of lipid, its elevated growth rates and low P demand. The use of a two-phase PBR (The first phase being nutrient replete, promoting cell growth and division, and the second phase nutrient deplete, promoting lipid production) for the mass culture of this species in industry is recommended.

ACKNOWLEDGEMENTS

I would like to thank my supervisors, Prof. V.M. Gray and Prof. S.D. Sym, for all their guidance, patience and assistance throughout the duration of the project. Gratitude is expressed to my family and friends for always being encouraging.

Special thanks to my mother, sister and boyfriend for their patience, love and unwavering support in all my endeavors.

The financial support of the South African National Energy Research Institute (SANERI), the National Research Foundation (NRF) and the University of the Witwatersrand are hereby acknowledged and greatly appreciated. Opinions expressed and conclusions arrived at, are my own work and not necessarily to be attributed to the NRF.

RESEARCH OUTPUT

Original Publications:

⇒ **Roopnarain, A., Gray, V.M. and Sym, S.** 2013. The Influence of Nitrogen Stresses on *Isochrysis galbana* strain U4, a candidate for biodiesel production. *Phycological Research*. (In Press).

⇒ **Roopnarain, A., Gray, V.M. and Sym, S.** 2014. Phosphorus Limitation and Starvation effects on *Isochrysis galbana* U4 for biodiesel production. *Bioresource Technology*. (In Press).

⇒ **Roopnarain, A., Sym, S and Gray, V.M.** 2014. The Effect of Nitrogen Source on Growth, Biochemical Composition and Ultrastructure of *Isochrysis galbana* U4. *Phycological Research*. (Revised).

⇒ **Roopnarain, A., Sym, S and Gray, V.M.** 2014. Time of Culture Harvesting Affects Lipid Productivity of Nitrogen-Limited *Isochrysis galbana* U4 for Biodiesel Production**.** *Journal of Experimental Botany*. (Submitted).

Conference Outputs:

⇒ **Roopnarain, A., Gray, V.M. and Sym, S.** 2010. Effect of nitrate on lipid production by *Isochrysis sp.*, a promising candidate for biodiesel production. Postgraduate Symposium (University of the Witwatersrand, Johannesburg; Poster presentation).

⇒ **Roopnarain, A., Gray, V.M. and Sym, S**. 2011. Biodiesel production by microalgae – Effect of nitrate on lipid production. Phycological Society of South Africa (PSSA) Conference (Magaliesberg, Johannesburg, South Africa; Oral presentation).

⇒ **Roopnarain, A., Gray, V.M. and Sym, S.** 2012. Flocculation induction in *Isochrysis* sp. Phycological Society of South Africa (PSSA) Conference (Kei mouth, East London, South Africa; Poster presentation).

⇒ **Roopnarain, A., Gray, V.M. and Sym, S.** 2012. Optimising dewatering of *Isochrysis* sp. by flocculation. Postgraduate Symposium (University of the Witwatersrand, Johannesburg; Poster presentation).

TABLE OF CONTENTS

CONTENTS	**Page**
DECLARATION	**ii**
ABSTRACT	**iii**
ACKNOWLEDGEMENTS	**iv**
RESEARCH OUTPUT	**v**
TABLE OF CONTENTS	**vi**
LIST OF FIGURES	**xii**
LIST OF TABLES	**xxiii**
LIST OF ABBREVIATIONS & UNIT	**xxvi**
CHAPTER ONE: Literature Review	**1**
1.1 General introduction	**2**
1.2 Biodiesel production from microalgae	**2**
1.3 Lipid accumulation pathways in microalgae	**5**
1.4 Algal selection & identification	**8**
1.4.1 Marine microalgae	**9**
1.4.2 Species identification	**11**
1.5 Mass culture of microalgae	**13**
1.5.1 Photobioreactor systems	**13**
1.5.2 Algal harvesting	**16**
1.6 Future prospects of algal based biofuels	**19**
1.7 Main objective	**21**
1.8 Aims	**22**
CHAPTER TWO: General Methodology	**23**
2.1 Medium preparation	**24**
2.2 Stock culture maintenance	**24**
2.3 Batch culture setup (1 L cultures)	**24**
2.4 Cell concentration measurements using a haemocytometer	**25**

2.5 Cell concentration measurements using spectrophotometry **25**
2.6 Lipid extraction **26**
2.7 Lipid content measurements using flow cytometry **27**
2.8 Dry cell weight measurements **28**
2.9 Biomass productivity measurements **29**
2.10 Lipid productivity measurements **29**
2.11 Growth rate, divisions per day and generation time determinations **29**
2.12 Morphological analysis **30**
2.12.1 Specimen embedding and sectioning **30**
2.12.2 Whole mounts of algal cells **31**
2.13 Culture medium composition measurements **31**
2.13.1 Nitrate measurements **31**
2.13.2 Ammonium measurements **32**
2.13.3 Phosphorous measurements **33**
2.14 Intracellular composition measurements **34**
2.14.1 Carbohydrate content determination **34**
2.14.2 Colorimetric determination of intracellular nitrogen **36**
2.14.3 Colorimetric determination of intracellular phosphorous **37**
2.15 Determination of chlorophyll content and carotenoid to chlorophyll ratio **39**
2.16 Light intensity measurements **41**
2.17 Statistical analysis **41**

CHAPTER THREE: Screening & Selection of a Marine Microalgal Species to be used as a Model Organism for Biodiesel Production **42**
3.1 Introduction **43**
3.2 Materials & Methods **44**
3.2.1 Algal selection **44**
3.2.2 Experimental setup **44**
3.2.3 Analytical methods **44**
3.3 Results & Discussion **45**
3.4 Conclusion **51**

CHAPTER FOUR: Morphological & Molecular Identification of the Model Organism **52**
4.1 Introduction **53**
4.2 Materials & Methods **54**
4.2.1 Morphological identification of model organism **54**
4.2.2 Molecular identification of model organism **55**
4.3 Results & Discussion **57**
4.3.1 Morphological identification **57**
4.3.2 Molecular identification **63**
4.4 Conclusion **65**
4.5 Supporting information **66**

CHAPTER FIVE: The Effect of Nitrogen Limitation and Starvation on *Isochrysis galbana* U4 **68**
5.1 Introduction **69**
5.2 Materials & Methods **70**
5.2.1 Experimental setup **70**
5.2.2 Effect of nitrogen depletion on *I. galbana* U4 **71**
5.2.3 Effect of varying starter nitrogen concentrations on *I. galbana* U4 **72**
5.3 Results & Discussion **73**
5.3.1 The effect of nitrogen absence/presence on algal growth, lipid yield and pigmentation **73**
5.3.2 Implications of nitrogen stresses on algal ultrastructure at varying growth stages **79**
5.3.3 The effect of varying nitrogen concentrations on *I. galbana* U4 **88**
5.4 Conclusion **96**
5.5 Supporting information **97**

CHAPTER SIX: The Effect of Nitrogen Source on Growth, Biochemical Composition and Ultrastructure of *Isochrysis galbana* U4 **98**
6.1 Introduction **99**

6.2 Materials & Methods **103**
6.2.1 Experimental setup **103**
6.2.2 Analytical methods **103**
6.2.3 Ultrastructural analysis and cellular measurements **104**
6.2.4 Statistical analysis **104**
6.3 Results **104**
6.3.1 Growth and carbon storage **104**
6.3.2 Variation in medium pH, ammonium and nitrate levels **110**
6.3.3 Algal pigmentation **115**
6.3.4 Intracellular fluctuations in nitrogen, phosphorous and the nitrogen to phosphorous ratio **119**
6.3.5 Cellular and sub-cellular analysis **124**
6.4 Discussion **127**
6.5 Conclusion **132**

CHAPTER SEVEN: The Effect of Phosphorus Limitation and Starvation on *Isochrysis galbana* U4 **134**
7.1 Introduction **135**
7.2 Materials & Methods **136**
7.2.1 Experimental setup **136**
7.2.2 Analytical methods **137**
7.3 Results & Discussion **137**
7.3.1 Nutrient uptake **137**
7.3.2 Growth and lipid accumulation **142**
7.3.3 Effect of P-Limitation on *I. galbana* pigmentation **146**
7.4 Conclusion **151**

CHAPTER EIGHT: Optimising the Dewatering Process of Cultures of *Isochrysis galbana* U4 by Flocculation **152**
8.1 Introduction **153**
8.2 Materials & Methods **156**

8.2.1 Experimental setup **156**
8.2.2 Flocculation efficiency measurements **156**
8.2.3 Sedimentation rate measurements **157**
8.2.4 pH-induced flocculation **157**
8.2.5 Medium recycling **157**
8.2.6 Chemical flocculation **158**
8.2.7 Autoflocculation **158**
8.2.8 Growth stage flocculation **159**
8.2.9 pH measurements **160**
8.3 Results & Discussion **160**
8.3.1 pH-induced flocculation and medium recycling **160**
8.3.2 Chemical flocculation **171**
8.3.3 Autoflocculation **173**
8.3.4 Effect of growth stage on flocculation efficiency **178**
8.4 Conclusion **182**

CHAPTER NINE: Culture of *Isochrysis galbana* U4 in Upscaled Photobioreactors **183**
9.1 Introduction **184**
9.2 Materials & Methods **185**
9.2.1 Photobioreactor setup **185**
9.2.2 Experimental setup and analytical methods **186**
9.3 Results & Discussion **190**
9.3.1 Comparison of microalgal growth in up-scaled PBRs (batch cultures) **190**
9.3.2 Seven liter batch cultures with varying light intensities **193**
9.3.3 Seven liter continuous culture with varying levels of nitrogen **196**
9.3.4 Sixteen liter continuous culture with flow rate variations **203**
9.4 Conclusion **210**

CHAPTER TEN: Summarising Discussion & Conclusion **212**
10.1 Screening, selection and identification **213**

10.2 Effect of nitrogen supply on *I. galbana* U4 **214**
10.3 Cost optimization for *I. galbana* mass culture **215**
10.4 *Isochrysis galbana* dewatering processes and mass culture **216**
10.5 Conclusion **216**

REFERENCES **218**

APPENDIX **253**

LIST OF FIGURES **Page**

Figure 1.1: Photosynthetic pathway resulting in the conversion of solar energy to chemical energy in the chloroplast (adapted and modified from Schenk *et al.*, 2008). **6**

Figure 1.2: Fatty acid biosynthesis pathway in chloroplast (adapted from Hu *et al.*, 2008). **8**

Figure 1.3 (A): Aerial view of opened, raceway photobioreactor (Chisti, 2007) and **(B)**: closed, tubular photobioreactor (www.bioenergy-noe.org). **14**

Figure 1.4: Schematic representation of a microalgal biorefinery system that minimises wastage, maximises economic yield and reduces the environmental impact (adapted and modified from Singh and Gu, 2010 and Greenwell *et al.*, 2010). **20**

Figure 2.1: Schematic representation of experimental setup. **25**

Figure 2.2: Standard curve depicting concentration of *I. galbana* cells with respect to absorbance readings at 650 nm. Error bars represent standard deviation (n = 3). **26**

Figure 2.3: Standard curve depicting nitrate concentration with respect to absorbance readings at 410 nm. Error bars represent standard deviation (n = 3). **32**

Figure 2.4: Standard curve depicting ammonium concentration with respect to absorbance readings at 635 nm. Error bars represent standard deviation (n = 3). **33**

Figure 2.5: Standard curve depicting phosphorous concentration with respect to absorbance readings at 820 nm. Error bars represent standard deviation (n = 3). **34**

Figure 2.6: Standard curve depicting glucose concentration with respect to absorbance readings at 490 nm. Error bars represent standard deviation (n = 3). **35**

Figure 2.7: Standard curve depicting nitrogen concentration with respect to absorbance readings at 660 nm. Error bars represent standard deviation (n = 3). **37**

Figure 2.8: Standard curve depicting phosphorous concentration with respect to absorbance readings at 820 nm. Error bars represent standard deviation (n = 3). **39**

Figure 3.1 (A): Nile red stained *Platychrysis* sp. cells viewed under a light microscope and **(B):** when the same cells were exposed to a different wavelength of light (450-500 nm). **46**

Figure 3.2: *Isochrysis* sp. growth curve showing the cellular concentration and lipid content observed over 18 days. Error bars represent standard deviation (n=3). **48**

Figure 3.3 (A): Light micrographs of a single *Isochrysis* sp. cell containing multiple lipid bodies (arrows indicate lipid bodies) and **(B):** algal floccules (observed on day 18) **49**

Figure 3.4: *Pleurochrysis* sp. growth curve showing the cellular concentration and lipid content observed over 18 days. Error bars represent standard deviation (n=3). **50**

Figure 3.5 (A–B): Light micrographs of single *Pleurochrysis* sp. cells containing multiple small lipid bodies (lipid bodies indicated by arrows; observed on day 18). **50**

Figure 4.1 (A-B): Light microscopy images of isolate cells showing a pair of equal length flagella and **(C):** shadow-cast cell with single flagella (the other was shed). Arrows indicate flagella. **58**

Figure 4.2 (A-D): Microphotographs of sections through isolate cells (seven day old culture). Abbreviations: N nucleus; Nu nucleolus; M mitochondria; C chloroplast; Py pyrenoid; G golgi apparatus; ER endoplasmic reticulum; V vacuole; R ribosomes; Sc scales. **60**

Figure 4.3: Diagrammatic representation of the general ultrastructural organization of a haptophyte cell. N = Nucleus, Py = Pyrenoid traversed by thylakoids, C = Chloroplast, GA = Golgi Apparatus, M = Mitochondrion, Sc = Scales, CM = Continuous chloroplast outer membrane and outer nuclear envelope, PE = Peripheral Endoplasmic Reticulum and F = Flagella. (Adapted from Solomon *et al.*, 1986). **61**

Figure 4.4 (A–B): Sections through the marginal region of the cell showing layers of superficial body scales and glancing sections of the scales. **62**

Figure 4.5: Schematic representation of the isolate body scales. **62**

Figure 4.6: PCR amplification products of the SSU nuclear ribosomal encoding region of the microalgal isolate separated on a 1% agarose gel. **M**: 100 bp plus DNA ladder, **1:** control lane (no DNA template), **2 - 7:** replicates of amplification with DNA template. **63**

Figure 4.7: Nucleotide sequence of the amplified region in the microalgal genome. **64**

Figure 4.8: Phylogenetic tree based upon a maximum likelihood analysis showing the relationships between 18s rDNA sequences of 23 species belonging to Clade C of the class Prymnesiophyceae (Edvardsen *et al*., 2000). *Pavlova gyrans* was used as the outgroup. Numbers at the nodes indicate bootstrap values (1000 replicates). The 18s rDNA sequence obtained from this study is indicated in bold. **65**

Figure 4.S1: Phylogenetic tree based upon a neighbor-joining analysis showing the relationships between 18s rDNA sequences of 23 species belonging to Clade C of the class Prymnesiophyceae (Edvardsen *et al*., 2000). *Pavlova gyrans* was used as the outgroup. Numbers at the nodes indicate bootstrap values (1000 replicates). The 18s rDNA sequence obtained from this study is indicated in bold. **66**

Figure 4.S2: Phylogenetic tree based upon a maximum parsimony analysis showing the relationships between 18s rDNA sequences of 23 species belonging to Clade C of the class Prymnesiophyceae (Edvardsen *et al*., 2000). *Pavlova gyrans* was used as the outgroup. Numbers at the nodes indicate bootstrap values (1000 replicates). The 18s rDNA sequence obtained from this study is indicated in bold. **67**

Figure 5.1: *Isochrysis galbana* U4 growth curve showing lipid accumulation under nitrogen-replete and deplete conditions. Error bars represent standard deviation (n = 3). **74**

Figure 5.2: Ambient nitrate depletion and intracellular nitrogen utilization in *I. galbana* U4 cells grown under nitrogen-replete and nitrogen-deplete conditions. Error bars represent

standard deviation (n = 3). **75**

Figure 5.3: The ratio of carotenoids to chlorophyll (car:chl) and the fluctuations in chlorophyll content observed in *I. galbana* U4 cells grown under nitrogen replete and nitrogen deplete conditions. Error bars represent standard deviation (n = 3). **79**

Figure 5.4.1 (A-D): Longitudinal sections through exponential phase cells. Abbreviations: C-Chloroplast; M-Mitochondria; N-Nucleus; Py-Pyrenoid; Nu-Nucleolus; Sc-Scales; V-Vacuole; G-Golgi apparatus. **85**

Figure 5.4.2 (A-D): Longitudinal sections through stationary phase cells. Abbreviations: C-Chloroplast; M-Mitochondria; N-Nucleus; Py-Pyrenoid; Nu-Nucleolus; Sc-Scales; L-Lipid. **86**

Figure 5.4.3 (A-D): Stages in lipid production. Abbreviations: C-Chloroplast; M-Mitochondria; N-Nucleus; Py-Pyrenoid; L-lipid. **87**

Figure 5.5: A decrease in the ambient nitrate concentration with respect to time in *I. galbana* cultures containing varying sodium nitrate levels as indicated. Error bars represent standard deviation (n = 3). **88**

Figure 5.6: The effect of varying nitrate concentrations on *I. galbana* biomass productivities observed over 15 days. Error bars represent standard deviation (n = 3). Different letters on the upper portion of each bar indicates where significant differences exist between treatments at various time intervals ($P < 0.05$). **89**

Figure 5.7: The effect of varying nitrate concentrations on *I. galbana* lipid yield observed over 15 days. Error bars represent standard deviation (n = 3). Different letters on the upper portion of each bar indicates where significant differences exist between treatments at various time intervals ($P < 0.05$). **90**

Figure 5.8: Observed densities of cultures at various nitrate concentrations (as marked on the vessels) 15 days after inoculation. **91**

Figure 5.9: The effect of varying nitrate concentrations on *I. galbana* lipid productivity observed over 15 days. Error bars represent standard deviation (n = 3). Different letters on the upper portion of each bar indicates where significant differences exist between treatments at the various time intervals ($P < 0.05$). **94**

Figure 6.1: Schematic representation of intracellular pathways involved in nitrogen uptake, storage, assimilation and partitioning in an algal cell (enzymes are italicized) (adapted and modified from South and Whittick, 1987 and Mulholland and Lomas, 2008). **101**

Figure 6.2: Structural representation of ammonium assimilation into glutamine and glutamate production (http://www.uky.edu/~dhild/biochem/24/fig08_05.png). **102**

Figure 6.3: *I. galbana* growth in *f/2* medium supplemented with various nitrogen sources. Error bars represent standard deviation (n=4). **105**

Figure 6.4: Lipid accumulation in *I. galbana* grown in *f/2* medium supplemented with various nitrogen sources. Error bars represent standard deviation (n=4). **107**

Figure 6.5: Carbohydrate accumulation in *I. galbana* grown in *f/2* medium supplemented with various nitrogen sources. Error bars represent standard deviation (n=4). **109**

Figure 6.6: the pH of *I. galbana* cultures supplemented with various nitrogen sources. Error bars represent standard deviation (n=4). Significant differences are indicated by different letters above the error bars ($P < 0.05$). **112**

Figure 6.7 (A): The decrease in ammonium-N and **(B):** nitrate-N in the medium of cultures with various nitrogen sources inoculated with *I. galbana* and control cultures lacking cells. Error bars represent standard deviation (n=4). **114**

Figure 6.8: The pH of control cultures (lacking cells) supplemented with various nitrogen sources as indicated. Error bars represent standard deviation (n=4). **115**

Figure 6.9: the chlorophyll content of *I. galbana* cultured in *f/2* medium supplemented

with various nitrogen sources. Error bars represent standard deviation (n=4). **116**

Figure 6.10: The carotenoid to chlorophyll ratio of *I. galbana* cultured in *f/2* medium supplemented with various nitrogen sources. Error bars represent standard deviation (n=4). **118**

Figure 6.11: The intracellular nitrogen content of *I. galbana* cultured in *f/2* medium supplemented with various nitrogen sources. Error bars represent standard deviation (n=4). **120**

Figure 6.12: The intracellular phosphorous content of *I. galbana* cultured in *f/2* medium supplemented with various nitrogen sources. Error bars represent standard deviation (n=4). **121**

Figure 6.13: The nitrogen to phosphorous ratio of *I. galbana* cells cultured in *f/2* medium supplemented with various nitrogen sources. Error bars represent standard deviation (n=4). **123**

Figure 6.14: The cell diameter of exponential and stationary phase *I. galbana* cells cultured in *f/2* medium supplemented with various nitrogen sources as indicated. Error bars represent standard deviation (n=50). Significant differences are indicated by different letters above the error bars ($P < 0.05$). **125**

Figure 6.15 (A): Exponential phase *I. galbana* cells cultured in *f/2* medium supplemented with ammonium, **(C):** urea and **(E):** nitrate. Photomicrographs on the right **(B, D and F)** represent magnified views of the plastids of the respective image on the left. White scale bars represent 1 um and black scale bars represent 0.5 um. **126**

Figure 7.1: Structural representation of polyphosphate (adapted from Stewart, 1974) **136**

Figure 7.2: Phosphorous depletion from the milieu due to uptake by *I. galbana* cells cultured in *f/2* medium supplemented with different starting P concentrations. Error bars represent standard deviation (n=4). **139**

Figure 7.3: *Isochrysis galbana* growth in *f/2* medium supplemented with various P concentrations. Error bars represent standard deviation (n=4). **140**

Figure 7.4: Nitrate depletion from milieu due to uptake by *I. galbana* cells cultured in *f/2*

medium supplemented with different starting P concentrations. Error bars represent standard deviation (n=4). **141**

Figure 7.5: Lipid accumulation in *I. galbana* grown in *f/2* medium supplemented with various P concentrations. Error bars represent standard deviation (n=4). **146**

Figure 7.6: The chlorophyll content of *I. galbana* cultured in *f/2* medium supplemented with various phosphorous concentrations. Error bars represent standard deviation (n=4). **148**

Figure 7.7: The carotenoid to chlorophyll ratio of *I. galbana* cultured in *f/2* medium supplemented with various phosphorous concentrations. Error bars represent standard deviation (n=4). **150**

Figure 8.1: The Electrical Double Layer that surrounds a charged particle in solution (Adapted from Omland, 2009) **154**

Figure 8.2: The decrease in the Electrical Double Layer potential as a function of the distance from the particle surface and the point at which the Zeta potential is measured (www.biochemistry-imm.org). **155**

Figure 8.3 (A): Flocculation efficiency of *I. galbana* at pH 9.5 brought about by the addition of various salts as indicated. Error bars represent standard deviation (n=3) and **(B):** resultant cultures four hours after the alteration of pH. **163**

Figure 8.4 (A): Flocculation efficiency of *I. galbana* at pH 10 brought about by the addition of various salts as indicated. Error bars represent standard deviation (n=3) and **(B):** resultant cultures four hours after the alteration of pH. **164**

Figure 8.5 (A): Flocculation efficiency of *I. galbana* at pH 10.5 brought about by the addition of various salts as indicated. Error bars represent standard deviation (n=3) and **(B):** resultant cultures four hours after the alteration of pH. **164**

Figure 8.6 (A): Flocculation efficiency of *I. galbana* at pH 11 brought about by the addition of various salts as indicated. Error bars represent standard deviation (n=3) and

(B): resultant cultures four hours after the alteration of pH. **165**

Figure 8.7: Appearance of sedimented *I. galbana* cells after being subjected to a pH of 10.5 brought about by various salts as indicated. Control refers to cells subjected to pH 8.3. Scale bar represents 10 µm. **165**

Figure 8.8: The rate of sedimentation of *I. galbana* in the indicated alkaline treatments at pH 10.5 and 11. Error bars represent standard deviation (n=3). **166**

Figure 8.9: Alkaline concentration required for *f/2* medium pH increase using the indicated basic solutions. **168**

Figure 8.10: *Isochrysis galbana* growth in medium recycled from the pH experiments using different drivers as indicated. Control refers to non-recycled *f/*2 medium. Error bars represent standard deviation (n=3). **169**

Figure 8.11: Flocculation of *I. galbana* using inorganic flocculants. Error bars represent standard deviation (n=3). **172**

Figure 8.12: Autoflocculation induction in *I. galbana* initiated by numerous growth conditions. Error bars represent standard deviation (n=3). **175**

Figure 8.13: *Isochrysis galbana* floccules observed in photobioreactor in response to agitation induced by bubbling. **176**

Figure 8.14: pH of autoflocculated *I. galbana* cultures after fourteen days. Error bars represent standard deviation (n=3). **177**

Figure 8.15: Growth curve of *I. galbana* showing points at which flocculation induction was attempted (circled; Error bars represent standard deviation, n=3). **179**

Figure 8.16: Flocculation induction of *I. galbana* at various growth stages. Error bars represent standard deviation (n=3). **180**

Figure 9.1: Schematic representation of the photobioreactor system used for the mass culture of *I. galbana*. **185**

Figure 9.2: *Isochrysis galbana* growth curve showing the cellular concentration and lipid content observed over 18 days of culture in a 7 L airlift PBR maintained under batch conditions **192**

Figure 9.3: *Isochrysis galbana* growth curve showing the cellular concentration and lipid content observed over 18 days of culture in a 16 L airlift PBR maintained under batch conditions **192**

Figure 9.4: *Isochrysis galbana* growth curves showing the effect of varying light intensities on cellular concentration when the alga was grown in a 7 L PBR, under batch conditions. Circled points depict points of changes in light intensities. (Key units: µmol photons/m^2/s) **195**

Figure 9.5: Michaelis-Menten curve showing steady state cell growth (velocity) versus nitrate concentration (substrate concentration) of *I. galbana* cells grown under continuous conditions. **197**

Figure 9.6: Bubbled (bubble column; —◆—) and non-bubbled (pond; —□—) *I. galbana* batch cultures obtained from the effluent of System 1 of the continuous PBR that was supplemented with 440 µM sodium nitrate. The cell concentration (**A**), lipid content (**B**), chlorophyll a content **(C**) and carotenoid to chlorophyll ratio (**D**) were monitored. Error bars represent standard deviation (n = 3). **198**

Figure 9.7: Bubbled (bubble column; —◆—) and non-bubbled (pond; —□—) *I. galbana* batch cultures obtained from the effluent of System 1 of the continuous PBR that was supplemented with 880 µM sodium nitrate. The cell concentration (**A**), lipid content (**B**), chlorophyll a content **(C**) and carotenoid to chlorophyll ratio (**D**) were monitored. Error bars represent standard deviation (n = 3). **199**

Figure 9.8: Bubbled (bubble column; —◆—) and non-bubbled (pond; —□—) *I. galbana*

batch cultures obtained from the effluent of System 1 of the continuous PBR that was supplemented with 1780 µM sodium nitrate. The cell concentration (**A**), lipid content (**B**), chlorophyll a content **(C**) and carotenoid to chlorophyll ratio (**D**) were monitored. Error bars represent standard deviation (n = 3). **200**

Figure 9.9: Bubbled (bubble column;) and non-bubbled (pond;) *I. galbana* batch cultures obtained from the effluent of System 1 of the continuous PBR that was supplemented with 1980 µM sodium nitrate. The cell concentration (**A**), lipid content (**B**), chlorophyll a content **(C**) and carotenoid to chlorophyll ratio (**D**) were monitored. Error bars represent standard deviation (n = 3). **201**

Figure 9.10: Growth curve showing *I. galbana* growth, lipid accumulation and medium pH when cultured in a 16 L PBR. Circled points indicate switches from batch to continuous mode at flow rates of 1.44, 2.16, 3.59 and 5.03 ml/min respectively. The culture was maintained in batch mode after 173 hours. **204**

Figure 9.11: Bubbled (bubble column;) and non-bubbled (raceway [shaken]; and pond [still];) *I. galbana* batch cultures obtained from the effluent of System 1 of the continuous PBR with a flow rate of 1.44 ml/min. The cell concentration (**A**), lipid content (**B**), chlorophyll a content **(C**) carotenoid to chlorophyll ratio (**D**) and pH (**E**) were monitored. **205**

Figure 9.12: Bubbled (bubble column;) and non-bubbled (raceway [shaken]; and pond [still];) *I. galbana* batch cultures obtained from the effluent of System 1 of the continuous PBR with a flow rate of 2.16 ml/min. The cell concentration (**A**), lipid content (**B**), chlorophyll a content **(C**) carotenoid to chlorophyll ratio (**D**) and pH (**E**) were monitored. **206**

Figure 9.13: Bubbled (bubble column;) and non-bubbled (raceway [shaken]; and pond [still];) *I. galbana* batch cultures obtained from the effluent of System 1 of the continuous PBR with a flow rate of 3.59 ml/min. The cell concentration (**A**), lipid content (**B**), chlorophyll a content **(C**) carotenoid to chlorophyll ratio (**D**) and pH (**E**) were monitored. **207**

Figure 9.14: Bubbled (bubble column; ◆) and non-bubbled (raceway [shaken]; ■ and pond [still]; ▲) *I. galbana* batch cultures obtained from the effluent of System 1 of the continuous PBR with a flow rate of 5.03 ml/min. The cell concentration (**A**), lipid content (**B**), chlorophyll a content **(C**) carotenoid to chlorophyll ratio (**D**) and pH (**E**) were monitored.

LIST OF TABLES **Page**

Table 2.1: Comparison of *Isochrysis* sp. and *Pleurochrysis* sp. growth and lipid parameters. **51**

Table 4.1: The oligonucleotide primers used for the amplification of the SSU nuclear ribosomal encoding region (18S rRNA). **55**

Table 4.2: A list of the species and corresponding GenBank accession numbers for the SSU nuclear ribosomal encoding sequences used in the phylogenetic analyses. The sequence in bold is from this study. **56**

Table 5.1: Sodium nitrate concentrations used in the study. **72**

Table 5.2: Rates of biomass productivity decrease in comparison with the increase in the rates of lipid accumulation and their corresponding regression coefficients in *I. galbana* cultures grown in the various treatments as indicated. **95**

Table 6.1: Rates of *I. galbana* growth (Day 2 – 7), their regression coefficients and the significant differences between the growth rates in the various treatments as indicated. **105**

Table 6.2: Rates of *I. galbana* growth (Day 7-14), their regression coefficients and the significant differences between the growth rates in the various treatments as indicated. **106**

Table 6.3: Rates of *I. galbana* lipid accumulation (Day 8-14), their regression coefficients and the significant differences between the rates in the various treatments as indicated. **108**

Table 6.4: Rates of *I. galbana* carbohydrate accumulation (Day 2-6), their regression coefficients and the significant differences between the rates in the various treatments as indicated. **110**

Table 6.5: Rates of *I. galbana* carbohydrate accumulation (Day 6-14), their regression coefficients and the significant differences between the rates in the various treatments as

indicated. **110**

Table 6.6: Rates of *I. galbana* pH change (Day 0-6), their regression coefficients and the significant differences between the rates in the various treatments as indicated. **111**

Table 6.7: Rates of *I. galbana* pH change (Day 8-14), their regression coefficients and the significant differences between the rates in the various treatments as indicated. **111**

Table 6.8: Rates of *I. galbana* chlorophyll synthesis (Day 2-6), their regression coefficients and the significant differences between the rates in the various treatments as indicated. **117**

Table 6.9: Rates of *I. galbana* chlorophyll synthesis (Day 8-14), their regression coefficients and the significant differences between the rates in the various treatments as indicated. **117**

Table 6.10: Rates of change in car:chl ratio (day 4-14) in *I. galbana* cultures, their regression coefficients and the significant differences between the rates in the various treatments as indicated. **119**

Table 6.11: Rates of intracellular nitrogen depletion in *I. galbana* cultures, their regression coefficients and the significant differences between the rates in the various treatments as indicated. **122**

Table 6.12: Rates of intracellular phosphorus depletion in *I. galbana* cultures, their regression coefficients and the significant differences between the rates in the various treatments as indicated. **122**

Table 6.13: Rates of change of N:P ratio in *I. galbana* cultures, their regression coefficients and the significant differences between the rates in the various treatments as indicated. **124**

Table 7.1: Rates of phosphorus uptake by cells of *I. galbana*, their gradients, regression coefficients and the significant differences between the rates in the various treatments as

indicated. **139**

Table 7.2: Rates of *I. galbana* growth (Day 4-14), their regression coefficients and the significant differences between the growth rates in the various treatments as indicated. **142**

Table 7.3: Rates of *I. galbana* lipid accumulation (Day 4-14), their regression coefficients and the significant differences between the rates in the higher P treatments. **146**

Table 8.1: Rates of *I. galbana* growth, their regression coefficients and the significant differences between the growth rates in the various treatments as indicated. **170**

Table 9.1: Differences in the configuration of System 1 and modified Schott® bottles **186**

Table 9.2: *Isochrysis galbana* mass culture experiments **186**

Table 9.3: Measurements of growth of *I. galbana* in PBRs with varying volumes **193**

Table 9.4: The effect of varying light intensities on the rate of *I. galbana* growth and maximal cellular yields **196**

LIST OF ABBREVIATIONS & UNITS

ACCase	Acetyl CoA Carboxylase
ACP	Acyl carrier protein
ADP	Adenosine diphosphate
Alum	Aluminium sulphate
ATP	Adenosine triphosphate
bp	base pair
car:chl	Carotenoid to chlorophyll ratio
Chl a	Chlorophyll a
cm	Centimetre
CO_2	Carbon dioxide
C_{Lipid}	Cellular Lipid Content
CTAB	Cetyltrimethylammonium bromide
DER 736	Diglycidyl ether of polypropylene glycol
DCW	Dry cell weight
$Div.day^{-1}$	Divisions per Day
DMAE	Dimethylaminoethanol
DNA	Deoxyribonucleic acid
EDTA	Ethylene diamine tetra acetic acid
EPS	Extracellular polymeric substances
ER	Endoplasmic reticulum
FFA	Free Fatty Acid
G	Gram
G3P	glyceraldehyde-3-phosphate
GOGAT	glutamine 2-oxoglutarate aminotransferase
GS	glutamine synthetase
HCl	Hydrochloric acid
Hrs	Hours
ITS	Internal Transcribed Spacer
L	Litre

M	Molar (moles per litre)
m	Meter
mM	milli molar
Mg	Milligram
mRNA	Messenger Ribose Nucleic Acid
N	Nitrogen
NADP	Nicotinamide adenine dinucleotide phosphate
Nm	Nano metres
NSA	Nonenyl succinic anhydride
P	Phosphorus
PBR	photobioreactor
$P_{Biomass}$	Biomass productivity
P_{Lipid}	Lipid Productivity
ppm	parts per million
PCR	Polymerase Chain Reaction
PSII	Photo system two
psi	pounds per square inch
RPM	Revolutions per minute
rRNA	ribosomal Ribose Nucleic Acid
RuBP	ribulose-1.5-bisphosphate
Rubisco	Ribulose-1,5-bisphosphate carboxylase/oxygenase
RSM	response surface methodology
s	Second
SC-RAPD	Single Cell Random Amplified Polymorphic DNA
SEM	Scanning Electron Microscopy
SRP	Soluble Reactive Phosphorus
SSU	Small Subunit
T_g	Generation time
TAGs	Triacylglycerols
TBE	Tris boric acid buffer
V	Volume

VCD	Vinylcyclohexane dioxide
μ	Growth rate
μl	Micro litre
μmol	Micro moles
°C	Degrees Celcius
3-PG	3-phosphoglycerate
18S rDNA	small ribosomal subunit deoxyribonucleic acid

CHAPTER ONE

Literature Review

1.1 General introduction

Microalgae are the most abundant primary producers in the world (Matsunaga *et al*., 2009; Msanne *et al*., 2012). Algae utilize water, carbon dioxide and radiant energy for rapid growth and can be harvested daily (Haag, 2007; Msanne *et al*., 2012). These photosynthetic microorganisms have significant potential in numerous applications that contribute to the food and feed industry, human healthcare, and the energy industry (Seshadri *et al*., 1991; Knuckey *et al*., 2006; Wijffels, 2007). Heavy metal bioremediation by microalgae is also currently widely researched (Matsunaga et al., 2009).

The production of biofuels such as biohydrogen (Kruse *et al*., 2005; Berberoglu *et al*., 2007; Hankamer *et al*., 2007; Beer *et al*., 2009, Mussgnug *et al*., 2010), biomethane (Gunaseelan, 1997; Mussgnug *et al*., 2010) and biodiesel (Chisti, 2007) from algae has received much attention of late. The focus of the current project is primarily on the successful production of biodiesel from microalgae. The lipids produced by microalgae can be transesterified into biodiesel (Chisti, 2007) and the excess biomass, after oil stripping, can be converted into animal feeds, biohydrogen, methane and ethanol (Haag, 2007). Excess carbon dioxide emitted from factories and power plants can be used to promote algal growth, in turn reducing the emission of greenhouse gases and having a positive impact on the current global warming crisis (Patil, 2007; Yeang, 2008). However, the successful production of biodiesel requires a system that enables the mass culture of algal strains that produce maximal lipid yield. Although much research has been conducted on systems used for the mass culture of microalgae no definitive success, in terms of commercial viability, has thus far been achieved in this field of research.

1.2 Biodiesel production from microalgae

Energy production by microalgae has been actively researched for the past sixty years. Initial studies focused on the production of methane gas from the carbohydrate portion of algal cells (Meier, 1955; Oswald and Golueke, 1960). Subsequent research into the utilization of the lipid portion of algae, for biofuel production, was motivated by the oil embargo that was proclaimed in 1973, which resulted in the beginning of extensive

alternate energy source studies (Hu *et al.*, 2008; Elshahed, 2010). The most comprehensive study focused on biodiesel from algae, was conducted by the US Department of Energy and was termed the Aquatic Species Program. The program spanned eighteen years (1978-1996) and was primarily focused on biodiesel production from oleaginous algae that were grown in open ponds, using waste carbon dioxide obtained from coal fired power plants (Sheehan *et al*., 1998). During the course of the program, 3000 algal strains were isolated. The algal collection was further narrowed down to 300 promising species that were selected based on lipid production and tolerance to severe environmental conditions. The role of nutrient depletion leading to lipid accumulation was observed early in the program and the enzyme Acetyl CoA Carboxylase (ACCase), used to catalyse a key step in oil synthesis, was discovered. The program ended in 1996 when it was concluded that the high production costs of biodiesel from algae make it a non-viable alternative to petro-diesel (Sheehan *et al*., 1998; Hu *et al*., 2008).

Due to the negative impact of the burning of fossil fuels on the environment, the surging petroleum prices and the ever-depleting petroleum supplies, renewed interest in biofuel production from microalgae has been sparked over the past decade (Akinci, 2008; Sharma *et al*., 2012). Fossil fuels are a non-renewable resource and the combustion of these fuels results in the utilization of "old" biomass with the concomitant release of "new" carbon dioxide into the atmosphere thus contributing to global warming. Conversely, the combustion of microalgal based lipids would result in the discharge of no new carbon dioxide, due to the consumption of the released gases for a cycle of new algal growth (McKendry, 2002). Biodiesel therefore forms an environmentally friendly alternative to fossil fuels (Chisti, 2007; Duan, 2012).

Commercial biodiesel is commonly extracted from soybean oil, palm oil, rapeseed oil, and waste cooking oil. Biodiesel production from these sources is however unsustainable due the limited availability of arable land for the cultivation of both energy and food crops (Liu *et al*., 2007; Elshahed, 2010). Microalgae can be mass produced in artificial waterways constructed on land that is agriculturally marginal and thus need not compete

with crop production. Certain algal species, such as *Botryococcus braunii*, are able to produce oil yields that exceed as much as 70% of their own dry weight. Oil crops, in comparison, produce oil that is approximately 5% of their total biomass since only the seeds, which store oils as an energy source enabling growth for subsequent plant generations, are available as a lipid source (Becker, 1994; Ohlrogge and Browse, 1995; Chisti, 2008). The rapid growth of microalgae, which commonly double their biomass within 24 hours, implies that a relatively small area of land would be required for its mass culture, making it more desirable as a fuel source relative to conventional oil seed crops (Chisti, 2007, 2008; Liu *et al*., 2007; Yeang, 2008).

A wide range of algal species produce various hydrocarbons, lipids and other complex oils. Many of these products may be used as feed for biodiesel (Chisti, 2007; Msanne *et al*., 2012). Lipid production may be further maximized via the alteration of numerous growth conditions. A few of these manipulations include nitrogen deprivation (Zhila *et al*., 2005), phosphorus limitation (Deng *et al*., 2009), decreased cultivation temperature (Xin *et al*., 2011), high salinity (Duan *et al*., 2012; Sharma *et al*., 2012), silicon deficiency (Ju *et al*., 2011), elevated light intensity (Roessler, 1990; Liu *et al*., 2012), co-immobilization in alginate beads with certain bacterial species e.g. *Azospirillum brasilense* (de-Bashan *et al*., 2002), high carbon dioxide concentrations (Chiu *et al*., 2009) and heavy metal stresses (Liu *et al*., 2007). When exposed to the above stated stressful conditions, photosynthetically fixed carbon is converted into storage products such as lipids. Since, under normal conditions, photosynthetically assimilated carbon is utilized for algal growth and reproduction, the accumulation of storage compounds would be at the expense of algal growth. It may therefore be deduced that an inverse relationship exists between algal cell growth and storage product accumulation in the form of lipids (Csavina, 2008; Li *et al*., 2008b).

The overall lipid yield, for biodiesel production, is however dependent on both algal growth rate and lipid yield (Griffiths and Harrison, 2009). A system therefore needs to be established that takes algal growth, through both cell division and lipid accumulation, into consideration. Thus a biphasic process, where growth occurs initially followed by

lipid accumulation in response to stress, is a central consideration in any attempt to produce maximal overall lipid yields.

1.3 Lipid accumulation pathways in microalgae

It is necessary to understand the underlying mechanisms by which cells accumulate lipid and the triggers initiating this process for the successful promotion of lipid accumulation in microalgal cells. Lipids have important physiological roles in plants and algae. They serve as energy storage, aid with the structural support of cells in the form of membranes and even serve as intracellular signaling compounds (Murphy, 2005; Lacour *et al*., 2012b). Storage lipids are desired for the production of biofuels since they are composed of glycerol esters of three fatty acids known as triacylglycerols (TAGs). TAGs are mostly stored in specialized cytosolic compartments, surrounded by monolayer membranes, which are referred to as lipid bodies (Ohlrogge and Browse, 1995; Hu, 2008; Yu *et al*., 2011; Sharma *et al*., 2012). TAG accumulation is generally triggered by the onset of unfavorable environmental conditions and results in the presence of an energy-rich reserve that may be catabolised upon the return of favorable conditions (Roessler, 1990; Yu *et al*., 2011; Sharma *et al*., 2012). TAGs may also serve as a free fatty acid (FFA) sink thereby preventing lipo-toxity that may occur as a result of the accumulation of excessive FFAs in the cytoplasm (Kurat *et al*., 2006).

The process of fatty acid biosynthesis in algae is not fully understood. However, much is known about lipid synthesis pathways in both animal and plant models and it is believed that the pathways in plants are similar to those evident in algae (Yu *et al*., 2011). Both carbon dioxide and energy, obtained from ATP and NAD(P)H, are required for the initiation of lipid synthesis (Schenk *et al*., 2008; Griffiths *et al*., 2011). These energy molecules are produced during the light phase of photosynthesis and carbon dioxide uptake is evident during the dark phase (Griffiths *et al*., 2011; Sharma *et al*., 2012). ATP and NADPH are consumed for the production of biomass in the dark phase, when normal growth conditions are prevalent. This results in the availability of ADP and $NADP^+$ as acceptor molecules for the light reactions of photosynthesis (Figure 1.1). Nutrient stresses lead to growth impairment, but photosynthesis continues due to light availability

thus ADP and $NADP^+$ are still required regardless of growth cessation. The pool of acceptor molecules can be replenished under growth-limiting conditions by fatty acid biosynthesis thereby preventing the damage of cell components (Thompson, 1996; Hu *et al*., 2008; Lacour *et al*., 2012a; Sharma *et al*., 2012).

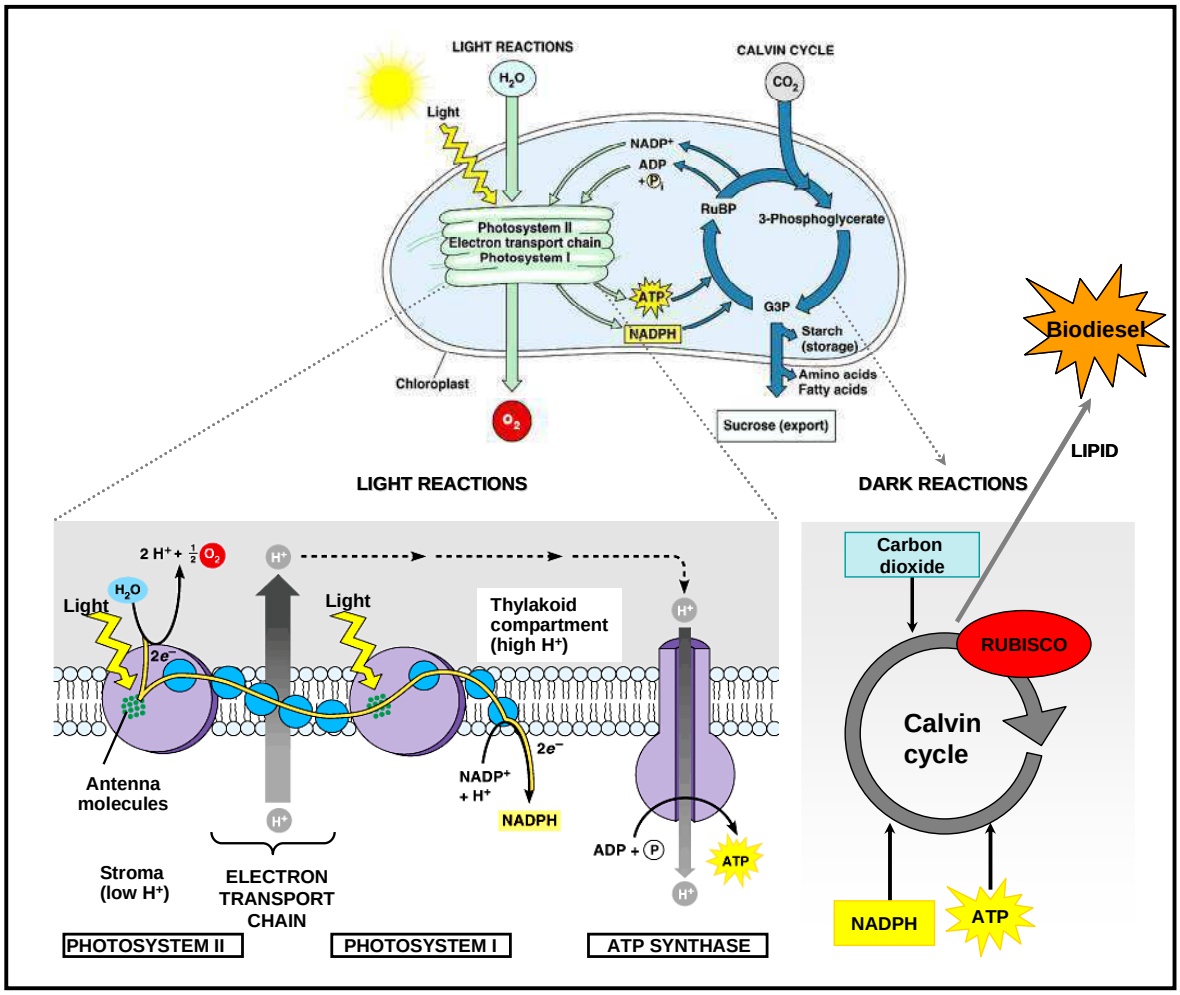

Figure 1.1: Photosynthetic pathway resulting in the conversion of solar energy to chemical energy in the chloroplast (adapted and modified from Schenk *et al.*, 2008).

The key steps in lipid synthesis occur during the dark phase of photosynthesis and are mediated by the Calvin cycle (Figure 1.1). During the Calvin cycle 3-phosphoglycerate (3-PG) production is catalysed by the enzyme Rubisco (ribulose-1.5-bisphosphate carboxylase/oxygenase) from the substrates ribulose-1.5-bisphosphate (RuBP), carbon dioxide and water. Reduction reactions follow, where 3-PG is converted to the final

output of the Calvin cycle, namely a three carbon compound, glyceraldehyde-3-phosphate (G3P) (Schenk, 2008; Figure 1.1). Upon glycolysis G3P is converted to the basic fatty acid precursor, acetyl CoA (Griffiths *et al*., 2011; Yu *et al*., 2011).

Like photosynthesis, fatty acid synthesis occurs in the chloroplast and is initiated by the carboxylation of acetyl CoA to form malonyl CoA by the enzyme acetyl CoA carboxylase (ACCase). This is considered the first committed, rate-limiting step in lipid biosynthesis (Wakil *et al*., 1983; Livne and Sukenik, 1992; Hu, 2008; Griffiths *et al*., 2011) hence the attempt to increase lipid yield via the over-expression of ACCase during the Aquatic Species Program (Sheehan *et al*., 1998). Elevated lipid yields were, however, not observed using this mechanism, possibly as a result of the complex regulation of ACCase (Scott *et al*., 2010) or the disruption of cellular metabolic equilibrium (the limited supply of carbon is required by multiple metabolic pathways and not only energy storage pathways) (Greenwell *et al*., 2010). ACCases have been successfully purified and characterized from two microalgal species, namely *Isochrysis galbana* (Livne and Sukenik, 1990) and *Cyclotella cryptica* (Roessler, 1994) and have been shown to be similar to those obtained from higher plants (Hu *et al*., 2008). The isolation and cloning of the gene encoding ACCase in *Cyclotella cryptica* (Roessler and Ohlrogge, 1993) showed the presence of an analogue of a trans-membrane signal sequence at the N-terminus, implying the possible translocation of ACCase via the endoplasmic reticulum to the site of lipid synthesis i.e. the chloroplast (Hu *et al*., 2008).

The central carbon donor for fatty acid synthesis is malonyl CoA (Ohlrogge and Browse, 1995). The malonyl group is transferred from CoA to a protein cofactor, acyl carrier protein (ACP), prior to entry into the fatty acid synthesis pathway (Figure 1.2). All subsequent reactions in the pathway leading to the production of a 16 to 18 carbon fatty acid, involve this ACP until the products are ready to be exported from the chloroplast or transferred to glycerolipids (Ohlrogge and Browse, 1995; Hu *et al*., 2008). The production of fatty acids from malonyl CoA requires at least 30 enzymatic reactions catalysed by enzymes that are located in the stroma of the chloroplast (Ohlrogge and Browse, 1995).

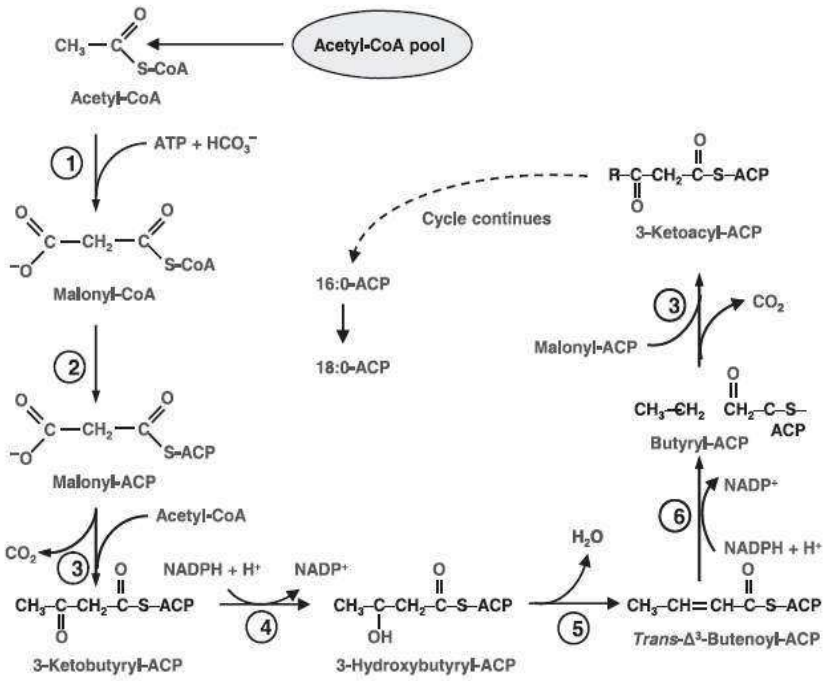

Figure 1.2: Fatty acid biosynthesis pathway in chloroplast (adapted from Hu *et al.*, 2008).

These fatty acids are then converted to acyl-CoA esters that are transferred to the endoplasmic reticulum (ER) for modifications and the production of membrane lipids or storage TAGs (Koo *et al.*, 2004). The Kennedy pathway for TAG biosynthesis, in the ER, was first described in the 1950s and involves the sequential, triplicate, acylation of glycerol-3-phosphate with acyl-CoAs with the aid of enzymes called acyltransferases (Kennedy, 1961; Yu *et al.*, 2011). The resultant TAGs, upon reaching specific concentrations, bud off from the ER, forming distinct lipid bodies (oleosomes) in the cytoplasm (Scott *et al.*, 2010).

1.4 Algal selection & identification

The selection of a suitable algal species, to be used in the production system, is imperative to obtain maximal oil yield (Zebib, 2008). Furthermore, species selection influences the bioreactor design, growth conditions, harvesting method, choice of location for algal mass culture and product range (Pulz and Gross, 2004; Griffiths *et al.*, 2012). At present, there are approximately 30 000 known microalgal species (Burton *et*

al., 2009). Species that display an elevated oil content include *Schizochytrium sp.* which produces between 50 and 77% oil relative to its dry weight, *Botryococcus braunii* that produces up to 75% oil and *Nannochloropsis sp.* that produce between 31 to 68% oil (Chisti, 2007).

The microalgal species selected for biodiesel production should portray elevated growth rates and high intrinsic lipid yields (Doan *et al*., 2011). The ability of the species to flocculate (clump) should also be taken into account when selecting an isolate. Harvesting (removal of the algae from water) is a costly process. Clumping would be advantageous, in the production system, due to the settling properties that it would create thus aiding in the harvesting of the algae i.e. the algal clumps will be heavier and fall out of suspension and may easily be collected. Many prymnesiophytes have been observed to flocculate. Clumping is, however, disadvantageous in that it creates a three phase system (gas/liquid/solid) that decreases mass transfer rates and results in the clogging of filters downstream from harvesting (Carvalho *et al*., 2006).

1.4.1 Marine microalgae

The dominant primary producers in aquatic systems are oceanic microalgae. These microorganisms are imperative in any marine ecosystem as they are the chief provider of energy, organic matter, essential fatty acids and food for other oceanic organisms. They therefore serve a major role at the base of the food chain (Zhukova and Aizdaicher, 1995; Matsunaga *et al*., 2009; Stephenson *et al*., 2011). Despite the fact that these organisms contribute to as little as 1% of the world's photosynthetic biomass, their annual global carbon fixation is similar to that accomplished by terrestrial photosynthetic organisms. This may be as a result of the elevated photosynthetic productivity and metabolic activity of marine microalgae in comparison to terrestrial plants (Field *et al*, 1998; Huntley and Redalje, 2007; Matsunaga *et al*., 2009; Stephenson *et al*., 2011). Marine microalgae consist of numerous species, which portray a high genetic diversity, thus enabling them to inhabit a vast range of sunlit niches and to withstand an array of extreme conditions. This assortment of genetic potential makes for a promising collection to be screened for

the selection of a candidate species for biofuel production (Harwood and Guschina, 2009; Stephenson *et al*., 2011).

Furthermore, marine microalgae do not require the limited supply of fresh water, as they grow and proliferate in seawater. They also compete marginally for land necessary for the growth of terrestrial crops, due to their ability to grow on arid land, making them ideal biofuel production candidates (Posten and Schaub, 2009; Stephenson *et al*., 2011; Schlesinger *et al*., 2012). Much research has been conducted on extremophile microalgal species. The extreme growth conditions enable their mass culture in open systems without much contamination risks (Huntley and Redalje, 2007; Burton, 2009). It is possible to culture any single species without much concern of contamination in closed cultivation systems. The potential for contamination is even more reduced when using marine species as many potentially contaminating agents cannot tolerate the high salinity of seawater.

The diverse array of microalgae include the prokaryotic cyanobacteria (blue-green algae), dinoflagellates, bacilliarophytes (diatoms), raphidophytes, haptophytes and chrysophytes (golden-brown algae) (Harwood and Guschina, 2009; Berry, 2011). Numerous species have been exploited for lipid production. However, research needs to concentrate on marine microalgal species due to the numerous, above-mentioned advantages associated with marine aquaculture (Chisti, 2007; Gouveia and Oliveira, 2009).

Of the various groups mentioned, one of the most promising for biodiesel production is the haptophytes. In the early 1900s, haptophytes were classified in the class Chrysophyceae. By the mid 1900s, sufficient ultrastructural data had been accumulated due to the advent of electron microscopy, to allow them to be placed into their own class known as the Haptophyceae (Daugbjerg and Anderson, 1997). Haptophyte algae have derived their name from the presence of a haptonema (Anderson, 2004). The haptonema is a unique filamentous structure that is located between two relatively equal length flagella. It ranges from being rudimentary (very short - only evident under the electron microscope) to very long (even longer than the flagella) and consists of fewer

microtubules than the flagella making it thinner (Hori and Green, 1985). The haptonema is used for the attachment to surfaces and the capture of prey. It may also play a role in the avoiding response (Kawachi *et al*., 1991; Jones *et al*., 1993; Inouye and Kawachi, 1994; Skovgaard and Hansen, 2003; Yoshida *et al*., 2006). At present the division Haptophyta is sub-divided into two classes, namely the Prymnesiophyceae and the Pavlovophyceae (Cavalier-Smith, 1998; Edvardsen *et al*., 2000).

The haptophytes that were screened for the current project included *Platychrysis* sp., *Isochrysis* sp. and *Pleurochrysis* sp. All of the screened isolates have been shown to store excess carbon as lipid (Moheimani and Borowitzka, 2006; Feng *et al*., 2011; Chen *et al*., 2012a; Sanchez *et al*., 2012; personal observation). However, no studies relating to biodiesel production has been conducted thus far with *Platychrysis* sp. Species of *Isochrysis* have been mass cultured but most studies were aimed at increasing algal yield to be used as aquaculture feeds (Juario and Storch, 1984; Enright *et al*., 1986; Helm and Laing, 1987; Renaud *et al*., 1991; Sukenik and Wahnon, 1991; Wikfors and Patterson, 1994; Borowitzka, 1997). In recent studies however, species of both *Isochrysis* (Feng *et al*., 2011; Chen *et al*., 2012a; Sanchez *et al*., 2012) and *Pleurochrysis* (Moheimani and Borowitzka, 2006) have been investigated as potential candidates for biodiesel production. Species of *Isochrysis* have also been highlighted in numerous biofuel reviews (Chisti, 2007; Deng *et al*., 2009; Harun *et al*., 2010; Mata *et al*., 2010; Singh and Gu, 2010; Verma *et al*., 2010).

1.4.2 Species identification

It is imperative to determine the identity of the model organism selected for biodiesel production. Morphological, physiological, biochemical and genetic characteristics may be compared with those of known algae to determine whether the current isolate is unique or not (Mason *et al*., 2003; Park *et al*., 2007; Li *et al*., 2008a).

Haptophyte taxonomy and classification may be broadly categorized with respect to the type of scales (coccoliths and organic) that these algae possess or do not possess. Generally it was believed that mineralised scales of haptophytes are calcified whilst those

of the Chrysophyceae are always silicified. Siliceous cyst formation was however recognized in the haptophyte *Prymnesium parvum* (Hibberd, 1980). Yoshida *et al*. (2006) also recently described a haptophyte bearing siliceous scales. Thus, a combination of taxonomic techniques need to be conducted to accomplish definitive algal identification, and not merely base it on morphological characteristics such as scale type. A similar observation was evident in the identification of the raphidophytes where the difficulty in classifying the algae, based on morphological methods, was due to some of the species displaying pleomorphology (Kai *et al*., 2006). Differences in size and shapes of a species of alga have been observed under varying environmental conditions resulting in ambiguous identifications. Numerous molecular methods, including nested single-cell PCR and single cell random amplified polymorphic DNA (SC-RAPD), proved valuable in the identification of these algal species (Kai *et al*., 2006).

Molecular methods for algal identification are at present widely applied. These techniques are possible due to evolutionarily-conserved sequences such as ribosomal RNA (Metting Jr., 1996). DNA may be extracted from the organism using numerous methods. The method used for DNA extraction from microalgae needs to be effective across a broad range of algal lineages, requires small amounts of cellular material and needs to be rapid and inexpensive. Current, successful techniques for algal DNA extraction are mostly based on variations of the cetyltrimethylammonium bromide (CTAB) method of Doyle and Doyle (1990) (Fawley and Fawley, 2004).

Specific regions of the extracted DNA may be amplified using the polymerase chain reaction (PCR). With the aid of appropriate primers that flank the region needing to be amplified, and optimal melting and annealing temperatures, multiple copies of the region of interest may be obtained. The PCR products may then be sequenced and the sequence obtained may be aligned with multiple previously-identified sequences of the same region, from various other algal species, to determine how similar the sequence of interest is in comparison to the known sequences in the Genbank® genetic sequence database. Bioinformatics tools such as PhyloDraw (Choi *et al*., 2000) may be used to construct a phylogenetic tree which would show sequence similarity based on the branch

lengths, distances from each other and bootstrapping analyses. Bootstrapping is a process that involves resampling from the original data multiple times and then determining the significance of the data in terms of a confidence interval (Fran *et al*., 2006). Branches with confidence intervals of 95% and greater are considered reliable. Using the above stated techniques the algal species may be identified or a novel species may be recognized.

The selection of the algal species to be used for biodiesel production should be one that produces maximal lipid yield. Attempts to further optimize the lipid yield of the organism via various methods including nutrient deprivation and genetic modification may also follow (Zebib, 2008; Leon-Banares *et al*., 2004).

1.5 Mass culture of microalgae

A low-cost, large-scale production system is required for the mass production of microalgae to be utilised for biodiesel generation. Numerous bioreactor designs have been established for this purpose but each design has its own set of associated shortcomings and benefits (Griffiths *et al*., 2011). Current commercial applications are primarily restricted to the low-volume/high-value product markets i.e. microalgal species are mainly mass produced for feed ingredients and specialty foods (Spolaore *et al*. 2006; Harun *et al*., 2010). The factors impeding the commercialization of microalgal oils for biodiesel production include low lipid productivities, elevated energy requirements for both the cultivation system and downstream harvesting of the biomass and expensive techniques used for the extraction of lipids (Hu *et al*., 2006; Feng *et al*., 2011)

1.5.1 Photobioreactor systems

Large-scale, commercial microalgal culture originated in the early 1960s, in Japan, where *Chlorella* was cultured. Numerous other ventures followed, with much attention being focused on the mass culture of *Spirulina* for health food. Algal culture during that period generally revolved around the use of fairly unsophisticated open air ponds that lacked artificial mixing (Borowitzka, 1999). At present the only practical methods for the large scale production of microalgae are tubular photobioreactors and raceway ponds (Chisti,

2007). The predominating culture systems currently also include fermenters, cascade systems and crude methods such as large transparent plastic bags (Borowitzka, 1999). The selection of the bioreactor system for algal mass culture is just as important as the selection of the model organism since the growth system controls the conditions under which the organism grows (Greenwell *et al.*, 2010). The factors that need to be considered when choosing a culture system include the nutrients required by the algae, the physiology of the algae, the cost of land, the energy required to run the system and water usage (Borowitzka, 1999).

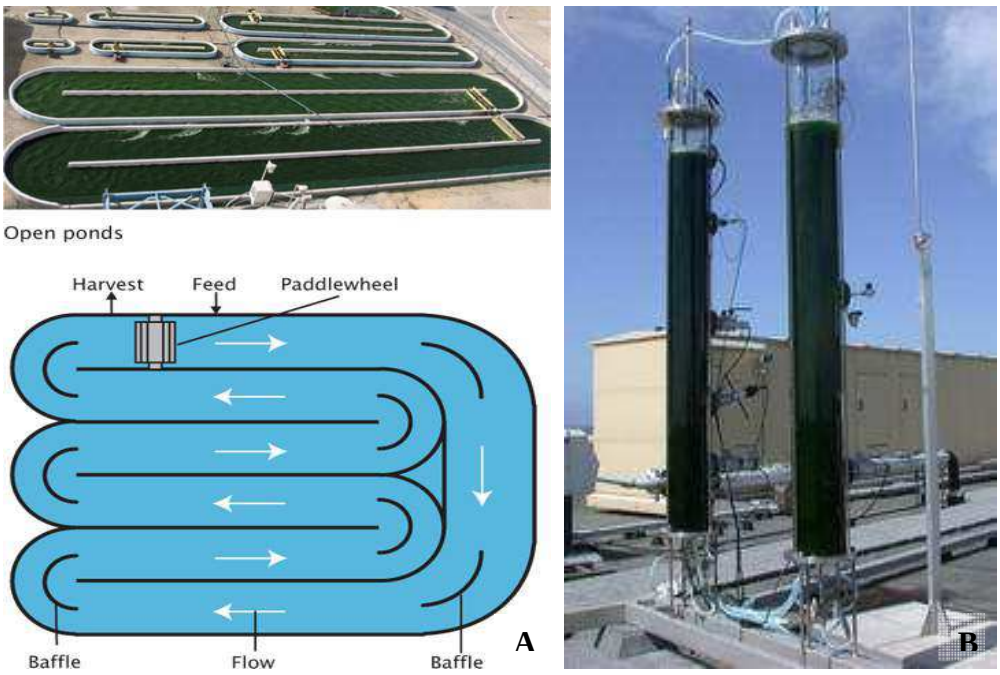

Figure 1.3 (A): Aerial view of opened, raceway photobioreactor (Chisti, 2007) and **(B):** closed, tubular photobioreactor (www.bioenergy-noe.org).

Majority of the large commercial systems that are currently in use are open-air systems due to the significantly elevated costs and scale up difficulties of closed systems (Borwitzka, 1999). Raceway ponds (Figure 1.3 A) are one of the most common forms of open-air systems. They consist of closed loop recirculation channels. Paddlewheels are used for mixing in these ponds and baffles are used for directing flow around the bends (Figure 1.3 A). Open-air systems are disadvantageous in that they produce low biomass yields in comparison to closed systems (Chisti, 2007).

Another short coming of the open culture system is the limited range of microalgae that may be maintained in monoculture. *Spirulina, Dunaliella* and *Chlorella* are the only genera that have been successfully monocultured using this system because they can tolerate extreme culture environments, e.g. low pHs not normally favoured by most other algal species. However the culture may still be contaminated with other organisms such as bacteria and fungi (Lee, 2001). The inability to control the climate is another problem associated with open air systems, which requires adequate illumination for maximal algal growth (Borowitzka, 1999).

Studies have focused on the use of closed systems for algal culture due to the need for increased biomass production and the ability to maintain monocultures under defined culture conditions (Lee, 2001). Tubular airlift photobioreactors (PBRs) (Figure 1.3 B) work optimally under non-limiting light levels only when the photosynthetically produced oxygen is continuously removed and when carbon dioxide supply is non-limiting. In addition, the temperature of the system needs to be controlled (Babcock Jr. *et al*., 2002). Light intensities within the photobioreactor also have a significant impact on cell growth. In dense cultures, light is rapidly attenuated within the photobioreactor, thus placing a limit on the maximum bioreactor diameter for optimal algal culture (Wu *et al*., 2004). Light distribution and algal cell exposure to incident radiation within the bioreactor is significantly affected by the mixing conditions and the geometry of the bioreactor (Babcock Jr. *et al*., 2002).

Mechanical mixing or airlift pumps may be used to maintain turbulent flow and mixing in PBRs. Airlift pumps are preferred and have been successfully utilized in numerous algal mass culture systems. Mechanical mixing may damage the biomass due to the rough mode of agitation (Chisti, 2007). Mixing in PBRs ensures the algal cells experience sufficient periodic cycling between the light and dark zones thus optimizing the exposure times of all cells to adequate amounts of light (Babcock Jr. *et al*., 2002; Wu *et al*. 2004). Mixing is also advantageous in that it prevents biomass sedimentation in tubes (Chisti, 2007) and minimizes biofilm formation on the internal surface of the bioreactor thus optimising light penetration (Loubiere *et al*., 2008). However, mixing may also be

counterproductive in that it creates shear forces that might be detrimental to the more fragile algal strains (Babcock Jr. *et al*., 2002).

A study conducted by Kazakis *et al*. (2007) showed that spargers (porous tubes or disks used for bubbling gases into liquids) used in bubble columns have a significant positive impact on the overall operating of the PBR system. The design parameters that need to be considered in these PBRs include the size of the bubbles and the duration of gas retention in the column (gas-holdup). The column geometry and the physical properties of the liquid phase coupled with the sparger pore diameter have been shown to influence gas-holdup (Kazakis *et al*., 2007).

A variety of spargers have also been used in systems for algae mass culture. Eriksen *et al*. (1998) utilised a dual sparging system in their continuous PBR system. The spargers had a dual function, one with small bubbles was for aeration (to deliver CO_2) and one with larger bubbles mixed the algal culture. The system lacked any form of mechanical mixing, to reduce shear stress to the algal cells. The incorporation of dual spargers provided a gentler method of mixing but still maintained comparable levels of productivity relative to those obtained in systems with mechanical mixing (Eriksen *et al*. 1998).

As evident from the above mentioned studies, numerous factors need to be taken into consideration when selecting the optimal system for microalgal mass culture. Upon rigorous analysis of the advantages and disadvantages associated with each culture method a choice may be established between a closed or opened system. Modifications and optimizations of the chosen production system should follow.

1.5.2 Algal harvesting

Harvesting refers to the solid-liquid separation resulting in the recovery of algal biomass for further processing. Microalgal harvesting may contribute to approximately 20 to 30% of the cost of biomass production (Grima *et al*., 2003; Mata *et al*., 2010). No radical advances in this field have been achieved since the 1960s (Golueke and Oswald, 1965)

however it is still an ongoing research area and various harvesting techniques are currently being optimized (Mata *et al*., 2010). The methods of cell harvesting that are frequently explored include sedimentation, filtration, flocculation, flotation, centrifugation and electrophoresis techniques (Mata *et al*., 2010; Uduman *et al*., 2010b; Griffith *et al*., 2011).

The chosen method is greatly species specific and also dependant on the desired final products (Shelef *et al*., 1984; Richmond, 2004; Uduman *et al*., 2010b). Species specific factors influencing the dewatering process include cell size, shape, density, motility, cell-surface properties and the variation of these properties at different life stages and in response to the cellular physiological state (Greenwell *et al*., 2010). Much research has been conducted on freshwater algal species and as a result studies on marine isolates have lagged behind. Since focus has been placed on oceanic algae, due to limited freshwater resources, it is imperative that methods of marine algal flocculation be established (Uduman, 2010b).

Various authors have analysed a range of harvesting strategies to optimize the downstream microalgal dewatering process:

- Millamena *et al*. (1990) analysed the effect of chemical flocculation, using aluminium sulphate (alum) and lime on the diatoms *Chaetoceros calcitrans* and *Skeletonema costatum* and the flagellates *Isochrysis galbana* and *Tetraselmis chui*. All species excluding *Isochrysis galbana* flocculated, resulting in greater than 80% cellular recovery, using both lime and alum. Optimal pH ranges for each treatment was however necessary to utilise the minimal chemical dose.

- Lee *et al*., (2009) used microbial colonies grown with various carbon sources (glucose, glycerine or acetate) to initiate the flocculation of *Pleurochrysis carterae*. Clumping occurs due the secretion of extracellular polymeric substances (EPS) by the flocculating bacteria, resulting in the adherence of microalgal cells to themselves and the bacterial consortia. This process is advantageous in that carbon sources, such as glycerol and acetate, are byproducts

of biodiesel production and no metallic flocculants are used that may lead to downstream contamination of the final product.

- Sanyano *et al*. (2011) carried out a study with the aid of the technique, response surface methodology (RSM) to determine the optimal parameters for the harvesting of *Chlorella* sp. using alum and ferric chloride. The duration required for maximal flocculation, pH and coagulant dosage was successfully determined using RSM thereby offering an alternate technique for harvesting experimental design. Ferric chloride resulted in the efficient flocculation of this species but is very expensive.

- Eldridge and colleagues (2012) used inorganic and organic coagulants to flocculate various marine microalgal species. Alum and iron sulphate resulted in more than 90% of *Tetraselmis suecica* and *Chlorococcum* sp. flocculating without any pH adjustments being necessary. Other species such as *Isochrysis galbana*, *Dunaliella tertiolecta* and *Nannochloropsis salina* were not as easily flocculated and required more then two times the coagulant concentration to achieve similar flocculation efficiencies. The factors contributing to the difference in the flocculation in the various species include cell size, surface area and surface composition.

Despite of the numerous studies conducted on microalgae harvesting and recovery, no single method may be seen as better than the next. This may be as a result of the affectivity of the methods being based on the species to be harvested, culture medium and end product (Shelef *et al*., 1984; Uduman, 2010b). A harvesting technique thus needs to be established post selection of the microalgae species to be used for biofuel production. This method should be economically feasible, require minimal energy, possess an elevated recovery efficiency with minimal cell damage and allow for the recycling of water and nutrients (Griffith *et al*., 2011).

1.6 Future prospects of algal based biofuels

A significant amount of research and development programs are conducted worldwide with the sole objective of ultimate algal biofuel commercialization. To date over 150 algal biofuel companies exist. The United States of America has dominated with approximately 80% of these companies based there followed by 13% in Europe and the remaining 9% elsewhere (Singh and Gu, 2010). Over 50% of the companies utilize closed systems for algal mass culture. Open ponds, regardless of their decreased cost implications, are only used by 25% of the companies and the remaining companies exploit natural settings for algal mass culture (Singh and Gu, 2010). The increase in the use of PBRs may be an outcome of cost reductions on more modern versions of these systems in the US resulting in approximately an equal expenditure for PBRs and open ponds (Piccolo, 2009).

One of the largest algae investments in the European Union (EU) is the £26 million project by the British company, Carbon Trust. The final goal of the project is to construct large algal farms in North Africa. Preferable regions for these algal farms are the coast of the Mediterranean Sea due to the warmer temperatures, which do not go below 15ºC year-long, experienced there (Piccolo, 2009). Countries such as Egypt, Algeria, Morocco and Tunisia, that lie on the south of the Meditteranean, are attractive for algal culture due to the vast desserts where these algal farms may be established. The development of such industries in Africa would be greatly beneficial in that they would create job opportunities and exposure of scientists to a vast array of technologies. The successful commercialization of algal-based biofuels would thus have numerous worldwide benefits both economically and environmentally (Piccolo, 2009; Singh and Gu, 2010).

The key strategies for algal biofuel commercialization include the selection of a fast growing and TAG-rich microalgal species, the development of a cheap and uncomplicated process for mass culture and harvesting and the development of an algal biorefinery (Greenwell *et al*., 2010; Singh and Gu, 2010). Most of this have already been discussed above but the biorefinery concept has not been mentioned thus far. A biorefinery may be defined as the processing of biomass to result in the production of a

wide array of end-products including energy thereby maximizing the value obtained from the biomass source. The recycling of water and nutrients involved in the process also contribute to the biorefinery concept (Greenwell *et al*., 2010; Singh and Gu, 2010; Alba *et al*., 2012). Products such as livestock feed, nutrients and food supplements for human consumption, chemicals required for the production of pharmaceuticals and pigments may be produced by algae (Brennan and Owende, 2010; Harun *et al*., 2010; Koller *et al*., 2012; Figure 1.4).

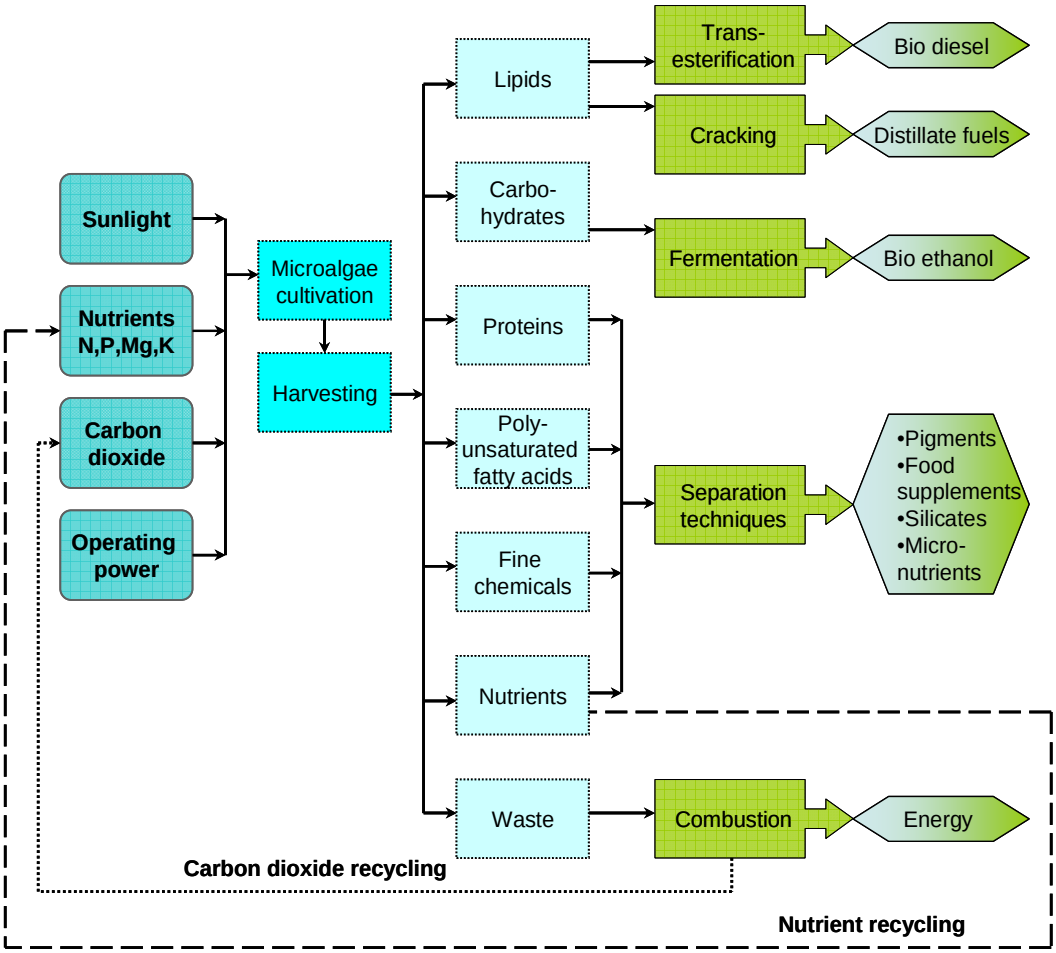

Figure 1.4: Schematic representation of a microalgal biorefinery system that minimises wastage, maximises economic yield and reduces the environmental impact (adapted and modified from Singh and Gu, 2010 and Greenwell *et al.*, 2010).

Williams and Laurens (2010) conducted an economic assessment that showed that harvesting and extraction processes account for approximately 15% of the operating budget and 50% of the labour costs indicating that they contribute significantly to the overall economic sustainability of biodiesel production from microalgae (Williams and Laurens, 2010). These costs may, however, be bypassed if algal species were able to naturally secrete lipids into the culture medium (Singh and Gu, 2010). Studies conducted on yeast cells have shown that the inactivation of certain genes involved in ß-oxidation and random mutagenesis resulted in the cells possessing the ability to secrete lipids (Nojima *et al*., 1999; Michinaki *et al*., 2003). The understanding of lipid secretion pathways is however still in its infancy. Microalgal cells may be genetically modified in attempts to promote lipid secretion when adequate knowledge of the routes to lipid secretion are elucidated. This would drastically decrease biodiesel production costs (Radakovits *et al*., 2010).

The selection of the ideal microalgal species, the optimisation of 'microalgal milking' (lipid secretion by microalgae cells) as termed by Singh and Gu (2010), the limitation of the cost of photobioreactors (Picollo, 2010) and the biorefinery process are the key factors that need to be solved to realise the viable commercialization of biofuel production from algae. With the current worldwide research drives, the successful establishment of real solutions, to aid in microalgal biodiesel commercialization, should be obtained in the near future resulting in further steps towards a viable solution to the world's environmental and energy concerns.

1.7 Main objective

To contribute to the knowledge on using microalgae for lipid sequestration, to be used as a feedstock for biodiesel production, as an environmentally friendly, sustainable alternative to fossil fuels.

1.8 Aims

1. To conduct batch culture experiments for the screening of a few pre-selected algal species and the selection of a model organism that produces maximal lipid yield, grows rapidly and flocculates (clumps).
2. To use molecular procedures and transmission electron microscopy (TEM) for the identification of the selected species.
3. To determine the optimal (cost-effective) conditions for cell growth and lipid production in batch cultures using bubble or gas sparge bottles.
4. To determine feasible harvesting strategies for the downstream concentrating of the selected species.
5. To develop a photobioreactor system, for the mass culture of the previously selected species and optimisation of the system to promote maximal cell growth rates and maximal levels of lipid accumulation.

CHAPTER TWO

General Methodology

2.1 Medium preparation

F/2 medium was used in all experiments. This medium is a commonly used, general enriched seawater medium that was specifically designed for the culture of diatoms and coastal marine algae (Guillard and Ryther, 1962). For the preparation of *f/2* medium natural seawater was filtered through bolting cloth and filter paper (Whatman No. 1), to remove any large contaminants, and then autoclaved for 30 minutes at 121 °C. The seawater was cooled and refiltered (using sterile Whatman No. 1 filter paper and an autoclaved funnel) inside a laminar flow bench. The second filtration step was conducted to remove any salt crystal rafts that formed during autoclaving which was observed to promote clumping. The microelements and vitamin solution (Appendix) were then added.

2.2 Stock culture maintenance

Every fortnight 1 ml of the unialgal cultures were aseptically transferred to a sterile 50 ml conical flask (autoclaved at 121 °C for 30 minutes) containing 20 ml *f/2* medium. These cultures were incubated at an illumination intensity of 110 µmol photons.m^{-2}.s^{-1} with a 10:14 light-dark cycle and were maintained at 23 ± 2 °C.

2.3 Batch culture setup (1 L cultures)

Batch culture (1 L) experiments were conducted in modified 1 L Schott Duran® bottles equipped with rectangular (2.5 cm x 1.5 cm), sand stone fish tank, air-spargers. Each bottle was equipped with a quick fit gas inlet, gas exhaust and an aeration tube. Plastic tubing (5 mm diameter) was used to attach the sparger to the outlet end of aeration tube, and for connecting the inlet side to an air pump (Labotec N 86 KN.18) which was operated at a pressure of 2.4 bar (Figure 2.1). The culture vessels were cleaned thoroughly and autoclaved for 30 minutes at 121 °C and air was pumped through the spargers to remove any dirt or debris which might have contaminated them prior to use. All batch (1 L) cultures were conducted at an illumination intensity of 110 µmol photons.m^{-2}.$s^{-1}$with a 10:14 light-dark cycle and were maintained at 23 ± 2 °C. The cultures were aerated with filtered air (Whatman uniflo 0.2 µm filter), at approximately 29.8 ml/sec, with the aid of an air pump (Labotec N 86 KN.18 with pressure of 2.4 bar). The lighting received by each culture was evened out by the random relocation (using a

number table – Microsoft Excel) of the growth vessels on the culture shelf relative to the unidirectional light source every alternate day.

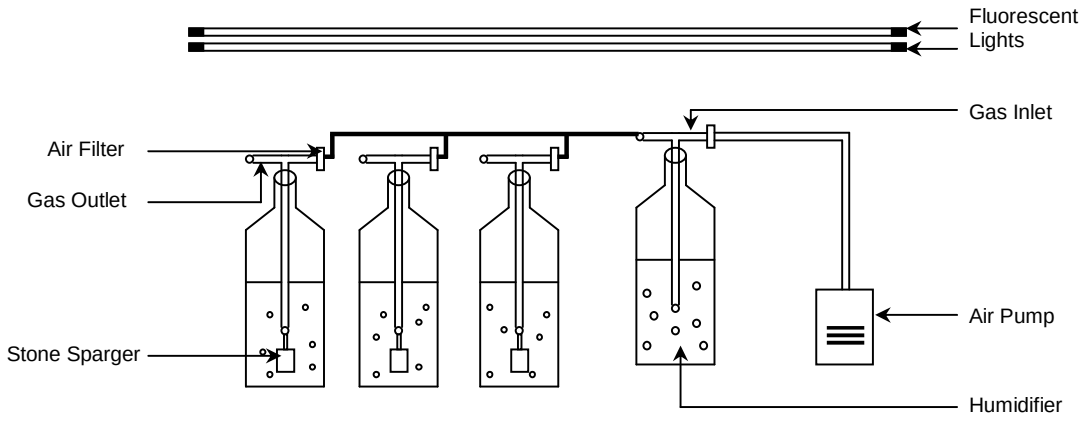

Figure 2.1: Schematic representation of experimental setup.

2.4 Cell concentration measurements using a haemocytometer

Cell numbers were measured using a Neubauer haemocytometer. A uniform cell suspension was obtained by mixing the culture with a Pasteur pipette (drawing the culture up and releasing multiple times). Motile cells were immobilized, prior to counting, by adding a drop of 1% Lugol's solution (Appendix) to 1 ml of the culture sample. The culture was diluted if the number of cells per 1 mm^2 exceeded fifty. Cell counts were conducted in quadruplicate.

2.5 Cell concentration measurements using spectrophotometry

A standard curve was constructed to determine cell numbers versus optical density with the aid of spectrophotometry. Cultures with varying cell densities were acquired through dilution. The cellular concentration of each culture was measured using a Neubauer haemocytometer (Section 2.4). The corresponding absorbance reading at 650 nm was determined (S2100 Diode Array Spectrophotometer) for each count and a standard curve was constructed (Figure 2.2).

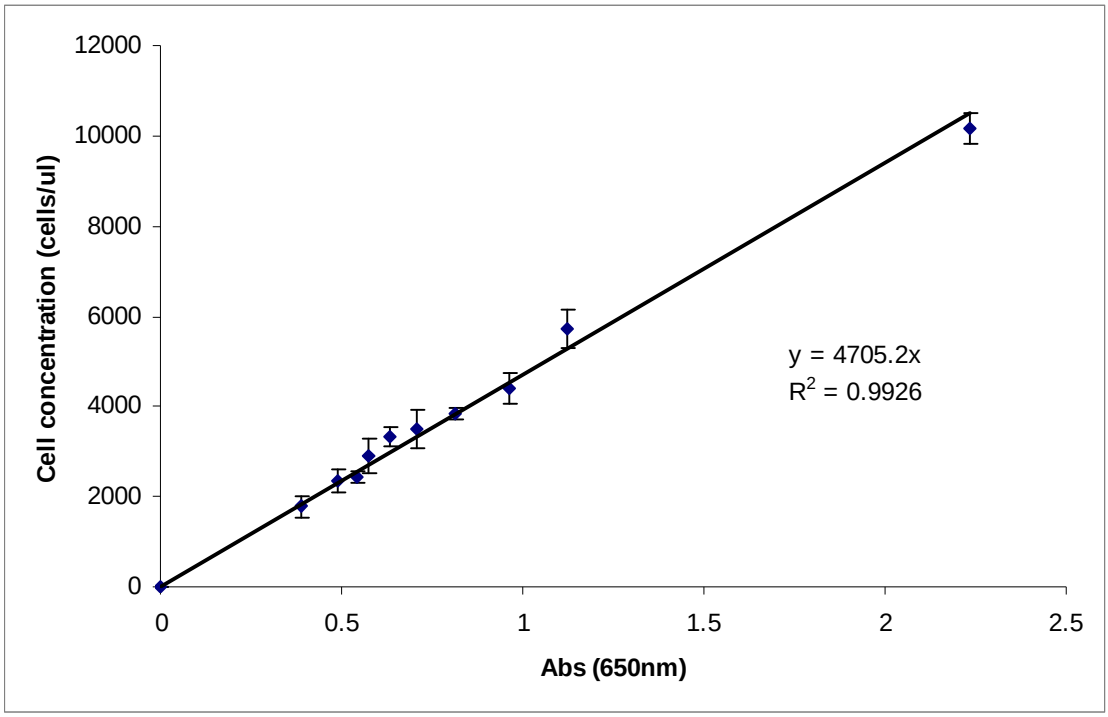

Figure 2.2: Standard curve depicting concentration of *I. galbana* cells with respect to absorbance readings at 650 nm. Error bars represent standard deviation (n = 3).

2.6 Lipid extraction

Aliquots (100 ml) of the algal culture were centrifuged, at 6000 rpm for 10 minutes. The pellet was removed, rinsed with 0.5 M ammonium bicarbonate to remove salt crystals (Zhu and Lee, 1997), placed on a glass sheet, and left to dry in a dessicator, containing silica gel crystals, at room temperature for 72 hours. The dried algal pellet was weighed and total lipids were extracted using a modified version of the Bligh and Dyer (1959) method as follows:

The initial stage of lipid extraction required the addition of chloroform, methanol and water in a 1:2:0.8 v/v ratio, i.e., 80 ml water, 100 ml chloroform and 200 ml methanol per unit gram dried cell mass, which resulted in a monophasic mixture. Autoclaved glass beads (0.1 mm diameter, Inqaba Biotech) were added to this mixture and the tube was vortexed at high speed for five minutes to disrupt the cells. Chloroform and water were then added to the previous mixture in a 1:1 ratio (i.e. 100 ml chloroform and 100 ml

water per unit gram dried cell mass) to produce a biphasic mixture. The resulting mixture was vortexed for an additional five minutes and transferred to micro filters which were placed in Zymo spin column collection tubes (ZR Fungal/Bacterial DNA Kit^{TM}). These tubes were centrifuged at 1500 rpm for five minutes. The resulting mixture, in the collection tube, was thus free of any cellular debris that may cause an inaccurate lipid yield result. A small volume (20 µl) of chloroform was then added to the glass beads in the filter. The filters in the collection tubes were re-centrifuged at 1500 rpm for five minutes. This process aided in rinsing out the filters thus ensuring that all the lipids were successfully transferred into the collection tube.

The chloroform phase was recovered from the resultant biphasic mixture in the collection tube using a sterile Pasteur pipette and placed in a clean, pre-weighed Eppendorf tube. The Eppendorf tube, containing the chloroform-lipid extract, was transferred to a 50 °C water bath and the chloroform was evaporated. The resultant residue in the Eppendorf tube represented the total extracted lipids from the algal biomass. The Eppendorf tube was incubated in a dessicator, with silica gel crystals, overnight and then weighed to determine the total lipid dry weight. The quotient of the total lipid dry weight and the algal biomass dry weight multiplied by 100 was used to calculate the percentage of total lipid.

2.7 Lipid content measurements using flow cytometry

Nile red stained and unstained cells were used for each lipid reading. The unstained cells represented the auto-fluorescence control. A 50 µl aliquot of Nile red in acetone (0.1 mg/ml) was added to 1 ml of algal suspension containing approximately 10^6 cells/ml. The suspension was then vortexed and incubated in the dark for 10 minutes in a 37 °C water bath. The fluorescence of Nile red is dependent on the polarity of the intracellular environment. The FL2 and FL3 flow cytometer channels detect Nile red fluorescence which exhibits yellow-gold and red fluorescence when dissolved in neutral and polar lipids respectively (de la Jara *et al*., 2003; da Silva *et al.*, 2008).

All the cytometric measurements were done using a BD FACSCalibur™ flow cytometer (Becton-Dickinson Instruments) equipped with a 488 nm argon laser. Calibration of the instrument was conducted, prior to each use, using BD CaliBRITE™3 beads for three-color flow cytometry setup. The following equation was used to determine total cellular lipid fluorescence:

Total cellular lipid fluorescence = (FL2/AF) + (FL3/AF)

Where FL2 refers to the mean fluorescence picked up by the FL2 channel that measures neutral lipids, FL3 refers to the mean fluorescence picked up by the FL3 channel that measures polar lipids and AF refers to the auto-fluorescence control picked up by the respective channels. Data was expressed in arbitrary fluorescence units (de la Jara *et al*., 2003; da Silva *et al.*, 2008).

Standard curves were constructed showing the correlation between Nile red fluorescence intensity, using flow cytometry, and microalgal lipid content, assayed by the method outlined in Section 2.6. Flow cytometry was the sole method used for lipid quantification after the construction of these standard curves.

2.8 Dry cell weight measurements

An aliquot of the microalgal suspension (100 ml) was centrifuged at 5000 rpm for ten minutes. The pellet was rinsed with 0.5 M ammonium bicarbonate to remove excess salts that would result in incorrect elevated dry weight measurements (Zhu and Lee, 1997). The pellet was then transferred to a pre-weighed glass sheet and allowed to dry in a dessicator, with silica crystals, at room temperature for 72 hrs. The dried biomass on the glass sheet was then weighed and the dry cell weight was calculated by subtracting the pre-determined weight of the glass sheet from the accumulative weight of the glass sheet containing the dried biomass.

2.9 Biomass productivity measurements

The following equation was used to determine biomass productivity over a specific duration:

$$P_{Biomass}\ (g/L/day) = \frac{DCW_{Start}\ (g/L) - DCW_{End}\ (g/L)}{Time\ (days)}$$

Where DCW_{start} refers to the dry cell weight at the beginning of the time interval, DCW_{end} refers to the dry cell weight at the end of the time interval and time refers to the algal cultivation period (from start to end; Rodolfi *et al*., 2009). The dry cell weight was determined as described in Section 2.8.

2.10 Lipid productivity measurements

The following equation was used to calculate lipid productivity:

$$P_{Lipid}\ (g/L/day) = \frac{C_{Lipid}\ (g/g) \times DCW\ (g/L)}{Time\ (days)}$$

Where P_{Lipid} refers to the lipid productivity, DCW refers to the dry cell weight, C_{Lipid} refers to the lipid content of the cells and time refers to the algal cultivation period (Li *et al*., 2008b; Widjaja, 2009). The lipid yield was obtained as described in Section 2.7 and dry cell weight was obtained as depicted in Section2.8.

2.11 Growth rate, divisions per day and generation time determinations

Cell concentration measurements were obtained as in Section 2.4 and Section 2.5 above. The following equation was used to determine growth rate (μ) (Barsanti and Gualtieri, 2006):

$$Growth\ rate\ (\mu) = \frac{lnN_2 / lnN_1}{t_2 - t_1} \quad ; \quad t_2 > t_1$$

Where N_2 and N_1 refer to the concentration of cells at time two (t_2) and time one (t_1) respectively.

Divisions per day ($Div.day^{-1}$) was calculated with the aid of the following equation (Barsanti and Gualtieri, 2006):

$$Div.day^{-1} = \mu / ln2$$

Generation/doubling time (T_g) was calculated with the aid of the following equation (Barsanti and Gualtieri, 2006):

$$T_g = 1 / Div.day^{-1}$$

2.12 Morphological analysis

2.12.1 Specimen embedding and sectioning

Algal cells were fixed for one hour in 2.5% glutaraldehyde in 0.1 M sodium cacodylate buffer in 0.5 M sucrose. Centrifugation followed at 3000 rpm for ten minutes and the supernatant was decanted. The pellet was then serially rinsed with 0.1 M sodium cacodylate buffer in a decreasing gradient of sucrose concentration (0.5 M, 0.4 M, 0.2 M and 0.1 M) for 15 minutes each. The cells were post-fixed for an hour in 2% osmium tetroxide in 0.1 M sodium cacodylate buffer without sucrose and then washed three times in the same buffer prior to dehydration. The material was dehydrated by passing it through a graded ethanol series (10%, 20%, 50%, 80%, 90% and a duplicate 100%) for fifteen minutes each. The dehydrated cells were infiltrated with 3:1, 1:1 and 1:3 mixtures of 100% ethanol and Spurr's Resin (Spurr, 1969) for twenty minutes each and then embedded in 100% Spurr's Resin according to the protocol outlined in Sym *et al*. (2011). The embedded samples were polymerized at 70 ºC for 16 hours.

Sections were cut using a diamond knife on a Reichert ultramicrotome and stretched using Xylol fumes. The sections were then picked up on a 300 mesh copper grid, stained

with 2% aqueous uranyl acetate and counterstained with Reynolds' lead citrate (1963) for fifteen minutes each and finally rinsed with distilled water. The sections were examined using a transmission electron microscope (FEI, T12 Tecnai G2 Spirit – Manufacturer: FEI Company, Eindhoven, Netherlands) at an accelerating voltage of 120 kV.

2.12.2 Whole mounts of algal cells

A drop (4 µl) of a healthy algal culture was placed on a formvar (0.5% w/v formvar in chloroform) coated 300 mesh copper grid. The cells were fixed via. the addition of a drop of 2% glutaraldehyde to the cells on the grid. After five minutes the liquid was removed with filter paper, without touching the grid. The grids were then rinsed with a drop of distilled water to remove salt crystals and then stained with 2% aqueous uranyl acetate and re-rinsed. The cells were shadowed with gold/palladium and examined using a transmission electron microscope (FEI, T12 Tecnai G2 Spirit – Manufacturer: FEI Company, Eindhoven, Netherlands) at an accelerating voltage of 120 kV.

2.13 Culture medium composition measurements

2.13.1 Nitrate measurements

The Cataldo method (Cataldo *et al.*, 1975) was used to determine the amount of nitrate in the culture medium. The microalgal culture was centrifuged at 3000 rpm for 10 minutes to remove the cells from suspension. A 50 µl aliquot of the supernatant was then transferred to a thoroughly cleaned glass vial. 200 µl 5% (w/v) salicylic (2-hydroxybenzoic) acid in pure sulphuric acid was added to the vial and the liquid was agitated briefly (shaken by hand) to ensure sufficient mixing of the contents. A ten minute incubation period, at room temperature, followed. 2 ml, 4 M sodium hydroxide was then added to the solution and the mixture was again shaken and left to incubate, at room temperature, for 20 minutes. The absorbance was then read at 410 nm (S2100 Diode Array Spectrophotometer). The absorbance readings obtained were back-plotted on a previously constructed nitrate standard curve (Figure 2.3) to determine the concentration of nitrate in solution.

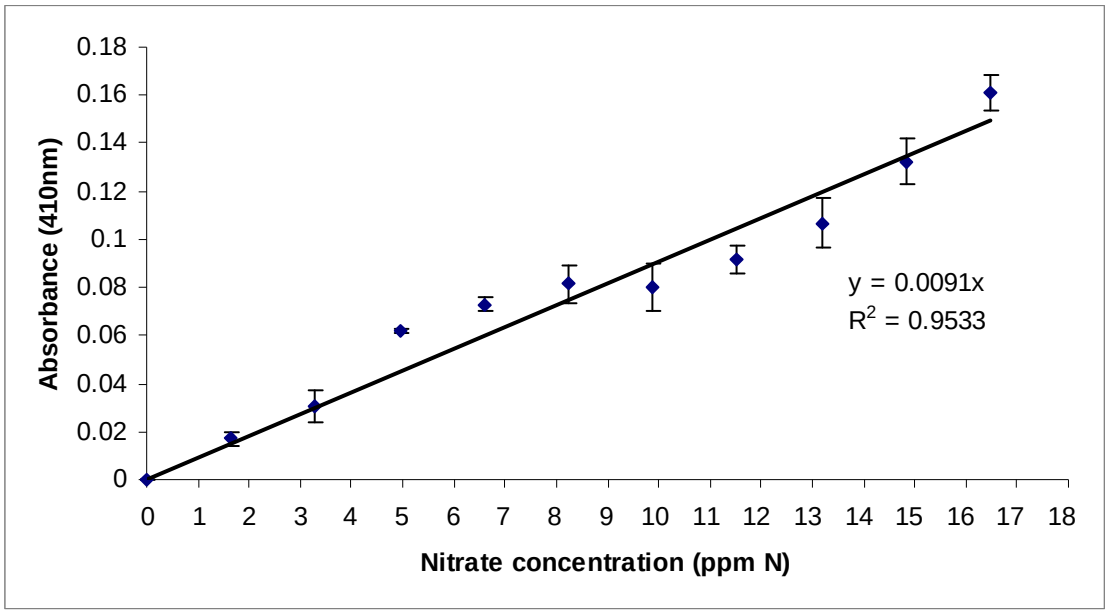

Figure 2.3: Standard curve depicting nitrate concentration with respect to absorbance readings at 410 nm. Error bars represent standard deviation (n = 3).

2.13.2 Ammonium measurements

The Indophenol Blue method (Scheiner, 1976) was used to determine the concentration of ammonium-N in the culture medium. This method required the preparation of a phenol-nitroprusside-buffer reagent and alkaline hypochlorite reagent. The phenol-nitroprusside-buffer reagent consists of 60 g phenol and 0.2 g sodium nitroprusside dissolved in 1 L of a buffer solution (30 g sodium phosphate tribasic and 30 g sodium citrate tribasic in 1 L distilled water). The alkaline hypochlorite reagent was prepared by adding 30 ml commercial bleach (3.5% available chlorine) to 400 ml 1 N NaOH and the solution was diluted to 1 L.

The algal culture was centrifuged at 3000 rpm and an aliquot of the supernatant (100 µl) was diluted to 2500 µl with distilled water. A 1 ml aliquot of the phenol-nitroprusside-buffer reagent was added to the diluted supernatant and the resultant solution was mixed. A 1.5 ml aliquot of the hypochlorite reagent was then added to the solution and the test tube was mixed well by inversion. Incubation followed, at room temperature, for 45 minutes. Absorbance readings were taken at 635 nm (S2100 Diode Array

Spectrophotometer) against a reagent blank that was carried out throughout the procedure with fresh seawater. The absorbance readings were used to determine the concentration of ammonium-N in the medium with the aid of a previously constructed standard curve, using known concentrations of ammonium chloride as a standard (Figure 2.4).

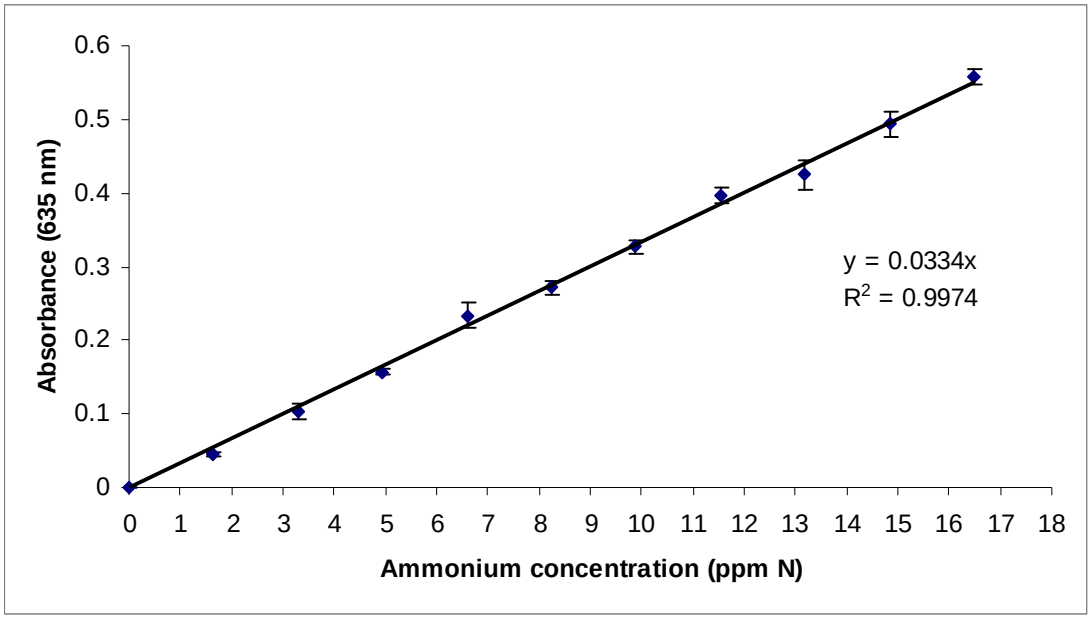

Figure 2.4: Standard curve depicting ammonium concentration with respect to absorbance readings at 635 nm. Error bars represent standard deviation (n = 3).

2.13.3 Phosphorous measurements

A method after Chen *et al*. (1956) was used to determine the levels of soluble reactive phosphorus (SRP) in the culture medium. This method required the preparation of fresh reagent C, which consists of 2 volumes distilled water, 1 volume 6 N sulphuric acid, 1 volume 2.5% ammonium molybdate and 1 volume 10% ascorbic acid, prior to each assay.

An aliquot of the microalgal culture was centrifuged at 3000 rpm for ten minutes. 1 ml of the supernatant and 1 ml reagent C was added to a 2 ml plastic Eppendorf tube and the Eppendorf tube was inverted several times to mix the solution. A blank was also made by using 1 ml fresh seawater, as opposed to the culture medium, in the step above. The

samples were then incubated at 37 °C for 90 minutes so that color development proceeded. After incubation absorbance readings were taken at 820 nm using a S2100 Diode Array Spectrophotometer (Biowave – Labotec). The resulting absorbance was used to determine the phosphorous content from a previously constructed standard curve, using known concentrations of sodium dihydrogen orthophosphate as a standard (Figure 2.5).

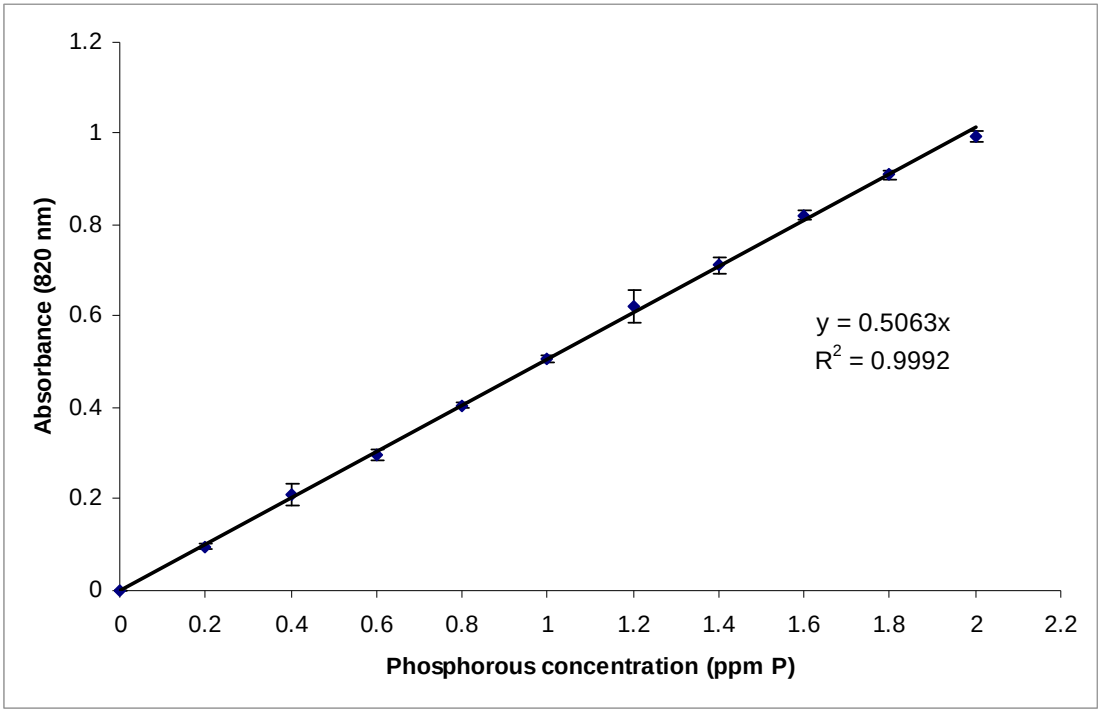

Figure 2.5: Standard curve depicting phosphorous concentration with respect to absorbance readings at 820 nm. Error bars represent standard deviation (n = 3).

2.14 Intracellular composition measurements

2.14.1 Carbohydrate content determination

Carbohydrates were extracted from the microalgal cells using a variation of the method adapted from Myklestad and Haug (1972). An aliquot of the culture (10 ml) was centrifuged at 5000 rpm for ten minutes. The supernatant was discarded and the pellet rinsed with 10 ml 0.5 M ammonium bicarbonate, to remove any salt residue (Zhu and

Lee, 1997). Re-centrifugation followed at 5000 rpm for 10 minutes and the supernatant was decanted. The algal pellet was then evaporated to dryness in an oven set at 50-55 ºC. Total carbohydrate was extracted by adding 80% sulphuric acid to the dried sample. This suspension was vortexed and incubated at 20 ºC for 20 hours.

The carbohydrate extract was then tested to determine the total carbohydrate content using the phenol-sulphuric acid method derived by Dubois *et al*. (1956). After incubation, the suspension was again vortexed thoroughly and a 100 µl aliquot was transferred to a well cleaned (washed and rinsed with distilled water) and dried test tube. A 500 µl aliquot of 4% phenol and 2.5 ml 96% sulphuric acid was added to the test tube and the resulting suspension was incubated at room temperature for 45 minutes. The absorbance of the solution was then read at 490 nm using a S2100 Diode Array Spectrophotometer (Biowave – Labotec). This absorbance value was used to determine the carbohydrate content from a previously constructed standard curve, using glucose as a standard (Figure 2.6).

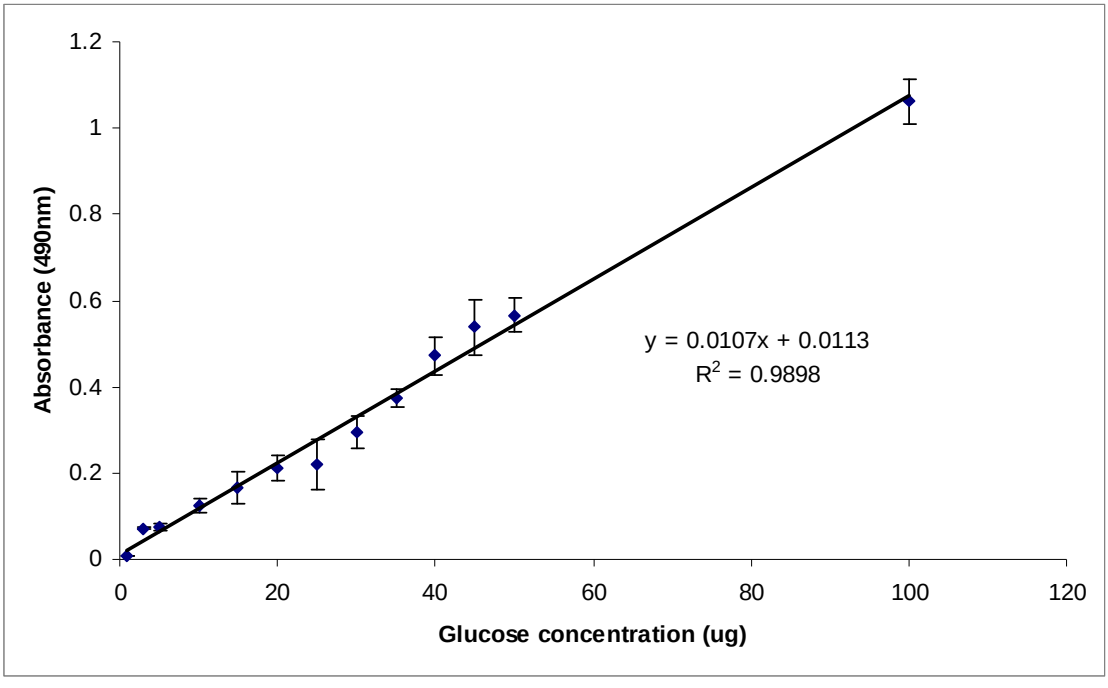

Figure 2.6: Standard curve depicting glucose concentration with respect to absorbance readings at 490 nm. Error bars represent standard deviation (n = 3).

2.14.2 Colorimetric determination of intracellular nitrogen

Digestion of the microalgal cells was conducted using a variation of the method described by Lindner and Harley (1942). A 10 ml aliquot of the algal culture was centrifuged at 5000 rpm for 10 minutes. The cell pellet was rinsed with 10 ml 0.5 M ammonium bicarbonate and re-centrifuged. The pellet was then dehydrated in an oven at a temperature of between 50 to 55 ºC. The dried pellet was weighed and transferred to a digestion tube. A 2 ml aliquot of 96% sulphuric acid was added to the digestion tube and the suspension was heated on a heating block (HI 839800 COD REACTOR – 2008 Hanna instruments) that was maintained at 105 ºC. The heating process was carried out in a fume hood until the dried cell pellet was partially disintegrated and dissolved (no cell clumps were observed). The solution was then cooled in an ice bath and 0.5 ml 30% hydrogen peroxide was added to the digestion tube. The resulting solution, in the digestion tube, was transferred to the 105 ºC heating block in the fume hood and was allowed to boil until it turned clear. The tube containing the digested cell solution was then allowed to cool in an ice bath and the solution was made up to 10 ml with distilled water.

A method developed by Dorich and Nelson (1983) was utilised for the nitrogen colorimetric assay. Reagents one and two were made up at least 24 hours prior to use. For reagent one, 17 g sodium salicylate, 12.5 g sodium citrate and 12.5 g sodium tartrate was dissolved in approximately 375 ml de-ionized water. Thereafter, 0.06 g sodium nitroprusside was added to the mixture. The solution was then made up to 500 ml with de-ionized water. For solution two, 15 g sodium hydroxide was dissolved in approximately 375 ml de-ionized water in a volumetric flask and was allowed to cool in an ice bath. A 5 ml aliquot of sodium hypochlorite was then added to the liquid in the volumetric flask and the solution was made up to 500 ml with de-ionized water.

A 20 µl aliquot of the digested cell solution, obtained using the procedure outlined above, was transferred to a sterilized (autoclaved for 30 minutes at 121 °C) and well dried test tube. Reagent one (1 ml) was added to the test tube and the resulting solution was mixed well and left to incubate at room temperature for 15 minutes. Reagent two (1 ml)

was then added to the test tube, the contents were mixed well and allowed to incubate at room temperature for an hour to ensure full color development. Absorbance readings were then taken at 660 nm using a S2100 Diode Array Spectrophotometer (Biowave – Labotec). The absorbance readings were used to determine the intracellular nitrogen content using a standard curve that was constructed using ammonium sulphate as a standard (Figure 2.7).

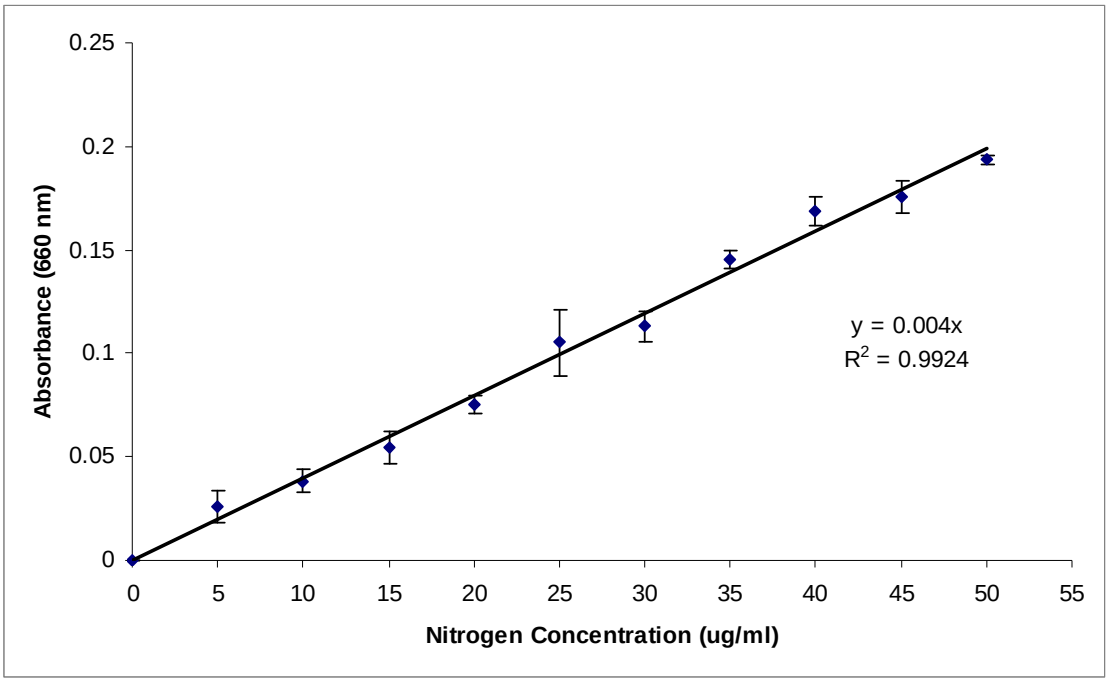

Figure 2.7: Standard curve depicting nitrogen concentration with respect to absorbance readings at 660 nm. Error bars represent standard deviation (n = 3).

2.14.3 Colorimetric determination of intracellular phosphorous

A similar procedure, as depicted in Section 2.14.2, was used for the digestion of microalgal cells for the phosphorous assay. The single variation was the volume of the digestion mixture (sulphuric acid and hydrogen peroxide mix). Where 2.5 ml was used for the nitrogen digestion procedure only 0.3 ml was used for this method. A 0.2 ml aliquot of 96% sulphuric acid was added to the dehydrated algal pellet and heated as stated in Section 2.14.2. Thereafter, 0.1 ml hydrogen peroxide was added to the solution in the digestion tube and reheated until the suspension turned clear. The resulting cell

digest solution was then made up to 10 ml with distilled water as in the previous nitrogen digestion process (Section 2.14.2).

A method developed by Dorich and Nelson (1983) was also utilised for the phosphorous colorimetric assay. This method required the use of molybdate reagent. For the preparation of molybdate reagent 4.3 g ammonium molybdate and 0.4 g antimony sodium tartrate were dissolved in 400 ml distilled water. A 54 ml aliquot of 96% sulphuric acid was then carefully added to the above solution. The resulting mixture was allowed to cool in an ice bath and thereafter made up to 1000 ml with distilled water.

A 0.5 ml aliquot of the cell digest, obtained using the protocol outlined above, was transferred to a sterilized (autoclaved for 30 minutes at 121 °C) and well dried test tube. 2 ml 1% ascorbic acid and 1.5 ml molybdate reagent was added to the test tube and the contents were mixed well using a vortex. An incubation period followed for an hour at room temperature for full color development. Absorbances of the resulting solution were then read at 820 nm using a S2100 Diode Array Spectrophotometer (Biowave – Labotec). The phosphorous content was determined with the aid of the absorbance readings and a previously constructed standard curve using potassium dihydrogen orthophosphate as a standard (Figure 2.8).

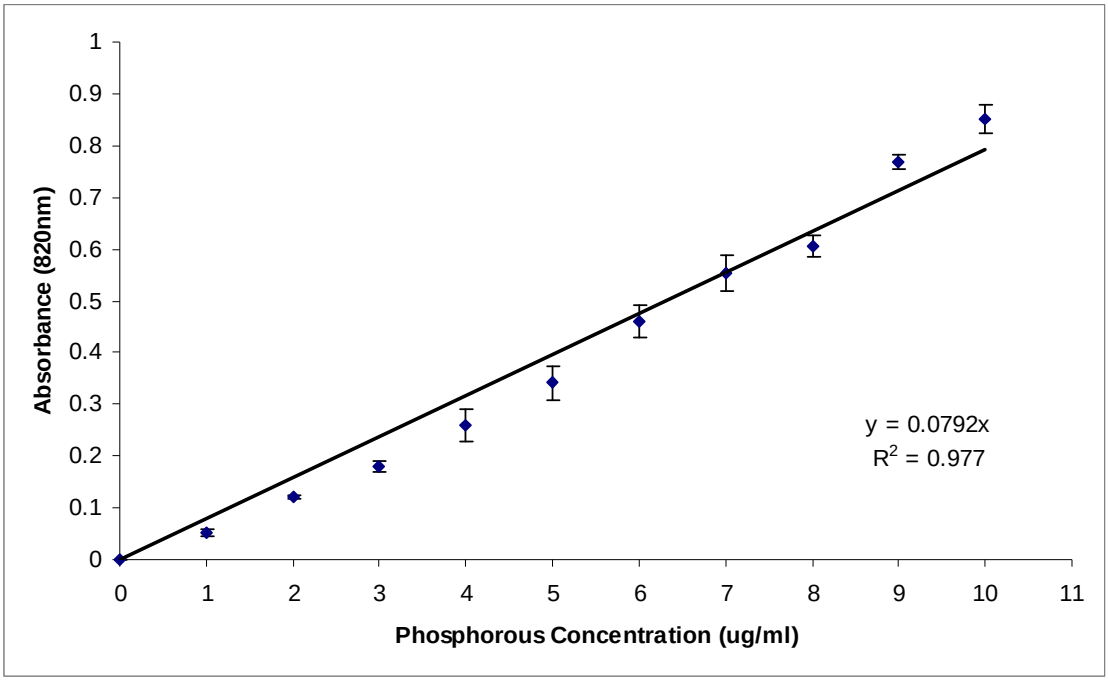

Figure 2.8: Standard curve depicting phosphorous concentration with respect to absorbance readings at 820 nm. Error bars represent standard deviation (n = 3).

2.15 Determination of chlorophyll content and carotenoid to chlorophyll ratio

An adaptation of the method described by Hansmann (1973) was used for pigment extraction. The microalgal culture (10 ml) was centrifuged at 5000 rpm for five minutes and the supernatant was decanted and replaced with 5 ml, 100% acetone. The small aliquot (approximately 0.5 ml) of culture medium that remains in the centrifuge tube, after decanting, results in a cell suspension with approximately 90% (v/v) acetone. The suspension was mixed vigorously (by shaking the centrifuge tube) for two minutes to resuspend the pellet and thereafter vortexed, to lyse all the cells, for ten minutes. The suspension, now consisting of white cell debris and the pigments in solution, was incubated at 4 °C, in the dark, for 24 hours. After incubation the suspension was centrifuged at 5000 rpm for 10 minutes. 1 ml of the supernatant was acidified with 20 µl 1 N HCl (producing a molarity of 0.02 N) mixed (by shaking) and left to incubate at room temperature for 90 seconds. The optical density of the unacidified and acidified supernatant was then read at 663 nm and 750nm. The optical density of the unacidified sample was further read at 650 nm and 480nm. The following equations were used to

determine the chlorophyll concentrations (Golterman, 1969) and the carotenoid to chlorophyll ratio (Heath *et al*., 1990):

$$^{U}E_{663(1cm)} = \frac{^{U}E_{663} - {}^{U}E_{750}}{Lightpath\ (cm)}$$

$$^{A}E_{663(1cm)} = \frac{^{A}E_{663} - {}^{A}E_{750}}{Lightpath\ (cm)}$$

Where $^{U}E_{663(1cm)}$ and $^{A}E_{663(1cm)}$ refer to the unacidified and acidified turbidity corrected extinctions respectively. $^{U}E_{663}$, $^{U}E_{750}$, $^{A}E_{663}$ and $^{A}E_{750}$ refer to the optical density at the specified absorbance indicated in the subscript of the unacidified and acidified samples (as indicated by U and A in the superscript, respectively). Lightpath refers to the width of the quartz cuvette in cms.

$$E_{chl(1cm)} = 2.43(^{U}E_{663(1cm)} - {}^{A}E_{663(1cm)})$$

Where $E_{chl(1cm)}$ refers to the extinction due to chlorophyll.

$$P_{chl}\ (\mu g/L) = E_{chl(1cm)} \times (1000/K_{chl}) \times (vol.\ extract(ml)/vol.\ culture(L))$$

Where P_{chl} refers to the quantity of chlorophyll measured in µg/L. K_{chl} refers to the extinction coefficient for chlorophyll which is 89, vol. extract refers to the volume of acetone used to extract the pigments and vol. culture refers to the volume of the culture centrifuged initially.

$$Car/Ch_a = OD_{480} / OD_{665}$$

Where Car/Ch_a refers to the carotenoid to chlorophyll a ratio and OD refers to the optical density reading at the specified absorbance indicated in the subscript.

Quartz cuvettes with a path length of 1 cm were used to obtain all the OD readings and if the readings exceeded 0.8 units the sample was diluted with acetone. The spectrophotometer was blanked with 90% acetone.

2.16 Light intensity measurements

A light meter (LI-250A Light meter – LI-COR® Biosciences) was used to determine the light intensity. Approximately ten readings were taken at various points around the bioreactor and the final light intensity was the average of these readings.

2.17 Statistical analysis

The software SPSS 20 (Statistical Program for Social Sciences 20) was used to perform statistical analyses. Differences amongst the various treatments were evaluated using one-way analysis of variance (ANOVA). Tukey's multiple comparison, post-hoc tests were conducted to compare the different means if the ANOVA effects were significant ($\alpha = 0.05$).

CHAPTER THREE

Screening & Selection of a Marine Microalgal Species to be used as a Model Organism for Biodiesel Production

3.1 INTRODUCTION

Globally, more than 100 000 microalgal species have been characterized and identified (Um and Kim, 2009). This vast resource makes the selection of a microalgal species for biodiesel production rather complicated (Griffiths and Harrison, 2009). At present the search for the optimal species for biodiesel production is keenly contested. Such a species should produce vast amounts of lipid and divide swiftly (Um and Kim, 2009). A species that easily can be harvested is an often-overlooked characteristic that is of great significance when selecting a species for biodiesel production. Ease of harvesting would greatly reduce operating costs which would prove to be beneficial in the downstream processing of the algae (Borowitzka, 1999; Griffiths and Harrison, 2009).

Numerous studies have shown that lipid yield and biomass productivity work antagonistically (Li *et al*., 2008a; Rodolfi *et al*., 2009; Um and Kim, 2009). Lipid accumulates in response to nutrient stress and cell division occurs rapidly when nutrient levels are optimal. The fact that lipid production takes place mainly in the non-dividing stationary phase poses a problem for the culture process for biodiesel production. A beneficial parameter used to select a species is lipid productivity. Lipid productivity is a function of both lipid yield and biomass productivity (Griffiths and Harrison, 2009). A microalgal species with an elevated lipid productivity was thus selected in this study as the model organism for biodiesel production.

In this study prymnesiophytes were chosen to be screened due to their ability to produce triacylglycerides as a storage lipid upon exposure to stressful conditions (Matsumoto, 2010). Furthermore, prymnesiophytes are marine and marine rather than freshwater microalgae were targeted for screening due to the abundant availability of sea water and a decrease in the likelihood of contamination when marine systems are used.

3.2 MATERIALS & METHODS

3.2.1 Algal selection

Three marine microalgal species, namely *Isochrysis* sp., *Pleurochrysis* sp. and *Platychrysis* sp. were selected for the screening process. The species selected are golden brown algae that are members of the Prymnesiales (Seoane *et al.*, 2009). The algal cultures were obtained from the algae collection in the School of Animal, Plant and Environmental Sciences at the University of the Witwatersrand (South Africa). Selection of these algal species for screening was based on the ability of these species to produce large amounts of lipids. This was clearly evident due to numerous lipid bodies visible in all three of the algal species when they were viewed using a Zeiss Axiophot microscope at 400 times magnification with Nomarski optics.

Each of the above-mentioned algal species were isolated as single cells to obtain unialgal/mono-species cultures. These cultures were maintained in *f/2* medium for the duration of the experiment (Guillard and Ryther, 1962; Appendix). *F/2* medium was prepared as outlined in Section 2.1 and all algal species were sub-cultured every forth-night to ensure that a healthy inoculum was available when required (Section 2.2).

3.2.2 Experimental setup

Experiments were conducted in 1 L modified Schott® bottles (Section 2.3). 800 ml sterile *f/2* medium was inoculated with approximately $3x10^6$ cells/ml, healthy (seven day old) microalgal cells (*Isochrysis* sp., *Pleurochrysis* sp. and *Platychrysis* sp.). These cultures were subjected to a constant illumination of 110 photons.µmol.m^{-2}.s^{-1} at approximately 25 °C and were aerated with filtered air (Whatman uniflo 0.2 µm filter). Cultures used for the construction of the growth curves were monitored every alternate day for a period of 20 days. All cultures were run in triplicate.

3.2.3 Analytical methods

The cell concentration and lipid content were determined as outlined in Sections 2.5 and 2.7, respectively. The lipid productivity and rate of growth were measured at various

time intervals (Section 2.10 and 2.11 respectively). Cells were viewed using a Zeiss Axiophot microscope at 400 times magnification with Nomarski optics to observe Nile red stained lipid bodies and cell clumps. The model organism was selected based on the growth rate, lipid yield, lipid productivity and ability to flocculate.

3.3 RESULTS & DISCUSSION

Distinct membrane-enclosed putative lipid storage bodies/droplets were observed in *Isochrysis* sp., *Pleurochrysis* sp. and *Platychrysis* sp. These droplets were hypothesized to be lipid in nature. To verify this, cells were stained with Nile red and observed using different wavelengths of light. Nile red is a selective fluorescent dye that was initially derived from Nile blue upon boiling in sulphuric acid. Studies conducted by Greenspan, Mayer and Fowler (1985) demonstrated the superior nature of Nile red in the detection of intracellular lipid droplets. They further described the dye as being an ideal lysochrome thus implying that the dye is strongly colored, highly soluble in the substance that it is intended to show by staining (lipids) and does not dissolve this substance.

Upon excitation at 450-500 nm Nile red stained lipid in the cells exhibit yellow-gold/red fluorescence (Greenspan *et al*., 1985). This characteristic is clearly evident in Figure 3.1. Similar fluorescence patterns were observed when analyzing all screened isolates. This implied that the intracellular droplets observed were indeed lipid in nature. Furthermore it may be deduced that the lipid droplets consist of neutral lipids since neutral lipids (storage lipids) exhibit a yellow-gold fluorescence whilst polar lipids (membrane lipids) exhibit red fluorescence (Greenspan *et al*., 1985).

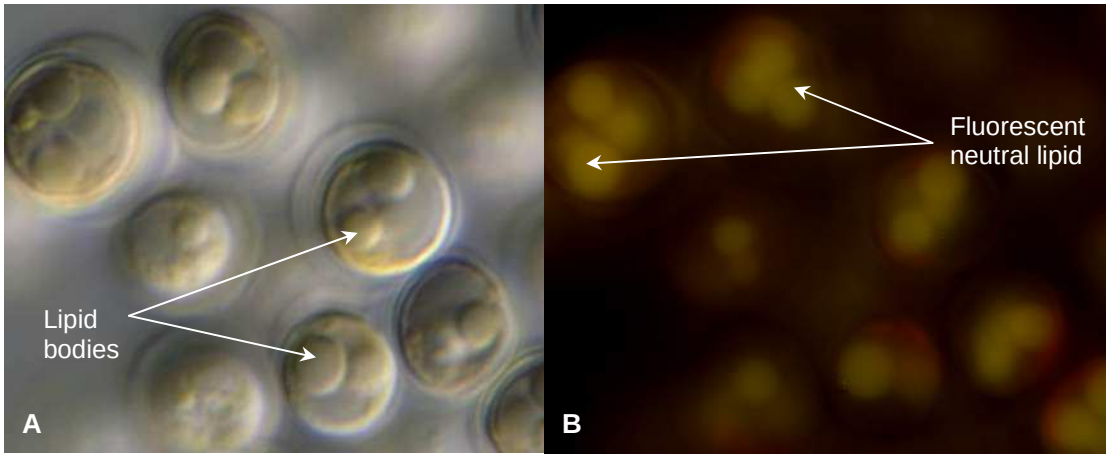

Figure 3.1 (A): Nile red stained *Platychrysis* sp. cells viewed under a light microscope and **(B):** when the same cells were exposed to a different wavelength of light (450-500 nm).

A method to quantify lipid in the cells was necessary to accurately select the ideal species to be used in the subsequent experiments. A flow cytometric method of lipid quantification was selected. The method was adapted from da Silva *et al*. (2008) where the relationship between lipid content and Nile red fluorescence was analysed in *Scenedesmus obliquus* and *Neochloris oleoabundans.* This method is advantageous in that it allows for the rapid, *in situ*, accurate, routine determination of lipid content in the cells. Standard curves were successfully constructed for all species screened (R^2 = 0.9978; 0.9503 and 0.9530 for *Isochrysis* sp., *Pleurochrysis* sp. and *Platychrysis* sp. respectively) and the flow cytometric method was henceforth used for all lipid measurements.

Platychrysis sp. was disregarded in the next step of the screening process due to its tendency to adhere to the surface of culture vessels observed when the cells were grown for the construction of lipid standard curves. This adherence tendency is disadvantageous in large scale bioreactors because they constantly would need to be cleaned. In addition, it also results in much of the biomass, which is most probably lipid rich, being lost since stressed cells are benthic. Such cells could potentially be suspended by decreasing the pH, but they would need to be re-flocculated afterwards (for lipid extraction) and both these steps would incur significant cost implications because of all the chemicals required. The cells that adhere to the culture vessels also reduce light penetration,

resulting in energy losses. Hence, the species was discounted at the outset as a potential organism for biodiesel production and was not pursued further. Hence, only *Isochrysis* sp. and *Pleurochrysis* sp. growth curves were constructed.

As evident in the *Isochrysis* sp. growth curve (Figure 3.2) the lipid yield was at an initial elevated level after which it decreased and became somewhat constant. It then increased again as the culture entered the stationary phase of cell growth. The initial elevated lipid yield may be due to the lipid present in the cells of the inoculum, which was 7 days old, and could have been nutrient-limited. As cell numbers increased the lipid yield decreased and became constant, as long as adequate nutrient supply, light and carbon dioxide levels were available. However, during the stationary phase an increase in lipid production was observed. This may be in response to the depletion of nutrients or the reduction in the light received by individual algal cells due to cell-cell shading when cultures become very dense. Algal cells produce lipid as an energy source to be used when normal growth conditions return (Rodolfi *et al*., 2009).

Cell concentrations decreased considerably after day 13 (Figure 3.2). This was as a result of the clumping of algal cells at the base of the culture vessel. Actual algae rafts formed which ranged from 1 to 3 cm. The cells that were counted were those that remained immersed in the culture medium. Hence, these counts merely indicate a decrease in single, free cells in culture and an increase in algae floccules. These algae floccules would be desirable in a bioreactor setup since it would aid in the settling and harvesting of the cellular material. Furthermore, this flocculation process was only evident during the lipid-rich, stationary phase i.e. the optimal instant for culture harvesting. Unlike in *Platychrysis* sp., the cells did not stick to the culture vessel (only to each other), which is also desirable since it does not impede light penetrating through the culture vessel and to the cells.

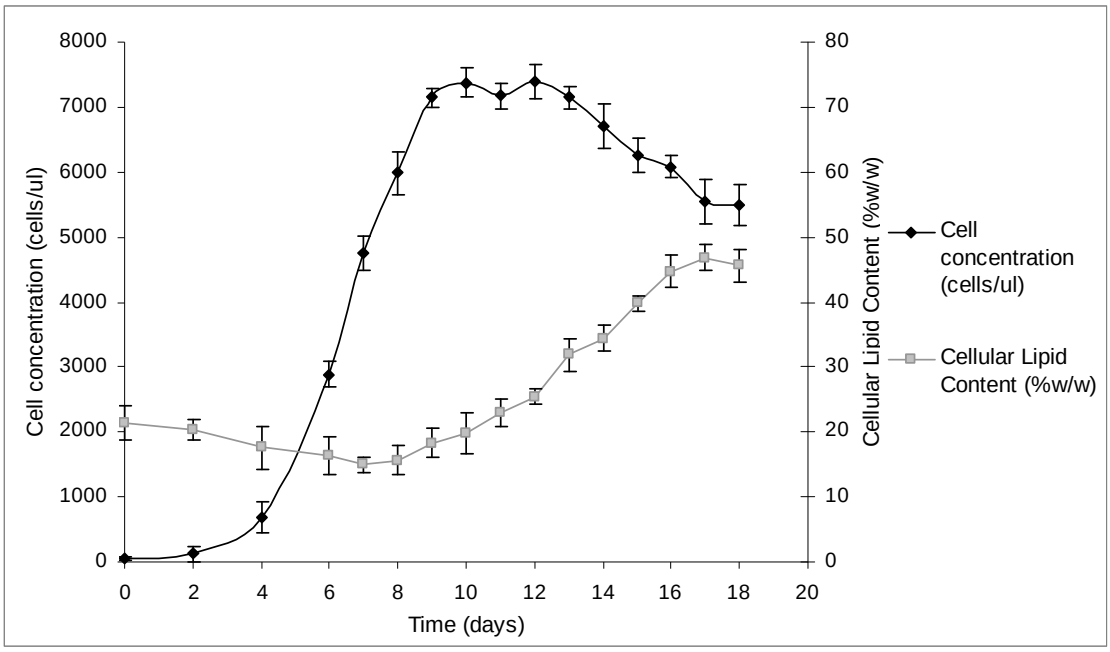

Figure 3.2: *Isochrysis* sp. growth curve showing the cellular concentration and lipid content observed over 18 days. Error bars represent standard deviation (n=3).

Multiple, distinct lipid bodies were evident in stationary-phase *Isochrysis* sp. cells (Figure 3.3 A) which corroborates the lipid data in Figure 3.2. These lipid bodies were as large as 1 µm in diameter ($1/5^{th}$ the size of the actual algal cell). *Isochrysis* sp. cells are relatively small (5 µm), in comparison to some other microalgal species, which would pose a disadvantage in terms of harvesting since small cells escape through filter pores. However, when the cells clump (Figure 3.3 B) their settling properties improve, due to the larger size and mass density of the clumps, which is a desirable property.

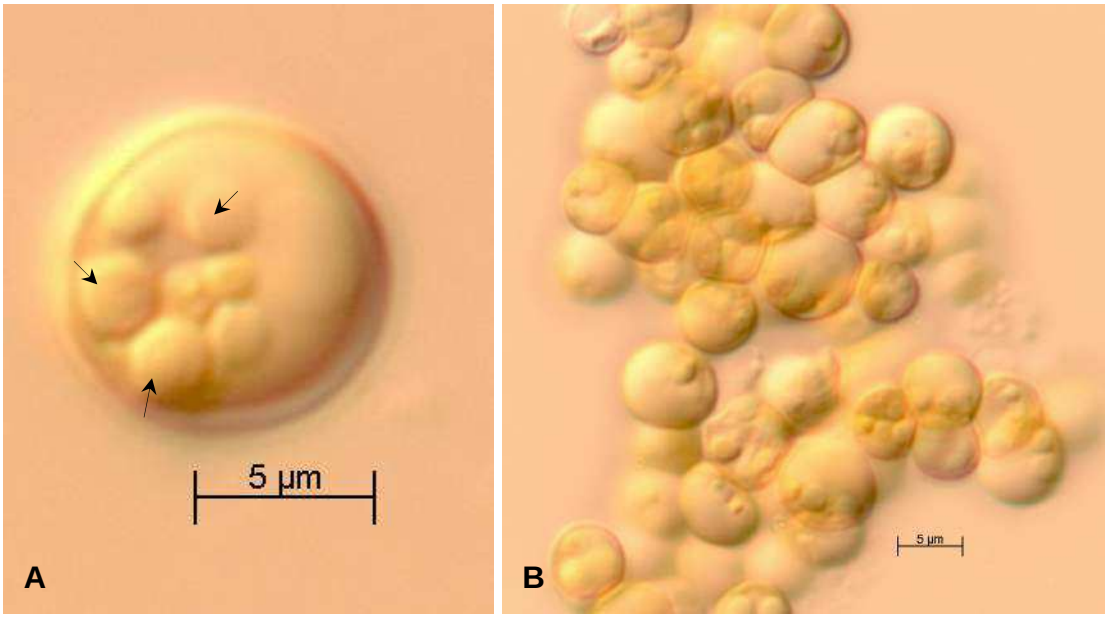

Figure 3.3 (A): Light micrographs of a single *Isochrysis* sp. cell containing multiple lipid bodies (arrows indicate lipid bodies) and **(B):** algal floccules (observed on day 18).

Pleurochrysis sp. cultures demonstrated a more gradual exponential phase in comparison to *Isochrysis* sp. (cf. Figures 3.2 and 3.4). Both the cellular and lipid yield were much lower than that observed in *Isochrysis* sp. (cf. Figures 3.2 and 3.4). Again, a gradual increase in lipid production was only observed during the stationary phase when nutrients and light were possibly limiting (Figure 3.4).

The photomicrographs of *Pleurochrysis* sp. show numerous minute lipid bodies, relative to the size of the cell, being produced on day 18 (Figure 3.5). These lipid bodies are smaller and more frequent when compared to those observed in *Isochrysis* sp. (cf. Figures 3.3 and 3.5). *Pleurochrysis* sp. cells are much larger in size than cells of *Isochrysis* sp. (*Pleurochrysis* sp. cell sizes are approximately 20 µm in length and 16 µm wide and *Isochrysis* sp. cells are approximately 5 µm in length and 4 µm wide). This characteristic would make *Pleurochrysis* sp. more suitable for biodiesel production, since larger cells are desirable in the final stage of settling and harvesting. The numerous advantages of using *Isochrysis* sp. however outweighs the properties associated with *Pleurochrysis* sp.

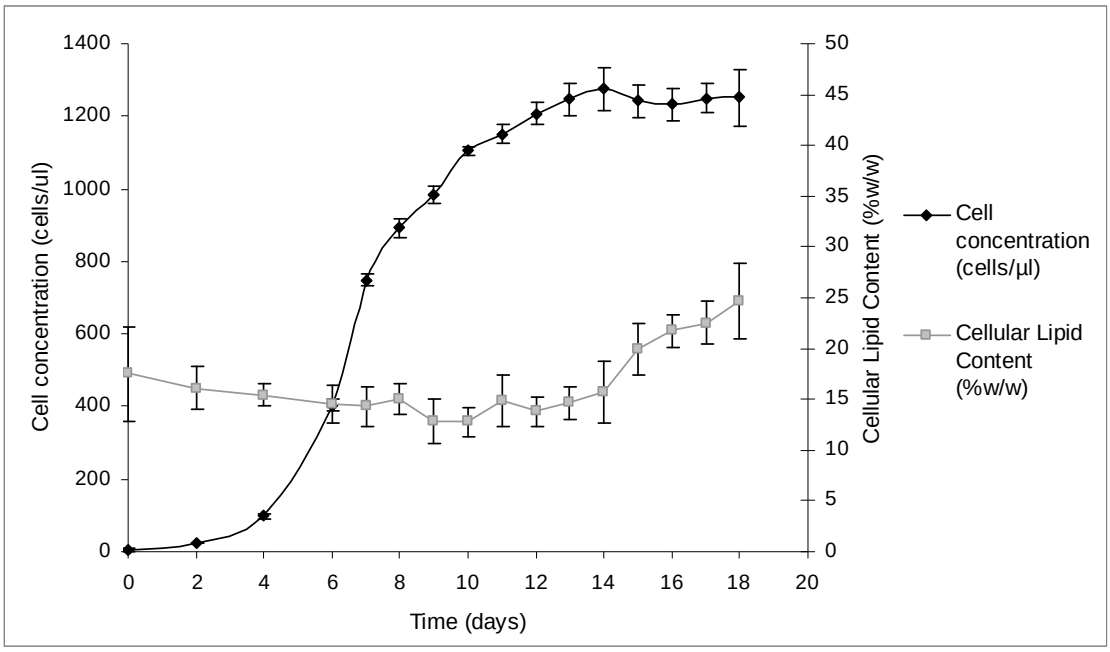

Figure 3.4: *Pleurochrysis* sp. growth curve showing the cellular concentration and lipid content observed over 18 days. Error bars represent standard deviation (n=3).

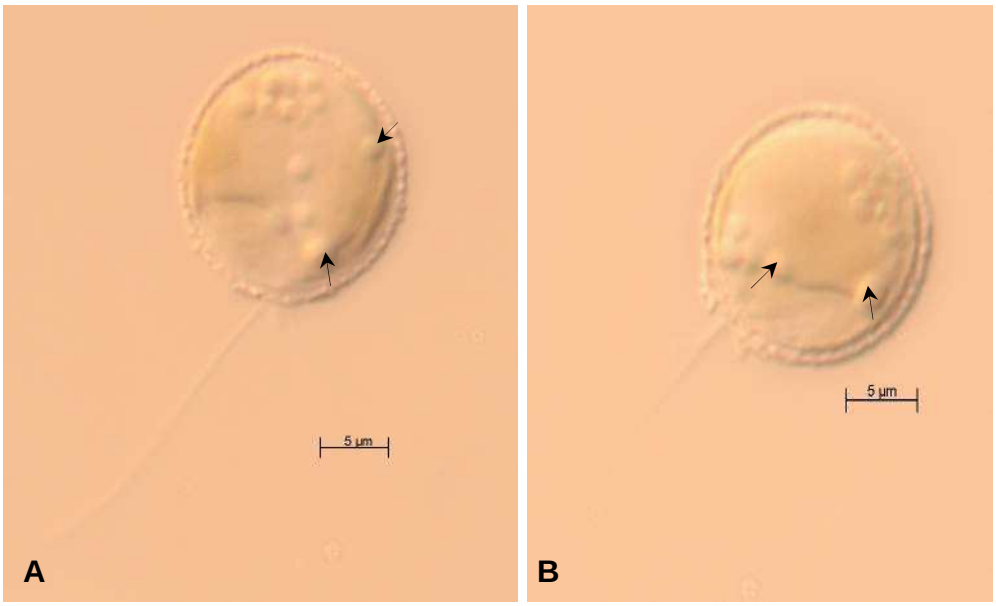

Figure 3.5 (A–B): Light micrographs of single *Pleurochrysis* sp. cells containing multiple small lipid bodies (lipid bodies indicated by arrows; observed on day 18).

A rapidly dividing and elevated lipid-bearing microalgal species is required for biodiesel production. Furthermore, a species that has an elevated lipid productivity is also sought.

Isochrysis sp. has a much higher growth rate, maximal lipid yield and lipid productivity than *Pleurochrysis* sp. (Table 2.1).

Table 2.1: Comparison of *Isochrysis* sp. and *Pleurochrysis* sp. growth and lipid parameters.

Species	**Growth Rate (cells/µl/day)**	**Divisions per day (div/day)**	**Generation time (days)**	**Maximal Lipid Yield (% w/w)**	**Lipid Productivity (mg/L/d)**
***Isochrysis* sp.**	0.332	0.479	2.088	≈ 45	≈ 29
***Pleurochrysis* sp.**	0.220	0.317	3.155	≈ 24	≈ 15

Hence, because of its clumping propensity, high lipid yield per cell and elevated volumetric lipid productivity, *Isochrysis* sp. was selected as the model organism to be used in all subsequent lipid production experiments.

3.4 CONCLUSION

Isochrysis sp. was selected as the model organism. Selection was based on the elevated lipid yield, growth rate and lipid productivity in comparison to *Pleurochrysis* sp. The ability of the *Isochrysis* sp. to form floccules is also advantageous in that it would decrease harvesting costs when used in industry. This study also confirmed that cell division was limited by nutrient and/or light supply and lipid accumulation was initiated upon approaching the stationary phase.

CHAPTER FOUR

Morphological & Molecular Identification of the Model Organism

4.1 INTRODUCTION

Light microscopy observations have been routinely used for the identification of algal species. However this method of microalgal identification may be inaccurate, unreliable and confusing since a very limited range of morphological attributes can be observed at this level of magnification. This makes any comparison between the unknown organism and other similar known species difficult (Nozaki *et al*., 1997). Hence, focus has been directed on using molecular methods and morphological observations at the electron microscope level of magnification for establishing algal species identification.

Morphological methods of microalgal identification are based on a comparison of the intracellular and extracellular features of the microalga of interest with other known species. Some external features of relevance include the presence of a haptonema, the length, number and the covering of the flagella and the type, size and orientation of scales if present. Intracellular features of interest when identifying species are mainly related to the internal composition, organization and structure of the organelles (Barsanti and Gualtieri, 2006).

The molecular identification of any species is based on the rationale that there is a correlation between similarities in the DNA structure and the interrelatedness of organisms. This method forms an alternative to identification based on visual observations since the genes encoding these observations may be identified and the extent of homology between these genes and that of other known species can be easily compared with the aid of the various phylogenetic programs that are currently available (Barsanti and Gualtieri, 2006).

Microalgae have been categorized into phyla primarily with respect to their basic cellular structure, pigmentation and life cycles (Khan *et al*., 2009). Nearly all members of the phylum Haptophyceae possess an appendage, located between two flagella, called the haptonema (Dodge, 1973). This appendage is ultrastructurally unlike the flagella in terms of the number and arrangement of the microtubules (Barsanti and Gualtieri, 2006).

The function of this organelle is at present uncertain however it may aid in attachment and capturing of microbes in heterotrophic haptophytes. Many members of this phylum are covered with organic (cellulosic) or calcified scales (Dodge, 1973). Haptophytes may be unicellular, coccoid, motile and may even form colonies (Green and Leadbeater, 1994). A distinguishing intracellular characteristic of this phylum is the continuous endoplasmic reticulum encapsulating the chloroplast and nucleus (South and Whittick, 1987; Barsanti and Gualtieri, 2006).

The haptophyte algae are generally considered as a single class, the Prymnesiophyceae Hibberd (= Haptophyceae) (Jordan and Green, 1994; Edvardsen *et al.*, 2000). The class may be further divided into four orders, namely the Coccolithales, consisting of majority of the coccolithophorids which bear calcified scales (coccoliths), the Isochrysidales, which possess a rudimentary haptonema or are completely devoid of the appendage, the Pavlovales, that possess haptonemas and stigmata (eyespots), and the Prymnesiales, that usually possess well-developed haptonemas (Tomas, 1997; Edvardsen *et al.*, 2000). The primary use of light microscopy, for the identification of haptophyte algae beyond the genus level, is often insufficient since these species are generally very small and are commonly distinguished based on scale morphology which require high magnifications (Tomas, 1997).

Both morphological (light and electron microscopy) and molecular characters were analyzed to ensure the unambiguous identification of the model organism used in the study.

4.2 MATERIALS & METHODS

4.2.1 Morphological identification of model organism

A healthy, exponential phase culture of the model organism was embedded in resin and sectioned (see Section 2.12.1). The sections were then viewed using a transmission electron microscope (FEI Spirit), at an accelerating voltage of 120 kV, to observe the morphological characteristics of the microalgal species. A whole mount of exponential

phase cells was also prepared (Section 2.12.2) and light microscopy images taken (Zeiss Axiophot microscope at 400 times magnification with Nomarski optics) to observe the structure of the flagella.

4.2.2 Molecular identification of model organism

4.2.2.1 Algal genomic DNA extraction

The algal genomic DNA was isolated from a seven day old monoculture of the model organism using the cetyltrimethylammonium bromide (CTAB) genomic DNA isolation method adapted from Murray and Thompson (1980; Appendix).

4.2.2.2 PCR amplification of the 18S rDNA region using universal primers

The small subunit nuclear ribosomal encoding region was amplified using two universal eukaryotic oligonucleotide primers (Table 4.1) synthesized by Inqaba Biotechnical Industries (PTY) Ltd.

Table 4.1: The oligonucleotide primers used for the amplification of the SSU nuclear ribosomal encoding region (18S rRNA)

Oligo Primer name	Sequence	T_m(°C)
1F forward primer	5'-AACCTGGTTGATCCTGCCAGT -3'	62.57
1528R reverse primer	5'-TTGATCCTTCTGCAGGTTCACCTAC -3'	64.58

The following constituents were added to PCR tubes (Whitehead Scientific 0.2 ml thin wall PCR® tube with domed cap) for the amplification of the sequence of interest:
25 µl 2X PCR Master Mix (Fermentas), 1 µl of each primer (sense and anti-sense) (Table 4.1), varying volumes (1, 2 & 4 µl) of the DNA template, obtained as stated in Section 4.2.2.1, and nuclease free water to make up the reaction volume to 50 µl. A control tube containing all the ingredients above with the exception of the DNA template was also included. These tubes were vortexed briefly to mix the suspension and thereafter centrifuged at 10000 rpm for 1 minute to settle the contents.

DNA was amplified in a Gene Amp® PCR express 2700 thermocycler (Applied Biosystems). The cyclic conditions were as follows: 3 minutes at 94 ºC, 35 cycles of denaturation at 94 ºC for 1 minute, rennealing at 50 ºC for 1 minute and extension at 72 ºC for 2.5 minutes, followed by 10 minute incubation at 72 ºC (Seoane *et al*., 2009).

4.2.2.3 Agarose gel electrophoresis of algal PCR products

A DNA ladder (5 µl 100 bp plus) was loaded in the first well followed by 5 µl of the PCR products, which were mixed with 1.5 µl 6X Orange Loading Dye Solution, in the subsequent wells of a 1% agarose gel (Appendix). Electrophoresis of these mixtures followed at 80 V in electrophoresis buffer (Appendix). The gel was than viewed with an ultraviolet trans-illuminator (BioRad Gel Doc System) and pictures were taken. Upon clear visualization of the PCR product on the gel, after electrophoresis, the sample was sent to the Central DNA Sequencing Facility in the University of Stellenbosch (South Africa), for sequencing. The resulting sequence has been deposited in GenBank (Accession number: JX868515).

4.2.2.4 Phylogenetic analysis

The sequence obtained from Stellenbosch was initially edited using Chromas (Bioinformatics Computer Laboratory, University of the Witwatersrand) and sequences that closely resembled the isolates sequence were acquired using BLAST. These sequences (Table 4.2) were used as references to establish the consensus sequences for the isolate sequence obtained.

Table 4.2: A list of the species and corresponding GenBank accession numbers for the SSU nuclear ribosomal encoding sequences used in the phylogenetic analyses. The sequence in bold is from this study.

Algal Species	**GenBank Accession Number**
Calcidiscus leptoporus (Murray and Blackman) Leblich and Tappan	AJ544116
Calcidiscus quadriperforatus (Kamptner) Quinn and Geisen	AJ544115
Calyptrosphaera sp.	AB183608
Coccolithus pelagicus (Wallich) Schiller	AJ246261

Cruciplaccolithus neohelis (McIntyre and Bé) Reinhardt	AJ246262
Emiliania huxleyi (Lohmann) Hay and Mohler	M87327
Emiliania huxleyi (Lohmann) Hay and Mohler	L04957
Gephyrocapsa oceanica Kamptner	AJ246276
Helladosphaera sp.	AB183607
Isochrysis galbana Parke emend. Green and Pienaar (Strain UIO 102)	AJ246266
Isochrysis sp. CCAP 927/14	DQ079859
Isochrysis galbana strain DB	GQ118682
Isochrysis sp. zhangjiangensi	DQ075203
Isochrysis sp. 3011	DQ071572
Isochrysis sp. 0318	EU924188
Isochrysis sp. 8701	DQ071573
***Isochrysis* sp. strain U4**	**JX8685151.1**
Pavlova gyrans Butecher emend. Green and Manton	U40922
Pleurochrysis carterae (Braarud and Fagerland) Christensen	AJ246263
Pleurochrysis elongata (Droop) Jordans	AJ246264
Pleurochrysis sp.	AJ246265
Reticulosphaera socialis	X90992
Umbilicosphaera foliosa (Kamptner) Geisen	AJ544119
Coccoid haptophyte	U40924

The program MEGA5 v5.05 (Tamura *et al.*, 2011) was used for multiple sequence alignment using Clustal W. A heuristic search procedure was used with 1000 replicates and gaps were treated as missing data. All characters were treated as equally weighted. Maximum likelihood, maximum parsimony and neighbor-joining phylogenetic trees were constructed. *Pavlova gyrans* was used as an outgroup to resolve the relationships among other species.

4.3 RESULTS & DISCUSSION

4.3.1 Morphological identification

Light microscopy observations of a healthy microalgal culture showed solitary, golden-brown, motile cells that were anteriorly truncate and posteriorly rounded (somewhat oval). The cells were 5 to 6 µm in length and approximately 4 µm in breadth and

possessed two equal length flagella (Figure 4.1 A & B). The presence of flagella implies that the isolate could belong to the class Cryptophyceae, Prasinophyceae, Dinophyceae or Prymnesiophyceae (Tomas, 1997). The absence of a gullet/furrow and ejectosomes verifies that the isolate is not a member of the cryptophyceae (Tomas, 1997). The shape of algal cells belonging to the class Prasinophyceae (quadrangular) is not consistent with the isolate shape implying that the isolate does not belong to this class. The isolate also does not belong to the Dinophyceae class since this class consists of algal cells that possess a traverse flagella which was not observed in the isolate. The light microscopy observations of the isolate are however consistant with descriptions of cells belonging to the Prymnesiophyceae class (Tomas, 1997). The isolate was obtained from Marina Beach (inshore waters), South Coast, Kwa-Zulu Natal. The sampling region is influenced by the Agulhas current and has been shown to be dominated by haptophytes amongst other species (Schluter *et al*., 2011). Hence, the isolate could indeed be a haptophyte.

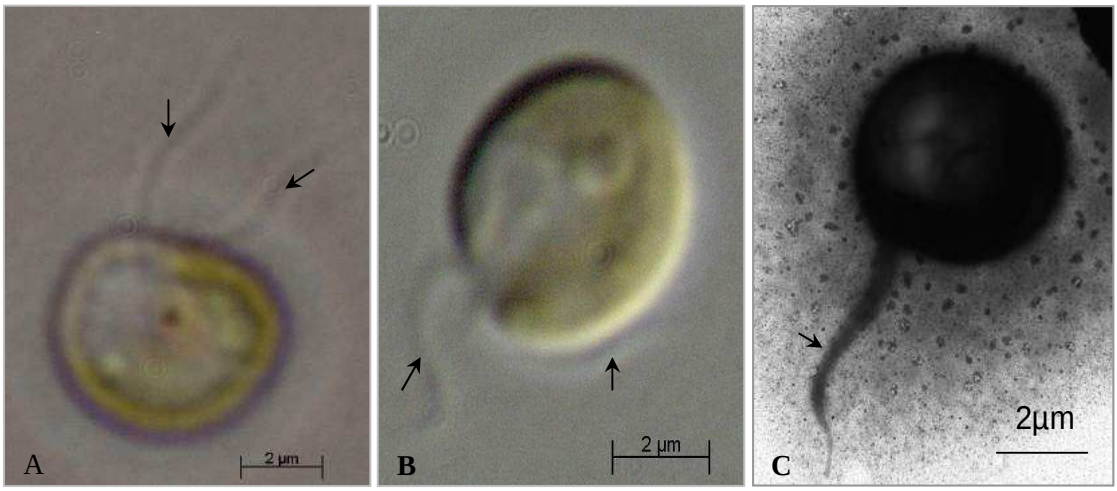

Figure 4.1 (A-B): Light microscopy images of isolate cells showing a pair of equal length flagella and **(C):** shadow-cast cell with single flagella (the other was shed). Arrows indicate flagella.

Ultrastructural observations, using electron microscopy, showed cells containing two chloroplasts (Figure 4.2 A). Each chloroplast contains a fusiform pyrenoid that is traversed by a pair of thylakoids (Figure 4.2 A and D). No girdle lamella was observed

in the plastids (Figure 4.2 A – D) and a continuous chloroplast outer membrane with the outer nuclear envelope was noted (Figure 4.2 D). Peripheral endoplasmic reticulum (ER) is situated beneath the plasmalemma (Figure 4.2 C and D) and a fan-like golgi apparatus, presumably were scales are produced, was observed (Figure 4.2 A and C). Multiple layers of scales surrounded the cells (Figure 4.2 A – D). All these features are consistent with members of the Haptophyta division (Figure 4.3; Green and Leadbeater, 1994; Jordan and Chamberlain, 1997; Edvardsen *et al*., 2000) implying that the isolate is indeed a haptophyte alga.

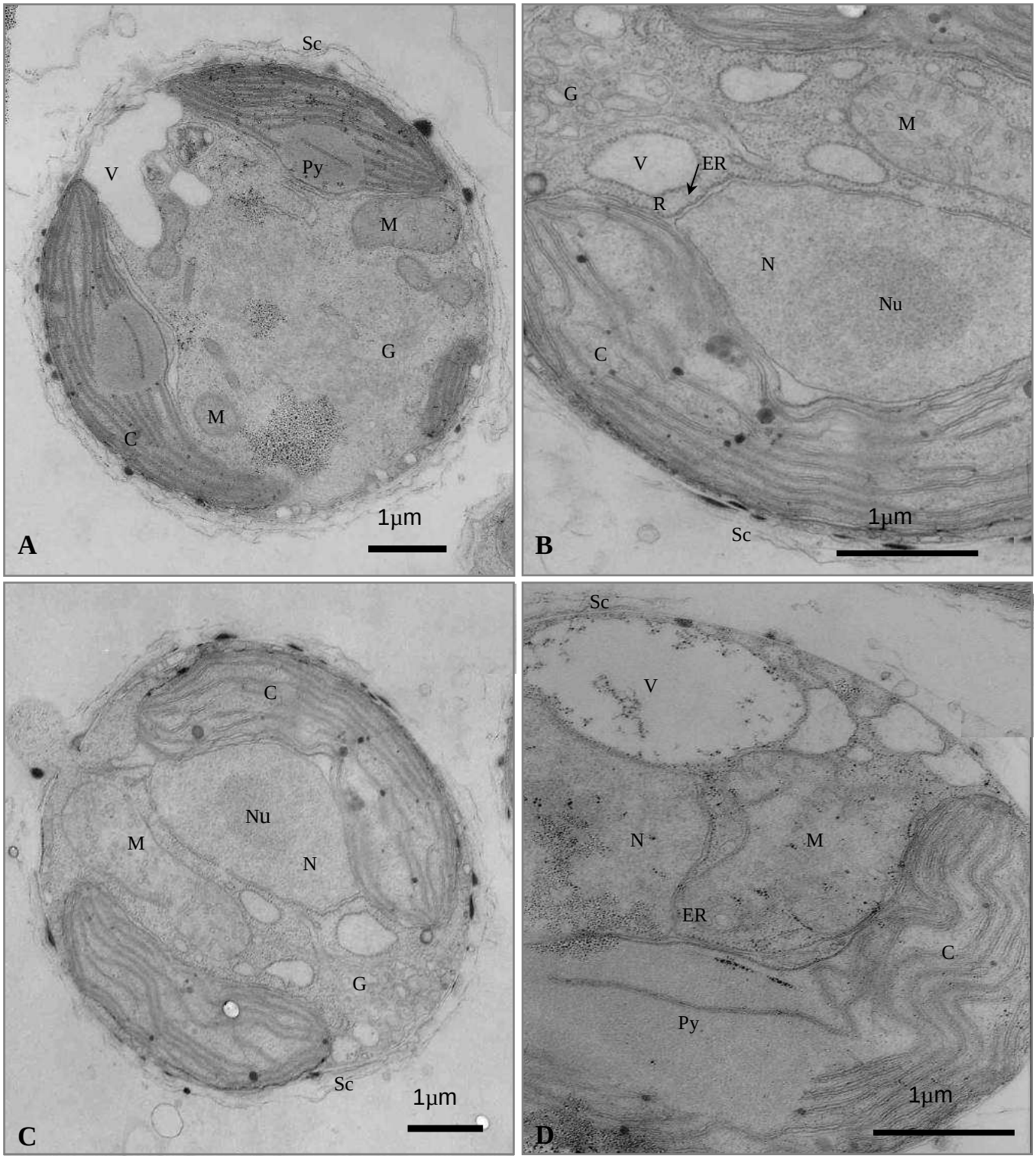

Figure 4.2 (A-D): Microphotographs of sections through isolate cells (seven day old culture). Abbreviations: N nucleus; Nu nucleolus; M mitochondria; C chloroplast; Py pyrenoid; G golgi apparatus; ER endoplasmic reticulum; V vacuole; R ribosomes; Sc scales.

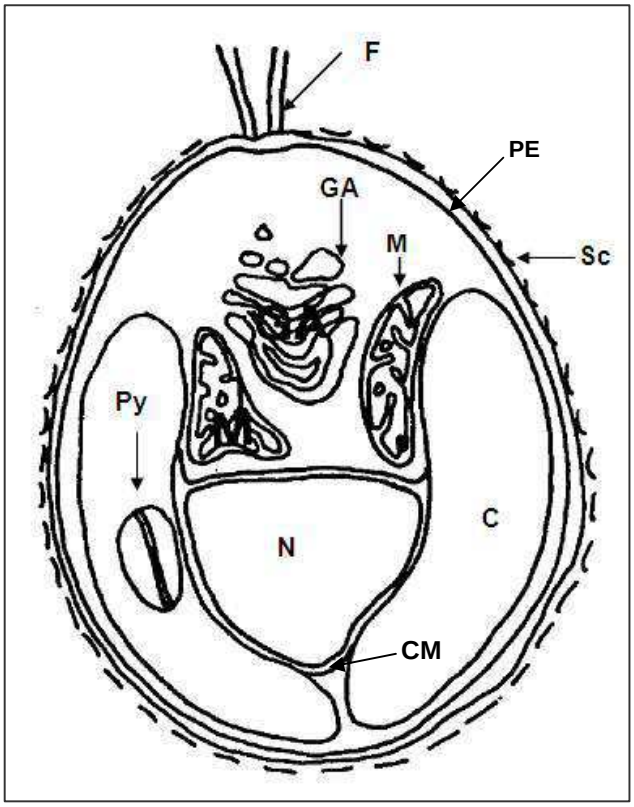

Figure 4.3: Diagrammatic representation of the general ultrastructural organization of a haptophyte cell. N = Nucleus, Py = Pyrenoid traversed by thylakoids, C = Chloroplast, GA = Golgi Apparatus, M = Mitochondrion, Sc = Scales, CM = Continuous chloroplast outer membrane and outer nuclear envelope, PE = Peripheral Endoplasmic Reticulum and F = Flagella. (Adapted from Solomon *et al*., 1986).

No haptonema was evident in the isolate cells. However, a rudimentary haptonema could be present but was probably not seen in any of the sections that were made. The absence of a haptonema or presence of a rudimentary haptonema, in the cells of the isolate, indicates that the species belongs to the Isochrysidales class (Edvardsen *et al.*, 2000). The isolate possessed two, equal length flagella (approximately 7 µm long; Figure 4.1 A & B) that were distally tapered (Figure 4.1 C), features that are consistent with the description of *I. galbana* flagella highlighted by Green and Pienaar (1977). The isolate was covered by multiple layers of body scales (Figure 4.4 A). Each scale carries a pattern of approximately 40 radial ridges that are arranged in four quadrants (Figure 4.5). The size of individual scales is depicted in Figure 4.5. The described scale morphology closely resembles that observed by Green and Pienaar (1977) when analyzing *Isochrysis galbana*. Haptophyte scales are so unique that they can be used to determine species

identification (Green and Leadbeater, 1994). Thus, it may be deduced that the isolate is presumably a strain of *I. galbana*.

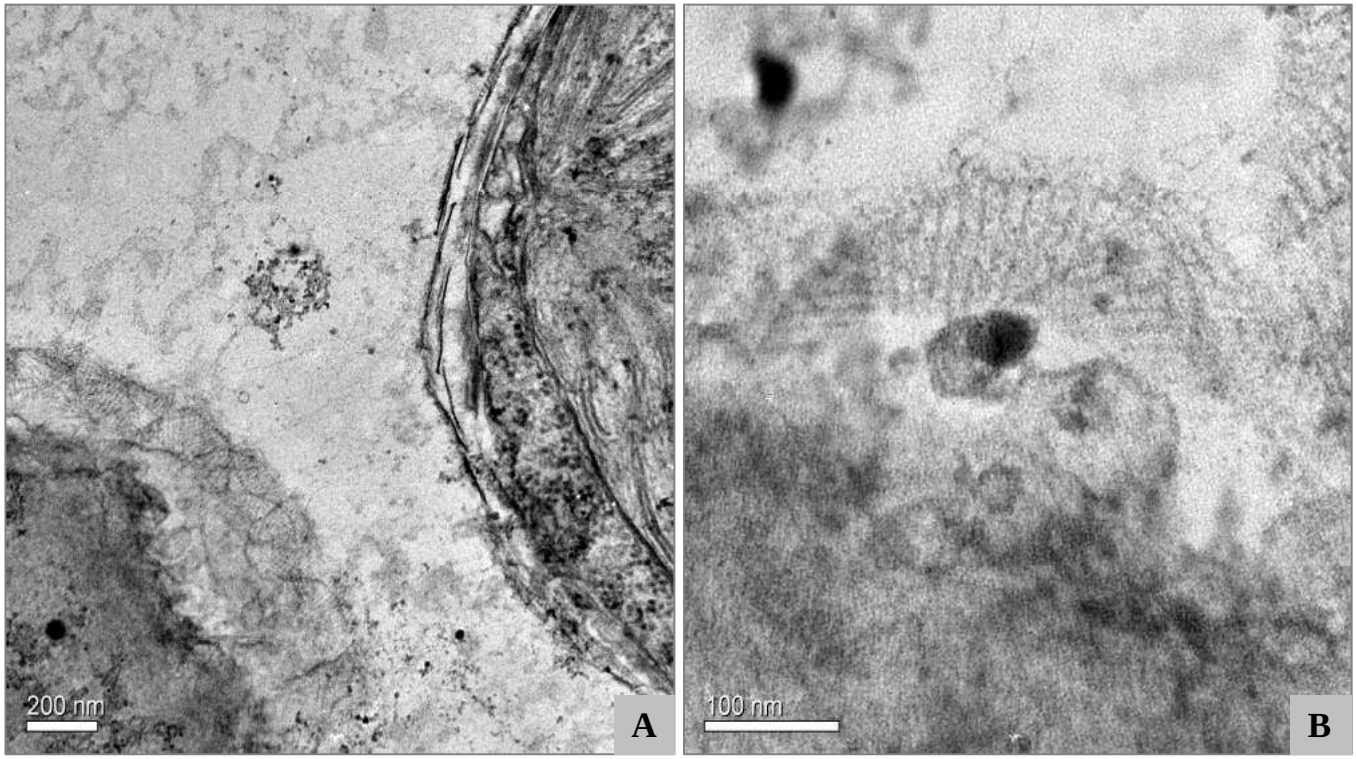

Figure 4.4 (A–B): Sections through the marginal region of the cell showing layers of superficial body scales and glancing sections of the scales.

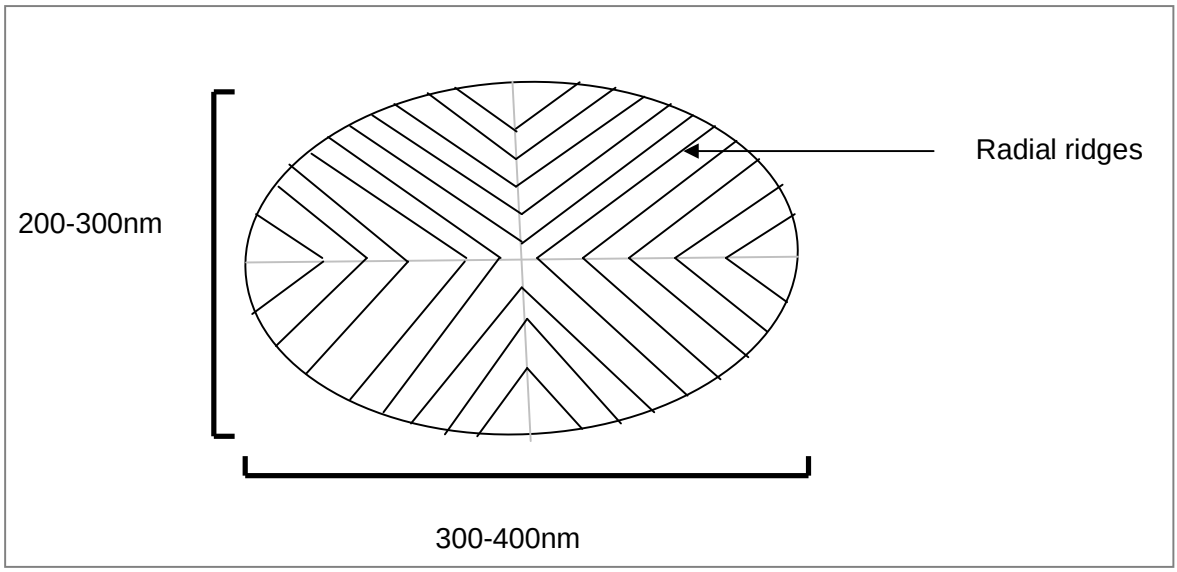

Figure 4.5: Schematic representation of the isolate body scales.

4.3.2 Molecular identification

A dual method of microalgae identification enables the definitive, unambiguous identification of the isolate. The morphological analysis revealed that the isolate is indeed a haptophyte belonging to the Isocrysidales class and possibly *Isochrysis galbana*. Molecular methods were used to verify these results.

The algal DNA was successfully amplified as indicated by the dark bands in lanes two to seven (Figure 4.6). Lane one represents the control lane that lacked any template DNA in the reaction mixture. A clear lane indicated no contamination of any PCR component which could lead to inaccurate results (Figure 4.6). The amplified region was sequenced and the nucleotide sequence, in Figure 4.7, was used for all downstream phylogenetic processing.

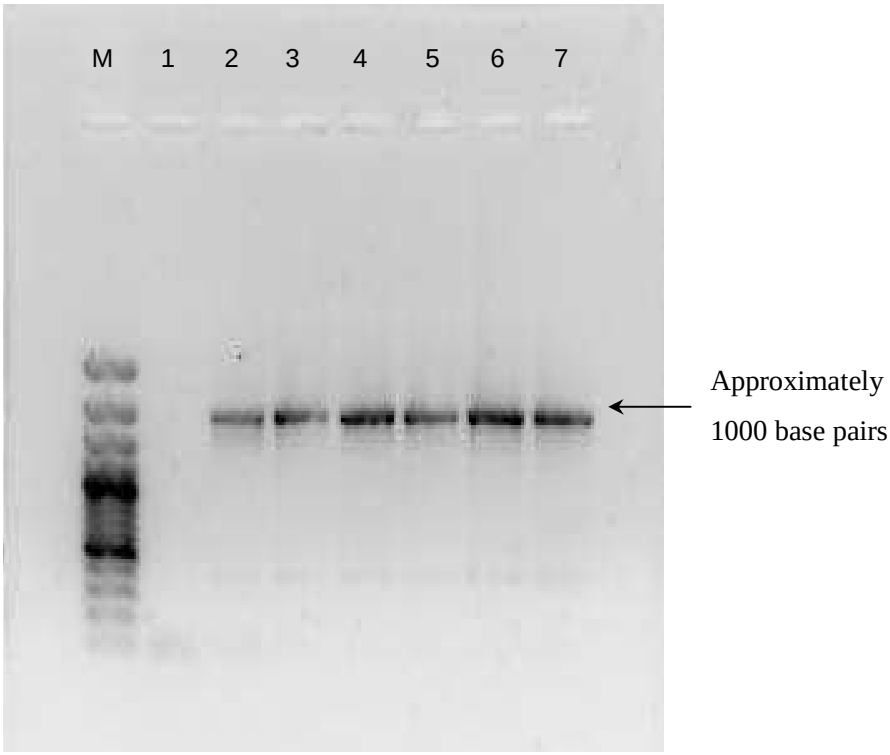

Figure 4.6: PCR amplification products of the SSU nuclear ribosomal encoding region of the microalgal isolate separated on a 1% agarose gel. **M**: 100 bp plus DNA ladder, **1:** control lane (no DNA template), **2 - 7:** replicates of amplification with DNA template.

1	TCAGAGTGTT	TCAAGCAGGC	AGTCGCTCTT	GCATGGATTA	GCATGGGATA	ATGAAATAGG
61	ACTCTGGTGC	TATTTTGTTG	GTTTCGAGCA	CCGGAGTAAT	GATGAACAGG	GACAGTCAGG
121	GGCACTCGTA	TTCCGCCGAG	AGAGGTGAAA	TTCTCAGACC	AGCGGAAGAC	GAACGACTGC
181	GAAAGCATTT	GCCAGGGATG	TTTTCACTGA	TCAAGAACGA	AAGTTAGGGG	ATCGAAGACG
241	ATCAGATACC	GTCGTAGTCT	TAACCATAAA	CCATGCCGAC	TAGGGATTGG	AGGATGTTCC
301	GTTTGTGACT	CCTTCAGCAC	CTTTCGGGAA	ACTAAAGTCT	TTGGGTTCCG	GGGGGAGTAT
361	GGTCGCAAGG	CTGAAACTTA	AAGGAATTGA	CGGAAGGGCA	CCACCAGGAG	TGGAGCCTGC
421	GGCTTAATTT	GACTCAACAC	GGGGAAACTT	ACCAGGTCCA	GACATTGTGA	GGATTGACAG
481	ATTGAGAGCT	CTTTCTTGAT	TCGATGGGTG	GTGGTGCATG	GCCGTTCTTA	GTTGGTGGAG
541	TGATTTGTCT	GGTTAATTCC	GTTAACGAAC	GAGACCGCAG	CCTGCTAAAT	AGTGTCCCCA
601	ACCCCTTGTT	GGGGCTCGCT	TCTTAGAGGG	ACAACTTGTC	TTCAACAAGT	GGAAGTTCGC
661	GGCAATAACA	GGTCTGTGAT	GCCCTTAGAT	GTTSTGGGCC	GCACGCGCGC	TACASTGATG
721	CATTCAGCGA	GTCGTCTCCC	TTGACCGAGA	GGTCCGGGTA	ATCTTGTGAA	CTTGCATCGT
781	GATGGGGATA	GATTATTGCA	ACTATTAATY	TTCAACGAGG	AATTCCTAGT	AAGCGTGTGT
841	CATCAGCGCA	CGTTGATTAC	GTCCCTGCCC	TTTGTACACA	CCGCCCGTCG	CTCCTACCGA
901	TTGAATGATC	CGGTGAGGCC	CCCGGASTGC	GGCGCCSCCG	CYGGTTCTCC	AGYSCTGGCG
961	TCGCGGGAAG	CTGTCCGAAC				

Figure 4.7: Nucleotide sequence of the amplified region in the microalgal genome.

A phylogenetic study using maximum likelihood (Figure 4.8), maximum-parsimony and neighbour-joining analyses (see Supporting Information Figures 4.S1 & 4.S2) produced similar trees. All trees confirmed that the isolate belongs to Clade C of the class Prymnesiophyceae (Edvardsen *et al*. 2000). More specifically it is a member of the Isochrysidales order and shows great sequence similarity to *Isochrysis galbana* Parke strain UIO 102 (Figure 4.8) implying that the isolate is a strain of *Isochrysis galbana* and will henceforth be called *Isochrysis galbana* strain U4.

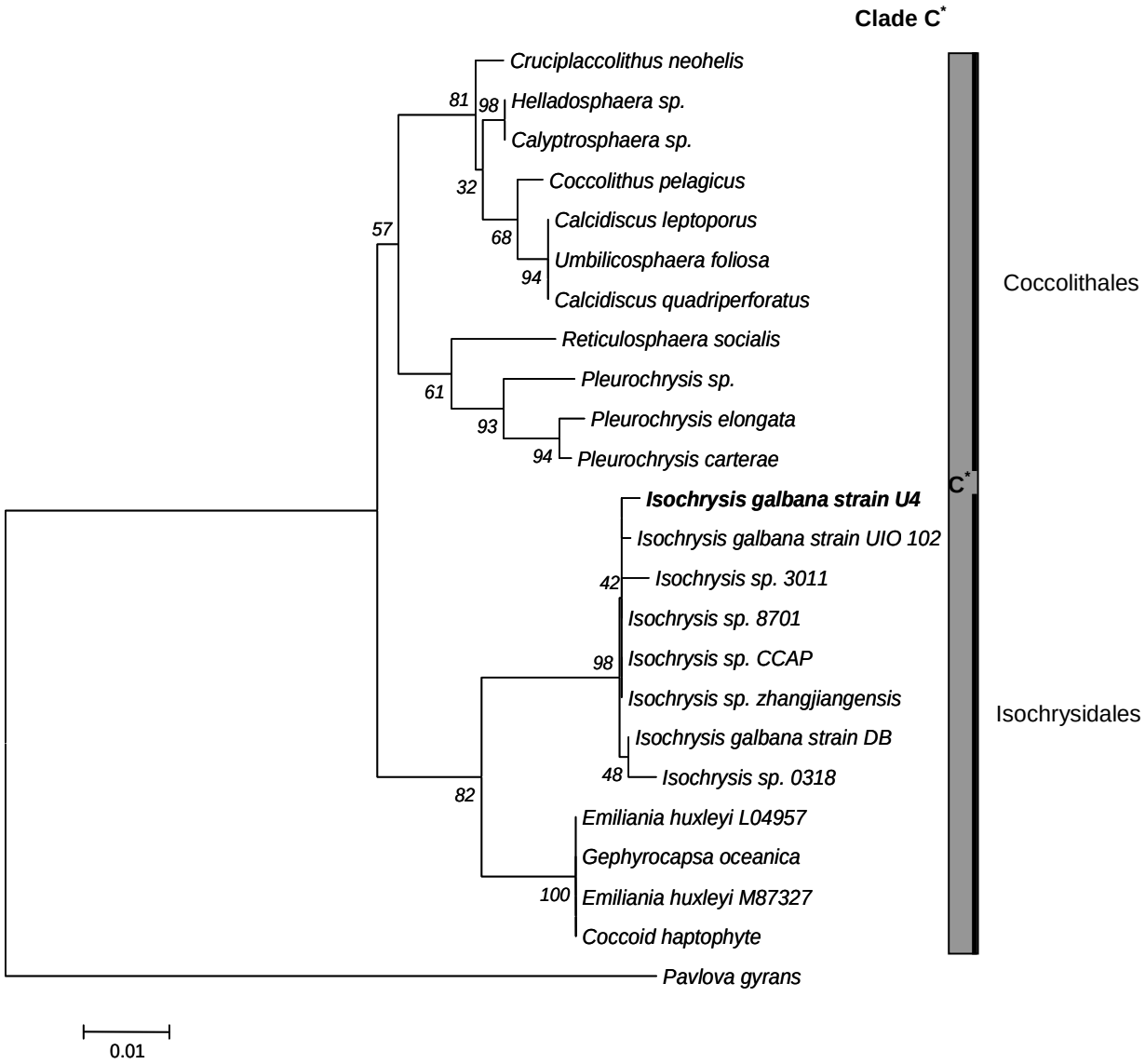

Figure 4.8: Phylogenetic tree based upon a maximum likelihood analysis showing the relationships between 18s rDNA sequences of 23 species belonging to Clade C of the class Prymnesiophyceae (Edvardsen *et al*., 2000). *Pavlova gyrans* was used as the outgroup. Numbers at the nodes indicate bootstrap values (1000 replicates). The 18s rDNA sequence obtained from this study is indicated in bold.

4.4 CONCLUSION

It may be concluded that the selected model organism is a Haptophyte, belongs to Clade C of the class Prymnesiophyceae (Edvardsen *et al*. 2000) and more specifically is a strain

of *Isochrysis galbana* and will be called *Isochrysis galbana* strain U4 henceforth since the culture was labeled U4 in the culture collection.

4.5 SUPPORTING INFORMATION

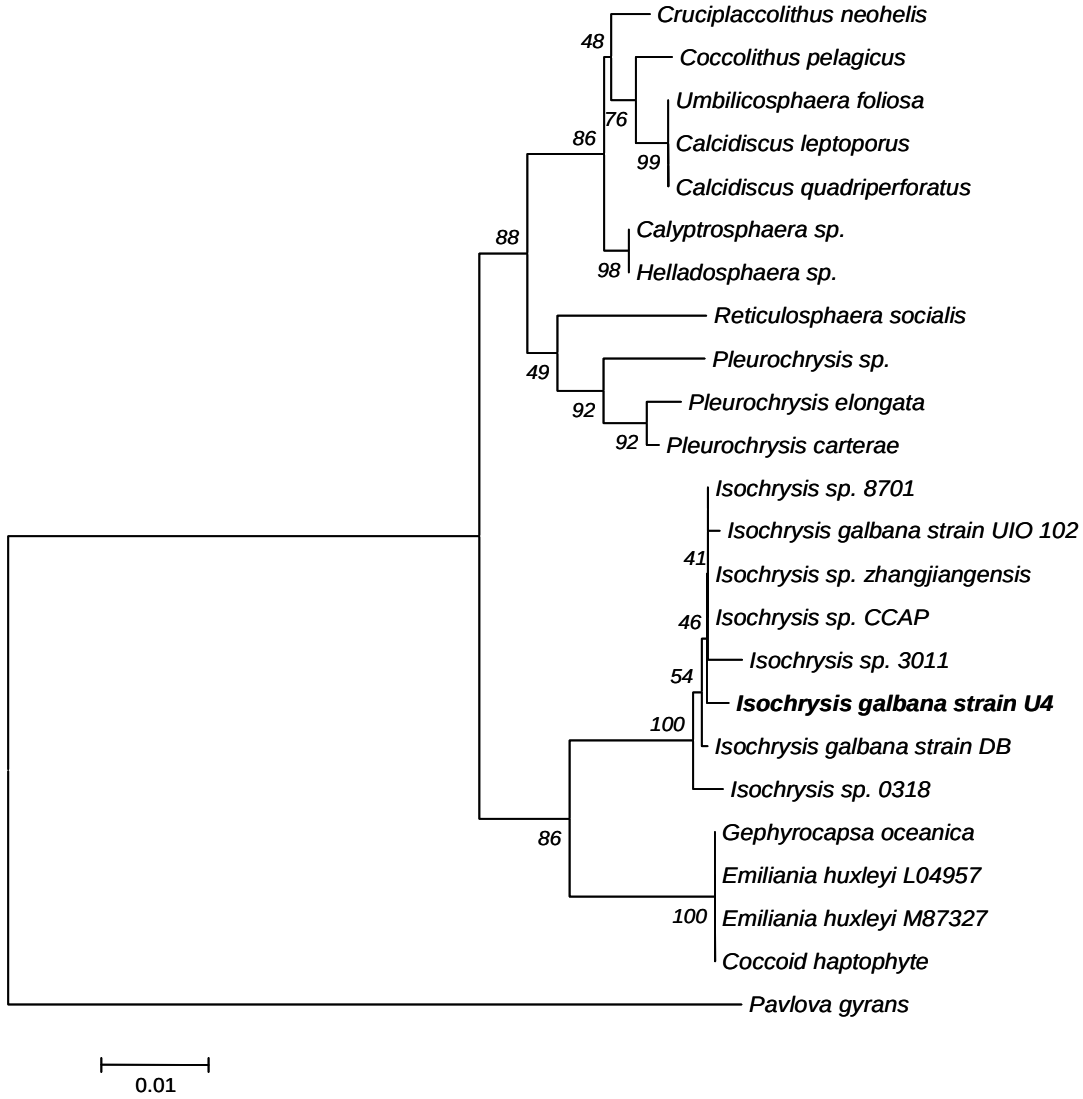

Figure 4.S1: Phylogenetic tree based upon a neighbor-joining analysis showing the relationships between 18s rDNA sequences of 23 species belonging to Clade C of the class Prymnesiophyceae (Edvardsen *et al*., 2000). *Pavlova gyrans* was used as the outgroup. Numbers at the nodes indicate bootstrap values (1000 replicates). The 18s rDNA sequence obtained from this study is indicated in bold.

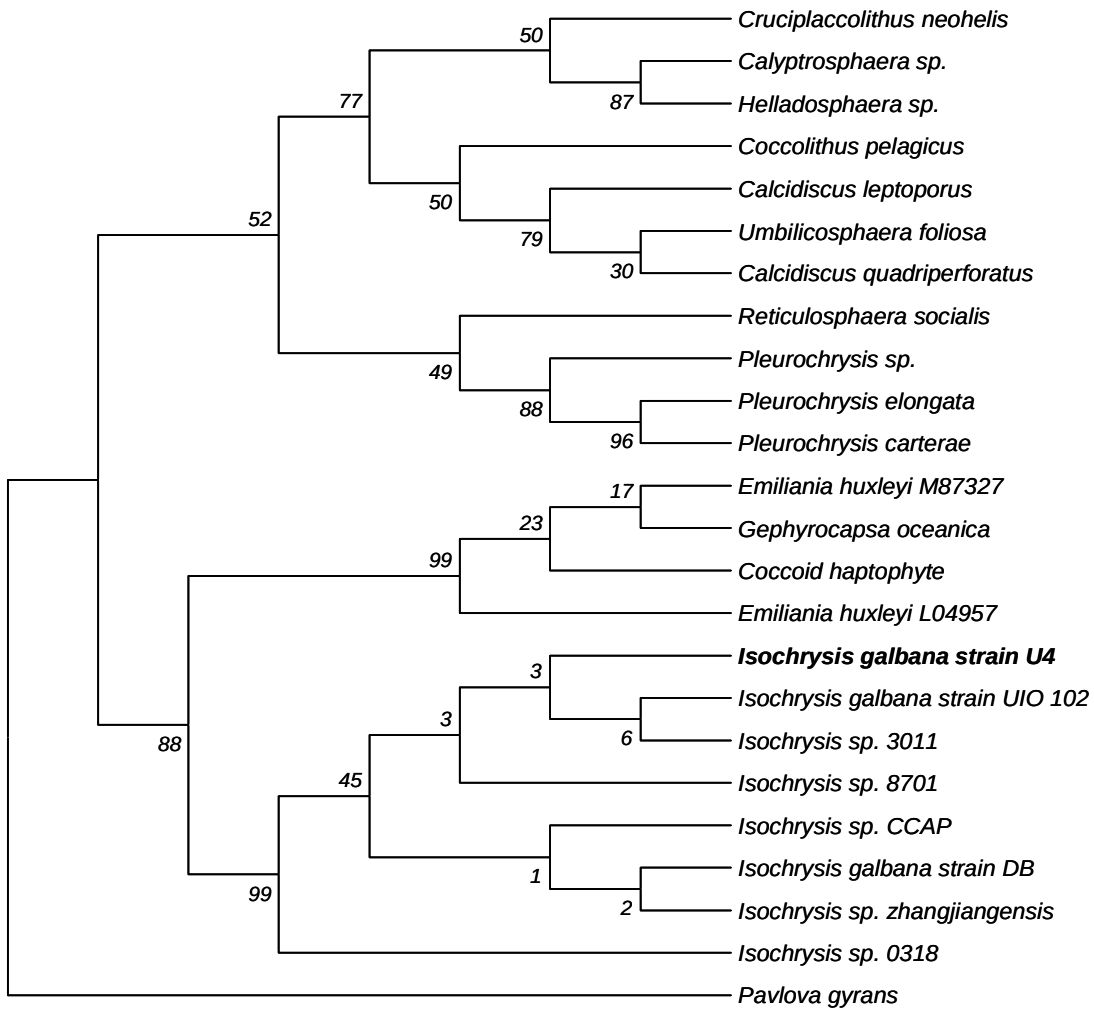

Figure 4.S2: Phylogenetic tree based upon a maximum parsimony analysis showing the relationships between 18s rDNA sequences of 23 species belonging to Clade C of the class Prymnesiophyceae (Edvardsen *et al*., 2000). *Pavlova gyrans* was used as the outgroup. Numbers at the nodes indicate bootstrap values (1000 replicates). The 18s rDNA sequence obtained from this study is indicated in bold.

CHAPTER FIVE

The Effect of Nitrogen Limitation and Starvation on *Isochrysis galbana* U4

5.1 INTRODUCTION

Alterations in the growth environment have a significant effect on the chemical composition and growth characteristics of microalgal cells (Fidalgo *et al*., 1998). Factors that may be manipulated in an attempt to alter lipid composition and content include the source and concentration of major nutrients such as nitrogen and phosphorous, light intensity and the temperature at which the system is maintained (Tedesco and Duerr, 1989; Rodolfi *et al*., 2009). Of these factors, the most widely reported inducer of lipid accumulation is nitrogen depletion (Li *et al*., 2008b; Merzlyak *et al*., 2007).

The induction of lipid synthesis in response to nitrogen stress is not new. It has been widely researched since the late 1940s after first being demonstrated by Spoehr and Milner (1949) where they showed that nitrogen starvation in *Clorella pyrenoidosa* resulted in the accumulation of approximately 85% lipid. Nutrient starvation results in the channeling of metabolic flux generated by photosynthesis to lipid biosynthesis upon nutrient stress (Li *et al*., 2008b). This is a mechanism used by microalgae to adapt to stress and to ensure that an energy rich reservoir is present when favorable conditions return to enable the population to recover once the stress is lifted. Lipid is a common energy reserve as it generates significantly greater amounts of energy than carbohydrates, upon oxidation (Roessler, 1990; Rodolfi *et al*., 2009).

Nitrogen is an essential component in genetic material, amino acids which make up peptides, proteins and enzymes, chlorophylls and energy transfer molecules such as ATP and ADP. It is therefore clearly evident that nitrogen is mandatory for cell growth and division (Lavin and Lourenco, 2005; Barsanti and Gualtieri, 2006; Li *et al*, 2008b). Under nitrogen replete conditions, photosynthetically assimilated carbon is utilised for algal growth and reproduction. The accumulation of storage carbon compounds, upon nitrogen stress, is at the expense of algal growth. It may therefore be deduced that an inverse relationship exists between algal cell growth and storage product accumulation in the form of lipids (Li *et al*., 2008b).

Lipid productivity is however the product of the lipid content (% dry weight) and the biomass productivity (grams dry weight per liter per day) and is a key characteristic when selecting a microalgal species for biodiesel production since it determines the eventual rate of lipid/oil production (Griffiths *et al.*, 2009; 2012). Thus a balance needs to be established between both parameters (lipid yield and biomass productivity) in order for significant lipid yields to be realized. Numerous authors have investigated the effect of nitrogen limitation on the final lipid yield in microalgal species (Reitan *et al.*, 1994; Sheehan *et al.*, 1998; Shifrin and Chisholm, 1981) but the temporal aspect of any analysis of lipid production and lipid productivity have been neglected. The understanding of the temporal tradeoff between lipid accumulation and growth is essential if nitrogen stresses are to be used as a tool to maximize the final lipid yield obtained from algal cells (Adams *et al.*, 2013).

A more in-depth understanding of the biochemistry and physiology of cells exposed to nitrogen stresses (nitrogen limitation and starvation) leading to lipid synthesis would also be beneficial as it may aid in optimizing lipid production. A study was conducted that focused on the growth, nitrogen uptake, pigmentation and lipid production rates in *I. galbana* cells grown in *f/2* medium. The ultrastructural changes associated with various growth phases in batch culture were analysed in an attempt to understand how individual cells react to nitrogen stresses.

5.2 MATERIALS & METHODS

5.2.1 Experimental setup

Modified aerated Schott® bottles (1 L; Section 2.3) were used to set up batch cultures of *I. galbana* U4 for both experiments (Sections 5.2.2 and 5.2.3). The bottles and glass tops were thoroughly cleaned and autoclaved (121 °C for 30 minutes) prior to use. All cultures were sparged with filtered (Whatman® uniflo 0.2 um) air and incubated at 23 ± 2 °C and under a photon flux density of 110 μmol photons.m^{-2}.s^{-1} with a 10:14 hour light-dark cycle.

5.2.2 Effect of nitrogen depletion on *I. galbana* U4

A study was conducted to demonstrate the effect of the natural uptake and consumption of nitrogen (progressive nitrogen depletion) by *I. galbana* cultured in *f/2* medium (Guillard and Ryther, 1962). Both nitrogen-replete experiments and controls lacking nitrogen were setup. The nitrogen-replete cultures were grown in standard *f/2* medium (Guillard & Ryther, 1962) whilst the nitrogen-deplete cultures (controls) were grown in a modified *f/2* medium that lacked sodium nitrate (the sole nitrogen source in *f/2* medium; Guillard & Ryther, 1962). Vessels containing 800 ml of the standard and nitrogen-free *f/2* medium were each inoculated with 4.8×10^6 cells of *I. galbana*. The stock culture for the inoculum was in the stationary phase to ensure that the cells were indeed nitrogen starved and to ascertain that no nitrogen was present in the inoculum. All treatments (nitrogen-replete and nitrogen-deplete) were undertaken in triplicate and monitored over two weeks under the conditions described above. Aliquots of the culture were extracted every alternate day and the cell concentration, lipid content, intracellular nitrogen content, nitrate concentration in the milieu and cellular pigmentation were determined as described in Sections 2.5, 2.7, 2.14.2, 2.13.1 and 2.15, respectively.

Cells, from the nitrogen-replete culture, were extracted during the lag, exponential and stationary phase and embedded in resin, sectioned and viewed using a transmission electron microscope as described in Section 2.12.1. A small aliquot of cells from each treatment (exponential and stationary), that was infiltrated with Spurr's resin for electron microscopy, was harvested prior to polymerization. This was mounted on a microscope slide, covered with a coverslip and the preparation was polymerized together with the electron microscopy preparation. Such slides were viewed with a Zeiss Axiophot light microscope with Nomarski optics at 1000 times magnification. Zeiss AxioVision microscopy software was used for pyrenoid size measurements (see Supporting Information; Section 5.5 – Figure S5.1). Sixty random pyrenoid measurements were conducted for each growth stage. The software SPSS 20 (Statistical Program for Social Sciences 20) was used to perform statistical analyses. Differences in the pyrenoid size between exponential and stationary phase cells were evaluated using an independent sample T-test.

5.2.3 Effect of varying starter nitrogen concentrations on *I. galbana* U4

The experiment was aimed at determining the effect of varying sodium nitrate concentrations on *I. galbana*. Fifteen vessels, containing 500 ml *f/2* medium each, were inoculated with approximately 3.0 x 10^6 cells of a healthy *I. galbana* culture. The cultures were grown for 14 days (until the late exponential phase/early stationary phase was reached). The cultures were then centrifuged, at 1000 rpm for five minutes, and the algal pellets were gently resuspended in 800 ml *f/2* medium with varying sodium nitrate concentrations (Table 5.1). Each concentration represented a percentage of the sodium nitrate required to make up normal *f/2* media. The treatments included 0%, 25%, 50%, 75% and 100% sodium nitrate, where 100% referred to 8.82 x 10^{-2} M sodium nitrate in the medium (i.e. the total sodium nitrate in normal *f/2* medium, Guillard and Ryther, 1962). Culture aliquots were extracted every third day to determine the lipid yield, biomass productivity and lipid productivity (Sections 2.7, 2.9 and 2.10 respectively). The nitrate concentration in the milieu was also monitored (Section 2.13.1).

Table 5.1: Sodium nitrate concentrations used in the study.

Percentage Sodium Nitrate	Sodium Nitrate Concentration (ppm)
0%	0
25%	18.75
50%	37.5
75%	56.25
100%	75

The rate of lipid accumulation and biomass productivity reduction were obtained from the slope of the best-fit curves of the respective nitrogen treatments. Triplicates of the control and all experimental treatments were conducted and the lighting received by each batch culture was evened out by random relocation of the vessels every alternate day.

5.3 RESULTS & DISCUSSION

5.3.1 The effect of nitrogen absence/presence on algal growth, lipid yield and pigmentation

Growth of *I. galbana* U4 was inhibited, after day 4, in nitrogen-deplete medium (Figure 5.1). This response is expected since nitrogen is mandatory for cell growth and division. Growth inhibition was accompanied by the rapid accumulation of lipid until day ten, after which it stabilized (Figure 5.1). Lipid accumulation occurs due to the excess fixed energy from photosynthesis, no longer capable of being used for growth, being shunted into lipid production to provide the cell with energy during times of metabolic imbalance (Lacour *et al*., 2012b). The cessation in lipid accumulation as the cells aged suggests that there is a possible limit to the amount of lipid that a particular cell is capable of storing which is a consequence of the limited volume of the cell that requires the storage of both essential organelles (e.g. nucleus, chloroplast) and lipid bodies. This could also simply be an inability of the cell to produce certain key proteins for lipid production.

In contrast, to the nitrogen-deplete cultures, cells grown in nitrogen-replete medium showed a distinct lag, exponential and stationary phase (Figure 5.1). The lag phase (Figure 5.1) was of similar duration (approximately three days) to that observed by Liu and Lin (2001) using another strain of *Isochrysis*. This prolonged lag phase, evident in the present study, may be attributed to the condition of the cells used for the inoculum. Previously nutrient-deprived cells, as expected, are lipid-rich and require more time to respond to conditions favorable to growth than those which are already actively growing because they have to reactivate processes essential for growth such as protein synthesis. The observed decrease in lipid yield, as the cells entered the exponential phase of growth, is indicative of the consumption of this energy rich reserve for the rebuilding of the cells (e.g. chlorophyll synthesis etc.) upon exposure to nutrient-rich conditions. A short exponential phase resulting in high cell densities was evident similar to that observed in other studies conducted using material of *Isochrysis* (Fabregas *et al*., 1986; Huerlimann *et al*., 2010). The lipid yield rapidly increased during the course of the stationary phase

highlighting the expected antagonistic relationship between growth rate and lipid accumulation.

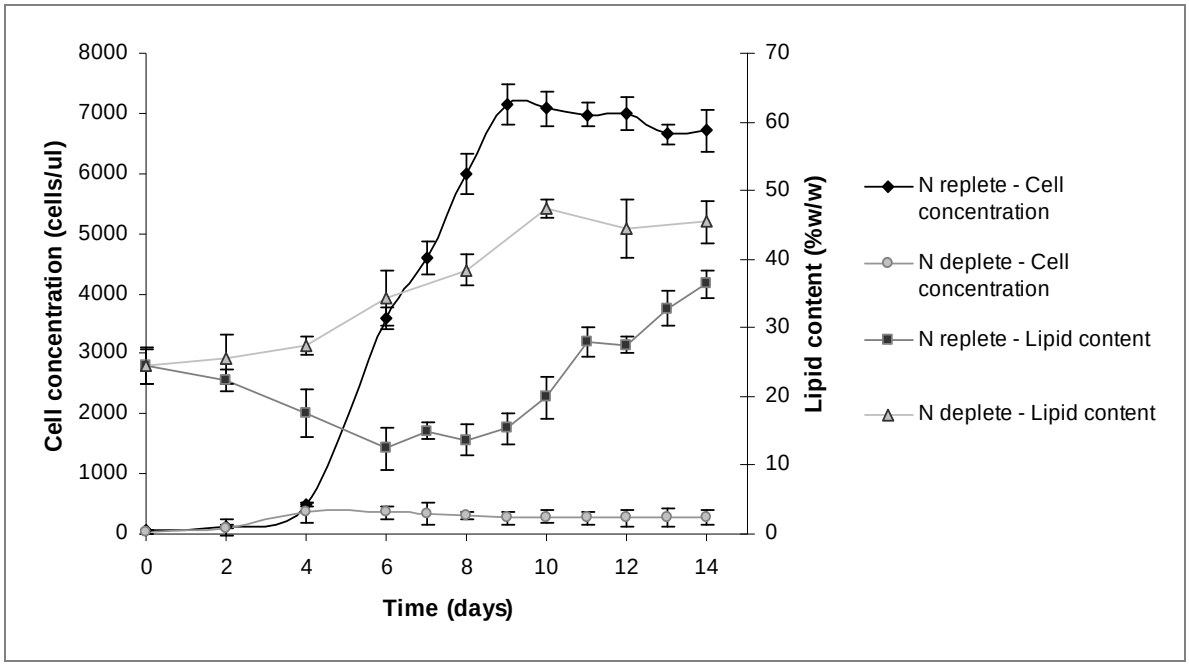

Figure 5.1: *Isochrysis galbana* U4 growth curve showing lipid accumulation under nitrogen-replete and deplete conditions. Error bars represent standard deviation (n = 3).

Interestingly, the stationary phase, in the nitrogen-replete treatment, did not coincide with the depletion of nitrogen in the culture medium, which was consumed by day six (Figure 5.2). Growth proceeded for three days post-exhaustion of all measurable nitrogen in the culture medium (cf. Figures 5.1 and 5.2). Likewise, cells inoculated into medium lacking any nitrogen were able to grow for the same three day period before growth stopped (Figure 5.1). This response to nitrogen limitation has been demonstrated in an array of other microalgal species (Dortch *et al*, 1984). However, it is known that nitrogen is mandatory for cell growth. Cell growth and division, in spite of the depletion of external nitrogen pools, means that nitrogen is somehow stored in the cells when abundant nutrients are available. These nitrogen reservoirs may then be utilised during stressful conditions. This is probably an evolutionary adaptation of algal species that experience erratic fluctuations in nutrient content in their natural environment. Therefore rapid, mass nutrient uptake (luxury uptake) would be beneficial to them (Dortch *et al*., 1984;

Lavin & Lourenco, 2005; Lacour *et al*., 2012a). Furthermore, this rapid nitrogen uptake may also enable algal species to out-compete or at least effectively compete with other species.

Luxury nitrogen uptake in this species of *Isochrysis* was evidenced by the large amount of intracellular nitrogen observed during growth in nutrient-replete medium and maintained as such even after all measurable external nitrogen became depleted (Figure 5.2). However, these intracellular nitrogen reserves slowly declined as growth proceeded due to its assimilation into structural components and became negligible at the time that the stationary phase was reached (cf. Figures 5.1 and 5.2). A rapid decline in the intracellular nitrogen levels was observed in cells cultured in nitrogen-deplete medium until day six, when it became undetectable (Figure 5.2). This coincided with the halt in cell growth and division (cf. Figures 5.1 and 5.1). This data collectively supports the notion that it is indeed the intracellular nitrogen that is limiting growth.

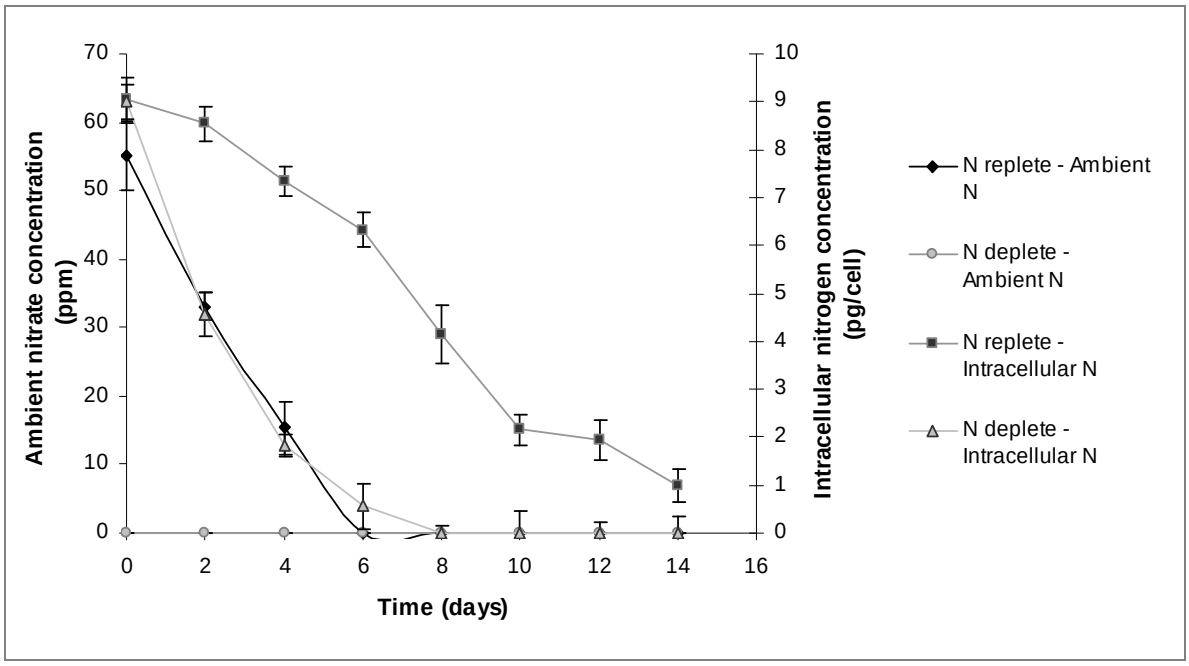

Figure 5.2: Ambient nitrate depletion and intracellular nitrogen utilization in *I. galbana* U4 cells grown under nitrogen-replete and nitrogen-deplete conditions. Error bars represent standard deviation (n = 3).

The continuation of cell division in *Isochrysis* in medium for a few days following the apparent exhaustion of nitrogen in this study is in agreement with the observations of many others (Herzig & Falkowski, 1989; Lavin & Lourenco, 2005). These authors suggest various mechanisms of nitrogen storage, including incorporation into inorganic nitrogen compounds such as ammonia, nitrate and nitrite and into organic compounds such as chlorophyll, amino acids, peptides, proteins, enzymes, nucleic acids and vitamins. The capacity to store nitrogen is widespread amongst microalgae but the degree of intracellular nitrogen accumulation is strongly species specific and dependant on factors such as the surface area to volume ratio of the cell and the activity of nitrogen-assimilating enzymes in various species (Dortch *et al*., 1984; Lavin & Lourenco, 2005). The species of *Isochrysis* used in the present study is approximately 5µm in length (Chapter 4). Because of their large surface area to volume ratio, such small cells would portray elevated mass nitrogen uptake capabilities relative to larger microalgal species.

In the nitrogen-replete treatment, the chlorophyll content increased until day six, a period which coincided exactly with the depletion in measurable nitrogen in the medium (cf. Figures 5.2 and 5.3). Similar observations have been made during the logarithmic phase of batch cultures of other species of *Isochrysis* (Fabregas *et al*. 1986; Davidson *et al*. 1991), but this study is unique in showing a clear, direct relationship between measurable ambient nitrogen levels and chlorophyll content. Cell division continues after the depletion of measurable ambient nitrogen because the cells draw on internal nitrogen reserves, but chlorophyll synthesis is essentially arrested with the result that the absolute content of chlorophyll per cell decreases. A rapid decrease in the chlorophyll content was evident during the stationary phase. A more pronounced chlorophyll reduction was observed in the nitrogen-deplete treatment where chlorophyll levels rapidly declined over the duration of the experiment until it approached critical levels (approximately 0.1 pg/cell) from day ten onwards (Figure 5.3). Interestingly, the reduction in chlorophyll to critical levels (Figure 5.3) occurred simultaneously with the arrest in lipid accumulation (Figure 5.1). Hence, the halt in lipid accumulation could be a consequence of the reduced chlorophyll levels since solar energy, which is captured by the photosynthetic apparatus,

is essential for the generation of the metabolic flux required for lipid synthesis and accumulation (Li *et al*., 2008b).

Chlorophyll contains four nitrogen atoms and so could be used as a nitrogen source when nitrogen is limited, but chlorophyll-derived nitrogen is minimal (less than 1% of the total cellular nitrogen in microalgae, Dortch *et al*., 1984). Thus, it is unlikely that the rapid decrease in chlorophyll content, under growth inhibiting conditions, is as a result of nitrogen mobilization from degraded chlorophyll. A metabolic imbalance occurs during nitrogen stress because photosynthesis continues but growth and cell division are arrested. This in turn leads to cellular oxidative stress. The production of lipids requires considerable amounts of energy (ATP) and reducing power (NAD(P)H), hence forms a sink for the excess electrons, and so initially reduces photochemical damage of the algal cells (Roessler *et al*., 1990; Lacour *et al*, 2012a). However, microalgal cells have a limit to the amount of lipid that they can store based on their volume and inability to grow (Lacour *et al*., 2012b). A reduction in the chlorophyll content can thus be viewed as an attempt by the cell to decrease photosynthetic rates and thus enable it to acclimate to a cessation in cell growth and division (Roessler, 1990; Lacour *et al*, 2012a).

The depletion of measurable ambient nitrogen coincided with an increase in the carotenoid to chlorophyll ratio in both nitrogen-replete and nitrogen-deplete cultures (cf. Figures 5.2 and 5.3). Because this ratio only increased after chlorophyll synthesis ceased in the nitrogen-replete cultures, it is clear that nitrogen stress results in an increase in the synthesis of carotenoids. The increased carotenoid production coupled with the decrease in chlorophyll synthesis resulted in a change in the color of nutrient stressed cultures from golden-brown to orange (not shown). Carotenoids are nitrogen-free pigments, the concentration of which increase in response to environmental stresses e.g. During the stationary phase, when the integral irradiance per cell cycle is elevated due to minimal cell divisions, the chlorophyll content decreases and the carotenoid levels increase as a protective response (Ben-Amotz & Avon, 1983; Davidson *et al*., 1991; Flynn *et al*., 1992). Amongst other functions, carotenoids play an important structural role in chloroplasts. When microalgal cells are stressed, the resultant carotenoids that are

rapidly produced form an association with chloroplast membrane lipids. This association in turn results in an increase in membrane thermostability, a decrease in membrane fluidity and a reduction in its susceptibility to lipid peroxidation (Havaux, 1998).

The observed increase in the carotenoid to chlorophyll ratio upon external nitrogen depletion means that the ratio can be used as a marker of nutrient stress in this species of *Isochrysis*. These findings correlate strongly with the findings of Heath *et al* (1990), where it was determined that this ratio is a reliable proxy of cellular nutrient status for an array of marine phytoplankton including *Isochrysis galbana*. Furthermore, the ratio of carotenoids to chlorophyll observed in the present study was in the same range as those observed by Heath *et al*. (1990). They found that absorption ratios in excess of 2.4 were exhibited by cells experiencing extreme levels of nitrogen deficiency and those below 1.4 were found in cells experiencing excessive nitrogen availability (Heath *et al*., 1990; Figure 5.3).

An elevated total carotenoid content in nitrogen stressed *Isochrysis* cells has also been reported elsewhere (Jalal *et al.*, 2013). An increase in the photoprotective carotenoid concentration in *Isochrysis galbana* cells exposed to elevated irradiances has also been observed (Fujiki and Taguchi, 2002) but no study characterized the carotenoid complement produced by this species when nitrogen-stressed. However, Geider *et al*. (1998) showed that the actual type of carotenoids favored by nitrogen stress in *Dunaliella tertiolecta* were the photoprotective (α and β carotenes) rather than the photosynthetic carotenoids. This shows that carotenoid accumulation in response to nitrogen depletion is not in an attempt to increase the photosynthetic ability of the cells when chlorophyll levels drop. The increase in photoprotective carotenoids rather than photosynthetic carotenoids may be in an attempt to increase functions such as quenching chlorophyll in response to increased exposure of the cells to elevated irradiances when cell division seizes (Geider *et al*., 1998).

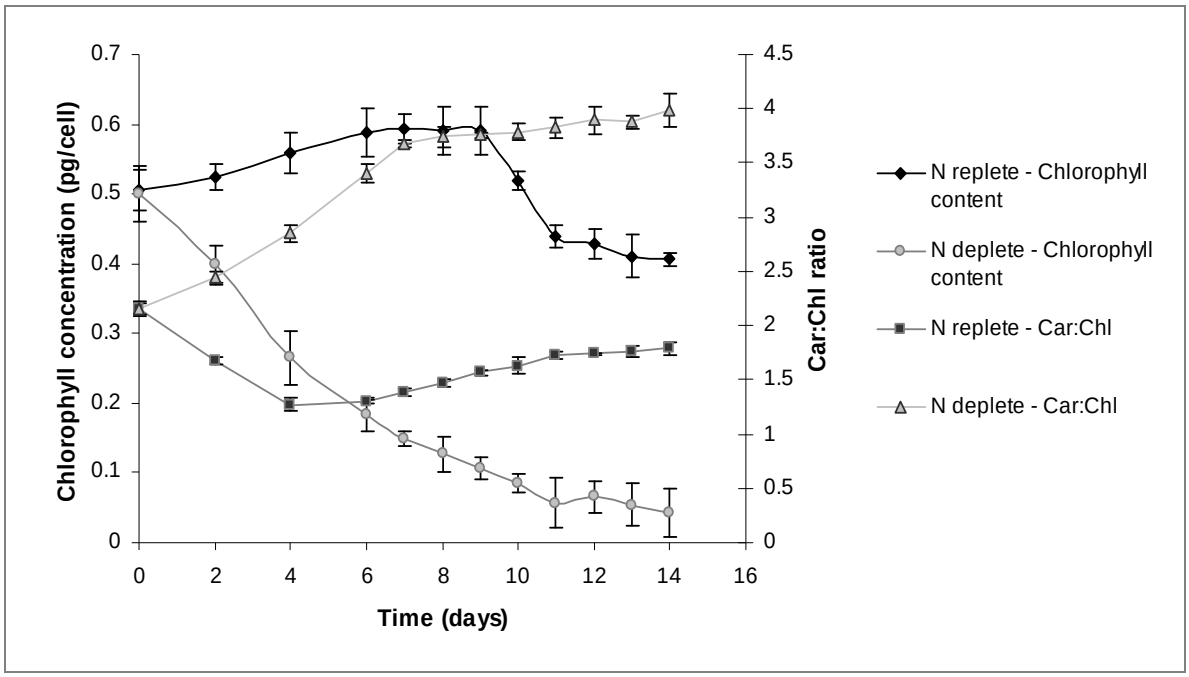

Figure 5.3: The ratio of carotenoids to chlorophyll (car:chl) and the fluctuations in chlorophyll content observed in *I. galbana* U4 cells grown under nitrogen replete and nitrogen deplete conditions. Error bars represent standard deviation (n = 3).

5.3.2 Implications of nitrogen stresses on algal ultrastructure at varying growth stages

The ultrastructure of healthy cells of species of *Isochrysis* has received much attention (Green & Pienaar, 1977), including aspects of cell division (Hori & Green, 1985) and the flagella root system (Hori & Green, 1991). More recently, attention has switched to the formation of lipid bodies in this genus (Liu & Lin, 2001; Eltgroth *et al*., 2005). In the present study, an analysis of ultrastructural changes in *Isochrysis galbana* U4 at various growth stages in batch culture (nitrogen-replete) revealed some interesting findings relating to the cessation of growth brought about by nutrient deprivation.

Healthy, exponential phase cells contained no lipid bodies and the chloroplasts were intact and contained large pyrenoids (Figure 5.4.1 A – D). The cells were also covered by multiple layers of glycoprotein scales (See inset image in Figure 5.4.1 B for scales). As previously observed by Flynn *et al*. (1992), Liu and Lin (2001) and Eltgroth *et al*.

(2005), the major change incurred by cells entering the stationary phase was the formation of cytoplasmic lipid bodies (Figures 5.4.2 A - D) and plastidial lipid bodies (Figure 5.4.3 A and B; See inset image in Figure 5.4.3 A for magnified plastidial lipid body). Plastidial lipid bodies have been considered to be sinks of surplus reducing power (Eltgroth *et al*., 2005). It was proposed that lipids are synthesized and packaged in the plastid and thereafter transported to the cytoplasm (Liu and Lin, 2001; Eltgroth *et al*., 2005). The latter proposal may be justified by the close proximity of the lipid bodies in the cytoplasm to the chloroplasts in *Isochrysis galbana* U4 (Figure 5.4.2 A- D and 5.4.3 B - D). Figure 5.4.3 represents a postulated pathway of lipid synthesis in *I. galbana* U4. As per the figures, lipid production is initiated in the chloroplast (Figure 5.4.3 A). The plastidial lipid bodies emerge from the chloroplast (Figure 5.4.3 B) and then form distinct membrane bound cytoplasmic lipid bodies (Figure 5.4.3 C) which may coalesce as the cultures age and more lipid is produced (Figure 5.4.3 D).

In *Dunaliella bardawil,* intrachloroplastic lipid bodies were mainly composed of carotenoids (Ben-Amotz and Avron, 1983) whereas those of another species of *Isochrysis* contain mostly poly-unsaturated long chain alkenes, alkenones and alkenoates (PULCA, Eltgroth *et al*. 2005). The exact function of these plastidial lipid bodies in the current *Isochrysis* isolate is unknown but this could be unraveled if they can be extracted and their composition determined. The large amount of cytoplasmic lipid bodies (Figures 5.4.2 A-D) accumulated upon the depletion of internal nitrogen reserves is a survival mechanism used by microalgae to ensure an energy-rich reservoir is present when growth-stimulating conditions return (Rodolfi *et al*., 2009).

A gradual disassembly of the chloroplast was evident as the stationary phase progressed (Figures 5.4.2 and 5.4.3 B and D). This was in contrast to the observations by Eltgroth *et al*. (2005) where no chloroplast breakdown was noted leading them to suggest that neutral lipid is actively produced in the chloroplasts rather than being scavenged from chloroplastic membranes during the stationary phase. The plastid disassembly, evident in the present study, may be in an attempt to reduce photosynthetic rates during growth-limiting conditions. Upon nitrogen limitation nuclear-encoded cytoplasmic proteins are

preferentially synthesized over those proteins encoded by plastid DNA (Falkowski *et al*., 1989). This may be due to the presence of most amino acids in the cytoplasm where nuclear encoded translation occurs. Most amino acids, made by transamination in the cytoplasm, would need to be transported back into the chloroplast prior to plastid encoded translation (Falkowski *et al*., 1989). The majority of the plastid proteins are encoded by chloroplast DNA. A decrease in plastid DNA translation brought about by nutrient deficiency would thus result in a decline in plastid membrane proteins, such as the D1/D2 proteins of PSII (reaction centre proteins) and stromal proteins. Membrane proteins form integral polar membrane components hence the membrane structure would be adversely affected upon their removal (Mock and Kroon, 2002). Nitrogen deficiency has also been shown to increase the activity of membrane galacto-lipid-specific acyl hydrolase in *Dunaliella salina* cells. This enzyme catalyses the breakdown of the chloroplast membranes and it was suggested that the chloroplast membrane fatty acids released could be incorporated into storage lipid reserves in response to nutrient stress (lipid recycling, Cho and Thompson, 1986). Chloroplast proteins may also be broken down to be used as a nitrogen source elsewhere which may result in plastid membrane dismantling if these proteins are located in the membrane rather than the plastid stroma.

An independent samples T-test revealed a statistically significant difference between the pyrenoid size in exponential and stationary phase cells ($t = 20.357$, $df = 113.358$, $p < 0.005$). The pyrenoid size of exponential phase cells ($M = 1.1961\mu m$, $SD = 0.20475$) was significantly larger than the pyrenoid size of stationary phase cells ($M = 0.3293\mu m$, $SD= 0.26199$). This was also obvious in sections of *Isochrysis galbana* U4 cells (Figure 5.4.1 in comparison to Figure 5.4.2). Furthermore, pyrenoids could not be found in late stationary phase cells (not shown). A similar lack of pyrenoids was also found in cells of *Isochrysis* that had been stored in alginate beads for a year (Chen, 2003). This observation may have been in response to severe nitrogen deficiency because such cells released into NH_4-replete medium rapidly took it up, but no explanation for this observation was provided (Chen, 2003).

Pyrenoids are dense, proteinaceous bodies located in the chloroplasts of hornworts and certain algal species. They are mostly composed of the bulky, nitrogen-rich enzyme Ribulose-1,5-bisphosphate carboxylase/oxygenase (Rubisco) that catalyses carbon dioxide fixation during the dark phase of photosynthesis. Pyrenoid size may be affected by the carbon dioxide concentration, light intensity and the light-dark cycle (Nagasato *et al*. 2003). A similar trend in pyrenoid investment with growth phase in batch culture was found in *Dunaliella tertiolecta* where the pyrenoid size increased during the exponential growth phase and decreased considerably during the stationary phase. This was monitored by the immunofluorescence of Rubisco which was either localized to the pyrenoid or immersed in the plastidial stroma (Lin and Carpenter 1997a).

In *Isochrysis galbana*, Rubisco constitutes approximately 23% of the total cellular protein under optimal growth conditions (Clark *et al*., 1999). Conflicting results were obtained when quantifying Rubisco levels in various microalgal species in response to nutrient depletion. Some investigators observed a decrease in Rubisco content upon nutrient stress (e.g. Falkowski *et al*., 1989) whereas others showed that the Rubisco levels remained constant during all growth stages (e.g. Lin and Carpenter, 1997b; Nagasato *et al*., 2003). No quantitative data of Rubisco levels through the various phases of development of the batch culture were currently pursued and hence a definitive corroboration for the decrease in the pyrenoid size was not obtained.

Numerous possible reasons for the decrease in the pyrenoid size exist. Pyrenoid reduction, in response to nitrogen stress, can be justified by the immobilization and breakdown of the nitrogen-rich protein, Rubisco, to be used as a nitrogen source elsewhere. This would result in the decrease in Rubisco levels in the microalgal cells. On the other hand, a constant Rubisco level concurrent with the decrease in the pyrenoid size can be explained by the redistribution of Rubisco in the plastid. Rubisco may be localized to the pyrenoid or dissolved in the plastid stroma. McKay *et al*. (1991) observed that Rubisco activase (an enzyme that catalyses the in vivo activation and regulation of Rubisco) is co-localized with Rubisco in the pyrenoid. This suggests that Rubisco located in the pyrenoid is catalytically active whereas stromal Rubisco is

inactive (McKay *et al*., 1991). A decrease in the pyrenoid size in nutrient stressed, stationary phase cells could be explained by the reduction in catalytically active pyrenoid-localized Rubisco thereby decreasing carbon dioxide fixation rates when conditions do not promote growth.

A more in-depth understanding of pyrenoid dynamics in *I. galbana* during nutrient stress can be obtained with the aid of immunofluorescence and electron microscopy immunogold analysis as conducted by Lin and Carpenter (1997a, 1997b). These techniques would enable the investigator to determine the location of the Rubisco (pyrenoid versus stromal) and even aid in the quantification of the enzyme.

Another difference between stationary and exponential phase cells was the presence of condensed masses in the nucleus in stationary cells (Figure 5.4.1 A and C compared to Figure 5.4.2 C). These masses may be the DNA that is transcribed (mRNA) but unable to be translated due to the lack of amino acids (Clark *et al*., 1999) or heterochromatin production. Nitrogen is necessary for amino acid and hence protein synthesis. Ambient nitrogen deficiency in phytoplankton results in the depletion of intracellular nitrogen reserves in a specific order. Initially inorganic nitrogen (ammonium, nitrate and nitrite) is utilized, followed by amino acids, a portion of the protein content, RNA and finally chlorophylls (Dortch *et al*., 1984; Lavin and Lourenco, 2005). The amino acid pool is thus consumed soon after the onset of nitrogen deprivation as it is abundant and easily accessible. This would result in decreased translation rates and increased accumulations of untranslated mRNAs accounting for the masses in the nuclei observed in this study. Dortch *et al*. (1984) showed that *Isochrysis galbana* does not contain a large amount of stored amino acids (1.5% particulate nitrogen) in comparison to other species which stored amino acids that constitute as much as 26.4% particulate nitrogen. It may therefore be deduced that the amino acids in *Isochrysis* cells would be rapidly consumed resulting in the early halting of protein synthesis.

The masses observed in the nuclei could also be heterochromatin since mRNA has a short half life. Heterochromatin is DNA that is tightly packed. The over-expression of

heterochromatin during the stationary phase may be the mechanism by which the organism protects its genetic material from damage during unfavorable growth conditions. This would represent the 'resting' stage inferred by Thinh (1994). The idea was supported by the ability of nutrient-stressed cells which were nitrogen starved for extended periods (up to two months) to recover when transferred into fresh medium (data not shown). Such recoveries have been noted in ageing (11 month old) *Isochrysis galbana* cultures (Thinh, 1994), although this author does not address any issues dealing with the bulk formation of heterochromatin.

Stationary phase cells either shed or resorb their flagella and became immotile (observed under light microscopy) and late stationary phase cells also shed a large amount of their glycoprotein scales. The loss of the flagella may be an energy-conserving strategy during stressful conditions. The loss of the glycoprotein scales, also observed by Chen (2003), may be attributed to a decrease in protein synthesis due to insufficient nitrogen supplies leading to the inability to produce more scales when the older scales are shed. Hence, there are multiple ultrastructural changes initiated by nitrogen depletion and cell growth cessation in *I. galbana* U4.

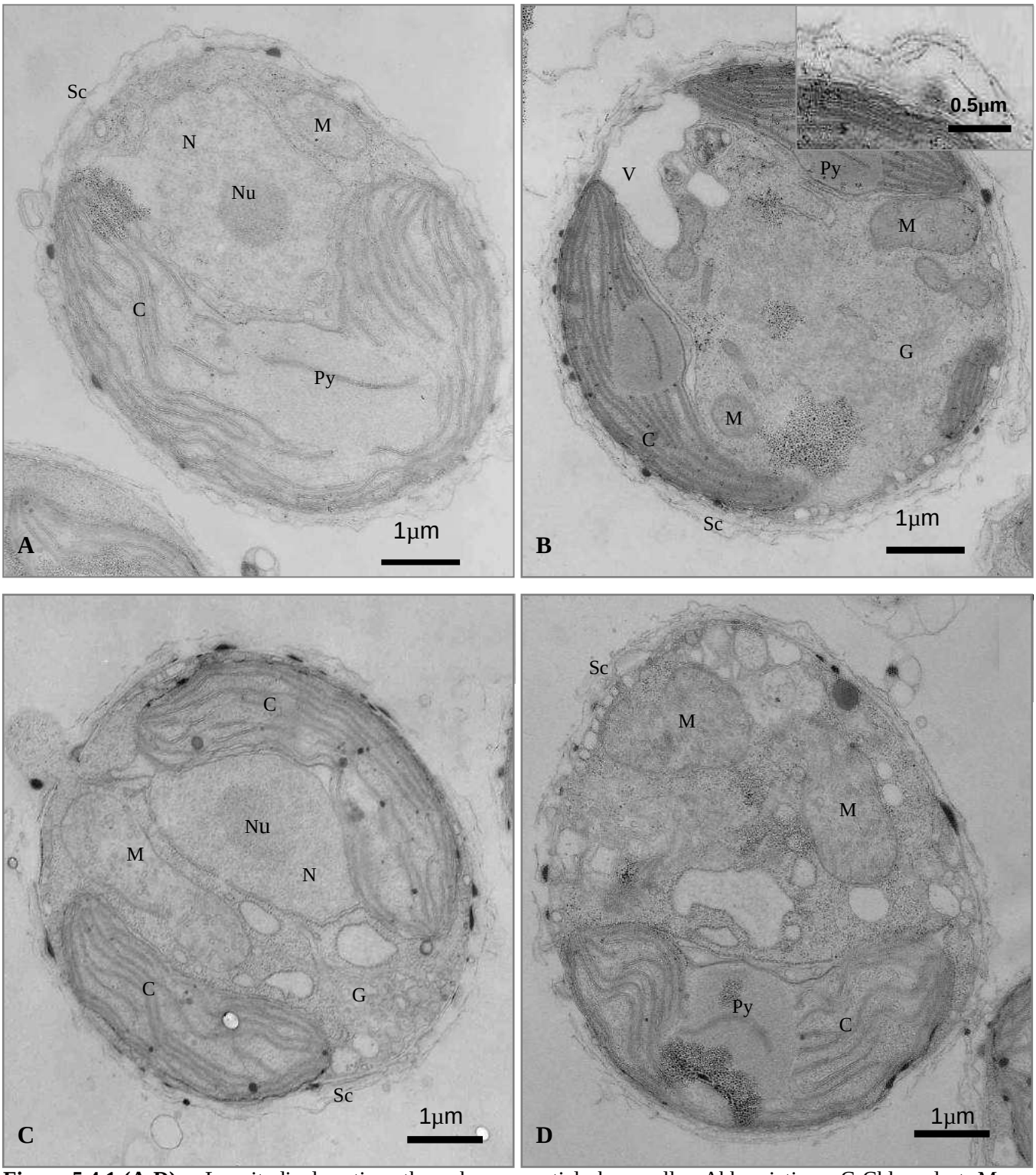

Figure 5.4.1 (A-D): Longitudinal sections through exponential phase cells. Abbreviations: C-Chloroplast; M-Mitochondria; N-Nucleus; Py-Pyrenoid; Nu-Nucleolus; Sc-Scales; V-Vacuole; G-Golgi apparatus.

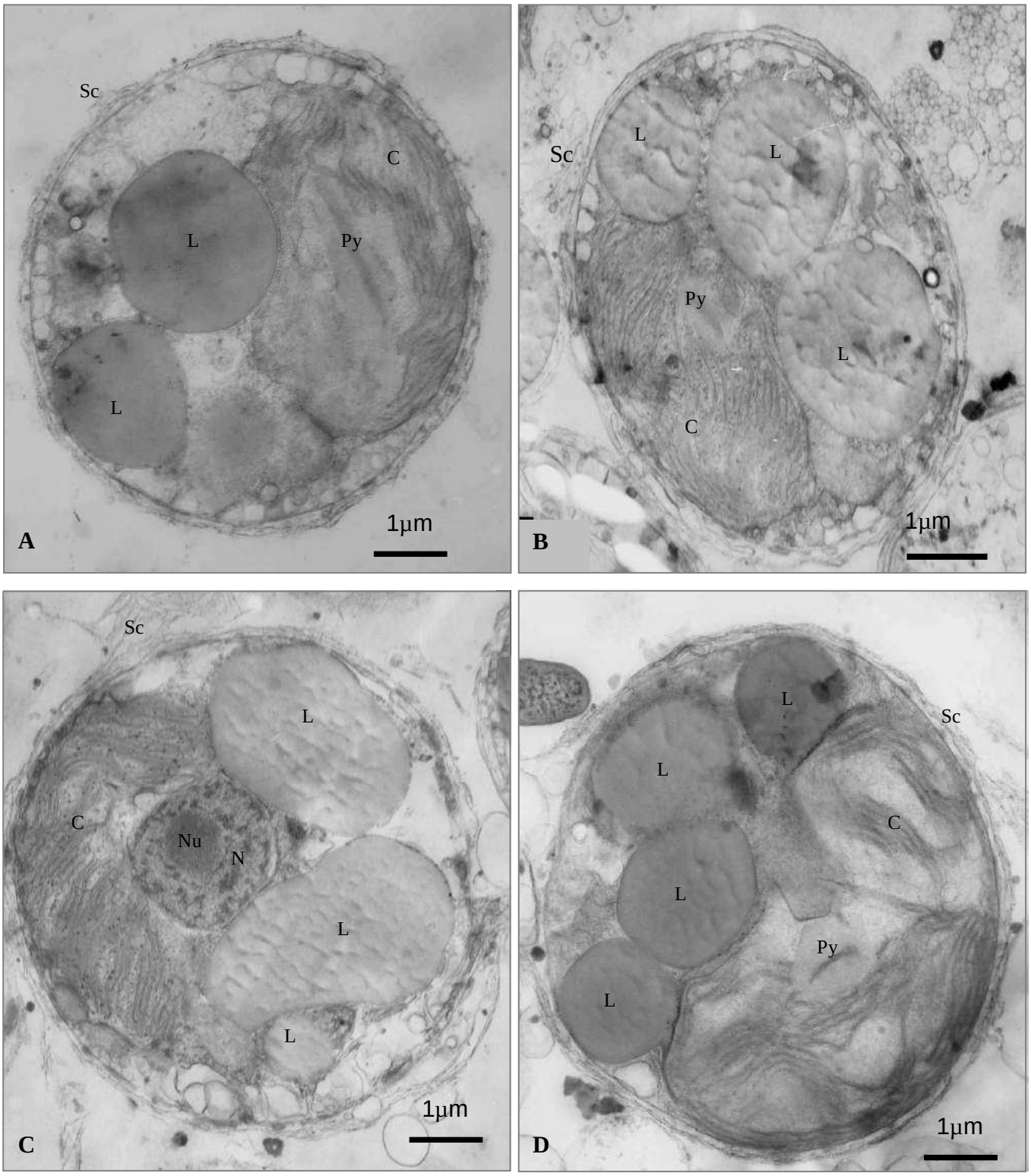

Figure 5.4.2 (A-D): Longitudinal sections through stationary phase cells. Abbreviations: C-Chloroplast; M-Mitochondria; N-Nucleus; Py-Pyrenoid; Nu-Nucleolus; Sc-Scales; L-Lipid.

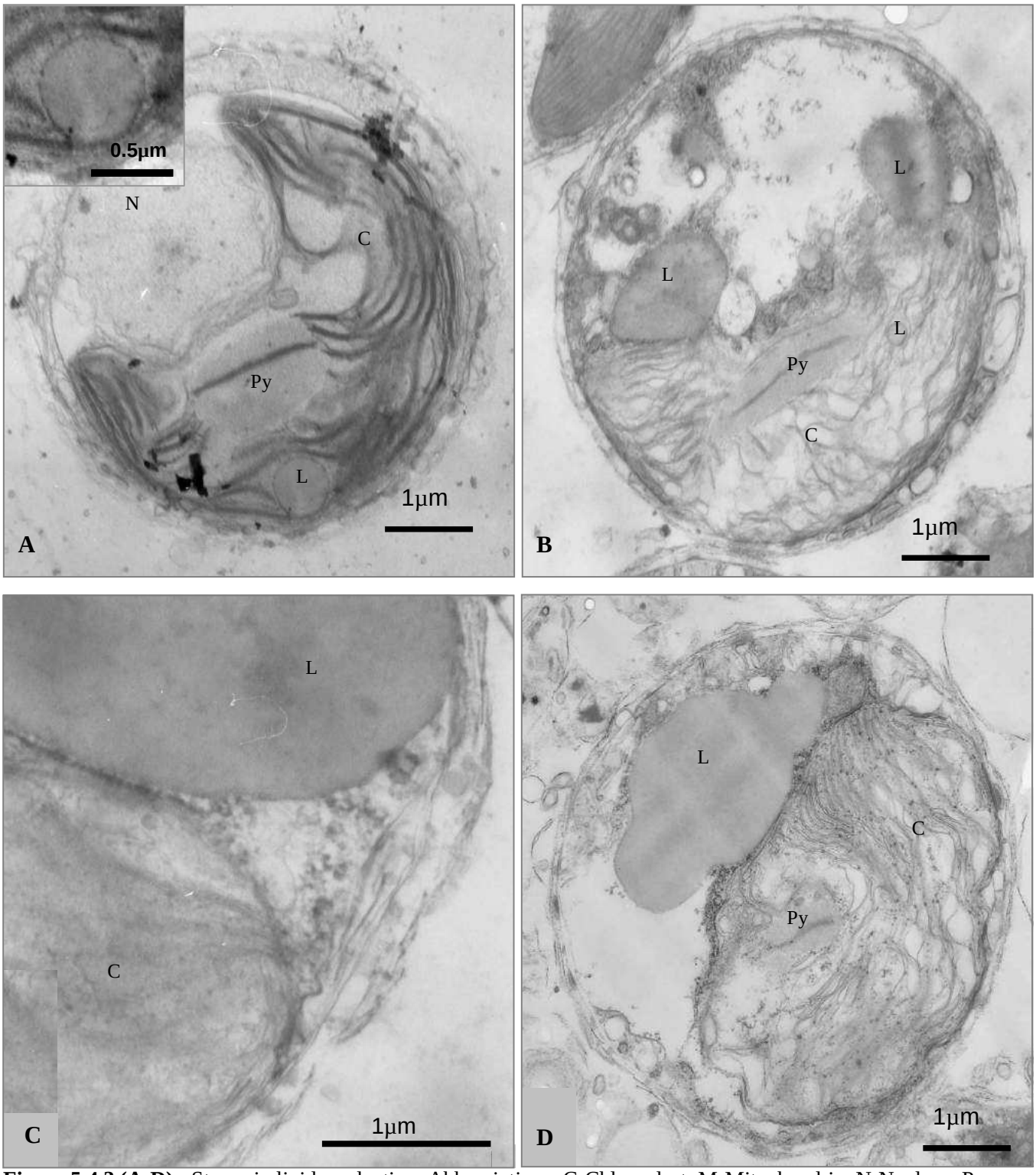

Figure 5.4.3 (A-D): Stages in lipid production. Abbreviations: C-Chloroplast; M-Mitochondria; N-Nucleus; Py-Pyrenoid; L-lipid.

5.3.3 The effect of varying nitrogen concentrations on *I. galbana* U4

Isochrysis galbana was cultured in *f/2* medium containing various levels of nitrogen which enabled the comparison of multiple nitrogen conditions ranging from nitrogen starved to nitrogen replete cultures. The luxury uptake of nitrogen was clearly demonstrated by *I. galbana* (cf. Figures 5.5 and 5.6). The complete uptake of all measurable levels of nitrogen from the medium did not correspond with a decrease in the biomass productivity in any of the nitrogen treatments (cf. Figures 5.5 and 5.6). This was expected since luxury uptake of nitrogen from the medium and gradual utilization of intracellular nitrogen by this microalgal species has been previously demonstrated (Section 5.3.1).

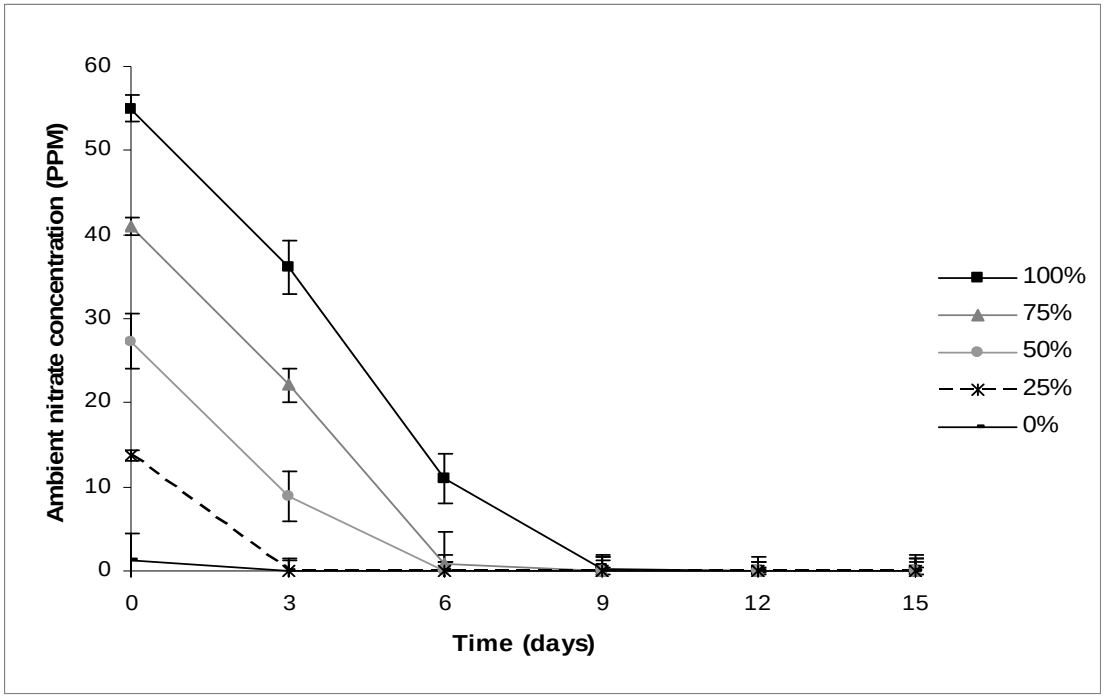

Figure 5.5: A decrease in the ambient nitrate concentration with respect to time in *I. galbana* cultures containing varying sodium nitrate levels as indicated. Error bars represent standard deviation (n = 3).

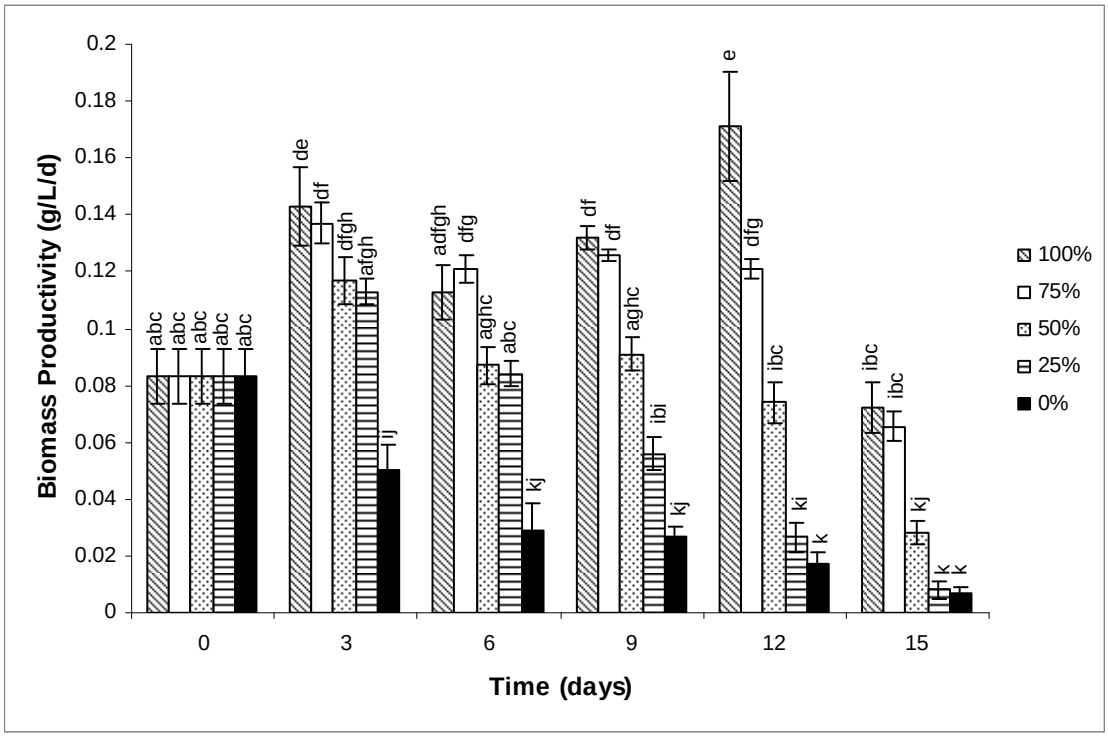

Figure 5.6: The effect of varying nitrate concentrations on *I. galbana* biomass productivities observed over 15 days. Error bars represent standard deviation (n = 3). Different letters on the upper portion of each bar indicates where significant differences exist between treatments at various time intervals ($P < 0.05$).

The biomass productivity in treatments supplied with nitrogen initially increased, but gradually decreased in the nitrogen starved treatment (0%) throughout the experiment (Figure 5.6). This is expected since nitrogen is mandatory for growth. However, the absolute halt in algal growth should be represented by biomass productivities closely bordering on zero since biomass productivity measures the change in biomass yield over a time period. Biomass productivities that were greater than zero in the nitrogen starved treatment, in spite of growth inhibiting conditions (no nitrogen), implies that the dry weight measurements are influenced by other factors excluding the concentration of cells.

An elevated biomass yield in the early stages of nitrogen starvation in microalgal species is not new (Li *et al.*, 2008b; da Silva *et al.*, 2009; Pruvost *et al.*, 2009; Pruvost *et al.*, 2011; Msanne *et al.*, 2012). Some investigators attribute this phenomenon to the *de novo*

synthesis of fatty acids which contributes to the weight of the cells (da Silva *et al.*, 2009). The cells cultured in the nitrogen starved medium would indeed be in the stationary phase of growth since late lag/early stationary phase cells were used as the inoculum and these cells were cultured under stressful conditions (N starvation). The stationary phase, in the species of *Isochrysis* used, is associated with the rapid accumulation of storage lipids (Chapter 3). The elevated lipid yield in the nitrogen starved cells in comparison to all other treatments is shown in Figure 5.7. Hence, the biomass productivity measurements in this study were most probably influenced by the cell growth stage and concomitant increase in intracellular lipid. The increase in the cell weight due to lipid accumulation is verified by the biomass productivity (in the nitrogen starved treatment – 0% nitrate) approaching zero towards day 15, when lipid accumulation started to cease (cf. Figures 5.6 and 5.7).

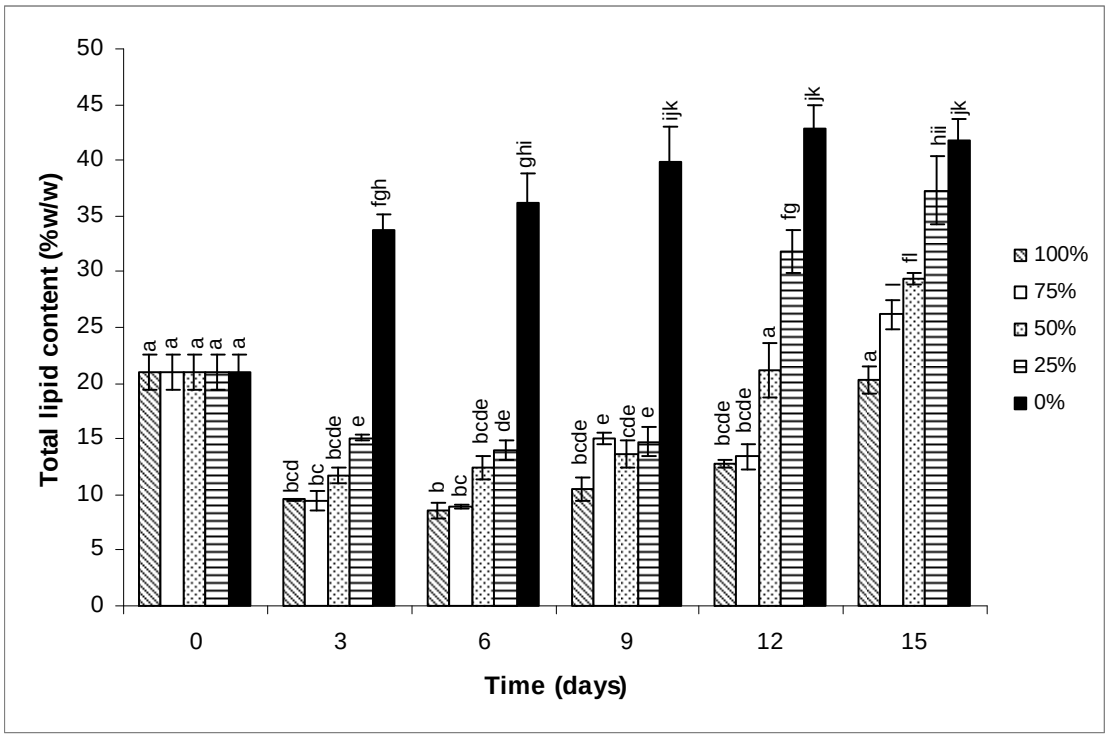

Figure 5.7: The effect of varying nitrate concentrations on *I. galbana* lipid yield observed over 15 days. Error bars represent standard deviation (n = 3). Different letters on the upper portion of each bar indicates where significant differences exist between treatments at various time intervals ($P < 0.05$).

A trend was noted in the cultures that were supplemented with nitrogen where the biomass productivity increased and thereafter declined. This observation was pronounced in the 100% nitrate treatment where the biomass productivity reached a peak on day 12 (Figure 5.6). Similar results (peaks in biomass productivities) with *I. galbana* have been observed elsewhere but have not been explained (Breuer *et al.*, 2012). A possible reason for the peak in the biomass productivity could be the initiation of lipid synthesis accompanied by the increase in the cell yield during that instant. As previously stated, lipid accumulation results in the increase in the cell weight. A slight increase in the lipid yield was observed in the 100% nitrate treatment on day 12 (Figure 5.7). That lipid increase, coupled with the increase in the cell yield, possibly resulted in the biomass productivity peak. The rapid decline in the biomass productivity that followed could be as a result of growth cessation (stationary phase reached), in response to nitrogen starvation or light limitation (Figure 5.8; 100% treatment demonstrated an elevated culture density which would inhibit light penetration). Hence, the reduced biomass productivity, on day 15 in the 100% treatment (Figure 5.6), was due to the cellular weight being solely attributed to lipid synthesis and not cell division.



Figure 5.8: Observed densities of cultures at various nitrate concentrations (as marked on the vessels) 15 days after inoculation.

The daily biomass productivities of each nitrogen treatment were a direct consequence of the concentration of nitrogen supplied and not any other nutrient or culture condition. This is indicated in Figure 5.6 where the biomass productivities, from day 3 onwards, were proportional to the nitrogen concentration in the medium (i.e. lower nitrogen concentrations resulted in reduced biomass productivities and vice versa). This is further supported by the appearance of the cultures on day 15 (Figure 5.8), the densities of which were proportional to the nitrogen concentration used in the medium.

The level of lipid in cells of the inoculum was considerably higher (about 20% w/w; Figure 5.7) than those normally experienced in rapidly growing cells (about 5 - 10%) and shows that these cells were nitrogen starved and in the early stationary phase upon commencement of the experiment. This validates the rapid increase in lipid yield in the nitrogen starved treatment (0%) by day 3 (Figure 5.7) since nutrient stressed cells rapidly accumulate storage lipids as a survival mechanism (Rodolfi *et al*., 2009). The elevated lipid yield in the nitrogen starved treatment (0%) could have been due to less growth being initiated in this treatment because of N-limitation, therefore less suspended cells resulting in lower levels of cell-cell self shading. This in turn results in reduced photo-limitation in the N-starved treatment than in all other treatments. Hence, individual N starved cells received adequate light energy to fuel lipid production. The treatments receiving nitrogen (25% - 100%) became very dense with time since the nitrogen levels stimulated growth and division (Figure 5.8). The denser the culture, the more self shading, resulting in lower levels of light being received by the cells to fuel lipid synthesis. Hence, the lipid yields in the treatments ranging from 25% to 100% were not as high as the yield obtained in the 0% treatment.

As nitrogen levels depleted in the milieu of those treatments receiving N, the lipid yield increased. It is likely that the lipid yields in the various N-fed treatments would have approached the level in the 0% treatment if the experiment had been pursued longer. The cells in the 25% treatment accumulated almost as much lipid as the cells in the 0% treatment by day 15 (Figure 5.7). The lipid yield tended to stabilize after the initial big spurt in the 0% treatment (Figure 5.7). This could be in response to the limited storage

capacity of the cells that need to store essential organelles (e.g. chloroplast, nucleus etc.) and the storage lipid reserves. A halt in lipid synthesis could also have been induced by the reduction in chlorophyll levels when N was limiting, since N is necessary for chlorophyll synthesis. These reduced levels of chlorophyll would result in a decline in the photosynthetic activity including lipid synthesis. Thus, there is an upper limit to the lipid accumulating capacity of *I. galbana* cells.

An initial, much higher lipid productivity was observed in the nitrogen-starved treatment (0%) in comparison to all other N treatments (Figure 5.9). This is due to the high lipid yield in this treatment (Figure 5.7) which compensates for the reduced biomass productivity (Figure 5.6; day 3). A more gradual increase in the lipid productivities was observed in the remaining treatments (25% - 100%) until day 3 (Figure 5.9). The initial increase in the lipid productivities in all treatments is attributed to the delay in the adaptation of the cells to new nitrogen conditions (Lacour *et al.*, 2012a). The N-starved cells in the inoculum were already in lipid overdrive and this is immediately switched off when intracellular N requirements are sated. This is more rapidly achieved in media with higher ambient concentrations of N, so a graded and differential response in lipid productivity is noted in response to varying levels of N in the medium.

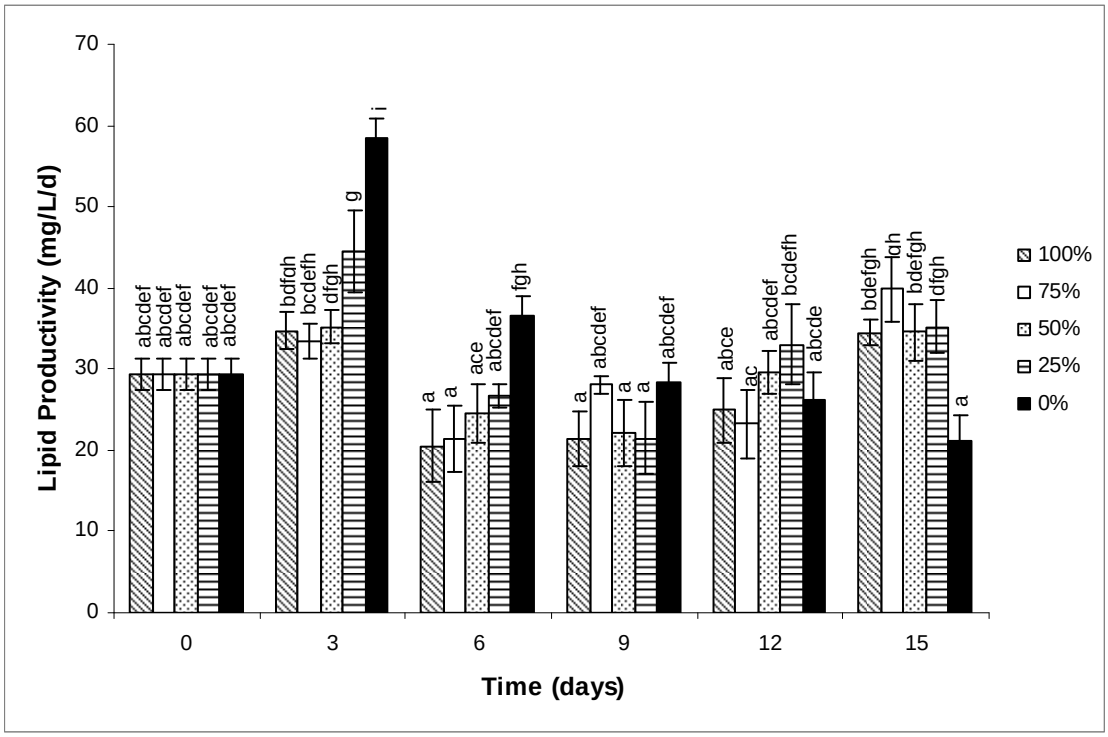

Figure 5.9: The effect of varying nitrate concentrations on *I. galbana* lipid productivity observed over 15 days. Error bars represent standard deviation (n = 3). Different letters on the upper portion of each bar indicates where significant differences exist between treatments at the various time intervals ($P < 0.05$).

As the experiment progressed (day 12-15; Figure 5.9) the lipid productivities of the N-fed treatments (25% to 100%) progressively overtook and ultimately became significantly greater than that of the N-starved (0%) treatment (Figure 5.9). As expected, accompanying these increases in the lipid productivities (Figure 5.9) was the decrease in the biomass productivities (Figure 5.6) and the increase in the lipid yield (Figure 5.7) in the cells of the respective treatments. It is clear that lipid yield, rather than biomass productivity has a greater influence on the eventual lipid productivity of this species since lipid accumulated at a higher rate than the reduction in the biomass concentration during the early stationary phase (Table 5.2). The dominating effect of lipid yield on lipid productivity measurements is proven by the reduced lipid productivities experienced in the N-starved (0%) culture as time progressed. The rate of lipid accumulation in this treatment dwindled with time, due to the maximal lipid capacity of the cells being reached, which impacted greatly on the lipid productivity which declined rapidly (cf.

Figures 5.7 and 5.9). Hence, the lipid productivity is reduced in highly stressed (late stationary) *I. galbana* cells.

Table 5.2: Rates of biomass productivity decrease in comparison with the increase in the rates of lipid accumulation and their corresponding regression coefficients in *I. galbana* cultures grown in the various treatments as indicated.

Treatment	**Rate of Biomass Productivity Decrease (% decrease/day)** [a]	**Regression coefficient**	**Rate of Lipid Accumulation (%w.w^{-1}/day)**	**Regression coefficient**
0% $Na(NO)_3$	-2.45	0.9342	5.87	0.8641
25% $Na(NO)_3$	-6.68	0.9944	8.72	0.8945
50% $Na(NO)_3$	-4.78	0.8533	5.85	0.9258
75% $Na(NO)_3$	-3.58	0.6547	4.99	0.7783
100% $Na(NO)_3$	-2.10	0.1302	3.72	0.8875

[a]Negative rates represent the decrease in the biomass productivity over time and the negative symbol can be disregarded when comparing the rates of lipid accumulation and biomass productivity reduction.

If the rate of lipid accumulation mirrored the rate of biomass reduction, a constant lipid productivity would have been observed. Lipid productivity in N-fed cultures was somewhat stable between days 6 and 9 (Figure 5.9). In this window period, the cells were not nitrogen starved and were growing exponentially (evidenced by a relatively reduced accumulation of storage lipid, generally highest levels of maintained biomass productivities and hence constant lipid productivities). During this window, no significant fluctuations in the lipid productivities ($P > 0.05$) were found, making levels of lipid productivity independent of the nitrogen concentration in the medium. However, the lipid productivity of cells in the N-free treatment, during this window was not stable (Figure 5.9), but rather irregular and relatively elevated and dependent on the levels of lipid being expressed and the levels of growth of the culture. Thus, fluctuations in lipid productivity are indeed initiated by cellular stresses such as N limitation as proven here.

The N limitation induced increases in lipid productivity observed here are in concert with those of Griffiths *et al*. (2012) working on numerous isolates including *Isochrysis*, but contradict those of the Aquatic Species Program (Sheehan *et al*., 1998). Several other investigators also show that lipid productivity may be improved by invoking nitrogen limitation (Takagi *et al*., 2000; Hsieh and Wu, 2009; Rodolfi *et al*., 2009). The finding of elevated lipid productivities in *I. galbana* under such conditions in the present study is important as it should inform the timing of culture harvesting. *Isochrysis* cells should ideally be harvested when lipid productivity peaks, so that the highest yield of lipid can be extracted without drastically effecting the concentration of biomass.

5.4 CONCLUSION

The intracellular nitrogen content determines the rate of growth, hence the initiation of lipid synthesis in *Isochrysis galbana* when the ambient N levels are depleted. It may be deduced that the pigment concentration (chlorophyll content and carotenoid to chlorophyll ratio) is strongly related to the nutrient status of the culture. Multiple ultrastructural changes are associated with internal nitrogen depletion. These include the dismantling of the chloroplast structure, the reduction in the pyrenoid size and the production of plastidial and cytoplasmic lipid bodies.

It is clearly evident that an elevated lipid productivity may be achieved in this species (as much as 60 mg/L/day). Although a distinct inverse relationship between lipid accumulation and biomass productivity was observed, lipid productivity, which a function of the two, was not constant throughout the growth period. This is because lipid productivity is influenced more by lipid yield than by biomass productivity. The greatest lipid productivities were obtained during the early stationary phase and declined towards the late stationary phase when lipid ceased to accumulate. Hence, lipid productivity is also influenced by the culture age. It is of great importance to select the appropriate instant for algal harvesting which corresponds to the maximal lipid productivity.

5.5 SUPPORTING INFORMATION

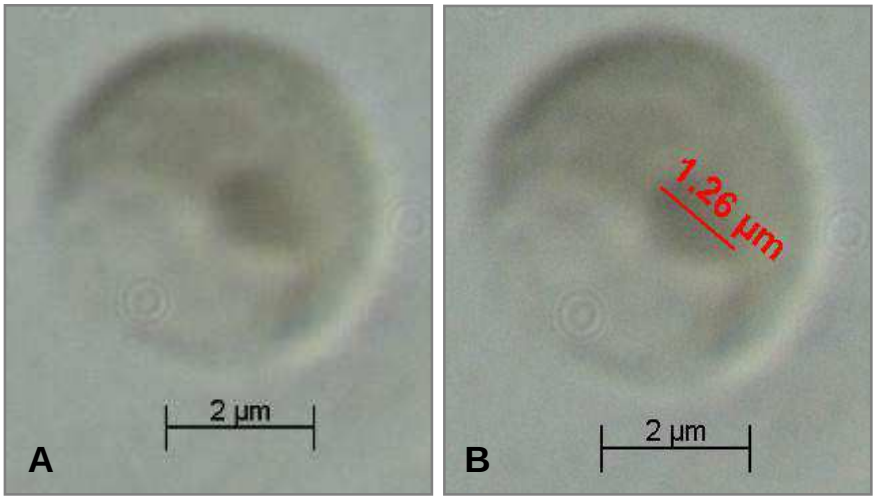

Figure S1: Light microscopy images of *Isochrysis galbana* U4 cells showing **(A):** pyrenoid located in the plastid and **(B):** pyrenoid measurement using Zeiss AxioVision microscopy software

CHAPTER SIX

The Effect of Nitrogen Source on Growth, Biochemical Composition and Ultrastructure of *Isochrysis galbana* U4

6.1 INTRODUCTION

Healthy microalgal cells consist primarily of carbon, oxygen, nitrogen and hydrogen (South and Whittick, 1987). Of these elements, carbon constitutes approximately half the dry cell weight and nitrogen accounts for about one-twelfth of healthy algal dry weight. Oxygen and hydrogen make up majority of the remainder of the algal cell but these elements are easily accessible from water (Syrett, 1988). Thus, algal growth is determined mostly by the availability of nitrogen and carbon. Alterations of these elements in the growth environment induce changes in the chemical composition of microalgal cells. One such alteration is the source of nitrogen in the growth medium (Xu *et al*., 2001).

Numerous forms of nitrogen are available in the natural environment, both inorganic and organic. The dominant sources of inorganic nitrogen include nitrogen gas, ammonium, nitrate and nitrite and of organic nitrogen include urea, glutamine and amino acids (Syrett, 1988; Levasseur *et al.*, 1993). Nitrogen gas is readily reduced to ammonia by some prokaryotes in a process referred to as nitrogen fixation. However, eukaryotic algae are incapable of fixing atmospheric nitrogen. They require fixed nitrogen (e.g. nitrate or ammonium) which they convert to organic nitrogen in a process referred to as nitrogen assimilation (Barsanti and Gualtieri, 1996). Regardless of the fixed nitrogen source, a conversion to ammonium is required prior to nitrogen incorporation into cellular organic compounds (Figure 6.1; South and Whittick, 1987).

When microalgal cells are cultured in medium containing nitrate, urea and ammonium the preferred nitrogen source is ammonium followed by nitrate and then urea (South and Whittick, 1987; Syrett, 1988; Levasseur *et al.*, 1990). This observation has been attributed to the much more reduced state of ammonium in comparison to nitrate. Urea and ammonium have a similar reduction state thus the preference of ammonium over urea may not be attributed to this factor (Levasseur *et al.*, 1993). The assimilation of urea requires energy that is not required with the direct assimilation of ammonium which is probably why ammonium is preferred over urea.

Nitrate reduction to ammonium occurs in a two-step process and requires the presence of two enzymes namely, nitrate reductase and nitrite reductase. Nitrate reductase utilizes NADPH for the catalysis of nitrate (NO_3^-) to nitrite (NO_2^-) via a double electron transfer:

$$NO_3^- + 2e^- + 2H^+ \rightarrow NO_2^- + H_2O$$

Nitrite is reduced to ammonium (NH_4^+) in a six-electron transfer reaction that is catalysed by nitrite reductase with the aid of ferrodoxin:

$$NO_2^- + 6e^- + 8H^+ \rightarrow NH_4^+ + 2H_2O$$

Thus eight electrons are required for the reduction of nitrate to ammonium (Figure 6.1; Barsanti and Gualtieri, 1996). This represents double the amount of electrons required for the reduction of carbon dioxide to carbohydrates, emphasizing the high energy requirement for nitrate assimilation (South and Whittick, 1987).

Like nitrate and nitrite, urea ($CO(NH_2)_2$) also needs to be converted to ammonium prior to assimilation. This process is catalyzed by the enzyme urease (Figure 6.1; Syrett, 1988; Levasseur *et al.*, 1993):

$$CO(NH_2)_2 + H_2O + 2H^+ \rightarrow CO_2 + 2NH_4^+$$

Urea reduction results in the production of two ammonium molecules.

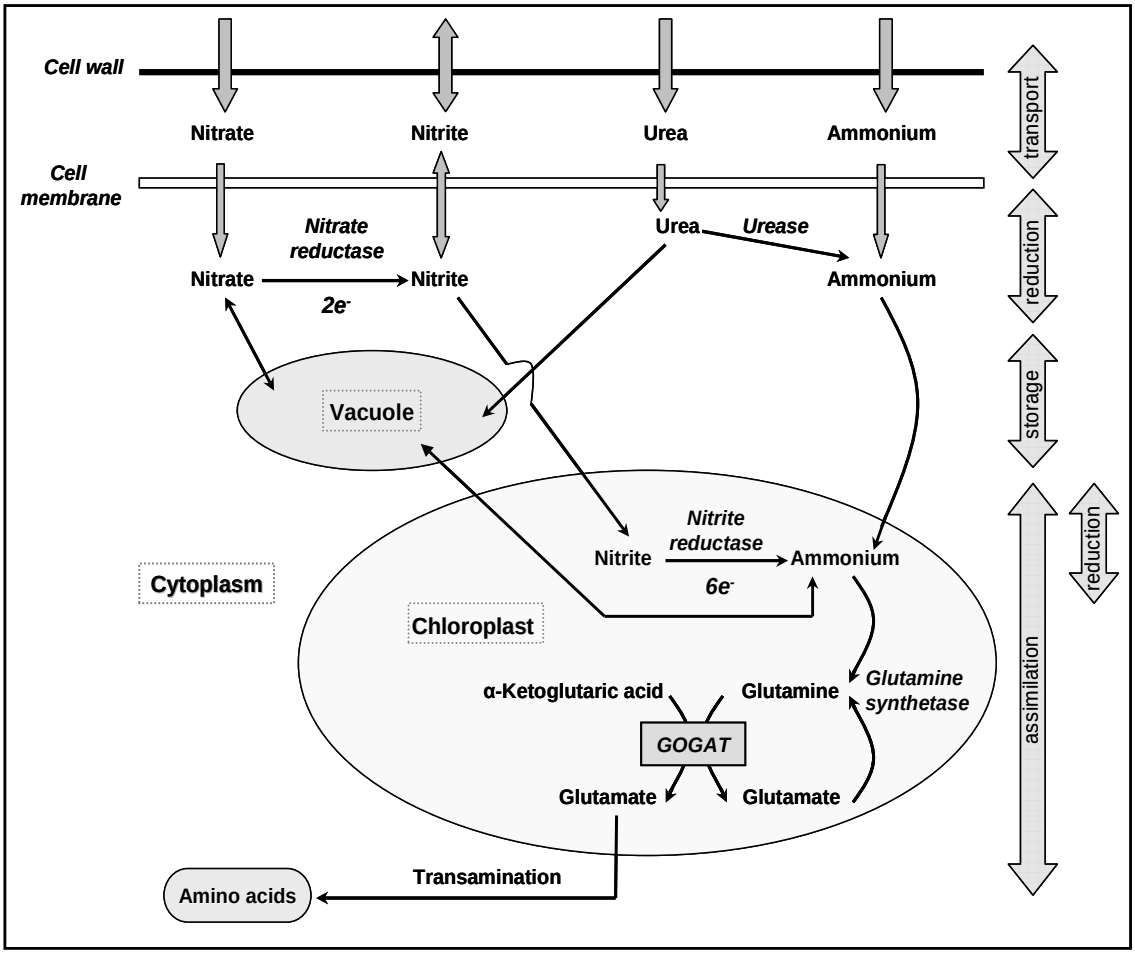

Figure 6.1: Schematic representation of intracellular pathways involved in nitrogen uptake, storage, assimilation and partitioning in an algal cell (enzymes are italicized) (adapted and modified from South and Whittick, 1987 and Mulholland and Lomas, 2008).

The production of amino acids from ammonium is carried out with the aid of two enzymes namely, glutamine synthetase (GS) and glutamine 2-oxoglutarate aminotransferase (GOGAT) (Figure 6.1 and Figure 6.2). Glutamate is required as the substrate for ammonium assimilation into glutamine by GS and the energy fueling the reaction is obtained from ATP (Figure 6.2). Two molecules of glutamate are then formed due to the transfer of the amino nitrogen of glutamine to α-ketoglutaric acid by GOGAT (Figure 6.2). One glutamate molecule is recycled back into the cycle whilst the other is mobilized to the cytosol. The cytosolic glutamate is the principal amino donor to other amino acids via. transamination reactions (Figure 6.1; South and Whittick, 1987; Barsanti and Gualteri, 1996).

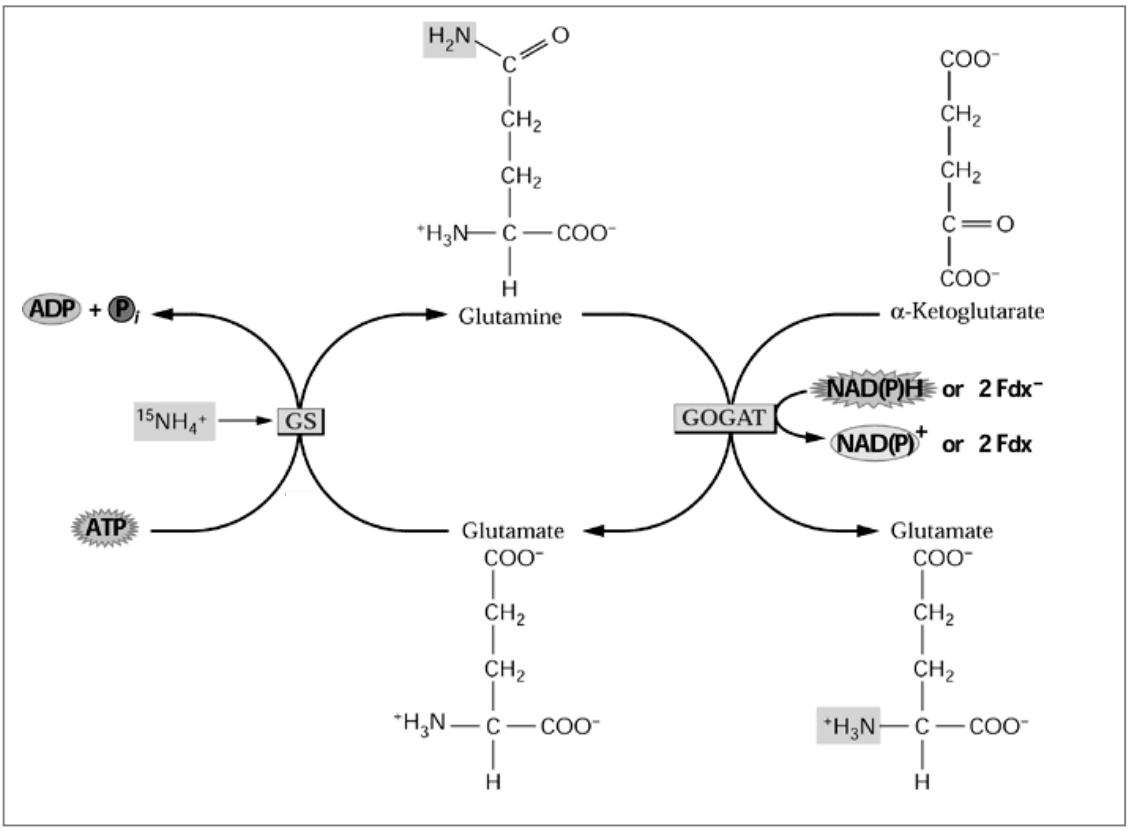

Figure 6.2: Structural representation of ammonium assimilation into glutamine and glutamate production (http://www.uky.edu/~dhild/biochem/24/fig08_05.png).

The choice of the nitrogen source to be used in the mass culture of microalgae has implications on the overall cost of the culture process. The use of a cheaper nitrogen source would be beneficial in terms of cost reductions but also needs to promote elevated levels of growth and lipid production capabilities. This study is aimed at selecting a cost effective nitrogen source for the mass culture of the *Isochrysis galbana* U4 and determining the effect of nitrogen source (nitrate, ammonium or urea) on the growth, biochemical composition (pigmentation, lipid and carbohydrate yield) and ultrastructure of the alga. The broad spectrum of nitrogen containing salts tested in the study enabled a clear comparison of treatments. The elevated energy requirement for the reduction of nitrate was taken into consideration when analysing the data obtained and a comparison between the responses to organic (urea) vs. inorganic (nitrate and ammonium) nitrogen sources was conducted.

6.2 MATERIALS & METHODS

6.2.1 Experimental setup

Growth experiments were conducted in 1 L modified aerated Schott® bottles (Section 2.3). The bottles and glass tops, equipped with the gas inlet and outlet, were thoroughly cleaned and autoclaved (121 °C for 30 minutes) prior to use. Seawater was filtered and autoclaved (Section 2.1) prior to use. All vessels were sparged with filtered (Whatman® uniflo 0.2 µm) air and incubated at approximately 25 °C and under a photon flux density of 110 µmol photons.m^{-2}.s^{-1} with a 10:14 light-dark cycle. The position-dependant influence of the light source on each culture vessel was minimized by the daily random relocation of each of them. Each nitrogen treatment was conducted in quadruplicate.

Seven nitrogen treatments were tested. These included sodium nitrate, potassium nitrate, ammonium nitrate, urea, ammonium sulphate, ammonium chloride and ammonium bicarbonate. All treatments experienced the same final nitrogen concentration as that in *f/2* medium (Guillard and Ryther, 1962).

6.2.2 Analytical methods

The cell concentration, lipid and carbohydrate content were determined as described in Sections 2.5, 2.7 and 2.14.1 respectively. The alkalinity of the medium was recorded using a pH meter (Precisa pH900). The chlorophyll content and the ratio of carotenoids to chlorophyll were determined as discussed in Section 2.15. Intracellular nitrogen and phosphorous was extracted from the algal cells and quantified using colorimetric measure as previously described (Sections 2.14.2 and 2.14.3 respectively). The salicylic acid method was used to determine the amount of nitrate (Cataldo, 1974; Section 2.13.1) and the Idophenol Blue method (Scheiner, 1976; Section 2.13.2) was used to determine the amount of ammonium in the culture medium. Ammonium and nitrate controls were setup. These controls were maintained under the conditions described previously (Section 6.2.1) and only differed from the experiments in that they were not inoculated with algal cells. The pH, ammonium and nitrate levels were monitored in the control treatments.

6.2.3 Ultrastructural analysis and cellular measurements

Exponential and stationary phase cells were embedded, sectioned and viewed using a transmission electron microscope (FEI Spirit) at an accelerating voltage of 120 kV, as described in Section 2.12.1. Embedded cells, polymerized under a coverslip on microscope slides, were viewed with a Zeiss Axiophot light microscope with Nomarski optics at 400 times magnification. Zeiss AxioVision microscopy software was used for cell measurements. Each value shown is an average of fifty cell measurements for each treatment.

6.2.4 Statistical analysis

The software SPSS 20 (Statistical Program for Social Sciences 20) was used to perform statistical analyses as mentioned in Section 2.17.

6.3 RESULTS

6.3.1 Growth and carbon storage

Isochrysis galbana U4 was capable of growing in *f/2* medium supplemented with all the different nitrogen sources used in the study (Figure 6.3) and none had a significantly different effect on the exponential growth rate of *Isochrysis* relative to the others (Table 6.1). The post-exponential growth rates varied significantly between the nitrate, ammonium and urea treatments (Table 6.2). Cultures grown with sodium nitrate resulted in the greatest rate of post-exponential growth and the highest final cell concentration. Potassium nitrate and urea grown cultures demonstrated similar post-exponential growth rates and final cell yields. Ammonium chloride and ammonium sulphate also showed a similar trend in post exponential growth however the final cell yield in these treatments were significantly lower than that obtained in the urea and nitrate treatments. The ammonium bicarbonate treatment resulted in the lowest final cell yield and the final cell yield in the ammonium nitrate treatment lies exactly between that obtained in the other nitrate and ammonium treatments (Table 6.2; Figure 6.3).

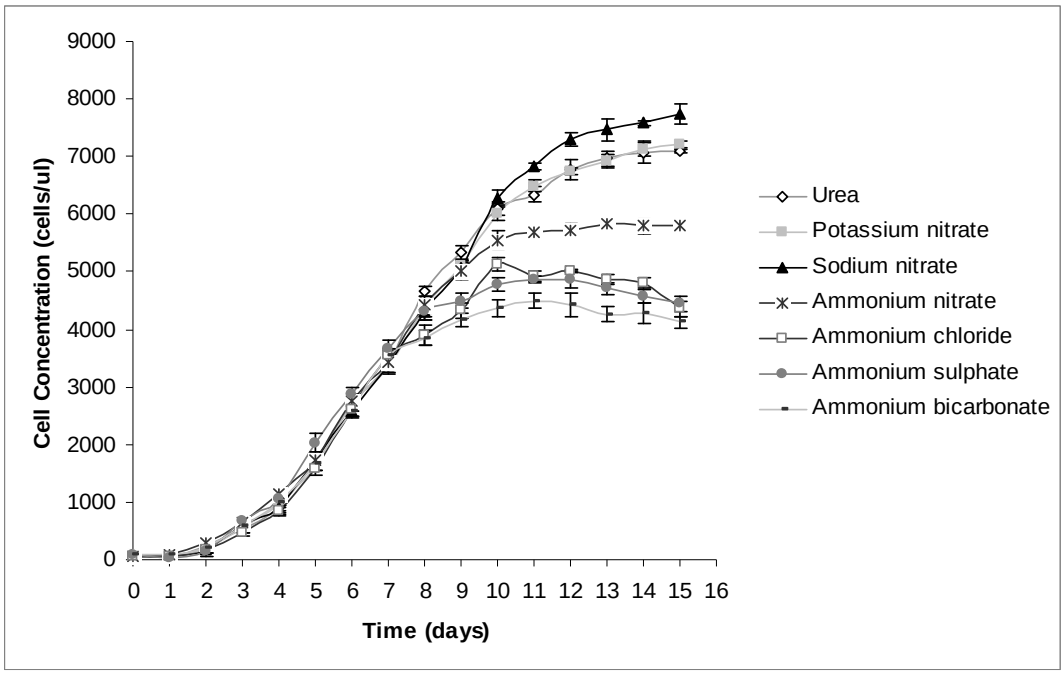

Figure 6.3: *I. galbana* growth in *f/2* medium supplemented with various nitrogen sources. Error bars represent standard deviation (n=4).

Table 6.1: Rates of *I. galbana* growth (Day 2 – 7), their regression coefficients and the significant differences between the growth rates in the various treatments as indicated.

Treatment	**Rate (Cells.ul^{-1}/day)**	**Regression coefficient**	**Significant differences***
Urea	0.2960 ± 0.0061	0.9617	A
Potassium nitrate	0.2995 ± 0.0037	0.9669	A
Sodium nitrate	0.3087 ± 0.0119	0.9724	A
Ammonium nitrate	0.2938 ± 0.0084	0.9722	A
Ammonium sulphate	0.3093 ± 0.0025	0.9809	A
Ammonium bicarbonate	0.2912 ± 0.0089	0.9632	A
Ammonium chloride	0.3056 ± 0.0021	0.9484	A

* Rates with the same letters are not significantly different (P > 0.05)

Table 6.2: Rates of *I. galbana* growth (Day 7-14), their regression coefficients and the significant differences between the growth rates in the various treatments as indicated.

Treatment	**Rate (Cells.ul^{-1}/day)**	**Regression coefficient**	**Significant differences***
Urea	0.1363 ± 0.0007	0.8661	A B
Potassium nitrate	0.1368 ± 0.0020	0.8868	A B
Sodium nitrate	0.1378 ± 0.0001	0.8984	A
Ammonium nitrate	0.1331 ± 0.0005	0.7191	B
Ammonium sulphate	0.1278 ± 0.0017	0.2880	C
Ammonium bicarbonate	0.1282 ± 0.0007	0.3390	C
Ammonium chloride	0.1282 ± 0.0007	0.3366	C

* Rates with the same letters are not significantly different (P > 0.05)

The nitrogen source had a significant effect on the rates of lipid accumulation in *I .galbana* (Table 6.3). Nitrate grown exponential cells demonstrated a greater lipid yield than cells grown in ammonium supplemented medium. However, as the cultures aged, a rapid increase in the lipid content of ammonium grown cells became evident (in comparison to nitrate grown cells; Figure 6.4). By day 14, the lipid accumulated per cell in cultures grown in ammonium-containing medium was approximately double that observed in the nitrate treatments (Figure 6.4). Cells grown in medium supplemented with urea also displayed an elevated lipid yield in comparison to the nitrate treatments (Figure 6.4; day 10 onwards).

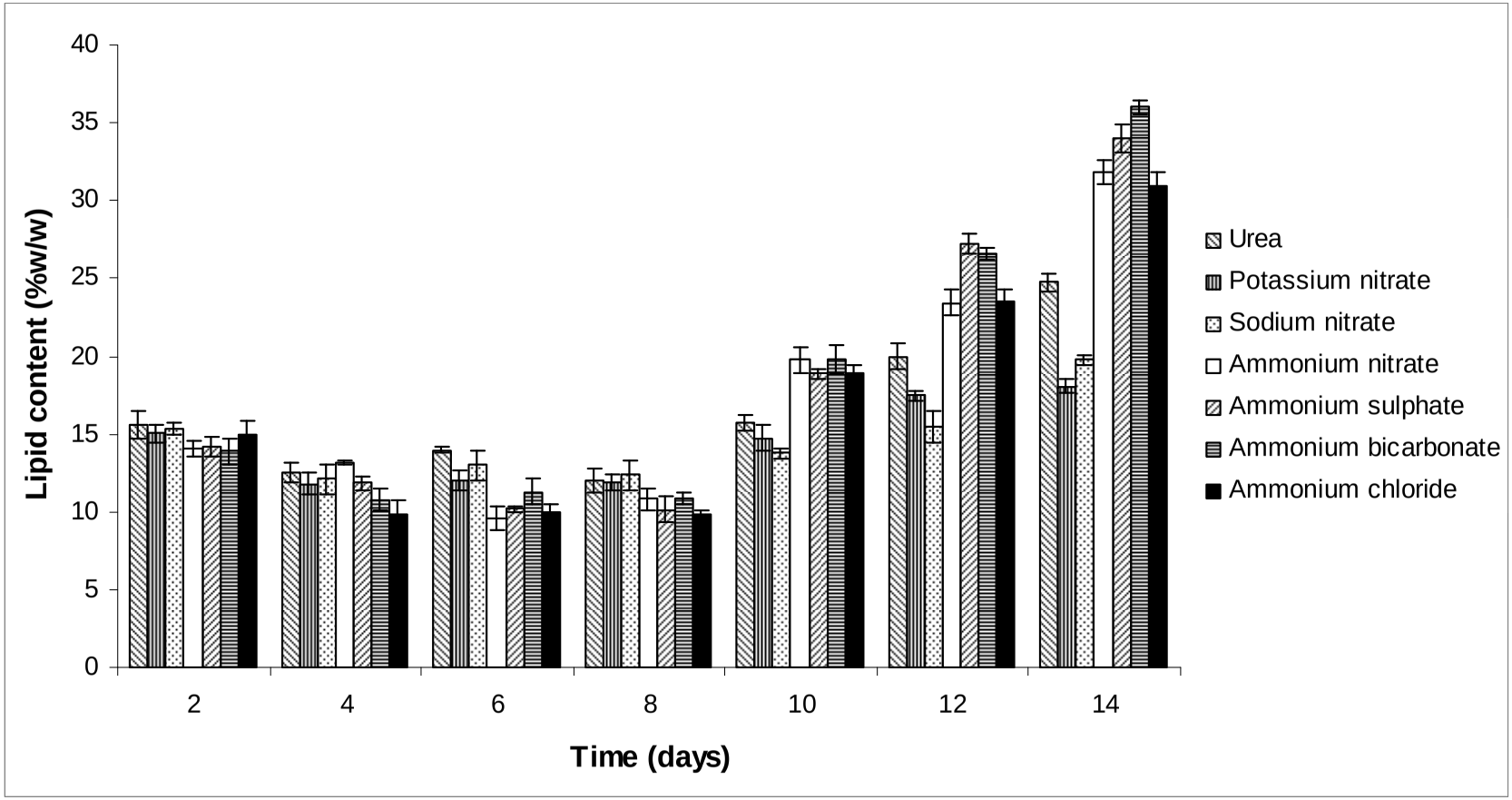

Figure 6.4: Lipid accumulation in *I. galbana* grown in *f/2* medium supplemented with various nitrogen sources. Error bars represent standard deviation (n=4).

Table 6.3: Rates of *I. galbana* lipid accumulation (Day 8-14), their regression coefficients and the significant differences between the rates in the various treatments as indicated.

Treatment	Rate (%w.w^{-1}/day)	Regression coefficient	Significant differences*
Urea	0.2153 ± 0.0042	0.9966	A B
Potassium nitrate	0.1961 ± 0.0050	0.9383	A
Sodium nitrate	0.1978 ± 0.0074	0.9233	A
Ammonium nitrate	0.2420 ± 0.0081	0.9781	B C
Ammonium sulphate	0.2539 ± 0.0074	0.9966	C
Ammonium bicarbonate	0.2505 ± 0.0030	0.9962	B C
Ammonium chloride	0.2499 ± 0.0003	0.9850	B C

* Rates with the same letters are not significantly different (P > 0.005)

In all nitrogen treatments, the carbohydrate content per cell decreased during exponential growth and increased again only as the stationary phase approached (cf. Figures 6.3 and 6.5). No apparent variations in the trends of the various groups of treatments (ammonium, nitrate and urea) were significant (Table 6.4 and 6.5). However, the carbohydrate content per cell in cultures exposed to the ammonium treatments far exceeded that prevalent in cells exposed to either nitrate or urea treatments. The trend in carbohydrate accumulation mirrored that of lipid accumulation with two exceptions i.e. carbohydrate accumulation was initiated prior to lipid accumulation (like in Li *et al*., 2011 and Msanne *et al*. 2012) and the late stationary phase carbohydrate levels in most treatments started to drop whereas the lipid levels continued to increase (cf. Figures 6.4 and 6.5).

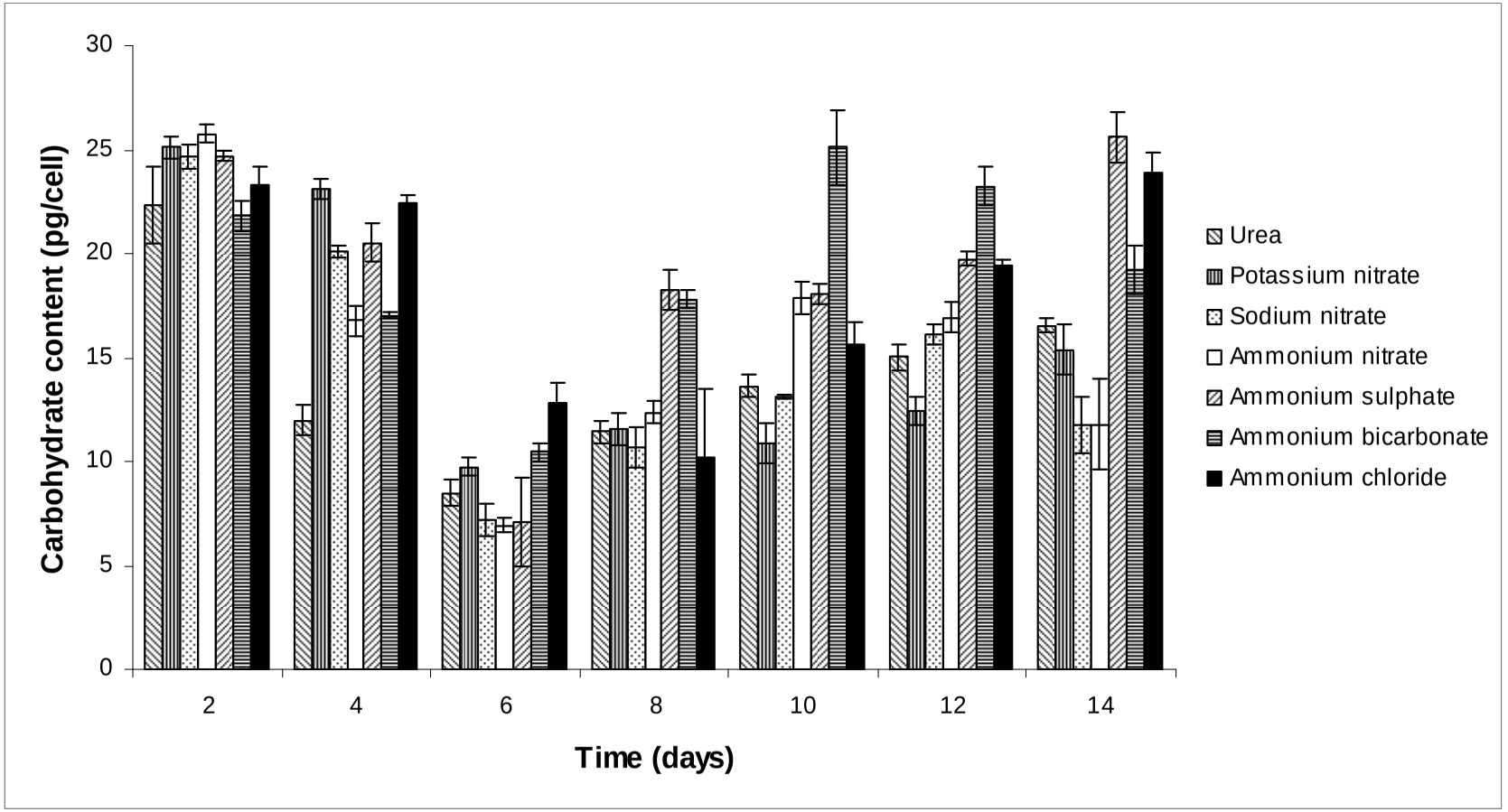

Figure 6.5: Carbohydrate accumulation in *I. galbana* grown in *f/2* medium supplemented with various nitrogen sources. Error bars represent standard deviation (n=4).

Table 6.4: Rates of *I. galbana* carbohydrate accumulation (Day 2-6), their regression coefficients and the significant differences between the rates in the various treatments as indicated.

Treatment	Rate ([Carbohydrate]/day)	Regression coefficient	Significant differences*
Urea	0.1722 ± 0.0110	0.9250	A B
Potassium nitrate	0.1765 ± 0.0021	0.8449	A B
Sodium nitrate	0.1538 ± 0.0094	0.9293	A
Ammonium nitrate	0.1488 ± 0.0030	0.9993	A
Ammonium sulphate	0.1528 ± 0.0121	0.9165	A
Ammonium bicarbonate	0.1903 ± 0.0025	0.9916	A B
Ammonium chloride	0.2025 ± 0.0037	0.8113	B

* Rates with the same letters are not significantly different (P > 0.005)

Table 6.5: Rates of *I. galbana* carbohydrate accumulation (Day 6-14), their regression coefficients and the significant differences between the rates in the various treatments as indicated.

Treatment	Rate ([Carbohydrate]/day)	Regression coefficient	Significant differences*
Urea	0.1645 ± 0.0073	0.9743	A
Potassium nitrate	0.1501 ± 0.0073	0.8148	A
Sodium nitrate	0.1600 ± 0.0011	0.4905	A
Ammonium nitrate	0.1590 ± 0.0157	0.2613	A
Ammonium sulphate	0.2075 ± 0.0171	0.8261	B
Ammonium bicarbonate	0.1575 ± 0.0059	0.4072	A
Ammonium chloride	0.1558 ± 0.0063	0.8419	A

* Rates with the same letters are not significantly different (P > 0.005)

6.3.2 Variation in medium pH, ammonium and nitrate levels

No significant differences in the rate of pH increase between all nitrogen treatments during the early exponential phase (Table 6.6; Figure 6.6) were found. The pH levels in all treatments reached a peak at around day 8 (Figure 6.6). The subsequent rate of pH decrease differed between the ammonium, nitrate and urea treatments (Table 6.7). A rapid decrease in the pH was evident in the ammonium treatments whereas a more subtle

decrease was noted in the nitrate treatments and a relatively stable pH was observed in the urea treatment (Figure 6.6). The rate of pH decrease in the ammonium nitrate treatment fell midway between that observed in the ammonium and nitrate treatments (Figure 6.6).

Table 6.6: Rates of *I. galbana* pH change (Day 0-6), their regression coefficients and the significant differences between the rates in the various treatments as indicated.

Treatment	Rate (pH change/day)	Regression coefficient	Significant differences*
Urea	0.1706 ± 0.0006	0.9709	A
Potassium nitrate	0.1709 ± 0.0004	0.9594	A
Sodium nitrate	0.1700 ± 0.0004	0.8885	A
Ammonium nitrate	0.1705 ± 0.0007	0.9366	A
Ammonium sulphate	0.1697 ± 0.0006	0.7364	A
Ammonium bicarbonate	0.1705 ± 0.0001	0.9889	A
Ammonium chloride	0.1703 ± 0.0006	0.8945	A

* Rates with the same letters are not significantly different (P > 0.05)

Table 6.7: Rates of *I. galbana* pH change (Day 8-14), their regression coefficients and the significant differences between the rates in the various treatments as indicated.

Treatment	Rate (pH change/day)	Regression coefficient	Significant differences*
Urea	0.1660 ± 0.0009	0.5658	A B
Potassium nitrate	0.1662 ± 0.0001	0.5502	A
Sodium nitrate	0.1665 ± 0.0001	0.2013	A
Ammonium nitrate	0.1658 ± 0.0006	0.3657	A B
Ammonium sulphate	0.1634 ± 0.0003	0.9270	B
Ammonium bicarbonate	0.1656 ± 0.0001	0.6164	A B
Ammonium chloride	0.1644 ± 0.0014	0.6075	A B

* Rates with the same letters are not significantly different (P > 0.05)

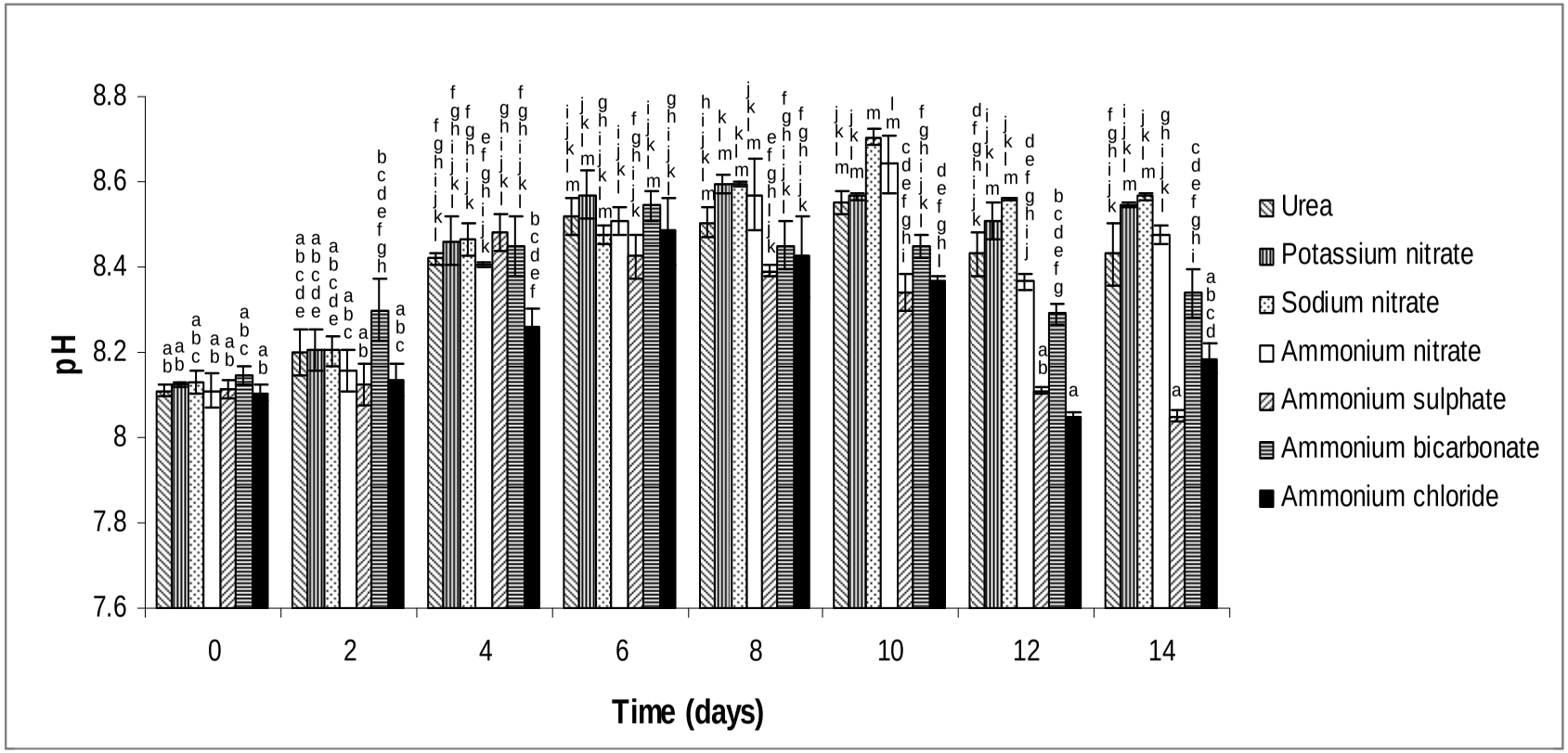

Figure 6.6: the pH of *I. galbana* cultures supplemented with various nitrogen sources. Error bars represent standard deviation (n=4). Significant differences are indicated by different letters above the error bars ($P < 0.05$).

The levels of both ammonium and nitrate in the culture medium decreased rapidly in all algal cultures irrespective of the salt used, but ammonium was depleted much earlier than nitrate was (Figures 6.7a and b; ammonium deplete by day 8 and nitrate deplete by day 10). Similarly, in the ammonium nitrate treatment, the medium was stripped of ammonium before the nitrate reserves began to fall. Controls of the various media containing ammonium salts but lacking cells showed a decrease in ammonium-nitrogen levels with time whereas the N levels in those with nitrate salts remained relatively constant throughout the duration of the experiment (Figures 6.7a and b). The pH of the experimental cultures fluctuated during the course of the experiment (Figure 6.6) but in the controls it remained relatively constant, around pH 8.3, for the duration of the experiment (Figure 6.8).

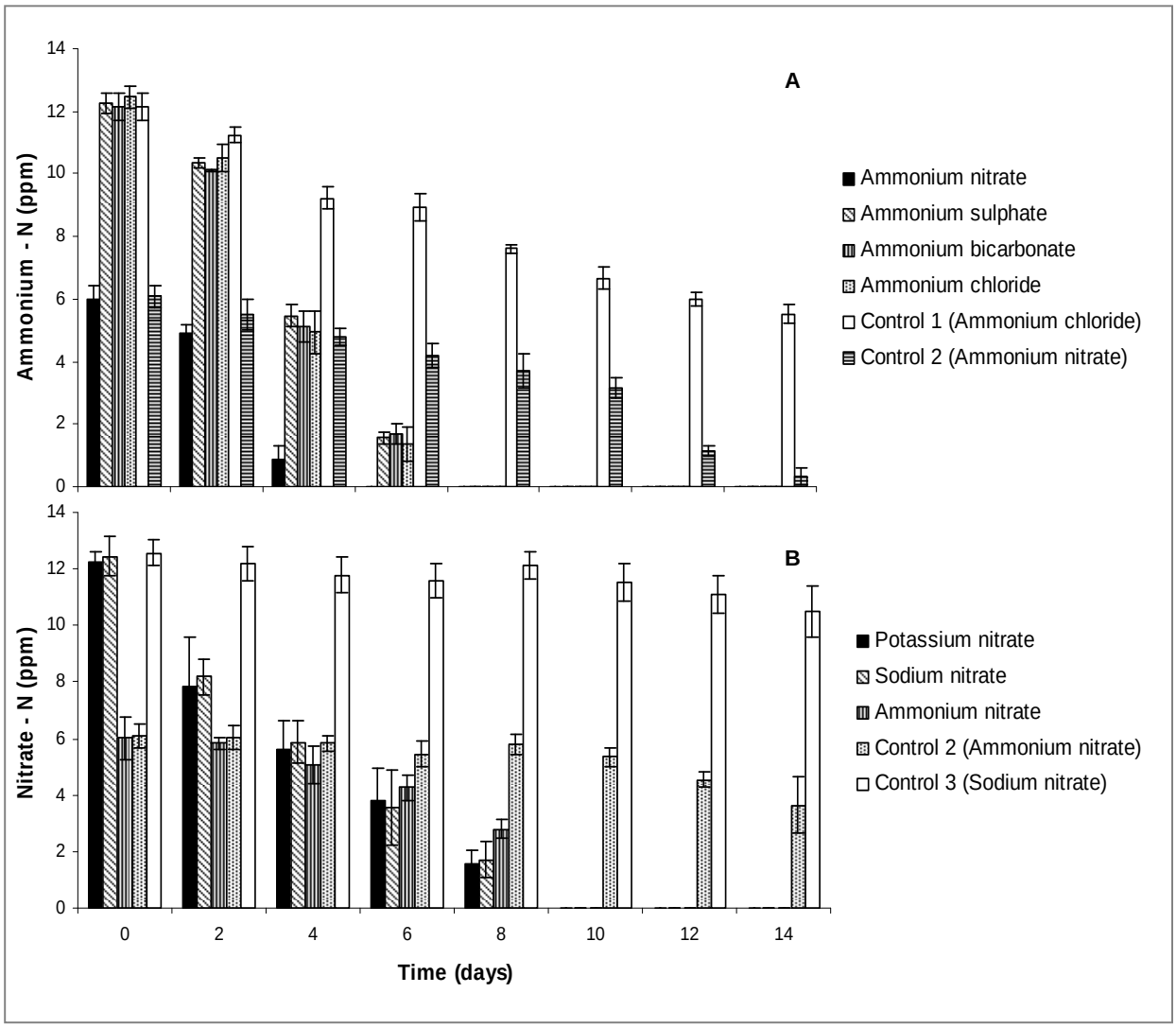

Figure 6.7 (A): The decrease in ammonium-N and **(B):** nitrate-N in the medium of cultures with various nitrogen sources inoculated with *I. galbana* and control cultures lacking cells. Error bars represent standard deviation (n=4).

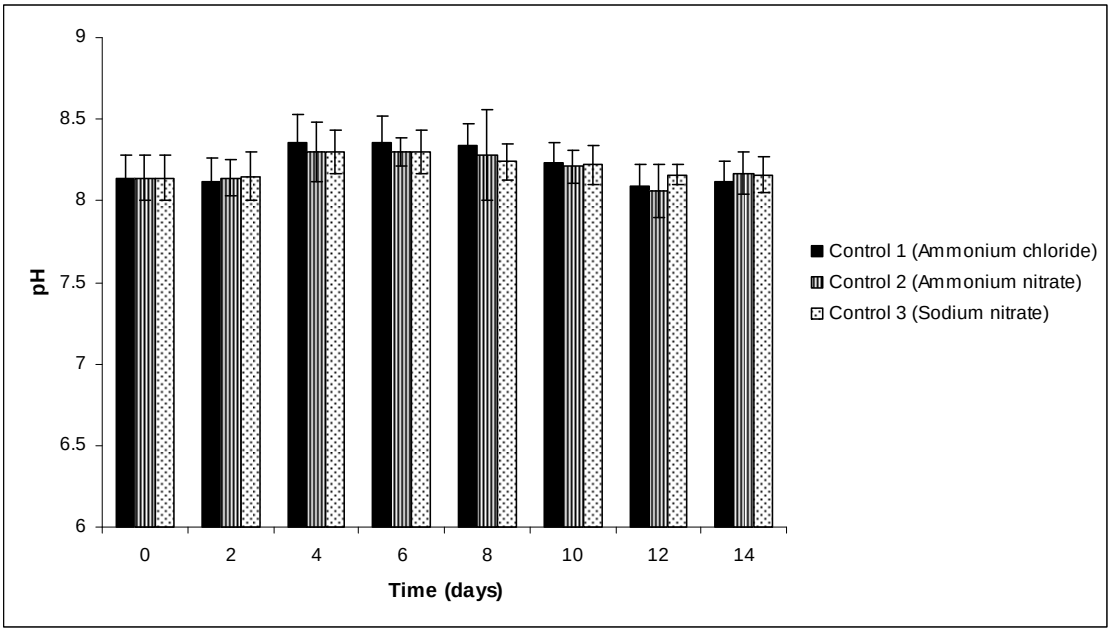

Figure 6.8: The pH of control cultures (lacking cells) supplemented with various nitrogen sources as indicated. Error bars represent standard deviation (n=4).

6.3.3 Algal pigmentation

The chlorophyll content in the cells subjected to any of the nitrogen salts was found to increase, stabilize and then decrease with time. The increase and stabilization of the chlorophyll content coincided with the exponential phase of growth while the decrease commenced with the advent of the stationary phase (cf. Figures 6.3 and 6.9). The rate of chlorophyll accumulation was initially significantly greater in the ammonium treatments (with the exception of ammonium chloride) than in the nitrate and urea treatments (Table 6.8). A rapid decline in the chlorophyll content in the ammonium treatments was found after day 6, but in the nitrate treatments it continued to rise until day 8, after which the decline was more gradual (Figure 6.9; Table 6.9).

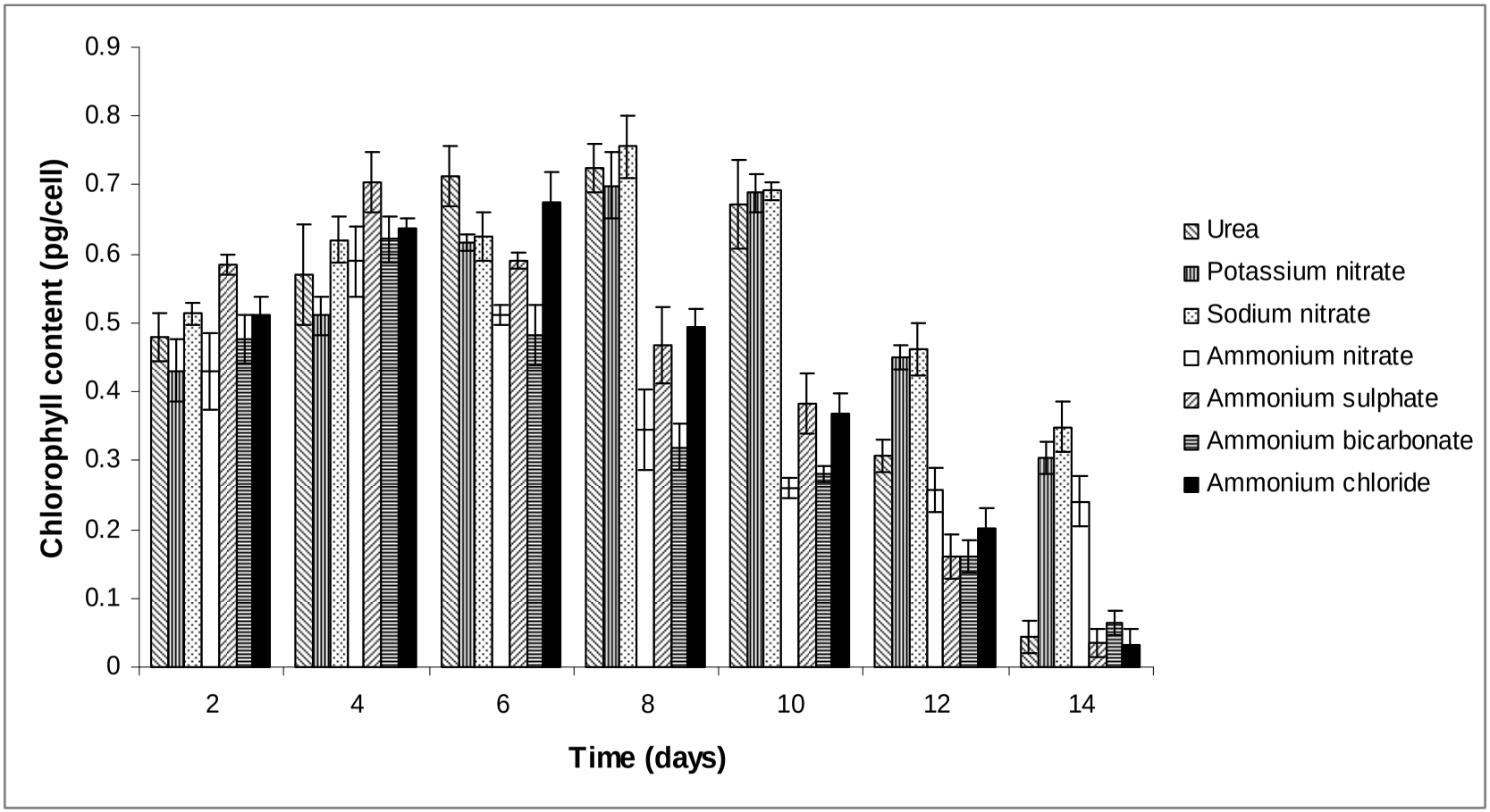

Figure 6.9: the chlorophyll content of *I. galbana* cultured in *f/2* medium supplemented with various nitrogen sources. Error bars represent standard deviation (n=4).

Table 6.8: Rates of *I. galbana* chlorophyll synthesis (Day 2-6), their regression coefficients and the significant differences between the rates in the various treatments as indicated.

Treatment	Rate ([Chlorophyll]/day)	Regression coefficient	Significant differences*
Urea	0.1146 ± 0.0094	0.9838	A
Potassium nitrate	0.1439 ± 0.0123	0.9940	A B
Sodium nitrate	0.1764 ± 0.0144	0.7761	B C
Ammonium nitrate	0.1993 ± 0.0228	0.2640	C D
Ammonium sulphate	0.2456 ± 0.0020	0.0018	D
Ammonium bicarbonate	0.2451 ± 0.0061	0.0017	D
Ammonium chloride	0.1460 ± 0.0134	0.9124	A B

* Rates with the same letters are not significantly different (P > 0.05)

Table 6.9: Rates of *I. galbana* chlorophyll synthesis (Day 8-14), their regression coefficients and the significant differences between the rates in the various treatments as indicated.

Treatment	Rate ([Chlorophyll]/day)	Regression coefficient	Significant differences*
Urea	1.6619 ± 0.0612	0.9359	A
Potassium nitrate	0.5608 ± 0.0743	0.9130	B
Sodium nitrate	0.6333 ± 0.0724	0.9584	B
Ammonium nitrate	0.2232 ± 0.0122	0.7602	C
Ammonium sulphate	0.7575 ± 0.0241	0.9732	D
Ammonium bicarbonate	0.4026 ± 0.0047	0.9657	C
Ammonium chloride	0.8482 ± 0.1206	0.9953	D

* Rates with the same letters are not significantly different (P > 0.05)

The carotenoid to chlorophyll ratio remained relatively constant, irrespective of the treatment, up to day 6 of culture, when it increased (Figure 6.10). The rate of increase was significantly higher in the ammonium treatments than that observed in the nitrate and urea treatments (Table 6.10).

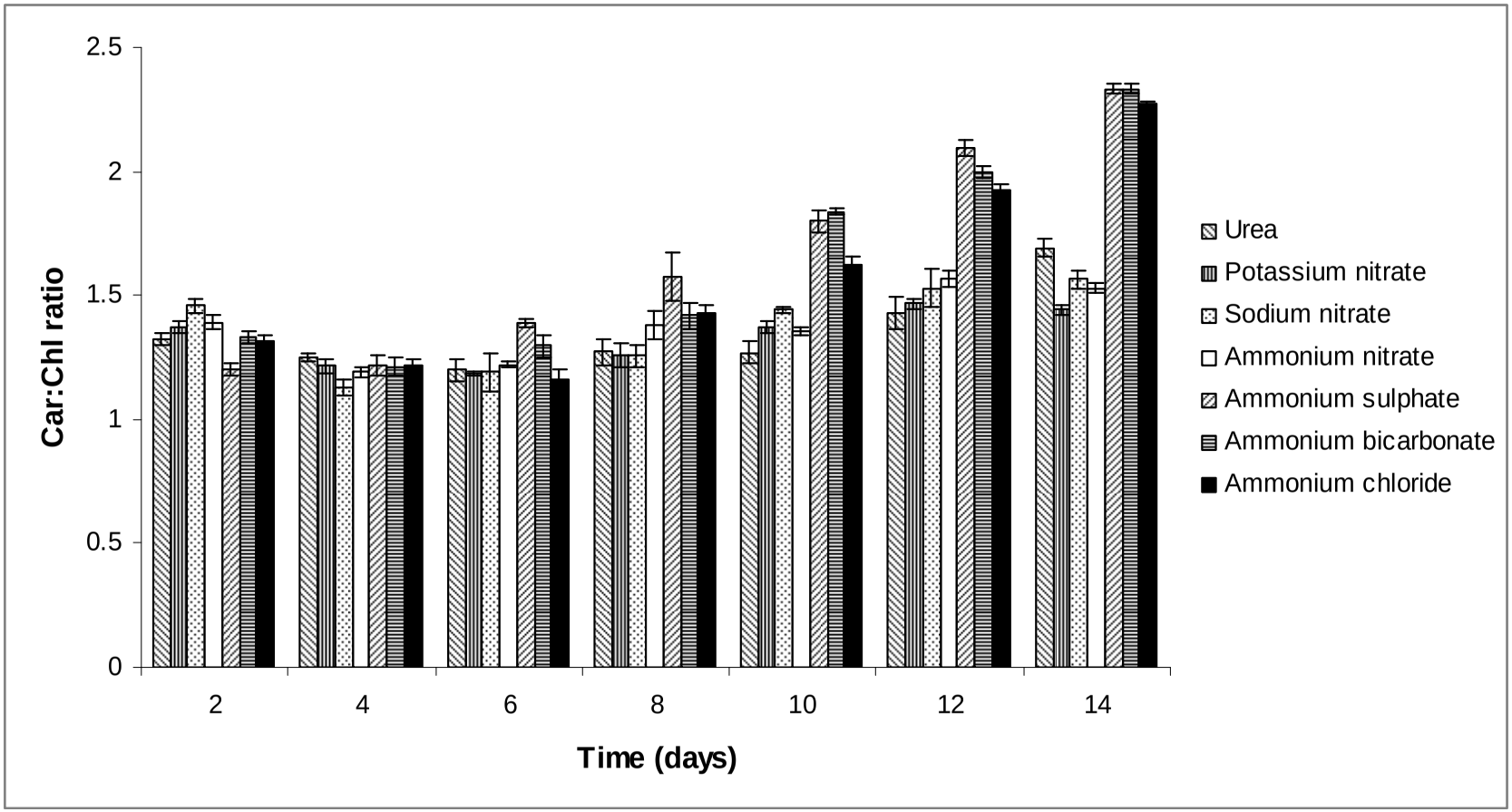

Figure 6.10: The carotenoid to chlorophyll ratio of *I. galbana* cultured in *f/2* medium supplemented with various nitrogen sources. Error bars represent standard deviation (n=4).

Table 6.10: Rates of change in car:chl ratio (day 4-14) in *I. galbana* cultures, their regression coefficients and the significant differences between the rates in the various treatments as indicated.

Treatment	Rate (Car:Chl/day)	Regression coefficient	Significant differences*
Urea	0.2349 ± 0.0006	0.7130	A
Potassium nitrate	0.1886 ± 0.0046	0.8714	A
Sodium nitrate	0.2308 ± 0.0072	0.9610	A
Ammonium nitrate	0.2448 ± 0.0077	0.8832	A
Ammonium sulphate	0.4300 ± 0.0165	0.9904	B
Ammonium bicarbonate	0.4479 ± 0.0791	0.9560	B
Ammonium chloride	0.4244 ± 0.0704	0.9292	B

* Rates with the same letters are not significantly different ($P > 0.05$)

6.3.4 Intracellular fluctuations in nitrogen, phosphorous and the nitrogen to phosphorous ratio

The initial intracellular nitrogen and phosphorous levels in all treatments were relatively high (Figure 6.11 and Figure 6.12). The rate of intracellular nitrogen depletion was not significantly different between any of the treatments (Table 6.11) with the exception of the ammonium bicarbonate treatment where the intracellular nitrogen was reduced to below measurable levels much earlier than in the other treatments. Interestingly, the ammonium bicarbonate treatment also experienced an early onset of the stationary phase and produced the lowest cell yield relative to all other treatments (Figure 6.3). The ammonium bicarbonate treatment also showed an earlier onset of carbon storage in the form of both carbohydrates and lipid and a maximal final lipid yield (Figure 6.4 and Figure 6.5).

The rates of intracellular phosphorous depletion in all treatments were not significantly different (Table 6.12). The intracellular phosphorous levels were less spectacular in their demise than the nitrogen levels (cf. Figures 6.11 and 6.12), a trend also observed by Ahlgren and Hyenstrand (2003). Interestingly, cells subjected to the ammonium bicarbonate treatment showed the greatest residual intracellular phosphorous content at

the end of the growth period (Figure 6.12) whereas they displayed the least intracellular nitrogen levels (Figure 6.11).

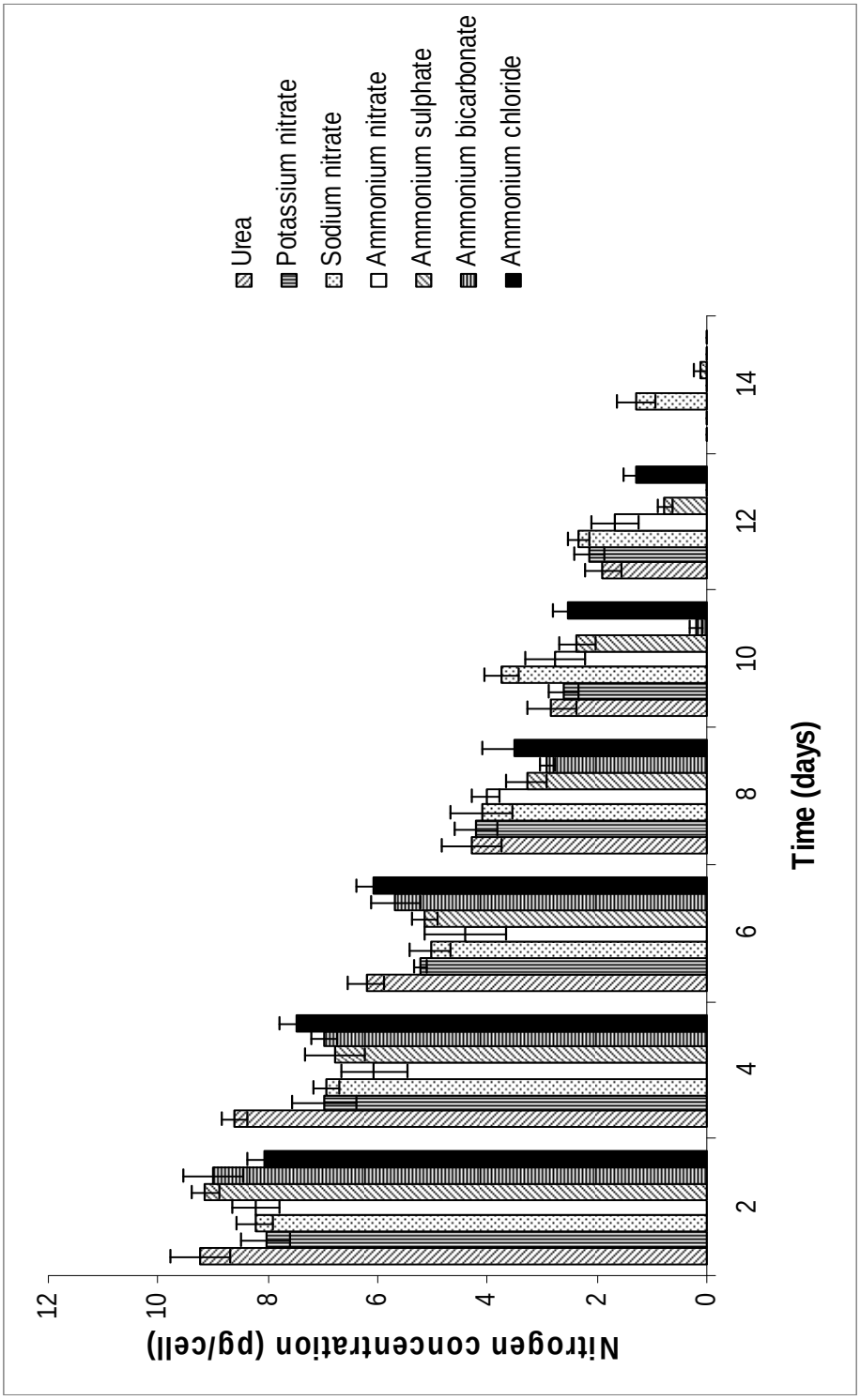

Figure 6.11: The intracellular nitrogen content of *I. galbana* cultured in *f/2* medium supplemented with various nitrogen sources. Error bars represent standard deviation (n=4).

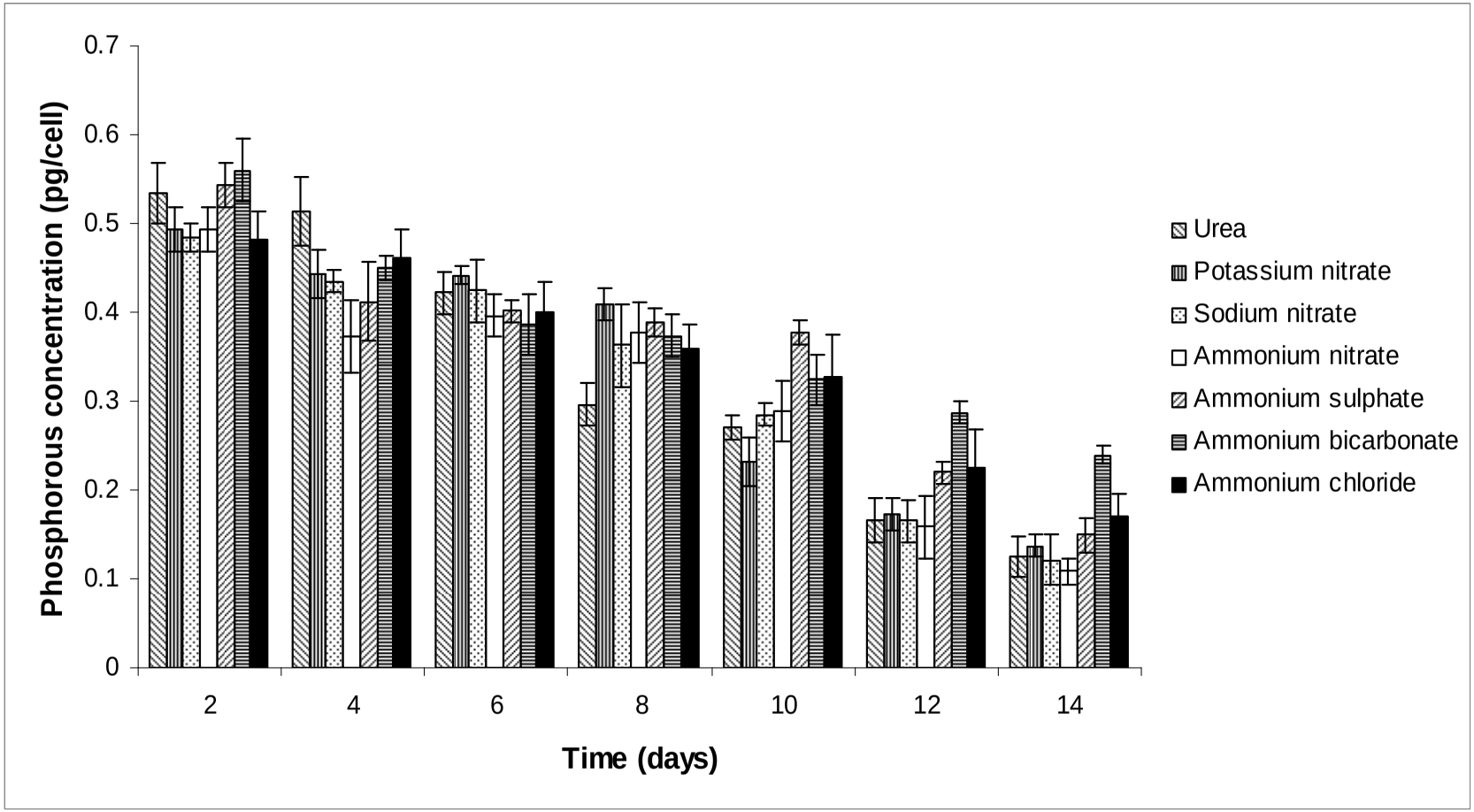

Figure 6.12: The intracellular phosphorous content of *I. galbana* cultured in *f/2* medium supplemented with various nitrogen sources. Error bars represent standard deviation (n=4).

Table 6.11: Rates of intracellular nitrogen depletion in *I. galbana* cultures, their regression coefficients and the significant differences between the rates in the various treatments as indicated.

Treatment	Rate ([Nitrogen]/day)	Regression coefficient	Significant differences*
Urea	0.0270 ± 0.0045	0.9858	A
Potassium nitrate	0.0363 ± 0.0054	0.9879	A
Sodium nitrate	0.0402 ± 0.0049	0.9773	A
Ammonium nitrate	0.0237 ± 0.0116	0.9752	A
Ammonium sulphate	-0.0124 ± 0.0078	0.9761	A
Ammonium bicarbonate	-0.0995 ± 0.0403	0.9297	B
Ammonium chloride	0.0112 ± 0.0083	0.9823	A

* Rates with the same letters are not significantly different (P > 0.05)

Table 6.12: Rates of intracellular phosphorus depletion in *I. galbana* cultures, their regression coefficients and the significant differences between the rates in the various treatments as indicated.

Treatment	Rate ([Phosphorous]/day)	Regression coefficient	Significant differences*
Urea	0.2795 ± 0.0525	0.9759	A
Potassium nitrate	0.2345 ± 0.0062	0.9107	A
Sodium nitrate	0.2437 ± 0.0173	0.9506	A
Ammonium nitrate	0.2640 ± 0.0363	0.9006	A
Ammonium sulphate	0.2615 ± 0.0369	0.8760	A
Ammonium bicarbonate	0.2960 ± 0.0122	0.9467	A
Ammonium chloride	0.2021 ± 0.0025	0.9689	A

* Rates with the same letters are not significantly different (P > 0.05)

The ratio of intracellular nitrogen to phosphorous in healthy cultures (day 2 – 4; Figure 6.13) was very close to the Redfield ratio (16 N: 1 P; Redfield, 1934). As the cultures aged a decrease in the ratio was evident in all treatments. The rate of this decrease differed significantly between the nitrate, urea and ammonium treatments (Table 6.13). The nitrogen to phosphorous ratio was reduced much earlier in the ammonium treatments than in the other treatments (Figure 6.13).

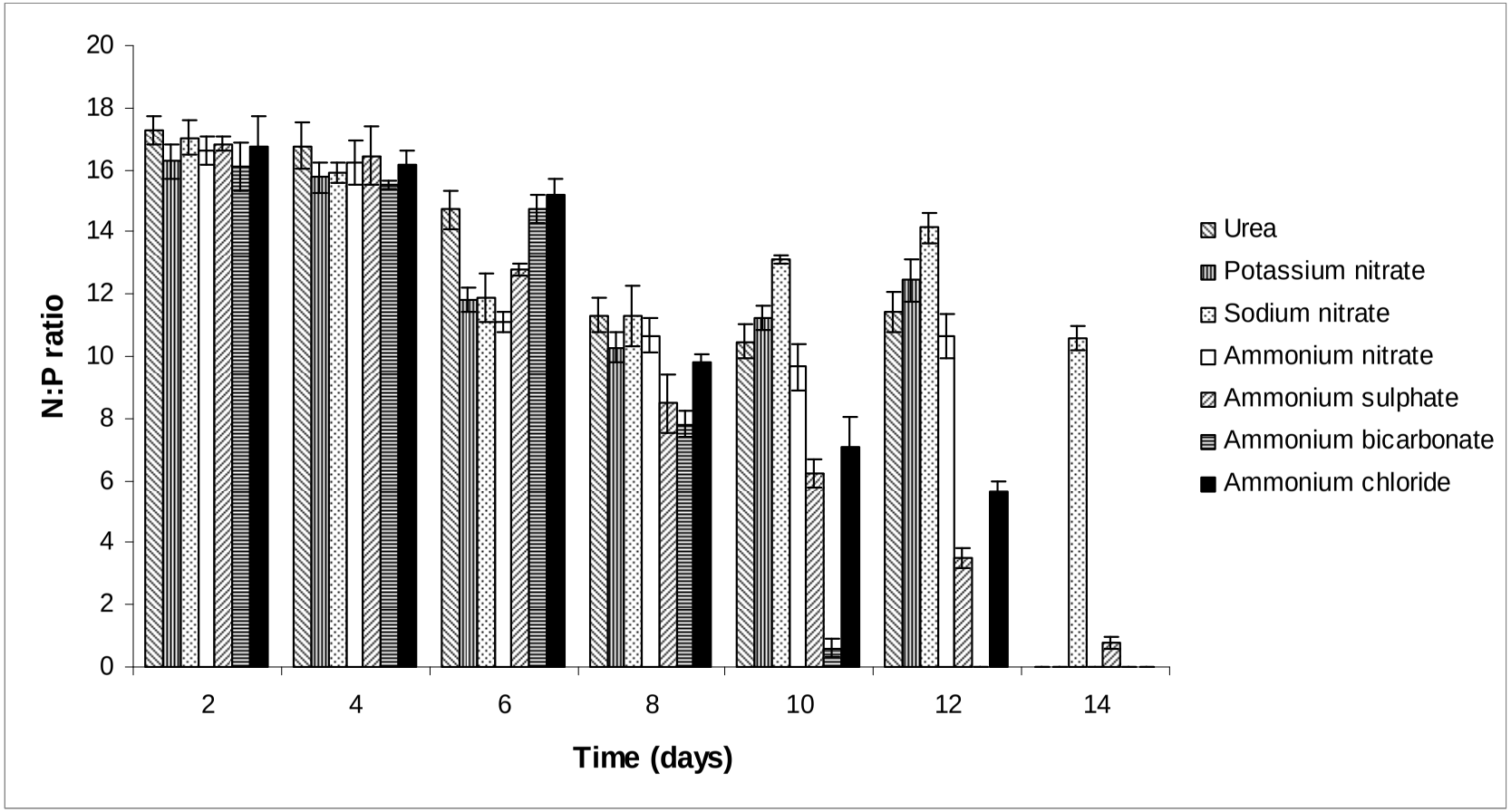

Figure 6.13: The nitrogen to phosphorous ratio of *I. galbana* cells cultured in *f/2* medium supplemented with various nitrogen sources. Error bars represent standard deviation (n=4).

Table 6.13: Rates of change of N:P ratio in *I. galbana* cultures, their regression coefficients and the significant differences between the rates in the various treatments as indicated.

Treatment	Rate (N:P/day)	Regression coefficient	Significant differences*
Urea	0.0855 ± 0.0027	0.7784	A B
Potassium nitrate	0.0904 ± 0.0031	0.6422	A B
Sodium nitrate	0.0935 ± 0.0002	0.4827	B
Ammonium nitrate	0.0840 ± 0.0016	0.7706	A
Ammonium sulphate	0.0441 ± 0.0030	0.9821	C
Ammonium bicarbonate	0.1234 ± 0.0013	0.8913	D
Ammonium chloride	0.0614 ± 0.0006	0.9466	E

* Rates with the same letters are not significantly different (P > 0.05)

6.3.5 Cellular and sub-cellular analysis

Stationary phase, ammonium grown cells were larger than stationary phase nitrate and urea grown cells (Figure 6.14). There was no superficial ultrastructural difference between the exponential *I. galbana* cells in the various nitrogen treatments, but closer observation showed that the organization of the plastid lamellae differed in the various treatments. All plastids have the typical grouping of three thylakoids as expected for this class of algae, but those cells exposed to ammonium salts had multiple thylakoid stacking, whilst those exposed to nitrate salts or urea had fewer, more widely-spaced thylakoids in their plastids (Figure 6.15).

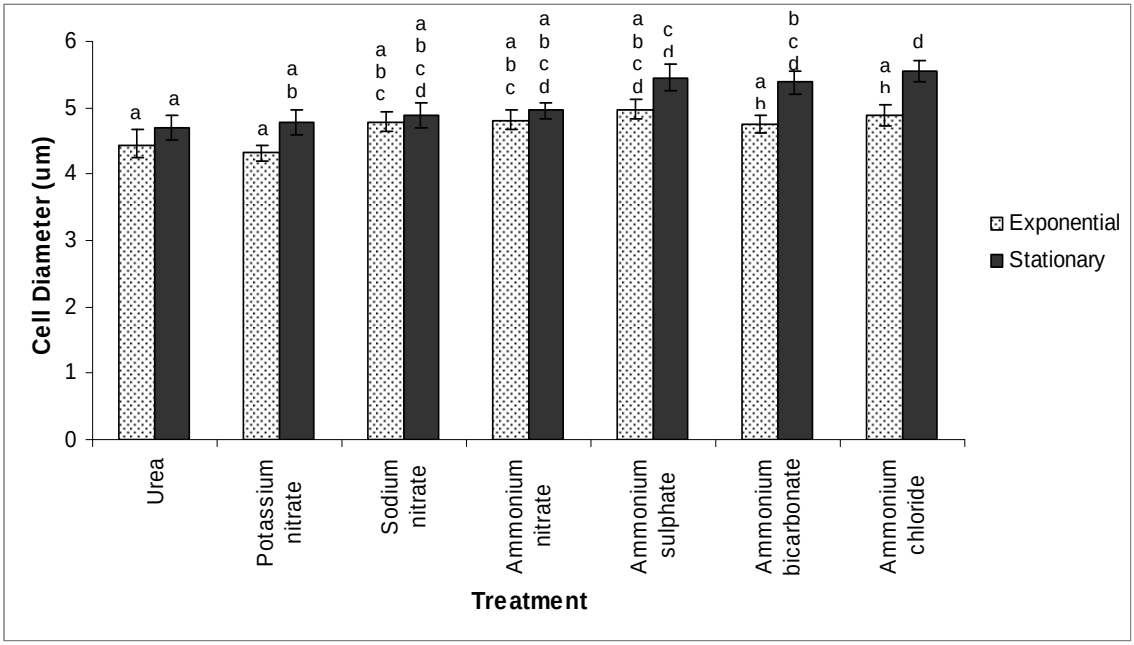

Figure 6.14: The cell diameter of exponential and stationary phase *I. galbana* cells cultured in *f/2* medium supplemented with various nitrogen sources as indicated. Error bars represent standard deviation (n=50). Significant differences are indicated by different letters above the error bars ($P < 0.05$).

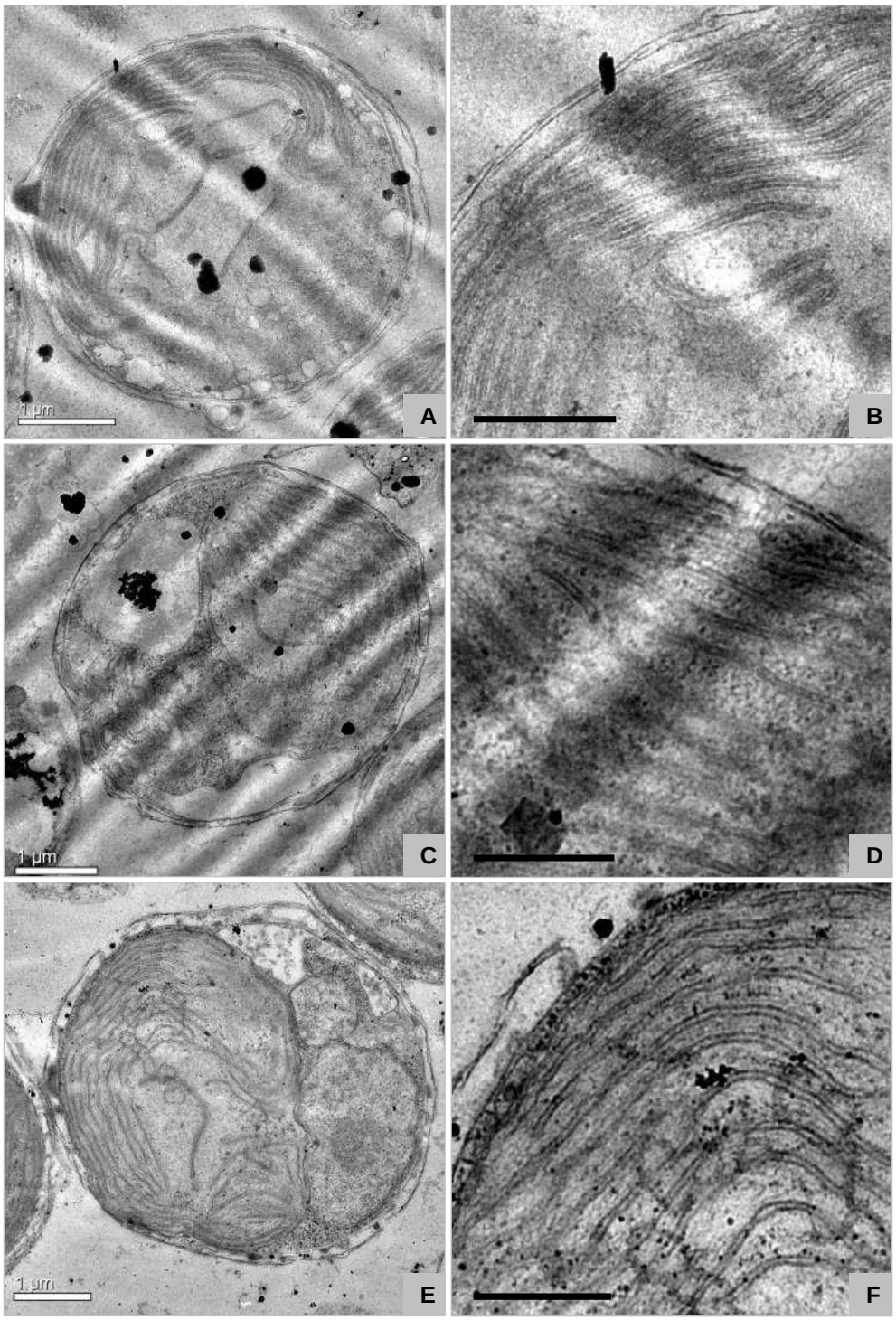

Figure 6.15 (A): Exponential phase *I. galbana* cells cultured in *f/2* medium supplemented with ammonium, **(C):** urea and **(E):** nitrate. Photomicrographs on the right **(B, D and F)** represent magnified views of the plastids of the respective image on the left. White scale bars represent 1 um and black scale bars represent 0.5 µm.

6.4 DISCUSSION

The recovery of similar growth rates of *I. galbana* when supplied with different forms of nitrogen is not novel amongst the algae (Carpenter *et al.*, 1972; Thompson *et al*., 1989; Flynn *et al*., 1993; Levasseur *et al*., 1993; Lourenco *et al*., 1997; Fidalgo *et al*., 1998; Liang *et al*., 2006). This is, however, counter-intuitive since nitrate reduction, which is required prior to N incorporation into biological molecules, requires an elevated energy cost relative to direct ammonium assimilation and thus reduced growth rates were expected in cultures fed nitrate-nitrogen. Similar growth rates in all nitrogen treatments indicate that the cells somehow acclimate to the nitrogen source.

A closer analysis of the growth curve showed that ammonium did stimulate a slightly elevated initial cell yield albeit not significantly so. This observation together with the observed increase in thylakoid development and the initial elevated chlorophyll levels in the exponential phase of ammonium-grown *I. galbana* cells supports the notion of ammonium as the preferred nitrogen source, relative to nitrate and urea. Alterations in the plastid structure in response to the nitrogen source has not been reported before for any microalga but has been followed in higher plants, such as wheat (Golvano *et al*., 1982). The correlation between enzymatic tests and ultrastructural analysis in that particular study led to the deduction that the chloroplast membrane system, photosynthetic ability and chloroplast development is accelerated by ammonium rather than nitrate (Golvano *et al.*, 1982) similar to the observations noted in the present study. Such a variation in *I. galbana* plastids contributes to the proposal that the carbon and nitrogen balance regulates the development of the chloroplast (Harris and Kirk, 1969). The uptake of ammonium prior to nitrate in ammonium nitrate grown cultures in *Isochrysis* verifies that ammonium is indeed the preferred source of nitrogen.

From the reasoning above, it is expected that ammonium-supplemented medium should result in an equal or even greater final biomass yields, than nitrate- and urea-grown cultures, since ammonium is the preferred nitrogen source and accelerated initial algal growth, chlorophyll accumulation and chloroplast development. However, the final cell

yield in nitrate- and urea-grown cultures were significantly greater than that observed in ammonium treatments. Such observations have been noted by other investigators working with various microalgal species (Costa *et al*., 2001; Xu *et al*., 2001; Dayananda *et al.*, 2006; Liang *et al*., 2006; Arumugam *et al*., 2013). Such an anomaly may be due to the rapid uptake and storage of such nitrogenous species, whereas rapid luxury storage of ammonium-nitrogen would be toxic (Goldman *et al*., 1982). In addition, ammonium-nitrogen was depleted before nitrate-nitrogen, as a result of both cellular uptake and the volatilization of ammonium-nitrogen (incurred by the increase in the pH of the culture medium). The loss through volatilization was corroborated by cell-free controls. As a result ammonium-fed cultures enter the stationary phase much earlier and result in much reduced final cell yields.

The stationary phase is indicative of some stress on the algal cells e.g. limited nutrients, carbon dioxide or light and is associated with the switch over to lipid synthesis to reduce the build up of carbon, oxygen, nitrogen, electrons and free radicals from photosynthesis, the latter of which would prove toxic to the cells. Hence, the early lipid accumulation in the ammonium treatment observed in the present study may actually be in response to the physiological state of the cells rather than the nitrogen source used. The elevated lipid yield in the early stationary phase of urea-fed cells relative to that of nitrate-fed cells, is desirable for biofeed plant managers because it reduces the time required to reach harvest and costs less because urea is a cheaper source of nitrogen.

Lipids are not the only energy reserve in microalgae. Carbohydrates also serve as carbon and energy sinks (Lacour *et al*., 2012a, b). The relationship between varying growth conditions and carbohydrate and lipid accumulation has been highlighted previously (Roessler, 1990). An elevated carbohydrate and lipid yield observed in nitrogen treatments that result in reduced eventual cell numbers observed in this study is in accordance with the results of Flynn *et al*., (1992) and Lourenco *et al*. (2002) when also working with *Isochrysis*. This is not unexpected since arrest of growth is associated with the accumulation of storage products (stress response). The initiation of carbohydrate accumulation prior to lipid accumulation verifies that carbohydrates are the primary

storage product and lipids are the secondary storage products in *Isochrysis galbana* U4 like in numerous other algal species (Klass, 2004; Li *et al*., 2011). The decrease in the carbohydrate content with the concomitant increase in the lipid content implies that the carbohydrates are converted to lipids, via the pentose phosphate pathway, when the cells become highly nutrient stressed (Feng *et al*., 2011; Li *et al*., 2011; Lacour *et al*., 2012a; Li *et al.*, 2012).

The initial increase in pH in the medium of all treatments was expected since rapidly growing cells require large amounts of carbon dioxide. Carbon fixation in turn results in the alkalization of the culture medium (Clark, 1999). The pH of the culture medium plays an important role in the growth of microalgae since different organisms thrive at various pH levels (pH optima). Furthermore, pH variations result in numerous abiotic phenomena e.g. pH levels that exceed 9.5 results in the production of various precipitates such as calcium carbonate, magnesium hydroxide and calcium phosphate (Sukenik and Shelef, 1984). This would be detrimental in that important nutrients such as phosphorus would no longer be available for algal growth (Kawasaki *et al*., 1981). Elevated values of culture pH (over 8) may also result in the conversion of ammonium-nitrogen to ammonia-nitrogen and its subsequent volatilization in this form resulting in the loss of nitrogen to the atmosphere (Bouldin *et al.*, 1974). The pH of all cultures rose above pH 8, as expected since seawater is always over a pH of 8. Because seawater contains a high concentration of salts it is also well-buffered. Hence, seawater is not an ideal medium in which to attempt ammonium as a nitrogen source since ammonia-nitrogen volatilization in this medium is inevitable as was observed in the study. This supports the previous assumption that the reduced final algal yields in the ammonium treatments were due to ammonia volatilization.

A nitrogen source-dependent rate of pH decrease was observed after pH peaks were reached since medium pH is primarily influenced by the inorganic ions of carbon and nitrogen in culture (Goldman *et al.*, 1982). CO_2 dissolves in seawater resulting in the production of carbonic acid (H_2CO_3) and hydrated CO_2. The hydroxylation of hydrated CO_2 and dissociation of H_2CO_3 results in the production of the bicarbonate ion (HCO_3^-)

(Raven, 2011). The photoassimilation of carbon by microalgae occurs according to the following reaction: $HCO_3^- \rightarrow CO_2 + OH^-$. This results in an increase in the culture pH. Hence, the observed, initial pH elevation of the culture medium in all nitrogen treatments when maximal photosynthesis was occurring in healthy algal cells.

The subsequent variations in the pH in the various treatments may be attributed to the nitrogen source used. Nitrate uptake and assimilation induces a pH increase due to the following reaction: $NO_3^- \rightarrow$ organic N + OH^-. Conversely, the uptake and assimilation of ammonium results in a decrease in the pH due to the following reaction: $NH_4^+ \rightarrow$ organic N + H^+. Urea uptake, in contrast, has no effect on the culture pH since urea is an uncharged chemical species (Goldman *et al*., 1982). Variations in pH values as a result of the source of nitrogen used only became clearly evident towards the end of the culture period. This is due to the effects of carbon uptake (pH increase) initially overshadowing the effects of nitrogen uptake and assimilation (pH increase in nitrate, pH decrease in ammonium and constant pH in urea) since the healthy algal cell is primarily composed of carbon (ratio of carbon to nitrogen of healthy cells is 5:1 when the rate of photosynthesis is elevated and the cells are not under any stress).

The observed decrease in the chlorophyll levels in cells that were ammonium-fed when they rise in nitrate- and urea-fed cells is consistent with observations of Lourenco *et al*. (2002). They also observed that elevated chlorophyll levels are evident in treatments that produce greater final cell yields (i.e. nitrate-grown cells; Lourenco *et al.*, 2002). This could be a consequence of the lower levels of nitrogen in the ammonium treatments due to volatilization, which in turn reduces the chlorophyll levels at an earlier stage of experimentation.

An increase in the carotenoid to chlorophyll ratio is generally associated with the stationary phase in *Isochrysis galbana* U4, when the cells are exposed to some environmental stress that inhibits further growth (Chapter 5). This increase may come about because of an increase in the net production of carotenoids, or a decrease in the chlorophyll content, or a combination of the two (Abalde *et al*., 1991). The rapid increase

in the carotenoid to chlorophyll ratio in the ammonium treatments verifies that the cells were experiencing some sort of environmental stress, in this case nitrogen depletion. The slightly elevated carotenoid to chlorophyll ratio in cells exposed to urea relative to that in those exposed to nitrate is a consequence of the rapid decrease in the chlorophyll content in the urea-grown cells or it may be due to the increase in the production of carotenoids in the urea treatment as observed by Abalde *et al*. (1991).

The initial elevated levels of intracellular nitrogen and phosphorus is indicative of luxury nutrient uptake since these nutrient levels only decreased as the cells aged (Spikes in the intracellular nitrogen and phosphorous levels, as growth proceeded, would have implied gradual nutrient uptake initiated by intracellular nutrient depletion). The highest level of lipid and carbohydrate storage induced by ammonium bicarbonate (in comparison to all other treatments) is expected since severely nutrient-limited cells (intracellular nitrogen was deplete earlier than in all other treatments) store carbon to be used for growth upon the return of optimal conditions. The effect of bicarbonate on algae has been reported elsewhere where it was shown to inhibit growth and induce lipid synthesis (Gardner *et al*., 2012).

A decrease in the nitrogen to phosphorus ratio (below 16) was observed in all treatments and is indicative of nitrogen limitation (Redfield, 1934), a situation which is further corroborated by the rapid decline in intracellular nitrogen, but a concomitant more gradual decline in intracellular phosphorous. The nitrogen to phosphorous ratio was reduced much earlier in the ammonium treatments than in the other treatments implying that the ammonium grown cells were nitrogen stressed much earlier. This early onset of nitrogen stress triggered the early cessation of cell growth and the early onset of carbohydrate and lipid accumulation.

The presence of larger cells during the stationary phase was expected and has been reported elsewhere (Sayegh and Montagnes, 2011; Chen *et al*., 2012b). The increase in the cell volume during the stationary phase is indicative of nutrient stress (Feng *et al*., 2011). Cell division is arrested in stationary phase cells resulting in larger cells.

Furthermore, multiple, large lipid bodies are evident in the cells which contribute to the cell size. Light intensity can also result in changes to cell size where the light level is directly proportional to the cell size (Harrison *et al.*, 1990). While light intensity was maintained at a constant level throughout the culture period in this study, self-shading becomes an issue when cultures become progressively denser. This is expected to result in a decrease in cell size with culture age but the opposite was observed which concurs with the deductions of Sciandra and colleagues (1997) that nitrogen limitation takes precedence over light limitation in cell volume regulation.

Greater cell volumes in cells that are ammonium-fed relative to those that are nitrate-fed were reported elsewhere (Paasche, 1971; Giordano, 1997; Lourenco *et al*., 2002) without explanation for the increase in cell size. In the present study, the early onset of the stationary phase in cultures of the ammonium treatments relative to those of the other nitrogen treatments resulted in an elevated cell size which probably reflects their nitrogen-deprived status. Nitrogen deprivation is expected to have a suite of cascade events, such as compromising membrane proteins and therefore making such stressed cells more susceptible to damage and thus more inclined to appear bloated upon fixation (Flynn *et al*., 1993).

6.5 CONCLUSION

A comparison of the array of nitrogen containing salts tested showed that all salts containing the same source of nitrogen (ammonium or nitrate) resulted in similar growth observations in *I. galbana* U4. Sodium nitrate was most effective at optimizing cell yield, followed by urea and then potassium nitrate. Despite ammonium-nitrogen being the most reduced form of inorganic nitrogen and therefore expected to support the best performance of the alga, cell yields in ammonium-fed cultures were significantly lower than in cultures grown with any other source of nitrogen and this is attributed to ammonia volatilization. Urea-fed cultures produced a greater initial lipid yield than nitrate-fed cultures. This, coupled with the ability of urea-fed cultures to produce similar cell yields as nitrate-fed cultures and the cheaper price of urea relative to all the other

nitrogen sources tested, leads to the conclusion that urea is the ideal nitrogen source for the mass culture of *Isochrysis galbana* U4.

CHAPTER SEVEN

The Effect of Phosphorus Limitation and Starvation on *Isochrysis galbana* U4

7.1 INTRODUCTION

Phosphate (PO_4) is necessary for the formation of phospholipids, nucleic acids and ester phosphates such as phosphorylated sugars (South and Whittick, 1987). Furthermore, PO_4 plays an important role in the generation and transformation of metabolic energy in the form of ATP and NADP (Stewart, 1974; El-Sheek and Rady, 1994). Hence, PO_4 is essential for the growth and division of algal cells. The most important inorganic form of phosphate used by algae is orthophosphate phosphorus. However, many algal species have the ability to utilize polyphosphates and organic phosphates. The hydrolysis of organic phosphates is initiated by plasmalemma-located phosphatases. In many instances, PO_4 limitation promotes the production of these alkaline phosphatases (South and Whittick, 1987).

Intracellular PO_4 levels fluctuate considerably in response to the levels of phosphorus (P) in the medium i.e. PO_4-limited versus PO_4-replete conditions (Stewart, 1974). As previously stated, P uptake and consumption is required for microalgal growth and division (Miyachi *et al.*, 1964). However, in most instances, the amount of P taken up by the cell far exceeds the need for immediate metabolic functions. This results in the accumulation of large quantities of storage PO_4 in the cells indicating luxury uptake of phosphate beyond the concentrations associated with the normal metabolic requirements of the cells. The luxury uptake of PO_4 is probably a strategy to ensure that PO_4 is available to the cell even when the ambient levels are limited (El-Sheek and Rady, 1994; South and Whittick, 1987). For most algal species this excess PO_4 is stored as polyphosphate granules, but some species also store ionic PO_4 in vacuoles (South and Whittick, 1987). The luxury uptake of PO_4 by algae is a well documented phenomenon (Droop, 1873; Stevenson and Stoermer, 1982) and it has been postulated that stored phosphate can additionally be utilized as a means of storing energy. This is plausible since polyphosphates possess energy rich P-O-P bonds (Figure 7.1; Meyerhof *et al.*, 1952; Stewart, 1974).

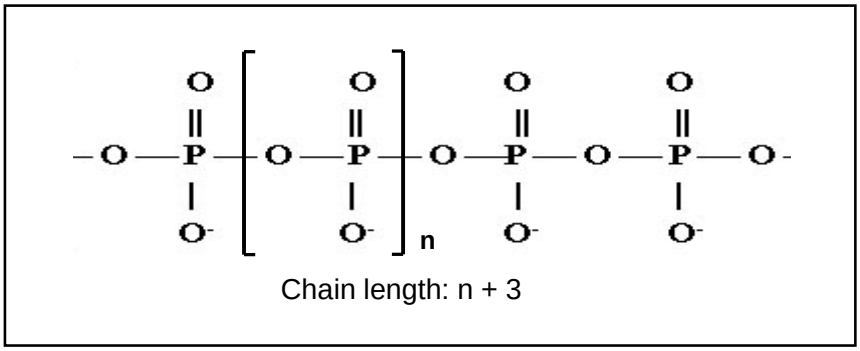

Figure 7.1: Structural representation of polyphosphate (adapted from Stewart, 1974)

The P requirements vary considerably between microalgal species, with the optimal P concentration, for maximal biomass productivity, ranging from 0.001 to 0.179 g/liter (Shelef and Soeder, 1980). Hence, studies need to be conducted to determine the response of individual algal species to varying levels of P. In comparison with nitrogen studies, P studies are limited.

This study is aimed at determining the effect of P limitation and starvation on *I. galbana* U4 cultures by monitoring growth, lipid accumulation and pigmentation. Unlike nitrogen, which is widely available, the supply of phosphorus is limited (Hannon *et al*., 2010). Hence, microalgae that have a low phosphorus demand are preferred for the successful commercialization of algal mass culture processes e.g. for biodiesel production. Furthermore, the use of low P demanding isolates would also aid in the reduction of the cost of the mass culturing process for eventual biodiesel production.

7.2 MATERIALS & METHODS

7.2.1 Experimental setup

The experiment was conducted in 1 L modified aerated Schott® bottles (Section 2.3). Both the bottles and glass tops, equipped with the gas inlet and outlet, were thoroughly cleaned with Teepol orange® (P-free soap) and autoclaved (121°C for 30 minutes) prior to use. Twenty vessels containing 800 ml, filtered and autoclaved (Section 2.1), modified *f/2* medium each, were inoculated with cells from an eight-day-old culture of *I. galbana* (approximately $3x10^6$ cells/ml). The cells were healthy and in the exponential growth

phase upon inoculation. All vessels were sparged with filtered (Whatman® uniflo 0.2um) air and incubated at 23 ± 2 °C under a photon flux density of 110 μmol photons.m^{-2}.s^{-1} with a 10:14 light-dark cycle. The position-dependant influence of the light source on each culture vessel was minimized by the daily random relocation of each of them

Eight different P treatments were used (0%, 1%, 5%, 12.5%, 25%, 50%, 100% and 150% phosphorus i.e. 0 ppm P, 0.01 ppm P, 0.05 ppm P, 0.125 ppm P, 0.25 ppm P, 0.5 ppm P, 1 ppm P and 1.5 ppm P respectively). These were achieved by altering the sodium dihydrogen orthophosphate dihydrate concentration in the medium (100% P is equivalent to the total P in *f/2* medium and represents the control treatment). Each P treatment was conducted in quadruplicate. The treatments in the range of 0.25 to 1.5 ppm P will henceforth be referred to as the 'higher P treatments' and the treatments in the range of 0 to 0.125 ppm P will be referred to as 'lower P treatments'.

7.2.2 Analytical methods

The cell concentration and lipid content was determined as outlined in Sections 2.5 and 2.7, respectively. The protocol in Section 2.13.3 was used to determine the concentration soluble reactive phosphorus (SRP) in the milieu. The nitrate levels in the culture medium (sole nitrogen source in *f/2* medium, Guillard and Ryther, 1962) were also monitored (Section 2.13.1) to verify that the growth cessation was initiated by phosphorus starvation and was not a function of nitrogen deficiency. The chlorophyll content and the ratio of carotenoids to chlorophyll were determined as discussed in Section 2.15. Statistical analyses were conducted using SPSS 20 software as outlined in Section 2.17.

7.3 RESULTS & DISCUSSION

7.3.1 Nutrient uptake

The P in the milieu was completely consumed by day 8 in all treatments (Figure 7.2), but cell growth continued until day 14 in the higher P treatments (Figure 7.3). Since cell growth is normally hindered in the absence of P (South and Whittick, 1987) the observed continuation of cell division in the absence of external P supplies could have been made

possible by P supply from storage reserves within the cells. This supports the species capacity for luxury P uptake and storage and its subsequent utilization of internal P reserves to support cell growth for a period following the depletion of external P in the surrounding medium.

The rate of P uptake varied between the different treatments ($P < 0.05$; Table 7.1). The P uptake rates were directly proportional to the concentration of P in the medium (Table 7.1). This concentration driven P uptake is most probably a function of P saturation when P concentrations are high since P uptake is an active process. The dependence of the rate of P uptake on the level of ambient P has been previously noted, but the type of polyphosphate that accumulated (acid-soluble versus acid-insoluble) varied in response to the external P concentration (Powell *et al.*, 2009). Acid-insoluble polyphosphate serves as a form of P storage whereas acid-soluble polyphosphate is used for immediate metabolic purposes (DNA and protein synthesis, Miyachi *et al.*, 1964). At low P levels, algal cells tend to accumulate acid-insoluble polyphosphate rather than the acid-soluble polyphosphate and at high P concentrations both forms of polyphosphate are accumulated (Powell *et al.*, 2009). Perhaps some trigger exists that promotes P storage (acid-insoluble polyphosphate) when P levels are low.

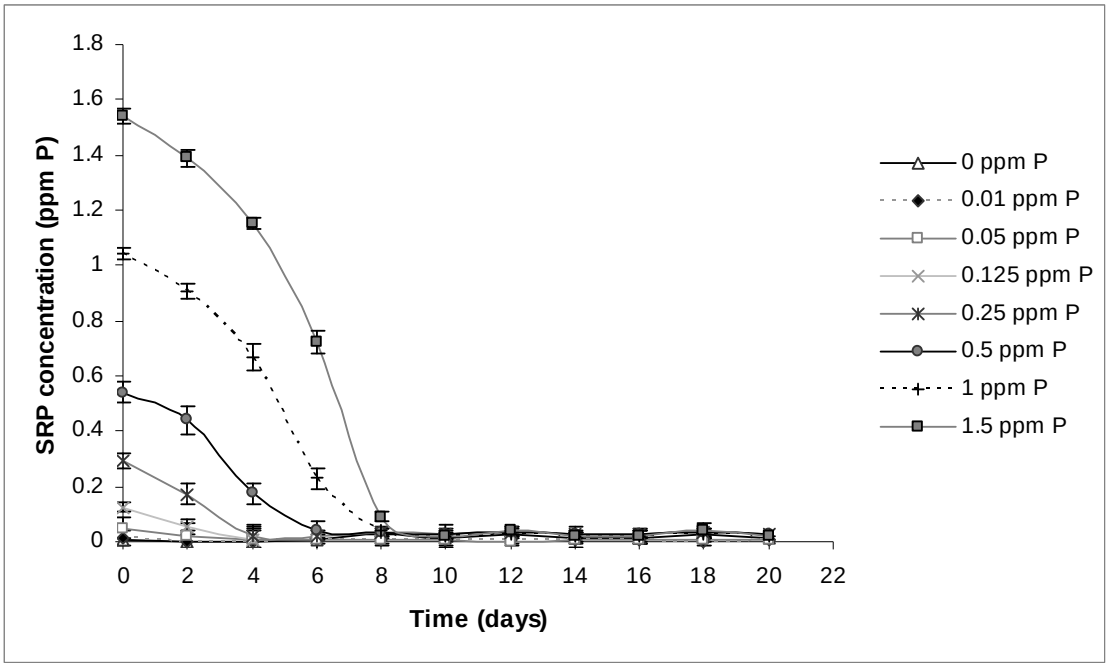

Figure 7.2: Phosphorous depletion from the milieu due to uptake by *I. galbana* cells cultured in *f/2* medium supplemented with different starting P concentrations. Error bars represent standard deviation (n=4).

Table 7.1: Rates of phosphorus uptake by cells of *I. galbana*, their gradients, regression coefficients and the significant differences between the rates in the various treatments as indicated.

Treatment	**Rate (ppm P/day)**	**Gradient (y=*M*x + c)**	**Regression coefficient**	**Significant differences[a]**
0.000 ppm P	-0.0033 ± 0.0008	-0.0020	0.9231	A
0.010 ppm P	-0.0056 ± 0.0006	-0.0025	0.8596	A
0.050 ppm P	-0.0149 ± 0.0006	-0.0116	0.9682	B
0.125 ppm P	-0.0355 ± 0.0021	-0.0299	0.9936	C
0.250 ppm P	-0.0678 ± 0.0030	-0.0678	0.9949	D
0.500 ppm P	-0.0838 ± 0.0021	-0.0886	0.9714	E
1.000 ppm P	-0.1353 ± 0.0025	-0.1340	0.9687	F
1.500 ppm P	-0.1816 ± 0.0615	-0.1786	0.9293	G

[a]Rates with the same letters are not significantly different (P > 0.05).

The initiation of the stationary phase on day 14 in all the higher P treatments shows that this concentration range of P had no detrimental effect on the algal growth (Figure 7.3). Hence, some other nutrient had become limiting by day 14 and triggered the initiation of the stationary phase. The most likely limiting nutrient was nitrogen. Thus nitrogen uptake was also monitored. Cells of *I. galbana* also displayed luxury uptake of nitrogen (Figure 7.4), and all the nitrogen was stripped from the medium by day 8 in the higher P treatments (Figure 7.4). However, the timing of cessation of nitrogen uptake coincided with the onset of cell growth cessation (day 4) in cultures lacking P (0 ppm, cf. Figures. 7.3 and 7.4). This is similar to the observations made by others (Xin *et al.*, 2010; Feng *et al.*, 2011). In the treatments that fall between these two extremes (0.01 – 0.125 ppm P), the relationship between the cessation of nitrate uptake and the onset of the cessation of cell growth was upheld (cf. Figures. 7.3 and 7.4) and shows that P was the limiting nutrient.

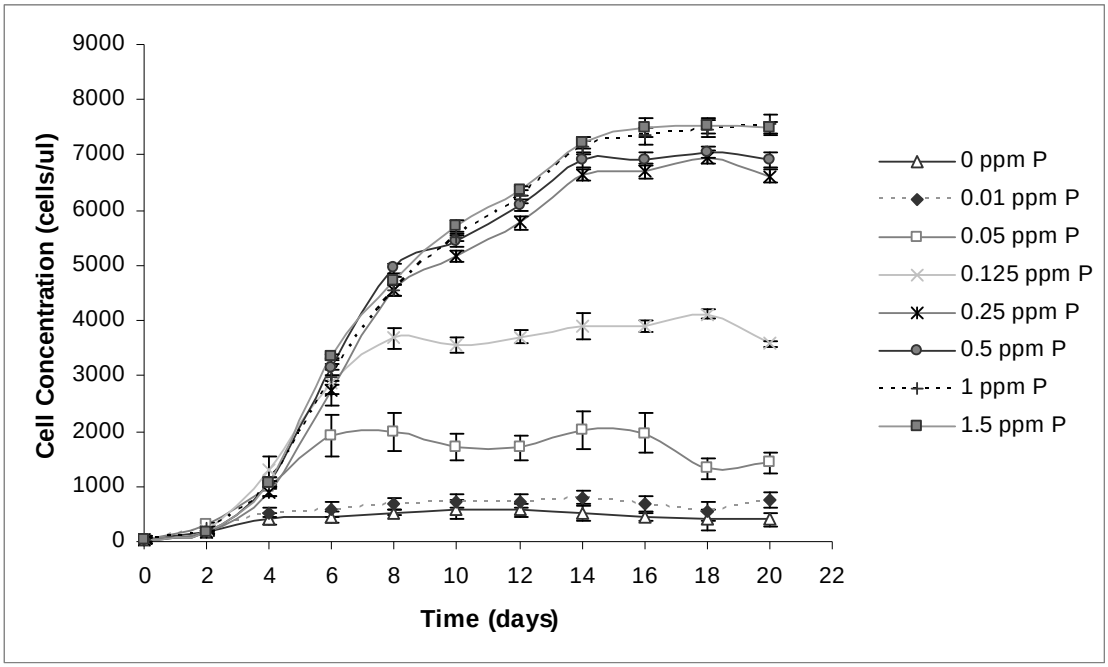

Figure 7.3: *Isochrysis galbana* growth in *f/2* medium supplemented with various P concentrations. Error bars represent standard deviation (n=4).

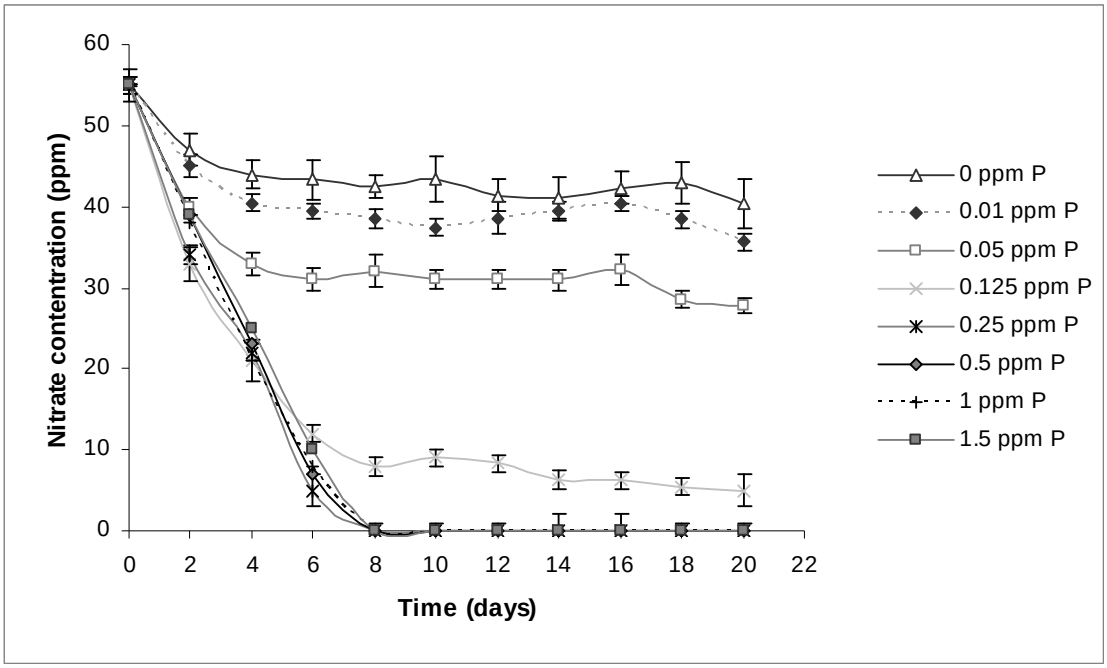

Figure 7.4: Nitrate depletion from milieu due to uptake by *I. galbana* cells cultured in *f/2* medium supplemented with different starting P concentrations. Error bars represent standard deviation (n=4).

Thus, nitrogen uptake was observed to be a function of P availability. It may therefore be deduced that maintenance of cell growth requires both nitrogen and phosphorus and the over-provision of one element has no impact on growth if the other is lacking. According to the threshold model for nutrient deficiency, only a single nutrient may be assumed to be limiting at any given instant (Droop, 1974) and since no variations were noted between the cultures grown under higher P levels, it may be concluded that growth in these treatments were eventually inhibited by N depletion rather than P depletion.

Conversely, growth in the lower P treatments was indeed inhibited by P concentration thus it is valid to examine responses of cultures in this range of P to see what effect its limitation has on lipid accumulation.

7.3.2 Growth and lipid accumulation

Isochrysis galbana grew in all P treatments (Figure 7.3), but the rate of growth varied significantly in cultures supplemented with the higher and lower range of P ($P < 0.005$; Table 7.2). All treatments of P at or in excess of 0.25 ppm resulted in the same rate of exponential growth (Table 7.2), proving that additions of P beyond the quarter strength level of the P concentration of *f/2* medium (0.25 ppm P) have no further beneficial effect. The similar growth rates and final cell yields observed in the higher P treatments (Table 7.2; Figure 7.3) leads to the conclusion that the P level in normal *f/2* medium (1 ppm P) was far in excess of the requirements for optimal *I. galbana* growth.

Table 7.2: Rates of *I. galbana* growth (Day 4-14), their regression coefficients and the significant differences between the growth rates in the various treatments as indicated.

Treatment	Rate (Cells.ul^{-1}/day)	Regression coefficient	Significant differences[a]
0.000 ppm P	0.1043 ± 0.0008	0.9784	A
0.010 ppm P	0.1005 ± 0.0094	0.9892	A
0.050 ppm P	0.1102 ± 0.0003	0.9359	A
0.125 ppm P	0.1157 ± 0.0027	0.9758	A B
0.250 ppm P	0.1293 ± 0.0015	0.9551	B
0.500 ppm P	0.1269 ± 0.0016	0.9380	B
1.000 ppm P	0.1277 ± 0.0008	0.9701	B
1.500 ppm P	0.1277 ± 0.0007	0.9550	B

[a] Rates with the same letters are not significantly different ($P > 0.005$)

The cell concentration in cultures starved of P (0 ppm) and those supplemented with low (0.01 ppm) levels of P initially increased very slightly (until day 4; Figure 7.3), but thereafter all growth ceased (Figure 7.3). The initial increase in growth was probably due to presence of intracellular PO_4 reserves already present in cells of the inoculum. Even the low amount of P added to the culture in the 0.01 ppm P treatment was sufficient to promote growth for a short duration, but cells ceased to grow and divide upon depletion of the P supply (intracellular P reserves and P in seawater). This observation verifies that P is essential for cell growth and division (Stewart, 1974; South and Whittick, 1987; El-Sheek and Rady, 1994).

Short durations of growth in P-starved cultures (0 ppm P) may also be attributed to the ability of phytoplankton to alter their cellular P requirements and rearrange the intracellular pool of P in an attempt to maintain optimal growth rates under P-limiting conditions until P-starvation occurs and growth ceases (Cembella *et al.*, 1984; Ji and Sherrell, 2008; Cade-Menun and Paytan, 2010). Such alterations include the synthesis of non-P containing membrane lipids (Van Mooy *et al.*, 2009) and the utilization of organic P. The switch to dependency on organic P is commonly initiated upon the depletion of the inorganic P supply (South and Whittick, 1987).

Generally, it has been widely noted that alkaline phosphatase in localized on the surface of the marine algal cells for the hydrolysis of extracellular organic P (Dyhrman and Palenik, 1997; Landry *et al.*, 2006; Xu *et al.*, 2006). However, alkaline phosphatase has been observed in intracellular locations in certain marine algal species including *Isochrysis* sp. (Gonzalez-Gil *et al*., 1998; Sun *et al.*, 2012). This leads to the assumption that *Isochrysis* has the ability to hydrolyze intracellular organic P when inorganic P levels are diminished. This was of particular importance in this experiment since fine-filtered, sterilized medium was used for algal culture which lacks a lot of the organic P present in the natural environment. Organic P may have been introduced with the algal inoculum and may be expelled into the medium by lysed algal cells or contaminating bacteria, but the levels of such contributions are minute in comparison with that evident in natural seawater. Hence, the use of both intracellular (to an extent since excessive use of this supply will be damaging to the cell) and extracellular organic P would be beneficial under severely P-limited conditions and would have contributed to the ability of *I. galbana* to maintain an elevated growth rate even under conditions of very limited P provided in the inorganic form.

Isochrysis showed a typical starvation response in the lower P treatments as evidenced by the saturation growth curves exhibited by this organism at these concentrations of P (Figure 7.3). Hence, P concentrations below 0.25 ppm initiated a P-induced limitation response in this species of *Isochrysis*.

Different microalgal species vary in their intracellular chemical composition. Hence, some species become P-limited in a particular medium whereas others become N-limited (Harisson *et al.*, 1990). The nitrogen to phosphorus ratio in *f/2* medium is 24:1 (Guillard and Ryther, 1962) and the Redfield N:P ratio (benchmark ratio for plankton) is 16:1 (Redfield, 1958). Thus, nitrogen is supplied in excess of its metabolic requirements in *f/2* medium if the Redfield ratio is applicable to this organism. Previous work on *I. galbana*, conducted by Kain and Fogg (1958), has shown that the minimum ratio of intracellular N to P is 52:1. The ability of the isolate to grow optimally in medium supplemented with quarter the P in *f/2* medium shows that the minimum N to P ratio lies above 96:1 highlighting the extent of the low P requirement of *I. galbana* U4. It is clear that the P content in *f/2* medium was supplied in excess of that needed by this species. Thus it may be deduced that, given the nutrient levels in *f/2* medium, growth cessation in *I. galbana* was initiated in response to other nutrient stresses (e.g. nitrogen starvation) or environmental factors (e.g. light limitation) rather than P-starvation.

P-starvation (0 ppm P) and limitation (0.01 - 0.125 ppm P) resulted in the highest recorded lipid yield, with algal cells accumulating up to approximately 50 % w/w lipid by day 14 (Figure 7.5). At this stage the cells are extremely stressed, as indicated by the growth curve (Figure 7.3). Such elevated lipid yields in *Isochrysis* has been observed elsewhere when exposing the alga to a growth-suppressing environment (Feng *et al.*, 2011). There was a reversal in lipid accumulation after day 12 in the 0 ppm P treatment (Figure 7.5). This was indicative of a cessation in lipid synthesis and the subsequent degradation or consumption thereof after a certain extent of cellular stress initiated by P-starvation (limited production of ATP and NADPH that is required to drive lipid synthesis). This also suggests that there was a possible limit to the amount of lipid that a particular cell was capable of storing, possibly a consequence of the limited volume of the cell that requires the storage of both essential organelles (e.g. nucleus, chloroplast) and lipid bodies. A halt in lipid synthesis in nutrient-stressed cells could additionally be ascribed to reduced chlorophyll levels resulting in a decline in the photosynthetic activity. The reduction on the chlorophyll content below a critical level (Figure 7.6; will be discussed later) impedes lipid accumulation, since solar energy which is captured by the

photosynthetic apparatus, is essential for the generation of the metabolic flux required for lipid synthesis and accumulation (Li *et al*., 2008a).

The reduction in the lipid yield in *I. galbana* cells exposed to extended periods of nutrient depletion has implications for the culturing of this species for lipid sequestration. It is imperative that the algal cultures are harvested and lipid extracted prior to or exactly when this maximal lipid content has accumulated in the cells (e.g. for the 0 ppm P treatment this window is between day 12 to 14; Figure 7.5) so as to avoid harvesting cells when lipid levels start falling during the post-maximal lipid accumulation phase. An increase in lipid yield in response to P-starvation is not new and has been reported by numerous investigators (El-Sheek *et al.*, 1994; Reitan *et al.*, 1994; Lynn *et al.*, 2000; Sigee *et al.*, 2007). Of particular interest was the study conducted by Reitan *et al.* (1994), since they used the same test organism. This study showed a direct correlation between the degree of P-limitation and lipid accumulation.

In the present study, there was no significant difference in the rate of lipid accumulation in higher P treatments ($P > 0.05$; Table 7.3). This was expected, since the P concentration tested (0.25 – 1.5 ppm P treatments) did not fall below the level that induces P-deficiency in this species (P limitation threshold lies somewhere between 0.125 and 0.25 ppm P; Figure 7.3). Hence, the cessation in growth and the subsequent induction of lipid accumulation was most probably stimulated by some other nutrient stress (most probably nitrogen evidenced by a decrease in the rate of growth in the higher P treatments on day 8 which correlated with the complete consumption of nitrogen in the milieu, cf. Figures, 7.3 and 7.4; the continuation of growth until day 14 was probably a consequence of the utilization of internal N reserves and the initiation of the stationary phase due to the depletion thereof; Figure 7.3). The treatments that were limited by the P concentration (0 – 0.125 ppm P) differed in that lipid synthesis was initiated earlier in P-starved cultures in comparison to P-limited cultures (i.e. greater levels of P-limitation initiated the earlier onset of the stationary phase concurrent with the initiation of storage lipid accumulation).

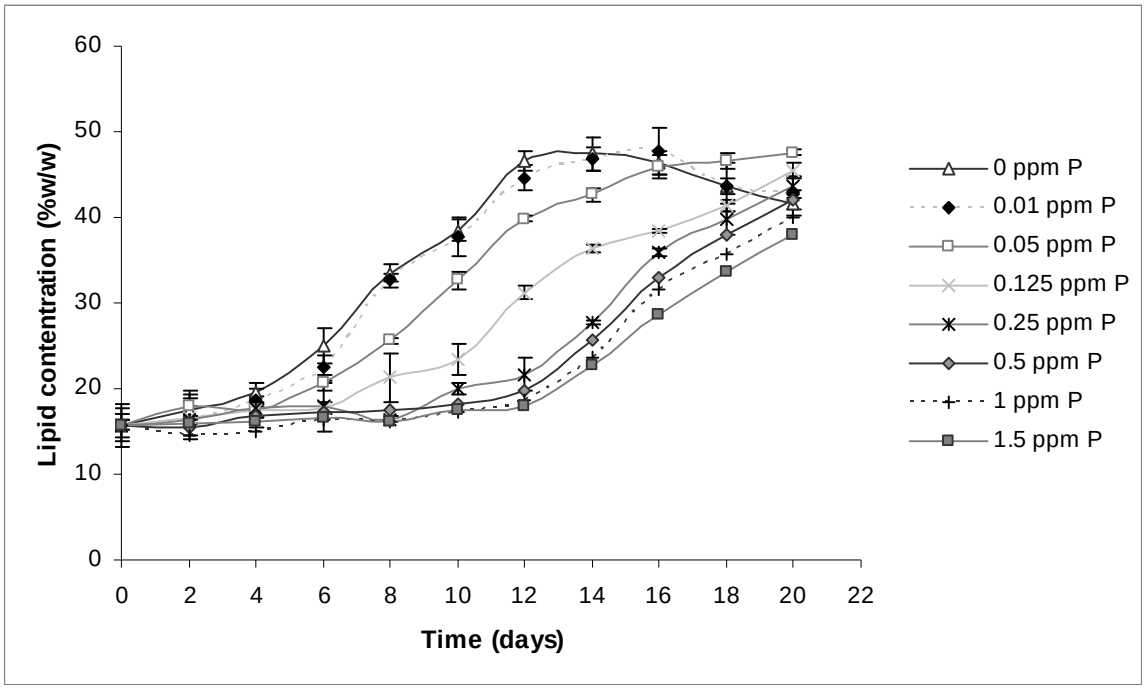

Figure 7.5: Lipid accumulation in *I. galbana* grown in *f/2* medium supplemented with various P concentrations. Error bars represent standard deviation (n=4).

Table 7.3: Rates of *I. galbana* lipid accumulation (Day 4-14), their regression coefficients and the significant differences between the rates in the higher P treatments.

Treatment	Rate (%w.w^{-1}/day)	Regression coefficient	Significant differences*
0.25 ppm Phosphate	0.1154 ± 0.0004	0.7103	A
0.50 ppm Phosphate	0.1152 ± 0.0011	0.7076	A
1.00 ppm Phosphate	0.1167 ± 0.0013	0.7752	A
1.50 ppm Phosphate	0.1126 ± 0.0952	0.6698	A

* Rates with the same letters are not significantly different (P > 0.05)

7.3.3 Effect of P-Limitation on *I. galbana* pigmentation

Cells that were not P-limited (0.25 – 1.5 ppm) showed a similar increasing trend of chlorophyll synthesis up to a plateau and followed by a decrease in the cellular chlorophyll content (Figure 7.6). Healthy cells accumulate chlorophyll for photosynthesis and growth and the chlorophyll levels decline during the stationary phase. All P-limited treatments (0 – 0.125 ppm) showed a decline in the chlorophyll content

relative to the levels of starvation (Figure 7.6). Chlorophyll does not contain P hence this decline can not be attributed to the breakdown of chlorophyll for P sequestration. When P becomes limiting, the majority of the photosynthate is directed towards the synthesis of storage products (e.g. lipids, Figure 7.5) and the biosynthetic pathways (e.g. leading to chlorophyll synthesis) become somewhat neglected (El-Sheek and Rady; 2004). The continuation of cell division concurrent with the halt in chlorophyll synthesis results in the reduction in the absolute content of chlorophyll per cell. The reduction in the chlorophyll content when growth ceases is in response to the inability to produce the energy molecules (ATP and NADPH) that drive chlorophyll synthesis when cells become P starved and the breakdown of the previously synthesized chlorophyll since chlorophyll has a short half-life.

The P-starved treatment (0 ppm P) resulted in cells with chlorophyll levels bordering 0.1 pg/cell by day 14 (Figure 7.6). This decrease in chlorophyll is important since the lipid levels in the 0 ppm P treatment also decline from day 14 (Figure 7.5). This corroborates the previous argument that lipid synthesis is halted and declines in response to below-critical (< 0.1 pg/cell) chlorophyll levels.

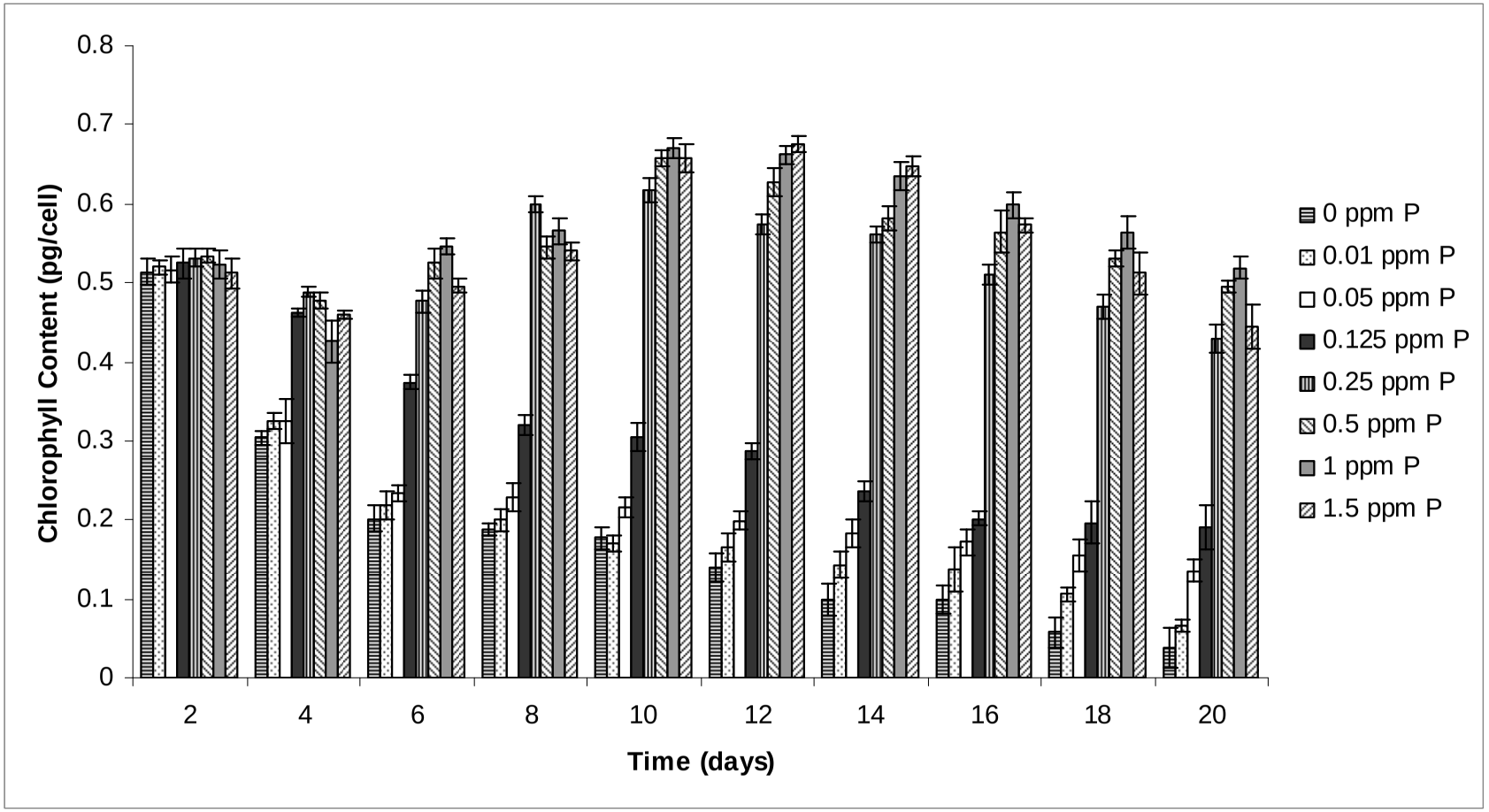

Figure 7.6: The chlorophyll content of *I. galbana* cultured in *f/2* medium supplemented with various phosphorous concentrations. Error bars represent standard deviation (n=4).

The carotenoid to chlorophyll ratio remained stable in the higher P treatments but increased rapidly in the P limited, lower P treatments (Figure 7.7). A stable ratio in the higher P treatments implies that the chlorophyll and carotenoid levels did not vary much. An increase in this ratio, in the P limited treatments, is indicative of an increase in the carotenoid content, a decrease in the chlorophyll content, or both. A definite decrease in the chlorophyll content was observed in the P limited treatments (Figure 7.6). The carotenoid concentration was not monitored however the rate of carotenoid to chlorophyll increase was greater than the rate of chlorophyll decrease hence the increase in the ratio was a function of both chlorophyll reduction and carotenoid accumulation. The increase in carotenoid concentration may have been a protective mechanism employed by the microalgal cells against photo-oxidative stress (Cade-Menun and Paytan, 2010).

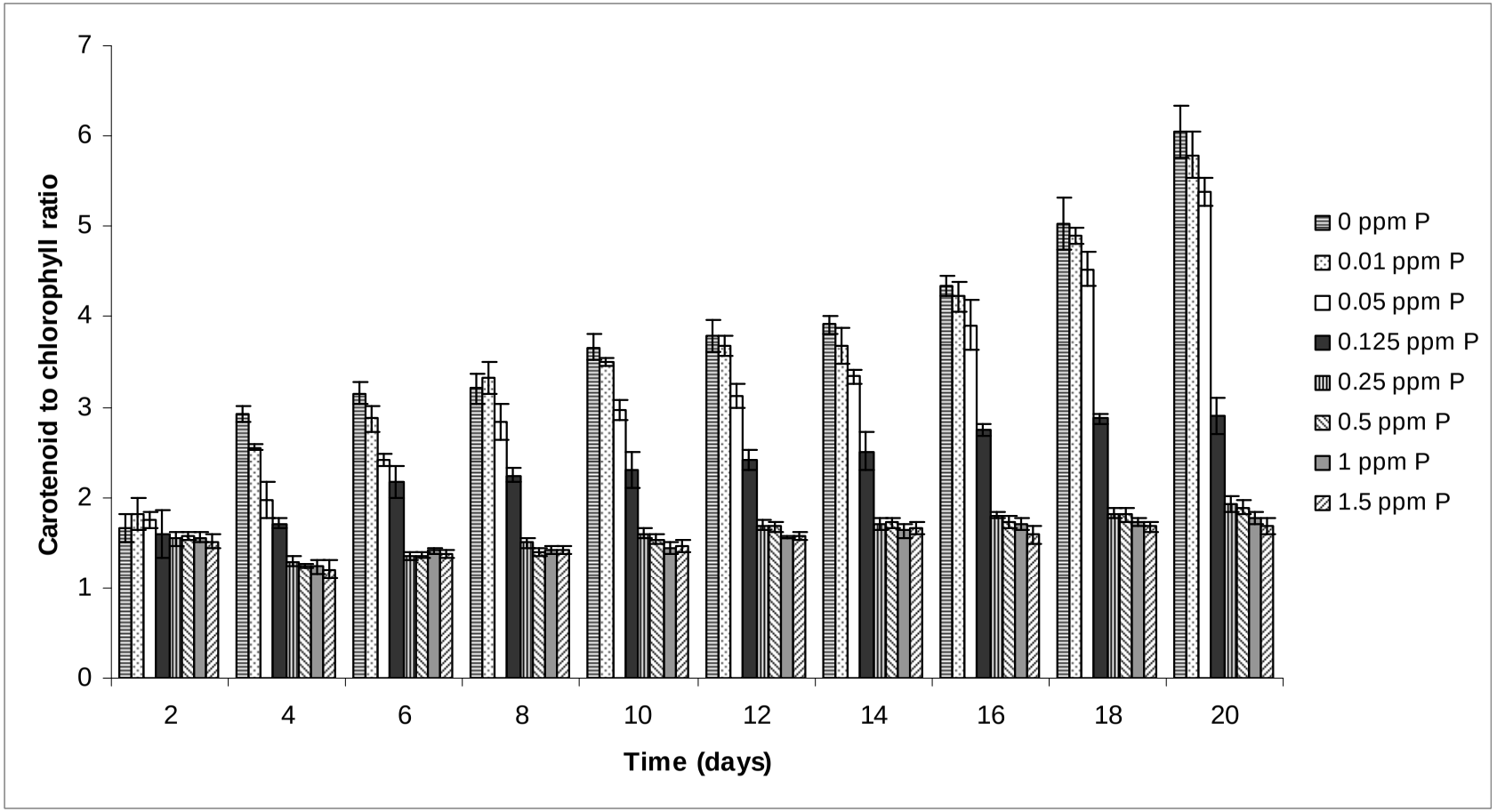

Figure 7.7: The carotenoid to chlorophyll ratio of *I. galbana* cultured in *f/2* medium supplemented with various phosphorous concentrations. Error bars represent standard deviation (n=4).

7.4 CONCLUSION

The growth rate, rate of lipid accumulation and pigmentation of *I. galbana* were unaltered when P was unlimited (higher P treatment; 0.25 – 1.5 ppm P). Thus, the P deficiency threshold for *I. galbana* lies below 0.25 ppm emphasizing the low P requirement of this organism. This has great implications for the mass culture of this species since reduced phosphorus requirements resulting in similar cell concentrations and photosynthetic rates would result in lower nutrient costs. The study also highlighted that *I. galbana* can store as much as six times the amount of P that it requires for maximum cell growth and division. Such elevated luxury uptake is advantageous in terms of species survival. Furthermore, the species can be used for P removal where excessive P levels become problematic in the environment.

CHAPTER EIGHT

Optimising the Dewatering Process of Cultures of *Isochrysis galbana* U4 by Flocculation

8.1 INTRODUCTION

It is usually necessary to first concentrate algal cultures before the lipid extraction process can commence. However, depending on the process selected, the cost of concentrating dilute cultures of microalgae may be unacceptably high (Uduman *et al.*, 2010a). Numerous techniques have been used for microalgae harvesting such as centrifugation, filtration, gravity sedimentation and flocculation (Sukenik *et al*., 1988; Edzwald, 1993, 1995; Danquah *et al*., 2009a,b; Lee *at al*., 2009; Uduman *et al*., 2010b; Zhang *et al*., 2010a,b). Each technique has its own set of associated disadvantages. Centrifugation is time-consuming, damaging to fragile species and requires costly equipment and high energy levels (Hung and Liu, 2006; Knuckey *et al*., 2006; Uduman, 2010a). Filtration requires the constant changing of screens, filters and membranes due to clogging, and gravity sedimentation is a lengthy process (Carvalho *et al*., 2006; Uduman, 2010a; Park *et al*., 2011). Conversely, if inexpensive, non-toxic flocculants are used and the coagulation process is optimised, flocculation is a low cost, rapid method that may be used for the treatment of large volumes of culture, making it a viable technique for microalgal concentration (Oh *et al*., 2001; Uduman, 2010a; Wu *et al*., 2012).

Flocculation refers to the process whereby particles in solution stick together, resulting in the formation of large aggregates called floccules (flocs), which settle out of solution due to increased mass and surface area. Generally, flocculation is induced by the addition of chemicals termed as flocculants (Knuckey *et al*., 2006; Uduman *et al*., 2010a; Show *et al*., 2012). Microalgal cells are negatively charged due to the ionization of surface functional groups (Ives, 1959; Folkman and Wachs, 1973; Edzwald, 1993). This negative charge results in the presence of electrostatic repulsive forces between the algal cells leading to the stability of the culture (Shelef *et al*., 1984). Destabilization of the system promotes flocculation due to the minimization of the electrostatic contact barrier between cells resulting in the dominance of attractive van der Waals forces over repulsive forces.

Particles in solution (colloids) possess an electric double layer at the interface between the particle and the solvent front (Hunter, 1988; Henderson *et al*., 2008). This double layer is formed due to the interaction between ions in the region surrounding the charged particle (interfacial region). The region closest to the charged particle attracts oppositely charged ions (counter ions) and repels ions of a similar charge to the particle. This region is referred to as the Stern layer. The layer of ions surrounding the Stern layer is termed the diffuse layer and consists of loosely bound counter-ions. Ions beyond the diffuse layer are in equilibrium with the solution (Omland, 2009; Figure 8.1).

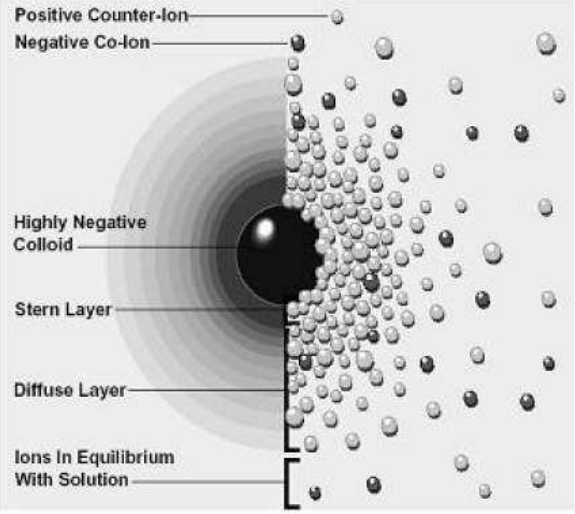

Figure 8.1: The Electrical Double Layer that surrounds a charged particle in solution (Adapted from Omland, 2009)

An exponential decrease in the potential energy of the electric double layer is evident with an increase in the distance from the surface of the charged particle (Figure 8.2; Omland, 2009). The Stern layer remains unchanged and is firmly attached to the colloidal particle however the charge of the diffuse layer is sensitive to factors such as pH changes and the ionic strength of the solvent (Hunter, 1988; Henderson *et al*., 2008; Omland, 2009). The measurement of the electric potential of the diffuse layer is referred to as the zeta potential (Figure 8.2; Hunter, 1988; Henderson *et al*., 2008). Zeta potential is thus the instantaneous, apparent charge on a particle in solution. As the zeta potential approaches the isoelectric point (zero zeta potential) the stability of the colloidal system

decreases resulting in the commencement of flocculation (due to decreased repulsive forces between particles) (Hunter, 1988). Hence, a reduction in the net electronegative charge on microalgal cells favors flocculation.

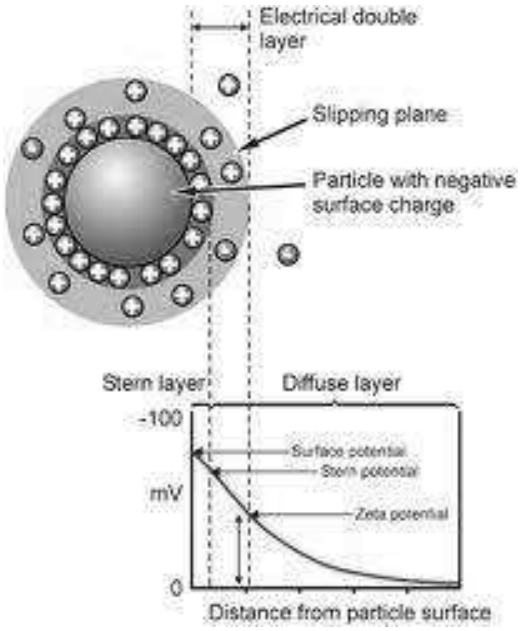

Figure 8.2: The decrease in the Electrical Double Layer potential as a function of the distance from the particle surface and the point at which the Zeta potential is measured (www.biochemistry-imm.org).

Factors that contribute to the degree of flocculation include temperature, culture age, hydrophobicity, cell density, ionic strength and pH of the culture medium, the type of flocculant used and cellular surface charges (Lee *et al*., 1998; Griffith *et al*., 2011; Eldridge *et al*., 2012). Commonly used microalgal flocculation methods include alterations in the pH of the medium (Elmaleh *et al*., 1991, 1992, 1998; Blanchemain *et al*., 1994; Yahi *et al*., 1994), chemical flocculation using metal salts (Sukenik *et al*., 1988) and autoflocculation (spontaneous flocculation without the addition of chemical flocculants) (Sukenik and Shelef, 1984; Spilling *et al*., 2011). A key factor when selecting a flocculation method is the ability to recycle excess medium post flocculation. Medium recycling would aid in the reduction of production costs since the pumping of medium to bioreactors would be minimized. For medium recycling to be possible the

flocculant used should not contaminate the growth medium or interfere with microalgal growth (Lee *at al*., 1998; Wu *et al*., 2012).

In this study various flocculation methods were tested to determine a cost effective dewatering process that will result in maximal cell recovery in *I. galbana* cultures. Furthermore, excess medium recycling and the effect of the algal growth stage on the flocculating ability of various flocculants were analysed.

8.2 MATERIALS & METHODS

8.2.1 Experimental setup

Non-axenic, monocultures of *I. galbana* U4 were used for all flocculation studies. Cultures were grown in filtered and autoclaved *f/2* medium (Section 2.1). A modification of the flocculation jar test, described by Uduman *et al*. (2010a), was used for all flocculation experiments. Experiments were conducted in 100 ml glass beakers (diameter = 5 cm, height = 7 cm) that were filled with 70 ml of the algal culture. The desired flocculant volume was added to the microalgal culture in the beaker while the culture was agitated, at a high speed, using a magnetic stirrer (Fried Electric, Model F-13). The speed was then decreased and agitation continued for two minutes. Settling followed for between 30 minutes to four hours, depending on the experiment to be conducted. Upon completion of the settling step a sample was pipetted from a fixed height in the jar (1 cm below the surface of the culture) and absorbance readings were taken to determine the cell concentration as described in Section 2.5. All experiments were conducted in triplicate.

8.2.2 Flocculation efficiency measurements

The following equation was used to determine flocculation efficiency:

$$\textit{Flocculation efficiency (\%)} = [(C_i - C_f) / C_i] \times 100$$

Where C_i refers to the concentration of cells prior to treatment and C_f refers to the final cell concentration upon completion of the settling stage (Harith *et al*., 2009). The final cell concentration was obtained by siphoning a culture sample 1 cm from the top of the culture. Absorbance readings of the sample were taken at 650 nm and the cell concentration was obtained from a previously constructed standard curve depicting cell concentration versus absorbance (Section 2.5).

8.2.3 Sedimentation rate measurements

The sedimentation rate was determined by measuring the distance of the cell front (sedimented sample) in mm from the top of the culture with respect to time (seconds) using a ruler and the naked eye (Spilling *et al*., 2011). Data points were obtained at ten random time intervals. These points were taken together to construct a best fit curve depicting the flocculation time with respect to the sediment height. The slope of the graph represented the maximum sedimentation rate (Harith *et al*., 2009).

8.2.4 pH-induced flocculation

Sodium hydroxide, potassium hydroxide and calcium hydroxide (the latter of which forms a fine suspension in water as milk of lime; all 2.5M) were used to induce pH stimulated flocculation in *I. galbana*. Jar tests were conducted as described in Section 8.2.1. The respective base was used to adjust the culture pH from pH 9.5 to pH 11 in 0.5 increments. The cultures were continuously agitated, using a magnetic stirrer (Fried Electric, Model F-13), upon addition of the base to ensure that the pH readings had settled. Cultures were then allowed to settle over four hours and intermittently sampled, on an hourly basis, to determine the efficiency of flocculation (Section 8.2.2). The movement of the flocculated cells through the medium was also monitored periodically to determine the rate of sedimentation (Section 8.2.3). The sedimented sample was viewed using a Zeiss Axiophot microscope with Nomarski optics.

8.2.5 Medium recycling

Once flocculation induced by pH was complete (approximately 100% flocculation efficiency achieved; Section 8.2.2) the remaining seawater, above the sedimented cells,

was siphoned off. This seawater was autoclaved at 121 °C for 30 minutes, allowed to cool and filtered under a laminar flow bench. The pH was adjusted, to that of normal seawater (pH 8.3), using 0.5 N sulphuric acid. Nutrients and vitamins were added to the seawater as recommended by the *f/2* medium preparation protocol (Guillard and Ryther, 1962; Appendix). A 20 ml aliquot of resultant medium from each flocculant treatment, was transferred to 100 ml Erlenmeyer flasks. The medium was then inoculated with $1.4*10^6$ seven day old *I. galbana* cells and growth was monitored over 17 days. Un-recycled *f/2* medium was used as a control. The position of the flasks on the culture shelf relative to the unidirectional light source was randomly shuffled to reduce error from experimental design.

8.2.6 Chemical flocculation

Ferric chloride, ferrous sulphate and aluminium sulphate were used as chemical flocculants. Jar tests (Section 8.2.1) were conducted where various concentrations of each flocculant was added to early stationary phase, *I. galbana* cultures to determine the optimal flocculant dosage i.e. the lowest chemical dosage resulting in maximal cell recovery (Sukenik *et al*. 1988). Prior to flocculation using ferric chloride and aluminium sulphate the culture pH was adjusted to pH 5.5 and pH 5 respectively using 0.5 N sulphuric acid to promote the formation of cationic hyrolysis products thus maximizing the efficiency of flocculation with the specific metal salt (Morraine *et al*., 1980; Shelef *et al*., 1984; Millamena *et al*., 1990; Uduman *et al*., 2010b). Furthermore, this pH adjustment was used successfully by Sukenik *et al*. (1988) for the flocculation of *I. galbana* cells. Ferrous sulphate did not require pH adjustment to optimize the flocculating ability. The flocculation efficiency for each flocculant concentration was measured after 30 minutes of settling (Section 8.2.2). .

8.2.7 Autoflocculation

Early stationary phase *I. galbana* cultures were exposed to the following conditions in an attempt to initiate autoflocculation:

(1) 3 °C, non-agitated and not aerated by bubbling, in the dark

(2) 22 °C, non-agitated and not aerated by bubbling, in the light
(3) 22 °C, non-agitated and not aerated by bubbling, in the dark
(4) 22 °C, agitated and aerated by bubbling, in the light and
(5) 22 °C, non-agitated and not aerated by bubbling, in the light, with double the biomass

In treatment four, the cultures were aerated using an air pump (Labotec with pressure of 2.4 bar). For treatment five, cells were centrifuged gently at 1000 rpm and the required volume of the pellet was resuspended in the culture to obtain double the biomass of microalgal cells. Non-agitated cultures were not moved for the duration of the experiment. As with the previous experiments, all the autoflocculation experiments were conducted in 100 ml beakers. The treatments were monitored over two weeks and the flocculation efficiency was measured every alternate day (Section 8.2.2). On the first and last days of the experiment pH measurements of all treatments were taken to determine if any flocculation observed was pH induced.

8.2.8 Growth stage flocculation

*F/*2 medium was inoculated with $1*10^6$ seven day old *I. galbana* cells. These cultures were subjected to a constant illumination of 110 µmol photons.m^{-2}.s^{-1} at 25 °C and were aerated with filtered air (Whatman uniflo 0.2 µm filter) with the aid of an air pump (Labotec with a pressure of 2.4 bars). Air was passed through a humidifier, prior to being pumped through the cultures, in an attempt to minimize culture evaporation. At various phases of the sigmoidal growth pattern of the batch culture jar tests (Section 8.2.1) were conducted to induce flocculation of the cells using the following treatments:

(1) Increasing the culture pH to 10.3 using potassium hydroxide
(2) Increasing the culture pH to 10.3 using sodium hydroxide
(3) Increasing the culture pH to 10.3 using calcium hydroxide
(4) Using a pre-determined concentration of ferric chloride
(5) Using a pre-determined concentration of ferrous sulphate and
(6) By gravity settling

The culture pH was adjusted to 5.5 prior to flocculation with ferric chloride and left unadjusted for ferrous sulphate flocculation experiments (Section 8.2.6). Aluminium sulphate was eliminated from this study due to its limited ability to flocculate *I. galbana* U4 cells. The cell front was allowed to settle for 30 minutes before the flocculation efficiency was determined (Section 8.2.2).

8.2.9 pH measurements

A pH meter (Precisa pH900) was used to measure the pH of the cultures. The pH probe was immersed into the cell suspension that was agitated using a magnetic stirrer (Fried Electric, Model F-13) to ensure even, constant mixing. Readings were taken only after the meter output stabilized.

8.3 RESULTS & DISCUSSION

8.3.1 pH-induced flocculation and medium recycling

Flocculation was evident in all base treatments (potassium hydroxide, sodium hydroxide and calcium hydroxide), at all pH levels but maximal flocculation (> 95%) was achieved at pH 10.5 and above (Figure 8.3 - 8.6). This pH-induced flocculation, at elevated pHs, has been observed in multiple studies with various microalgal species (Elmaleh *et al*., 1991, 1992, 1998; Blanchemain *et al*., 1994; Yahi *et al*., 1994; Nurdogan and Oswald, 1995; Lee *et al*., 1998; Knuckey *et al*., 2006; Vandamme *et al*., 2012). Authors have attributed this observation to the neutralization of negatively charged algal cells by the addition of bivalent cations such as calcium and magnesium (Nurdogen and Oswald, 1995). In earlier studies investigators have suggested that this process occurs as a result of the production of positively charged precipitates which interact with the algal cells and promote flocculation (Sukenik and Shelef, 1984).

The use of calcium hydroxide as an algal flocculating agent has been extensively studied due to its comparatively low cost, its non-toxicity and the desirability of calcium cations in animal feed. The flocculating ability of calcium hydroxide observed by some authors

was only prevalent if the culture medium had a high concentration of magnesium ions (Folkman and Wachs, 1973). The medium used in this study (*f*/2 medium) is enriched seawater and basal seawater contains approximately 1294 ppm magnesium (Kester *et al*., 1967). This high concentration of magnesium ions may have assisted in the flocculation process (Elmaleh *et al*., 1998). Other authors attributed flocculation to the precipitation of positively charged calcium phosphate which neutralizes algal cells and promotes agglomeration (Sukenik and Shelef, 1984). *F/2* medium contains 1 ppm phosphorous which is completely scavenged from the medium during the early exponential phase (Chapter 7). Hence, calcium phosphate precipitation does not explain the calcium hydroxide initiated flocculation evident in this study due to all the phosphate in the medium being consumed prior to initiation of the experiment.

Calcium hydroxide induced flocculation may also be a consequence of the formation of calcium carbonate which results due to the reaction between calcium hydroxide and dissolved carbon dioxide in the culture medium. Calcium carbonate may precipitate out of solution and entrap the particles via 'sweep coagulation' which refers to the enmeshment of the cells in large amounts of precipitate. This would result in an increased density of the settling particles consequently leading to gravity sedimentation (Leentvar and Rebhun, 1982). This process could explain the observations in the jar experiments where a distinct sedimentation front was observed at pH 10.5 and above (Figures 8.5 B and 8.6 B). Sedimented cells (Figure 8.7) showed a gelatinous precipitate between the cells further justifying the 'sweep coagulation' theory. Calcium carbonate precipitate carries a negative charge at all pH levels that it exists (Larson and Buswell; 1940; Folkman and Wachs; 1973; Leentvar and Rebhun, 1982; Smith and Davis; 2012). This implies that calcium carbonate would play no role in charge neutralization of the negatively charged microalgal cells. Calcium ions, conversely, are positively charged. Thus, it may be deduced that the dissolved species contribute significantly to charge neutralization whereas the precipitates play an integral role in 'sweep flocculation' (Henderson *et al*., 2008).

However, neutralization of the microalgal cells may also have been achieved by the formation of positively charged, gelatinous magnesium hydroxide precipitate (Larson and Buswell; 1940; Folkman and Wachs; 1973; Leentvar and Rebhun, 1982; Smith and Davis; 2012), due to the large amount of magnesium in seawater, which would aid in the dual role of charge neutralization and agglomeration (Elmaleh *et al*., 1998; Schlesinger *et al*., 2012). The large open structure of magnesium hydroxide precipitate implies that it would easily entrap algal cells (Duan and Gregory, 2003). The role of magnesium in microalgal destabilization and concentration was proven in a study conducted by Wu *et al*., (2012) where the elemental composition of pH-induced, algal flocs was deduced using energy-dispersive X-ray (EDX) analysis. This analysis revealed large amounts of magnesium in the sediment and a decrease in the magnesium concentration of the culture medium inferring the importance of magnesium in agglomeration.

Increases in the culture pH induced by potassium hydroxide and sodium hydroxide, may have resulted in similar observations of adsorption and flocculation where magnesium hydroxide, calcium carbonate and magnesium and calcium cations contribute to the agglomeration process. However, direct observation of the cells sedimented by the introduction of calcium hydroxide shows them to be very different to those that flocculate via the other two treatments. As evident in Figure 8.7, the calcium hydroxide treatment favoured far more clumping of cells as indicated by the larger amount of precipitate between the cells. The increased amount of precipitate is also observed in the jar experiments, post sedimentation, (Figures 8.5 B and 8.6 B) where the algal sludge from the calcium hydroxide treatment was much whiter in comparison with the other two treatments (the whiter sludge implies that more white precipitate relative to green cells is evident in the calcium hydroxide treatment than in the other two treatments). This elevated precipitate in the calcium hydroxide treatment could be as a result of the inability of calcium hydroxide to dissolve in the medium (calcium hydroxide dissociates in water preferentially at different pHs). This could also be due to the rapid formation of large amounts of calcium carbonate which would precipitate out of solution above a solubility limit.

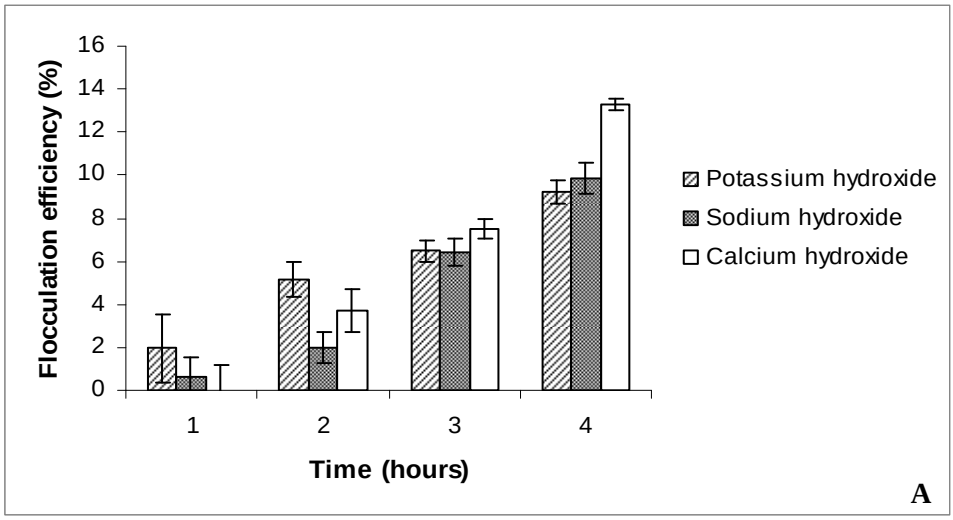

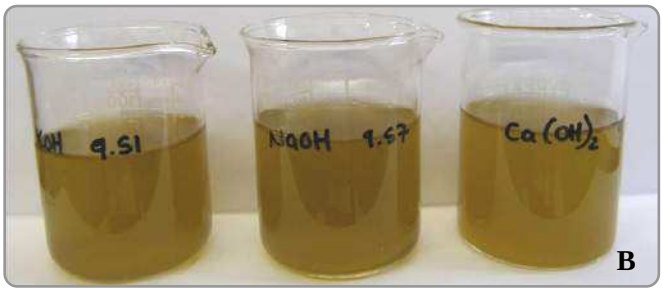

Figure 8.3 (A): Flocculation efficiency of *I. galbana* at pH 9.5 brought about by the addition of various salts as indicated. Error bars represent standard deviation (n=3) and **(B):** resultant cultures four hours after the alteration of pH.

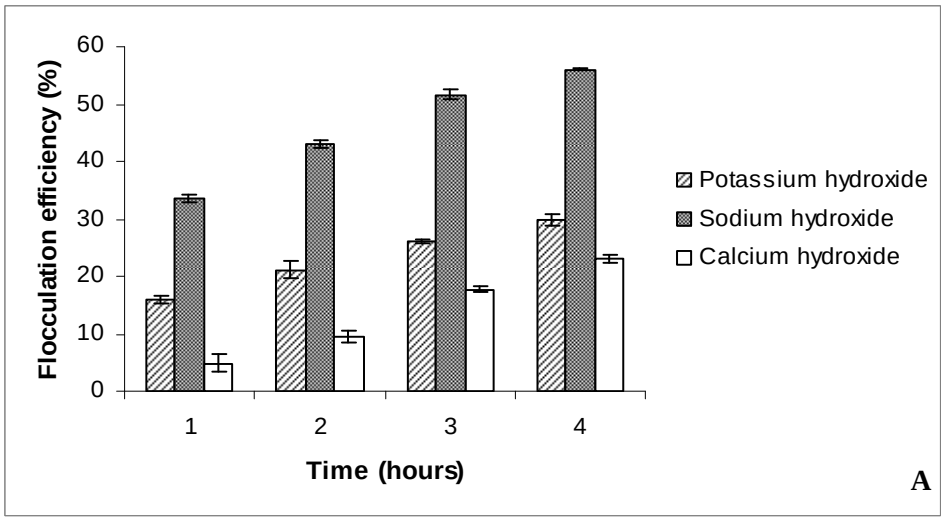

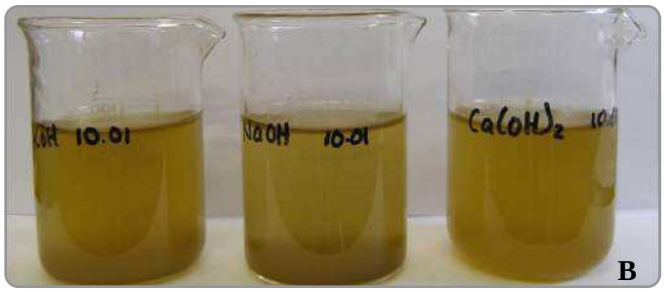

Figure 8.4 (A): Flocculation efficiency of *I. galbana* at pH 10 brought about by the addition of various salts as indicated. Error bars represent standard deviation (n=3) and **(B):** resultant cultures four hours after the alteration of pH.

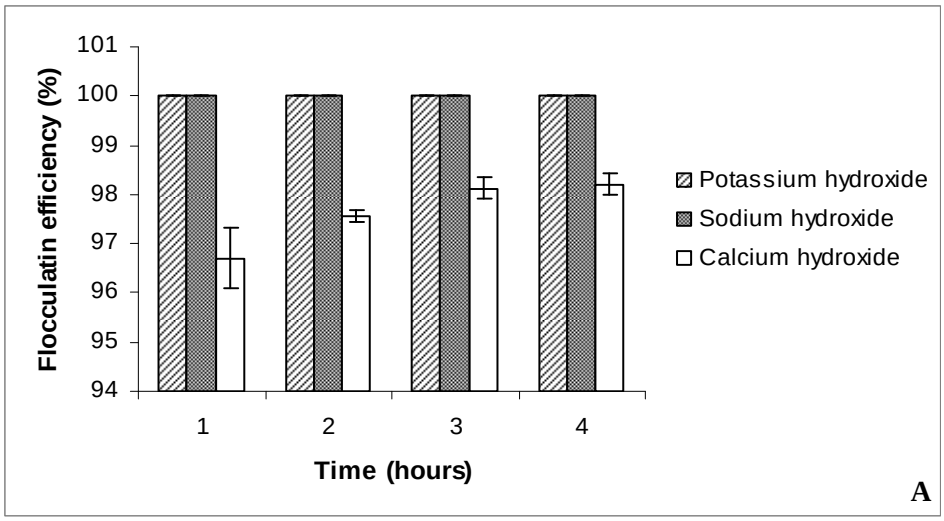

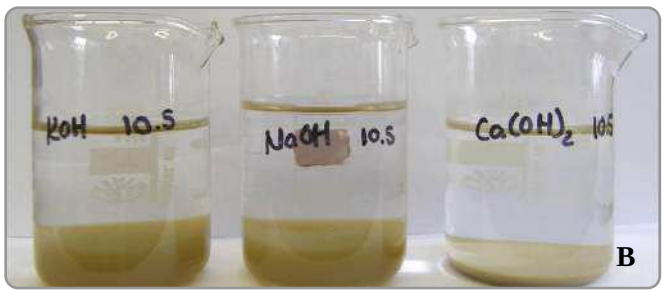

Figure 8.5 (A): Flocculation efficiency of *I. galbana* at pH 10.5 brought about by the addition of various salts as indicated. Error bars represent standard deviation (n=3) and **(B):** resultant cultures four hours after the alteration of pH.

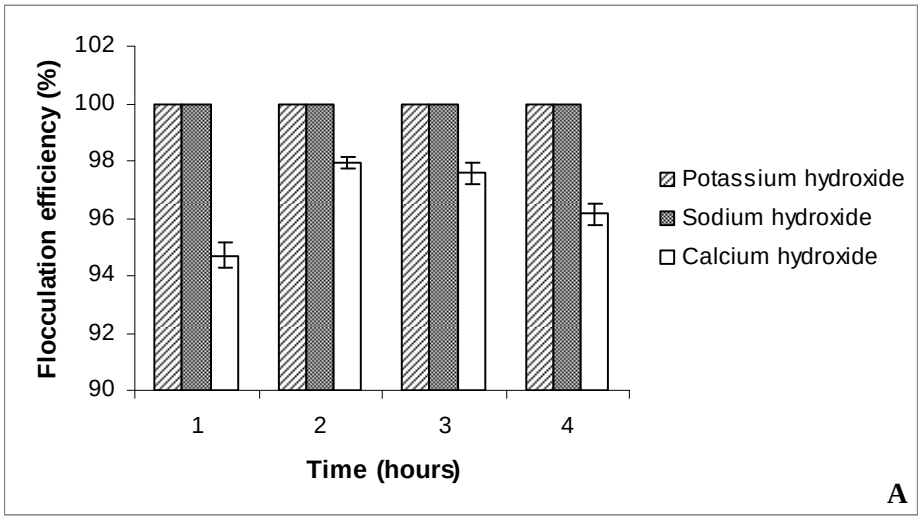

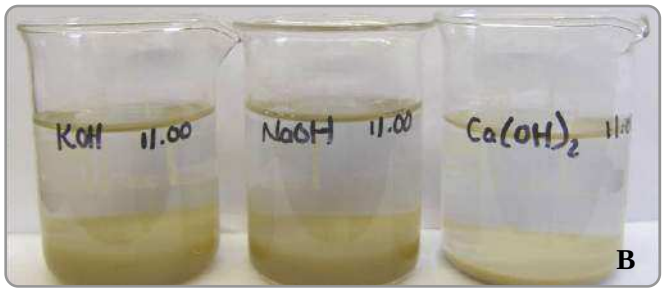

Figure 8.6 (A): Flocculation efficiency of *I. galbana* at pH 11 brought about by the addition of various salts as indicated. Error bars represent standard deviation (n=3) and **(B):** resultant cultures four hours after the alteration of pH.

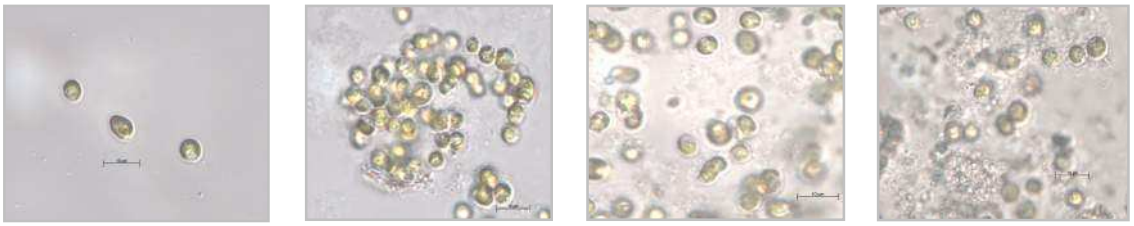

Control | **Potassium hydroxide (pH 10.5)** | **Sodium hydroxide (pH 10.5)** | **Calcium hydroxide (pH 10.5)**

Figure 8.7: Appearance of sedimented *I. galbana* cells after being subjected to a pH of 10.5 brought about by various salts as indicated. Control refers to cells subjected to pH 8.3. Scale bar represents 10 µm.

Another factor that may have contributed to the flocculation of the algal cells observed in this experiment, is the variation in the surface charge of the cells. Zeta potential

measurements were not monitored in this study however numerous other authors analysed this parameter in microalgal flocculation experiments (Henderson *et al*., 2008; Danquah *et al*., 2009b; Beach *et al*., 2012; Wu *et al*., 2012). Wu *et al*. (2012) showed that in marine microalgal systems pH increases led to a concomitant increase in the zeta potential. This results in a reduction in the microalgal repulsive forces thus aiding flocculation. In the study, *Nannochloropsis oculata* and *Phaeodactylum tricornutum* were used as test marine organisms. The zeta potential of *N. oculata* rose from -40 mV to -15 mV upon pH increase from 7.3 to 10 and that of *P. tricornutum* increased from -10 mV to approximately 0 mV within the same pH range. These observations indicate a species specific decrease in the surface charge of the microalgal cells at elevated pHs. A similar occurrence would have been observed in the present pH-induced flocculation study with *I. galbana*, but no zeta potential studies were undertaken on this species to validate this.

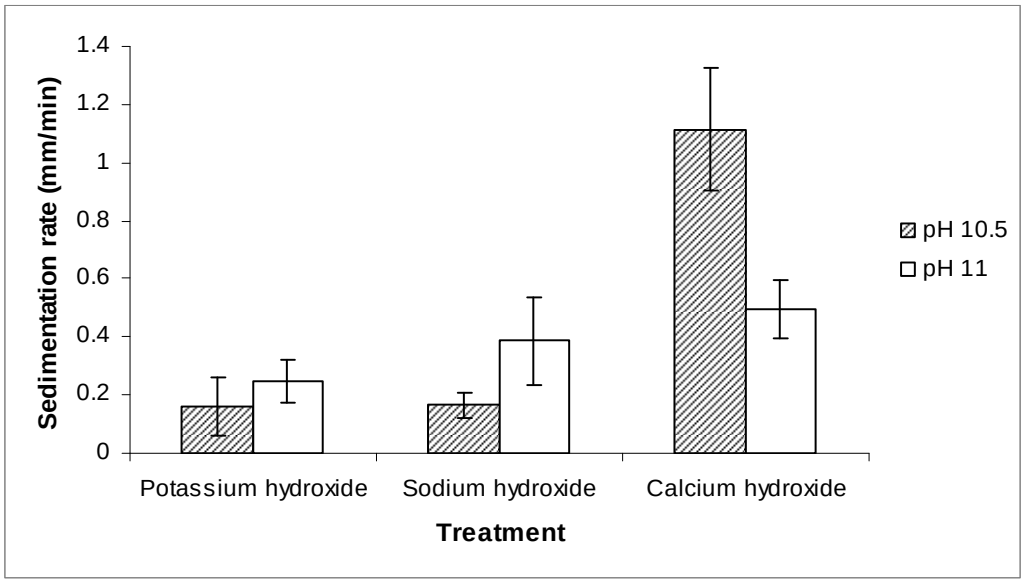

Figure 8.8: The rate of sedimentation of *I. galbana* in the indicated alkaline treatments at pH 10.5 and 11. Error bars represent standard deviation (n=3).

The settling velocity of the microalgal sludge is pH dependant and increased with an elevation of pH when using KOH and NaOH but decreased when similarly using $Ca(OH)_2$ (Figure 8.8). The increased rate of sedimentation brought about by elevated pH

via the addition of potassium hydroxide and sodium hydroxide is attributed to the increase in the algal sludge density due to an elevated amount of precipitate being produced upon addition of more basic solution. This is further verified by the jar test pictures (Figure 8.5 B and 8.6 B) where the algal sludge in the pH 11 treatment is lighter green (more white precipitate than green cells) in comparison to the pH 10.5 sludge, indicating more precipitate at a greater pH.

The algal sludge generated by calcium hydroxide at pH 10.5 sedimented out of solution approximately six times quicker then the corresponding sodium hydroxide and potassium hydroxide algal sludges implying that superior thickening and dewatering may be achieved when using calcium hydroxide. The elevated density of the calcium hydroxide generated algal sediment is also clearly evident from the jar tests where the sedimentation front is much lower than that observed in the other two treatments after four hours (Figures 8.5 B and 8.6 B). This, elevated density of the calcium hydroxide (pH 10.5) generated algal sludge is advantageous in that the resulting sludge has a lower water content, which would result in cost reductions if further dewatering using methods such as centrifugation is required prior to oil extraction, since a smaller volume of algal sludge would need to be concentrated.

Interestingly a decrease in the sedimentation rate was observed in the calcium hydroxide treatment upon pH increase from 10.5 to 11. This observation is counter-intuitive since an elevated pH would result in a larger precipitate yield that would presumably result in the increased settling rate due to an increase in the density of the sedimentation front (cell-precipitate combination). No doubt the calcium hydroxide (pH 11) treatment had the largest amount of precipitate in comparison to all other treatments (this is clearly observed in Figure 8.6 B where the algal sludge in the pH 11, calcium hydroxide treatment looked whiter than that observed in the other treatments implying the largest precipitate to cell ratio in this treatment). The reduced sedimentation rate in the pH 11, calcium hydroxide treatment may actually be attributed to the observed excess in precipitate. Microalgal floccules that form as a result of precipitate binding to cells have loose structures (not closely-packed). Moreover, all the floccules formed are not of the

same size hence some floccules would settle quicker than others. When excess precipitate is evident in the medium algal floccules tend to attach to each other, due to the formation of precipitate bridges resulting in the formation of large floccule-precipitate networks. These networks result in a reduction in fluid movement (between flocs) and prevent larger floccules from passing smaller ones so all floccules sediment at the same time causing a reduction in the sedimentation rate (Smith and Davis, 2012).

The sedimented cells post-flocculation were stained with tryphan blue to determine if the pH treatments were harmful to the cells. This test showed no damaged cells since none of the cells took up the stain implying that *I. galbana* is tolerant to exposure to elevated pHs. Furthermore, the direct observation and comparison of the flocculated and non-flocculated cells (Figure 8.7; pH flocculated compared with control) showed that all cells were intact and looked the same. Similar observations were evident in flocculation experiments conducted by other investigators where microalgal cells were unaffected by short durations of pH increases (Blanchemain and Grizeau, 1999; Ravi and Sivasankara, 2002; Knuckey *et al*., 2006; Spilling *et al*., 2011).

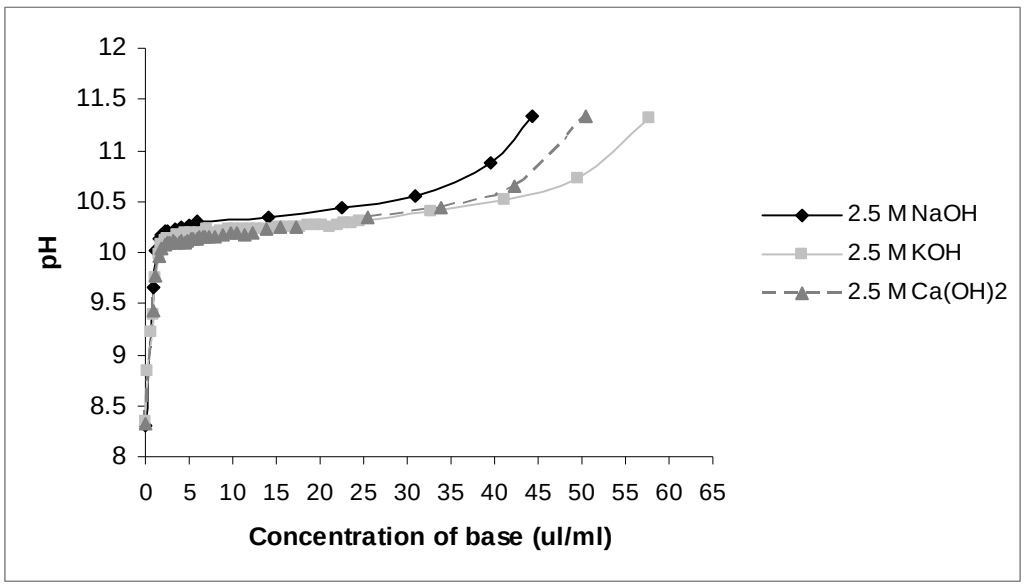

Figure 8.9: Alkaline concentration required for *f/2* medium pH increase using the indicated basic solutions.

The medium was very buffered against pH change between 10.2 and 10.5 irrespective of the driver of pH change (Figure 8.9). Sodium hydroxide treatments required a smaller volume of the basic solution to reach the same pH as the other two treatments. This implies that sodium hydroxide would be advantageous in the scale-up of this process. However, the cost of the actual chemicals also need to be taken into account as larger quantities of calcium hydroxide may still be cheaper then smaller quantities of sodium hydroxide. The vast volumes of all base solutions required for the slight pH increase, from 10.2 to 10.5, may be attributed to the inherent buffering ability of seawater (Knuckey at al., 2006).

As the pH values approached the buffer zone of the medium a fine white precipitate appeared irrespective of the driver used. More precipitate formed as more alkali was added to the culture medium. This precipitate interacted with the cells in suspension and contributed to the bulk of the resultant sludge observed post-settling.

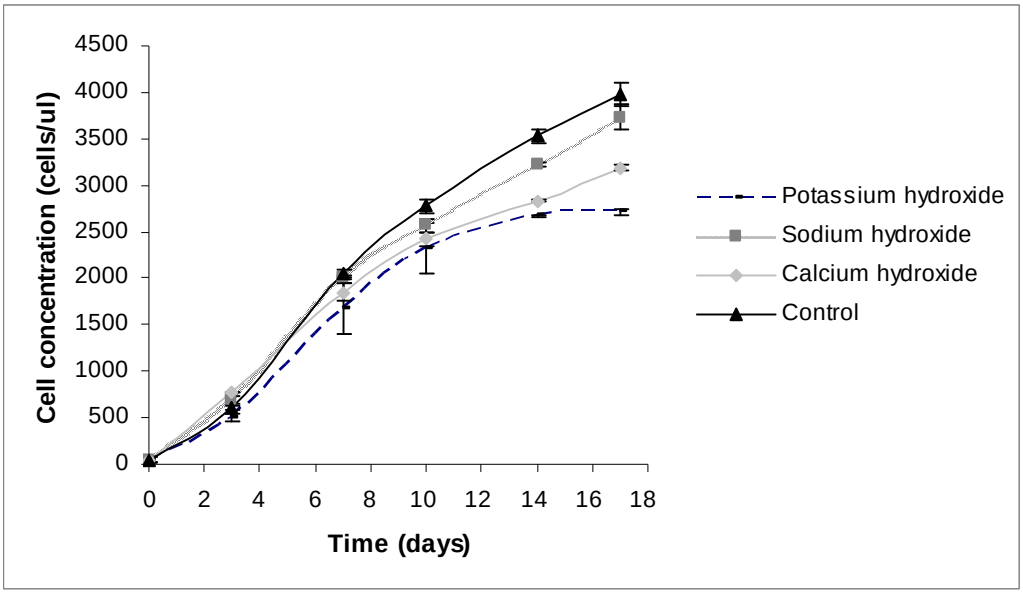

.

Figure 8.10: *Isochrysis galbana* growth in medium recycled from the pH experiments using different drivers as indicated. Control refers to non-recycled *f*/2 medium. Error bars represent standard deviation (n=3).

Table 8.1: Rates of *I. galbana* growth, their regression coefficients and the significant differences between the growth rates in the various treatments as indicated.

Treatment	Rate (Cells.ul^{-1}/day)	Regression coefficient	Significant differences*
Potassium hydroxide	0.1716 ± 0.0016	0.9382	A B
Sodium hydroxide	0.1718 ± 0.0024	0.9671	A B
Calcium hydroxide	0.1674 ± 0.0007	0.9537	A
Control	0.1764 ± 0.0016	0.9739	B

* Rates with the same alphabet are not significantly different (P > 0.005)

Isochrysis galbana growth and division was not inhibited in all post-flocculation, recycled medium (Figure 8.10). Both the recycled potassium hydroxide and sodium hydroxide medium treatments yielded growth rates that were significantly similar to the control treatment (P > 0.005; Table 8.1) implying that medium recycling after algal flocculation using these treatments is feasible. However, the growth rate in the calcium hydroxide treatment was significantly different from the control growth rate (P < 0.005; Table 8.1). Cell clumps were observed in cultures grown in the recycled medium from calcium hydroxide treatments. This could have been as a result of the presence of calcium hydroxide precipitate in the growth medium even after the pH alteration (back to pH 8.3), which resulted in some flocculation as growth proceeded hence fewer cells in suspension. This would not adversely affect the process of medium recycling since a similar cell concentration, as in the control, might still be obtained eventually when harvesting the cells.

From the above pH induced flocculation experiments, it may be deduced that the addition of alkaline solutions to microalgal cultures, above the solubility limit (resulting in saturated solutions), induces flocculation (Davis and Foust, 1969). These alkaline treatments allow for the separation of microalgal cells from culture medium but also contaminate the cells with the salts used (Figure 8.7). This is not a major obstacle since small quantities of such salts are non-toxic. Alkaline treatments such as calcium hydroxide are preferred since it is cost effective and calcium is not harmful in animal feed (Schlesinger *et al*., 2012). Potassium hydroxide and sodium hydroxide residues in

the concentrated microalgal sludge are also advantageous in that they act as catalysts in the transesterification process, leading to biodiesel production (Cavalho *et al.*, 2011).

A recent study disproved the theory that the amount of alkali necessary to flocculate cells increases as a linear function of the number of cells in the culture. In this study Schlesinger *et al*. (2012) showed that denser cultures require smaller concentrations of the alkaline solution to induce flocculation. In the present study no experiments were conducted to determine the effect of cell concentration on the pH at which flocculation was initiated in *I. galbana*. A decrease in the volume of the basic solution to flocculate dense cultures would be beneficial in that it would result in a cost decrease and increased biomass yield of pH-induced flocculation. It would also reduce the amount of inorganic precipitate in the microalgal sludge.

8.3.2 Chemical flocculation

The mechanism by which flocculation occurs, when metal salts are used, is via charge neutralization due to the adsorption of cations by the negatively charged microalgal cells (Folkman and Wachs, 1973; Uduman *et al*., 2010b). Ferrous sulphate resulted in maximal flocculation (approximately 30% efficiency) at 120 mg/l, followed by ferric chloride that resulted in approximately 20% flocculation efficiency at 160 mg/l. Aluminium sulphate was ineffective as a flocculant for *I. galbana* U4 (Figure 8.11). None of the metal salt treatments yielded flocculation efficiencies that would warrant their serious consideration as feasible dewatering agents.

Sukenik *et al*. (1988) conducted a similar study where they observed almost complete flocculation of a culture of *I. galbana* when high aluminium sulphate and ferric chloride doses (within the range of the current study) were used. In that study a comparison of the flocculation efficiency of marine and freshwater species showed that much larger amounts of the flocculant was required in the marine system and they attributed this to the high salinity of marine cultures resulting in the reduction in the activity of the flocculant due to the masking of its active sites. Moreover, the elevated amount of flocculant required to flocculate *I. galbana* was also attributed to the motility of the

species (Sukenik *et al*., 1988). A high coagulant demand for this species was also observed by Eldridge *et al*. (2012), where aluminium sulphate and iron sulphate were used as flocculating agents. The results obtained in this study were similar to that acquired by Knuckey *et al*., (2006) were they observed poor flocculation (less than 30%) of an unidentified species of *Isochrysis* using ferric chloride. They attributed this to an 'incompatible cell surface chemistry' but did not elaborate on this inference. The poor flocculating ability of aluminium sulphate evident in this study was also observed in a study conducted by Millamena *et al*. (1990) where they attempted to flocculate *I. galbana* using alumimiun sulphate.

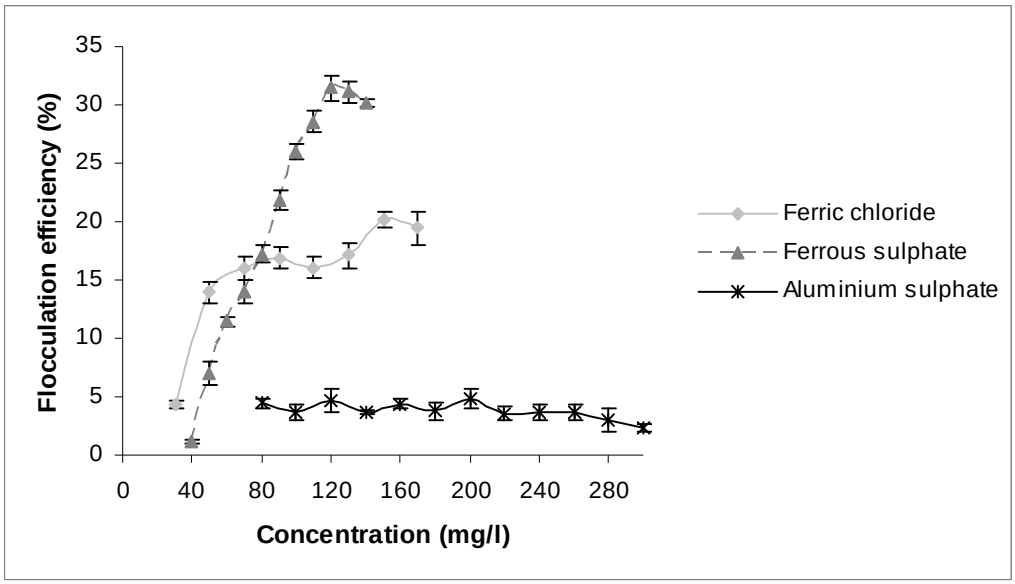

Figure 8.11: Flocculation of *I. galbana* using inorganic flocculants. Error bars represent standard deviation (n=3).

The limited success using metal salts to flocculate *I. galbana* may be due to the properties of the cells of this species, such as the small size (4-5µm) and motility. This species of *Isochrysis* does not possess a cell wall but is covered by numerous layers of small glycoprotein scales that are hydrophilic in nature (Green and Pienaar, 1977; Chapter 4). This cell covering would aid in the stability of the cells in suspension and the shedding of these scales in layers may contribute to the elevated coagulant demand required by the cells (the cells that are neutralized by the cations or precipitate would lose the neutralized

scales and require additional precipitate and cations for the repulsive forces to be decreased again). The inability of this species to be flocculated using aluminium sulphate may be augmented by the rapid decrease in the culture pH incurred by the addition of large aluminium sulphate doses (Eldridge *et al*., 2012). This would result in a decrease in the zeta potential and hence incur a greater negative charge to the cells, which would then strongly repel each other and resist coagulation.

The use of multivalent metal salts, such as those used in this experiment, is disadvantageous in aquaculture (and other applications) due to their toxic nature (Grima *et al*., 2003; Schlesinger *et al*., 2012). Hence, this method of flocculation would not be favoured for biodiesel production as excess algal material after oil extraction should be used as animal feed or in the production of various other products to maximize its use. The cost implications of using such flocculants also count against their use in an upscaled version of this process even if this model organism could be dewatered successfully using this technique.

8.3.3 Autoflocculation

Autoflocculation refers to the spontaneous formation of algal floccules in culture. Generally, this phenomenon results in response to an elevated pH which occurs in culture due to the consumption of carbon dioxide by photosynthesizing algal cells (Sukenik and Shelef, 1984; Show *et al*., 2012). This would result in the precipitation of hydroxides and carbonates that would aid in agglomeration and gravity sedimentation (Section 8.3.1). Another factor that may contribute to auto-flocculation is the secretion of extracellular polymeric substances (EPS) by the algal cells. Numerous algal species have been shown to have the capacity to secrete this substance (Hanlon *et al*., 2006; Mishra and Jha, 2009; Bellinger *et al*., 2010) and it has even been linked with flocculation in the ocean (e.g. diatoms, Kiorboe and Hansen, 1993). The secretion of EPS by bacterial cells may also assist in microalgae autoflocculation (Sukenik and Shelef, 1984; Lee *et al*., 2009).

In the present study, early stationary phase microalgal cells were exposed to various conditions in an attempt to induce algal autoflocculation. Cultures that were incubated in

the dark at 3 ºC were completely flocculated within four days. A gradual increase in cell removal (up to about 70% efficiency) from aerated cultures and cultures incubated in the dark at 22 ºC was evident over the duration of the experiment. The flocculation efficiency in the other two treatments tested remained constant (around 50% efficiency or lower) throughout the incubation period (Figure 8.12). The pH values of the various culture treatments were monitored on day fourteen to determine if flocculation was induced by an elevated pH (starting pH was 8.3 when the experiment was initiated).

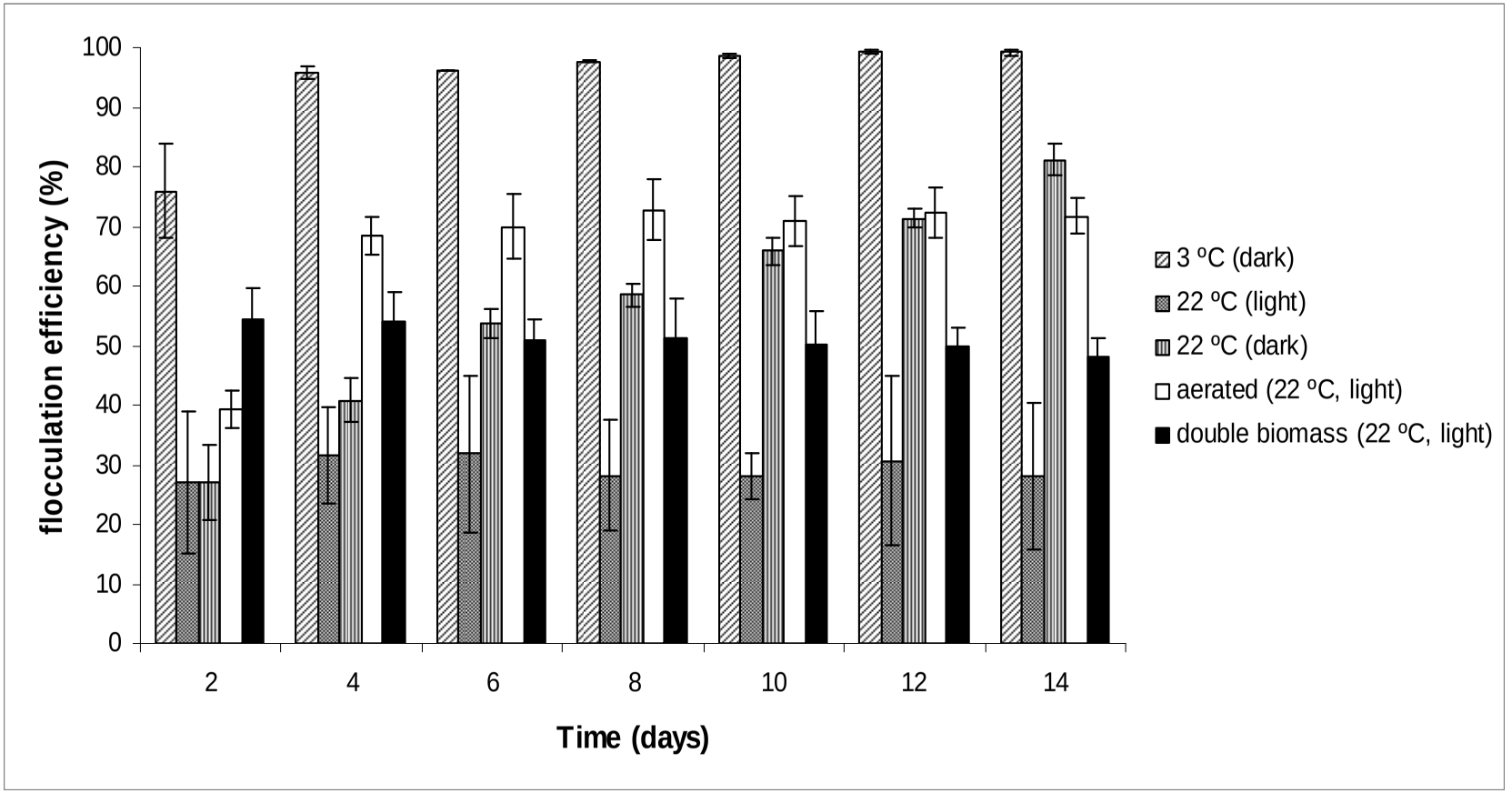

Figure 8.12: Autoflocculation induction in *I. galbana* initiated by numerous growth conditions. Error bars represent standard deviation (n=3).

Light is essential for photosynthesis to occur. The cultures that were maintained in the dark would be unable to photosynthesize resulting in low rates of metabolism and reduced amounts of energy resulting in decreased motility. This would aid in the settling of the algal cells. Furthermore, studies have indicated that microalgal cells with a reduced metabolism tend to agglomerate in response to an increase in the zeta potential (Danquah *et al*., 2009b). This would result in cells becoming less electronegative resulting in a decline in the repulsive forces. The rapid complete flocculation of cells in the dark at 3 ºC may also be attributed to a decrease in the viability of the cells at such low temperatures.

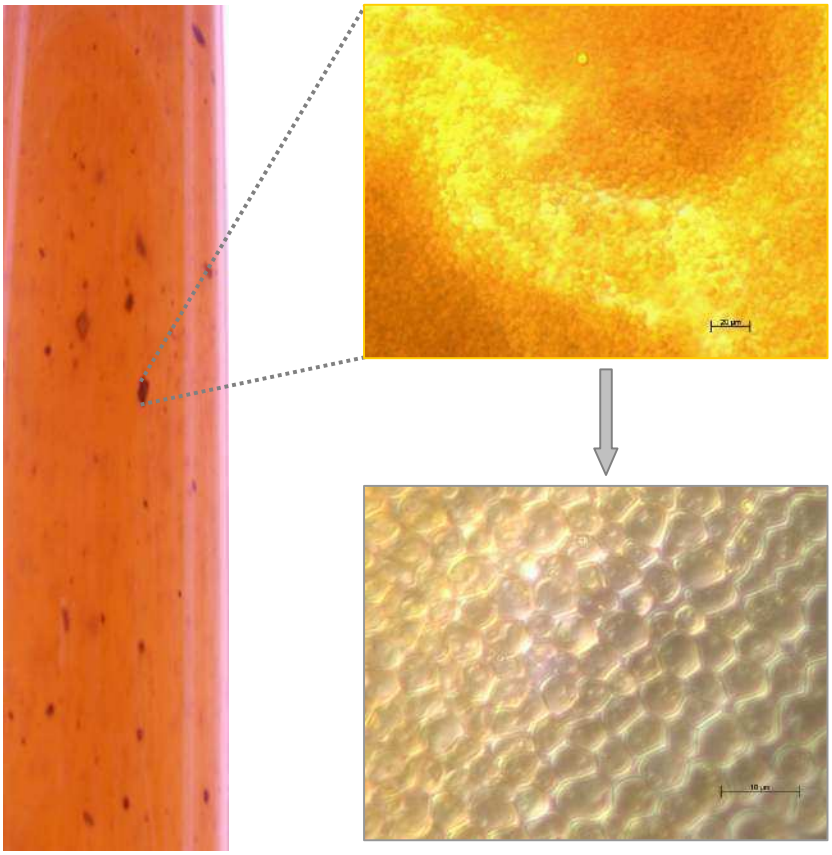

Figure 8.13: *Isochrysis galbana* floccules observed in photobioreactor in response to agitation induced by bubbling.

Agitation by bubbling led to the formation of distinct floccules that easily settled out of solution due to their high densities (Figure 8.13). The formation of these floccules may

be due to the high concentration of cells in the culture and increase in the frequency of collisions between these cells in bubbled cultures. Floccule formation due to agitation in dense cultures may be further justified by the equation $dN_A/dt \propto N_{cells}^2$ which shows that the rate of aggregation and the frequency of collisions are directly proportional to the number of cells in solution squared (Hunter, 2001; Eldridge *et al*., 2012). The formation of these flocs may also be due to the secretion of EPS by the cells. Secretion of EPS is mostly prevalent during early lag phase and the late stationary phase (Metting Jr., 1996; Eldridge *et al*., 2012). EPS secretion during the late stationary phase is possibly a mechanism used by stressed microalgal cells to remain attached to a substrate, and utilise minimal energy, until optimal growth conditions return. The cells in this experiment would be in the late stationary phase. EPS secretion increases the 'stickiness' of the cells. This would aid in the adhesion of the cells to each other upon collision. The cultures used were non-axenic implying that the interaction between bacterial EPS and the cells could have also contributed to cell 'stickiness' and floccule formation. During the late stationary phase the metabolic activity of the cells would have decreased, due to nutrient depletion, which would lead to an increase in the zeta potential. Hence, a reduction in the repulsive forces which would also contribute in floccule formation.

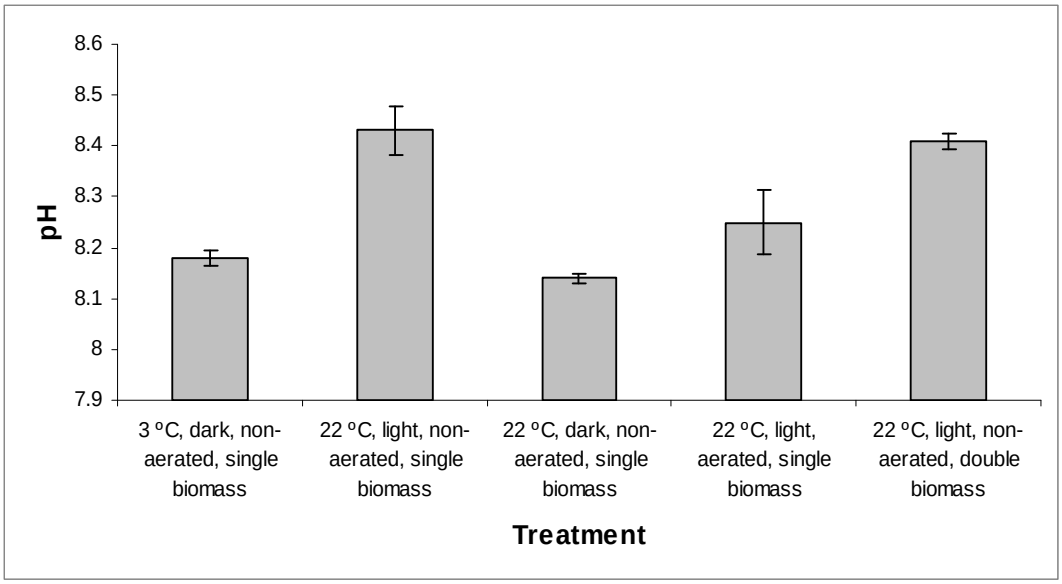

Figure 8.14: pH of autoflocculated *I. galbana* cultures after fourteen days. Error bars represent standard deviation (n=3).

The culture containing double the biomass resulted in approximately two times the flocculation efficiency in comparison to the culture maintained under the same conditions with the normal biomass content. This may be as a result of the increased cell concentration increasing the probability of interactions between the cells resulting in flocculation and sedimentation. A similar, elevated pH was observed in the both cultures regardless of the cell concentration (Figure 8.14). This elevated pH is due to carbon dioxide consumption by the cells that are metabolically active due to their exposure to light. But the same pH levels in the single and double concentration cultures is unexpected since more cells would result in more carbon dioxide uptake which should result in a higher pH observed in the double cell concentration treatment. The similar pH in both treatments may be attributed to the decreased light exposure in the culture with double the biomass, due to cell shading in such a dense culture, which would have resulted in a reduction in photosynthetic rates (decreased carbon dioxide uptake rate resulting in more carbon dioxide in the medium thus maintaining the pH at a similar level to the culture with half the cell concentration). The elevated pHs in both treatments would result in an increase in the zeta potential which would aid in flocculation. The decrease in the electronegative charge of the cells would be more beneficial in the double biomass treatment as a large number of cells would result in the cells being in closer proximity to each other resulting in coagulation.

The pH levels in all culture treatments were below pH 9 (Figure 8.14) implying that the autoflocculation observed in this experiment was not related to the precipitation of hydroxides and carbonates (which occur at pHs greater than 10; Section 8.3.1).

8.3.4 Effect of growth stage on flocculation efficiency

Isochrysis galbana was cultivated in batch culture over nineteen days. The growth kinetics of the algal cells is depicted in Figure 8.15. The results show a gradual increase in the cell concentration, up to approximately 10 000 cells/µl, on day sixteen followed by a plateau in cell numbers till day nineteen when cultivation was halted. The lag phase was observed between day zero and three followed by the exponential phase between day three and eight and the stationary phase was evident beyond day 16. Flocculation

induction (using various treatments) was attempted throughout all growth phases to see whether an optimum time for harvesting, that correlates with optimal lipid accumulation, could be determined.

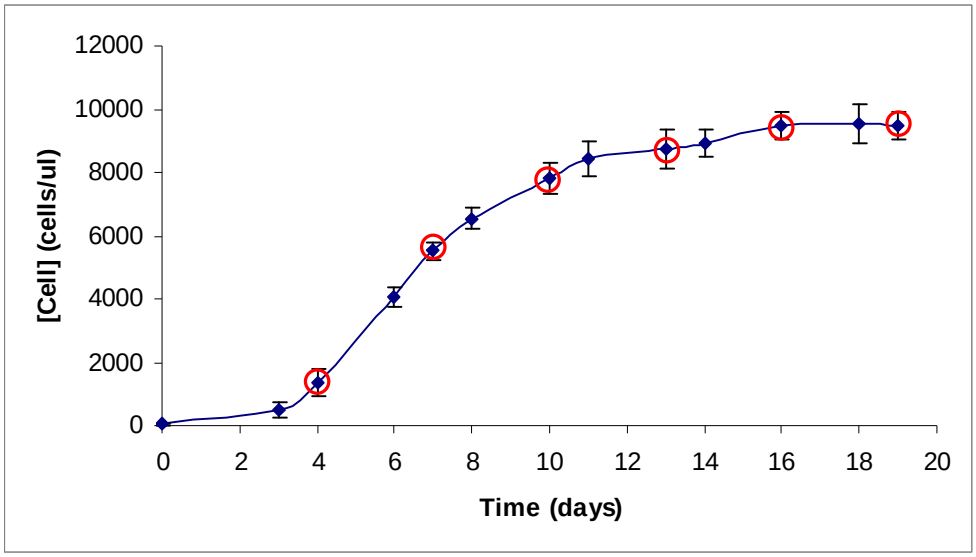

Figure 8.15: Growth curve of *I. galbana* showing points at which flocculation induction was attempted (circled; Error bars represent standard deviation, n=3).

pH-induced flocculation was initiated using potassium hydroxide, sodium hydroxide and calcium hydroxide to elevate the microalgal culture pH to 10.3. A pH value of 10.3 was used instead of the value of 10.5 (Section 8.3.1), so that smaller amounts of the alkaline solutions were needed and thus keep costs to a minimum when upscaling the process. Aluminium sulphate was eliminated from the study as it is unsuccessful in the flocculation of *I. galbana* U4 (Section 8.3.2) but ferric chloride and ferrous sulphate were both tested as flocculating agents.

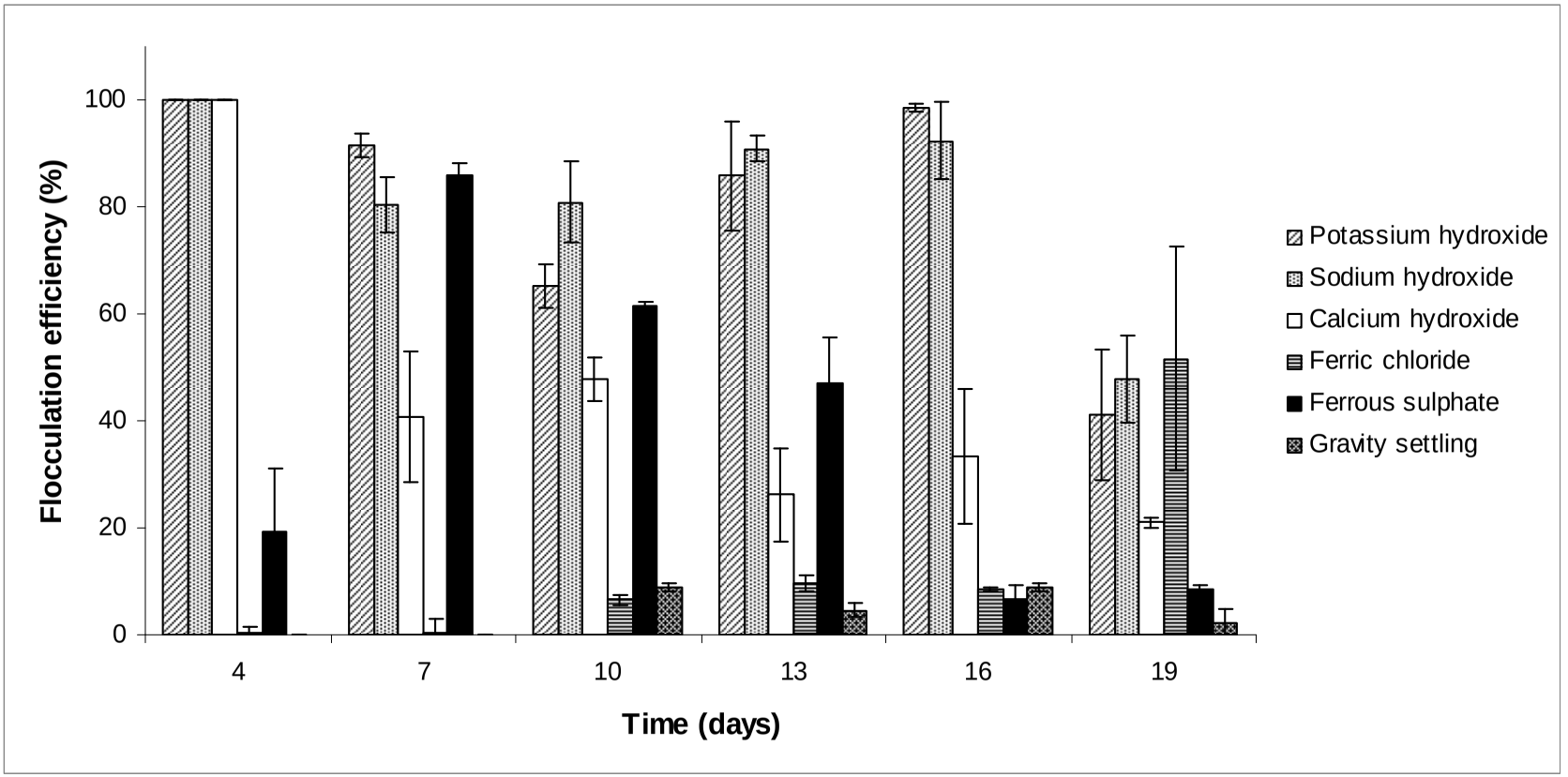

Figure 8.16: Flocculation induction of *I. galbana* at various growth stages. Error bars represent standard deviation (n=3).

Complete flocculation was evident using all alkaline treatments on day 4 (lag phase) (Figure 8.16). This may be as a result of the secretion of EPS by the cells during this phase interacting with the precipitate to form flocs that settle out of solution. At this early phase phosphate would not have been completely consumed by the algal cells. Hence, calcium phosphate precipitate may aid in the flocculation process. This observation would correlate with that observed by Sukenik and Shelef (1984) where they achieved algal flocculation at lower pHs (8.5-9.0), relative to the present study, which they attributed to the precipitation of calcium phosphate. However, harvesting at such an early stage would be undesirable due to the low cell concentration and the minimal level of lipid in the cells at this stage.

An elevated ferrous sulphate flocculating ability (≈ 90% efficiency) was initially evident (day 7) followed by a downward trend in the flocculating ability, as the exponential phase proceeded (Figure 8.16). The reasons for the initial increased ability of the flocculating agent is unknown. Harvesting at this growth stage would also be undesirable due to the decreased lipid levels. During the stationary phase, when large amounts of lipid-rich cells are prevalent in culture, potassium hydroxide and sodium hydroxide resulted in maximal flocculation (Figure 8.16). This may be due to the loss of the flagella during this growth phase (Chapter 5). Danquah *et al.* (2009b) showed that a multi-strain culture of *Tetraselmis suecica* and *Chlorococum* sp. had a lower net electronegative zeta potential during the low growth rate phase (stationary phase) as compared to cultures in the high growth rate phase (exponential phase) (Danquah *et al*., 2009b). If this is applicable to *I. galbana* as well, a reduction in the electronegative charge on the cells during the stationary phase would also account for the increased flocculating ability observed in this study using alkaline induced flocculation during the stationary phase. The pH used (10.3) was not feasible for calcium hydroxide flocculation implying that this alkaline treatment requires a higher pH for microalgal flocculation to proceed.

8.4 CONCLUSION

It may be concluded that optimal flocculation of this species of *Isochrysis* is achieved by increasing the pH of the medium using potassium hydroxide, sodium hydroxide or calcium hydroxide. Calcium hydroxide is preferred because it is cheaper and because it induces superior rates of sedimentation. All multivalent metal salt treatments were not as effective as pH dependant flocculation in flocculating this species. Autoflocculation was observed in cultures agitated by bubbling and resulted in distinct, large flocs that easily settle out of solution. This is advantageous in that it introduces no additional chemicals and therefore is cheaper. The bulk of separated seawater in such procedures can additionally be used as the inoculum seed and the medium for further culturing and lipid biofeed production. During the stationary phase, when lipid-rich cells are expected to dominate the culture, pH-induced flocculation can be used to maximum effect in recovering the most cells.

CHAPTER NINE

Culture of *Isochrysis galbana* U4 in Upscaled Photobioreactors

9.1 INTRODUCTION

Microalgae can be commercially cultured in either opened or closed systems. Both these systems have associated advantages and disadvantages. A closed tubular, bubble-column photobioreactor (PBR) system was used in the current study since it enables the maintenance of a more controlled environment, it is less prone to contamination and higher biomass levels can be achieved using this system in comparison to opened systems (Borowitzka, 1999).

Early studies using PBRs date back to the 1940s, when *Chlorella* was cultivated to investigate photosynthesis. Gradual improvements of that system have been tested since. Numerous categories of PBRs exist today including tubular, horizontal, inclined and spiral varieties (Barsanti and Gualtieri, 2006). Multiple parameters need to be taken into consideration when designing a PBR system. These include gaseous-exchange, methods of mixing that are not hazardous to the microalgae, light intensities, methods to maintain the temperature of the system and a way to control the carbon dioxide and oxygen content in the system (Borowitzka, 1999).

In the present study a simple design of a tubular bubble-column PBR was used. Minor variations of the systems configuration and growth conditions were carried out throughout the study in an attempt to maximize the growth rate and lipid yield of the microalgal species.

A two-phase continuous system was tested for the mass culture of *Isochrysis galbana* U4. This two-phase PBR or two-stage configuration was used because it has been established that *Isochrysis galbana* U4 cells divide when nitrogen is abundant and accumulate lipid in response to nitrogen depletion. Hence, cell division and lipid accumulation do not take place concurrently. In the two-phase PBR set up the first photobioreactor is replete with respect to nitrogen and the second photobioreactor is nitrogen deplete. Hence, cell growth occurs in the first phase and lipid accumulation occurs in the second phase. Theoretically, this two-phase system would be ideal for the mass culture of *I. galbana*.

9.2 MATERIALS & METHODS

9.2.1 Photobioreactor setup

The two-phase or two-stage PBR system consisted of two interconnected photobioreactor systems, System I and System II respectively. Algal cell division occurs in System I and lipid accumulation takes place in System II. The first stage PBR, also called System I consisted of a cylindrical Perspex tube equipped with a nutrient and air inlet. The effluent overflow from the first stage was collected into the second phase PBR also referred to as System II which consisted of a 5 L conical flask (Figure 9.1). The bioreactors were illuminated with multiple vertical (unlike in Figure 9.1) fluorescent lights. Filtered air (Whatman uniflo 0.2 µm filter) was pumped through distilled water (humidifier) prior to entry into the bioreactor, with the aid of an air pump (Labotec with a pressure of 2.4 bar). The filtered air was bubbled into System 1 using a sand-stone fish tank sparger. When this configuration was run in continuous mode, fresh *f/2* medium was supplied into System 1 by means of a peristaltic pump (Watson & Marlow, 520S) and the culture overflow was collected in System 2 (Figure 9.1). Batch cultures were conducted in System 1 only.

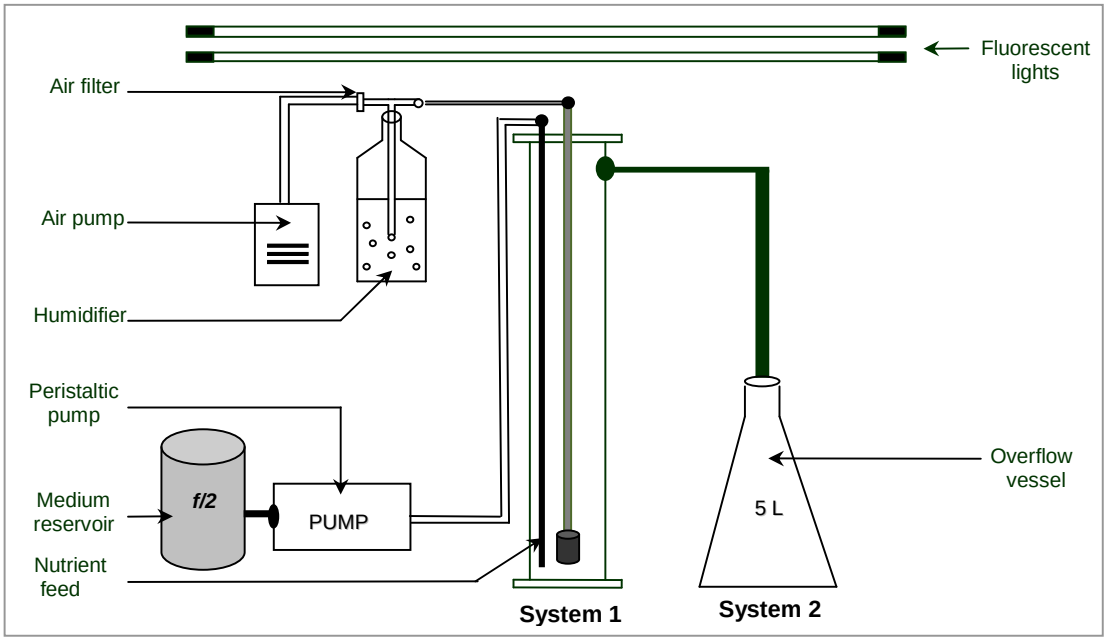

Figure 9.1: Schematic representation of the photobioreactor system used for the mass culture of *I. galbana*.

Two configurational variations (Configuration I and Configuration II) of the above PBR setup were tested. During the initial testing phase the volume of System 1 was 7 L. Thereafter an up-scaled variation of System 1 was constructed and tested (16 L). The second configuration of System 1 varied in both the volume and the design (Table 9.1). System 2 remained unchanged in both trials (7 and 16 L) of the continuous system however the algal culture collected in System 2 was transferred to different growth vessels and grown under varying conditions (e.g. various light intensities/ bubbled vs. non-bubbled cultures and agitated cultures grown in vessels maintained on an orbital-shaker).

Table 9.1: Differences in the configuration of System 1 and modified Schott® bottles

Configuration	**Volume System I (L)**	**Height (m)**	**Diameter (cm)**	**Base**
Configuration I	7	1	11	Flat
Configuration II	16	1.4	13	Funnel
Modified Schott® bottles*	1	0.25	9	Flat

* Used for all experiments conducted thus far and added for comparison purposes

9.2.2 Experimental setup and analytical methods

Multiple experiments were conducted using the PBR configurations described (cf. Tables 9.1 and 9.2).

Table 9.2: *Isochrysis galbana* mass culture experiments

	Batch	**Continuous**
Configuration I (7 L)	1. Only System I for 14 days 2. Only System I with varying light intensities	3. Varying levels of nitrate in influent (*f/2* medium) and exposure of effluent to multiple growth conditions (bubbled and non-bubbled)
Configuration II (16 L)	4. Only System I for 14 days	5. Varying flow rates and effluent growth conditions (bubbled, non-bubbled still and non-bubbled agitated/shaken)

9.2.2.1 Experiment 1 (7 L batch culture)

An initial batch PBR experiment was conducted to determine the growth dynamics of *I galbana* in a larger volume (7 L photobioreactor as apposed to the 1 L sparged bottles). For the batch run only System 1 was used. 6.5 L *f/2* medium (prepared as in Section 2.1) was inoculated with a 7 day old *I. galbana* culture (inoculum concentration = approximately 6.5 x 10^7 cells). The system was illuminated at 186 µmol photons.m^{-2}.s^{-1} with a 10:14 light-dark cycle and incubated at approximately 25 °C. Aliquots of the algal culture were extracted every alternate day for cell counts (Section 2.5) and lipid yield measurements (Section 2.7).

9.2.2.2 Experiment 2 (7 L batch with varying light intensities)

Batch (only System 1; 7 L) photobioreactor experiments were conducted to determine the effect of increased illumination on *I. galbana* growth. The illumination was modified by varying the number of lights that were switched on. The light intensities used included 186, 215, 361 and 720 µmol photons.m^{-2}.s^{-1} with a 10:14 light-dark cycle and the temperature was maintained at approximately 25 °C. Initially, batch cultures were conducted with a single light intensity thereafter sequential changes in the light intensities during the course of the batch run were tested. For all runs 6.5 L *f/2* medium (prepared as in Section 2.1) was inoculated with a 7 day old *I. galbana* culture (inoculum concentration = approximately 6.5 x 10^7 cells). The cell concentration and lipid content were monitored for the duration of the experiment (Sections 2.5 and 2.7 respectively). The rate of growth, divisions per day and generation times were calculated for each batch culture exposed to the various light intensities (Section 2.11).

9.2.2.3 Experiment 3 (7 L continuous culture with varying levels of nitrogen)

An experiment was conducted to determine the influence of nitrogen supply concentration on the growth of *I. galbana* cells cultured in a continuous setup. *I. galbana* (800 ml) was grown to mid-log phase in a 1 L modified Schott Duran® bottle (Section 2.3). This culture was used as the inoculum for System 1 which contained modified *f/2* medium supplemented with 440 µM $NaNO_3$ (half the $NaNO_3$ concentration of normal *f/2* medium). The bioreactor was run in continuous mode with modified *f/2* medium (440

µM $NaNO_3$) as the nutrient feed. The nutrient feed rate (ml/min) was adjusted until the cell density remained relatively constant (i.e. quasi-steady state reached; rate of growth = rate of cell washout). The following formula was used to calculate the steady-state cell growth rate:

Steady State Cell Growth Rate (cells/min) = Dilution Rate (ml/min) x *Algal Cell Density (cells/ml)*

1.4 L of the culture effluent (from System 2) was collected. 700 ml of this effluent was transferred to a 1 L modified Schott Duran® bottle (Section 2.3; bubbled culture) and the remainder of the culture (700 ml) was transferred to a 2 L Erlenmeyer flask. The bubbled cultures in modified Schott Duran® bottles simulated a closed photobioreactor setup for System 2 (i.e. the second, lipid–accumulating, phase of the bioreactor run) whilst the non-bubbled cultures in Erlenmeyer flasks simulated a pond setup for System 2. Both bubbled and non-bubbled cultures were subjected to an illumination intensity of 110 µmol photons.m^{-2}.s^{-1} with a 10:14 light-dark cycle and were maintained at approximately 25 °C. Growth (Section 2.5), lipid accumulation (Section 2.7) and algal pigmentation (Section 2.15) were monitored for 10 days.

When the 'quasi-steady' state was reached and an adequate amount of effluent was obtained for the second phase (1.4 L) the nitrate supply in the nutrient feed was increased to 880 µM $NaNO_3$ (normal $NaNO_3$ concentration in *f/2* medium). The nutrient feed rate (ml/min) was then adjusted upwards until the cell density remained somewhat constant (i.e. 'quasi steady' state reached for increased nitrogen). The resulting effluent was cultured in bubbled and non-bubbled vessels for 10 days and the cell concentration, lipid yield and pigmentation were monitored as described above.

The process was repeated for 1760 µM $NaNO_3$ (double the $NaNO_3$ concentration in *f/2* medium) and 1980 µM $NaNO_3$ (2.25 times the $NaNO_3$ concentration in *f/2* medium) and the resulting effluent from the respective treatments was cultured as stated above.

9.2.2.4 Experiment 4 (16 L batch culture)

A batch PBR run was conducted to determine the ability of *I. galbana* to grow on a much larger scale (16 L PBR as apposed to the 1 L sparged bottles and 7 L PBR). For the batch run only System 1 was used. 15 L *f/2* medium (prepared as in Section 2.1) was inoculated with a 7 day old *Isochrysis galbana* culture (inoculum concentration = approximately 6.5 x 10^7 cells). The system was illuminated at 186 µmol photons.m^{-2}.s^{-1} with a 10:14 light-dark cycle and incubated at approximately 25 °C. Aliquots of the algal culture were extracted every alternate day for cell counts (Section 2.5) and lipid yield measurements (Section 2.7).

9.2.2.5 Experiment 5 (16 L continuous culture with flow rate variations)

A 16 L, continuous experiment was conducted to determine the influence of the flow rate on the growth of *I. galbana* and the duration of the second phase. 14 L *f/2* medium (prepared as in Section 2.1) was inoculated with 1 L, 7 day old *I. galbana* culture (inoculum concentration = approximately 1.5 x 10^{10} cells). The cells were allowed to grow for 4 days in batch culture (System 1). The PBR was illuminated at 186 µmol photons.m^{-2}.s^{-1} with a 10:14 light-dark cycle and incubated at approximately 25 °C.

On day 4 the bioreactor was switched to continuous mode. The nutrient feed consisted of freshly prepared *f/2* medium (Section 2.1). The initial flow rate was 1.44 ml/min. The flow rates were then increased to 2.16, 3.59 and 5.03 ml/min respectively. Each flow rate was maintained for a day and the resulting effluent was transferred to a 500 ml modified Schott Duran® bottle (bubbled) and 2 Erlenmeyer flasks (non-bubbled). The bubbled cultures in modified Schott Duran® bottles simulated a closed photobioreactor setup for System 2. One of the cultures in Erlenmeyer flasks was kept on an orbital shaker (maintained at 90 RPM) which simulated a raceway setup due to the slight agitation and the other was left on the culture shelf which simulated a pond setup for System 2 since the culture was not agitated. All effluent cultures were subjected to an illumination intensity of 110 µmol photons.m^{-2}.s^{-1} with a 10:14 light-dark cycle and were maintained at approximately 25 °C. Growth (Section 2.5), lipid accumulation (Section 2.7), algal pigmentation (Section 2.15) and the culture pH were monitored for 14 days.

9.3 RESULTS AND DISCUSSION

9.3.1 Comparison of microalgal growth in up-scaled PBRs (batch cultures)

Isochrysis galbana was grown in batch culture in both the 7 L and 16 L PBRs to determine if upscale in volume of the PBR system has an impact on algal growth and lipid accumulation dynamics. Growth proceeded similarly in both cultures with a distinct lag, exponential and stationary phase (cf. Figures 9.2 and 9.3) however the rate of growth was higher in the 7 L PBR than in the 16 L PBR (Table 9.3). Furthermore, the growth rate of *I. galbana* cultured in modified 1 L Schott® bottles was greater than that observed in cultures grown in both the PBRs tested (Table 9.3; 1 L Schott® bottle data from Chapter 3). Hence, the rate of *I .galbana* growth is inversely proportional to the volume of the culture vessel.

PBRs can be up-scaled by increasing the tubes diameter, height or both (Molina *et al.*, 2000; 2001). The increase in the diameter of PBRs results in a decrease in the surface area to volume ratio thus reducing the exposure of the individual cells to the incident light as the density of the algal culture increases (cell-cell shading; Xu *et al.*, 2009). Increases in the PBR height may result in a decrease in the gradient of carbon dioxide between the gas entry and exit points which would consequently result in the starvation of cells closer to the gas exit due to the complete consumption of all carbon dioxide closer to the gas inlet. Furthermore, increases in the length of the PBR may also result in the retention of large amounts of oxygen which inhibits photosynthesis when in excess due to photoxidation (Xu *et al.*, 2009). The volume of the PBRs used in the present study were increased by enlarging both the height and diameter in an attempt to decrease the effects of the individual changes. The reduction in the growth rate with respect to the PBR size could be an accumulative effect of both the height and diameter increases i.e. due to both carbon dioxide and light limitation. Furthermore, with increasing photobioreactor volume the mass flow dynamics and mixing rates may have impacted on cell growth rates due to limitations in the gas exchange and nutrient supply rates.

Regardless of the variations in the rates of growth the final cell yields in both PBRs and in the 1 L modified Schott® bottles were similar (between 7500 and 8000 cells/µl in all vessels; cf. Figures 9.2, 9.3 and 3.2; Chapter 3). This implies that growth cessation was not in response to growth-limiting levels of light or carbon dioxide and was most probably induced by nutrient depletion, more specifically nitrogen depletion (Chapter 5, 6 and 7).

Elevated levels of lipid accumulation (> 30% w/w) were only observed during the late-stationary phase (Figure 9.2) in the up-scaled PBRs. This differed from *I. galbana* cultures in 1 L modified Schott® bottles where lipid accumulation was initiated in the early stationary phase and lipid levels exceeded 30% w/w during the mid-stationary phase (Chapter 3; Figure 3.2). Low levels of lipid accumulation in up-scaled PBRs may be a consequence of the reduced light and carbon dioxide in the PBRs which are essential components for lipid accumulation (Ratledge and Cohen, 2008; da Silva *et al.*, 2009). During the stationary phase the cell density is at the highest level. As the concentration of cells in the PBR increases an exponential decrease in the light intensity is prevalent due to cell-shading effects (Chen *et al*., 2011). The elevated concentration of cells would also require much more carbon dioxide. Similar light and carbon dioxide-limitation effects, due to increases in the cellular concentration, may have resulted in the slightly diminished rate of growth from day 6 to 12 (in comparison to day 4 to 6 when cell concentrations were lower) in the 16 L PBR batch culture (Figure 9.3).

Lipid levels started to rise when the cellular concentration declined in the 7 L PBR (Figure 9.2). The decline in the cell concentration was as a result of the rapid clumping of cells as the stationary phase progressed hence fewer, free cells were left in the culture medium. Thus, the cells in suspension were exposed to slightly elevated light levels due to a decrease in cell-shading effects. An increase in the exposure to light may have supplied adequate energy for lipid accumulation resulting in the lipid increase observed in Figure 9.2.

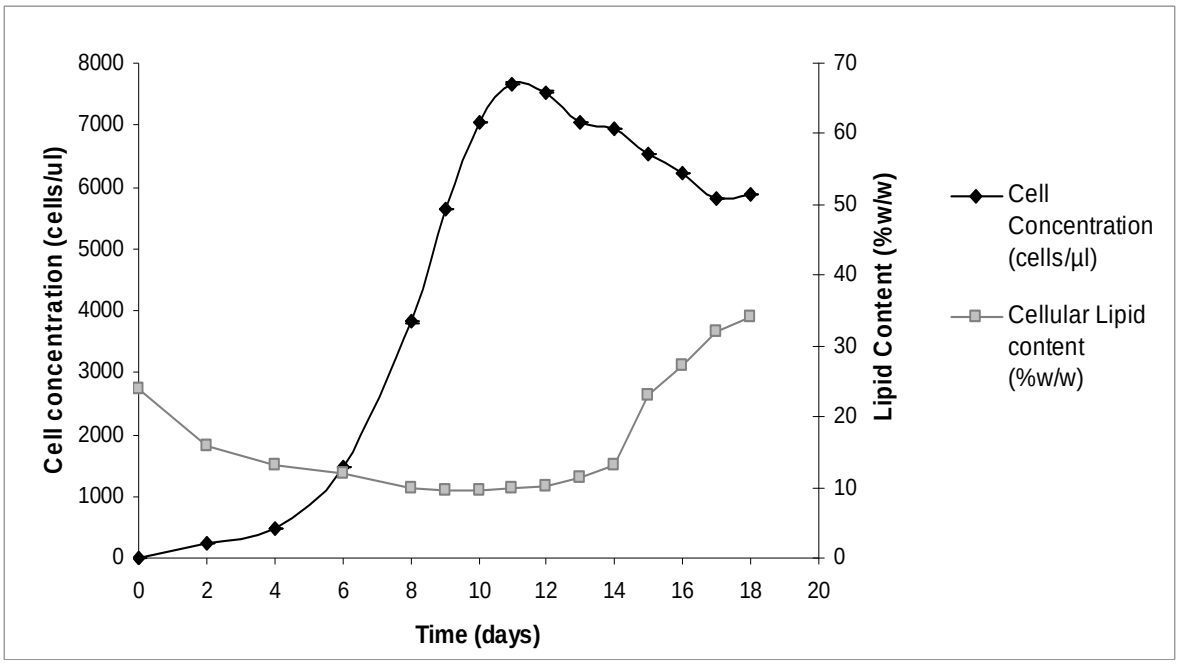

Figure 9.2: *Isochrysis galbana* growth curve showing the cellular concentration and lipid content observed over 18 days of culture in a 7 L airlift PBR maintained under batch conditions

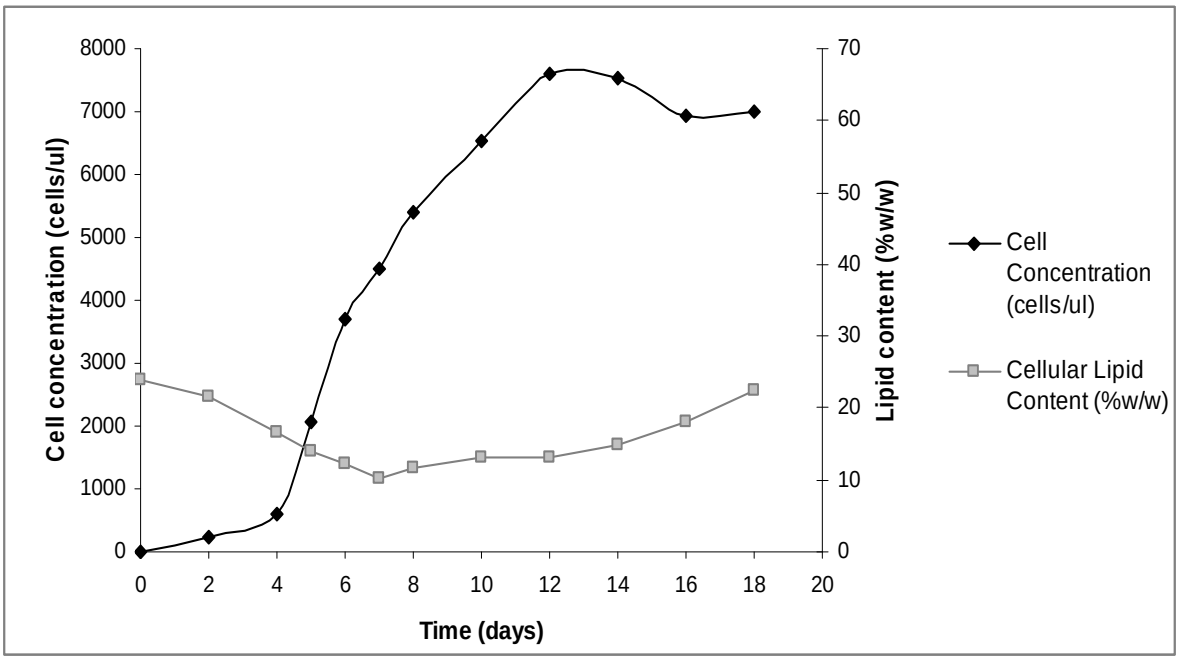

Figure 9.3: *Isochrysis galbana* growth curve showing the cellular concentration and lipid content observed over 18 days of culture in a 16 L airlift PBR maintained under batch conditions

Table 9.3: Measurements of growth of *I.galbana* in PBRs with varying volumes

System volume (L)	Growth rate (cells/µl/day)	Divisions per day (div/day)	Generation time (days)
1*	0.3320	0.4789	2.0880
7	0.2570	0.3707	2.6975
16	0.2295	0.3311	3.0202

* Data from Chapter 3

9.3.2 Seven liter batch cultures with varying light intensities

The PBR batch culture experiments (Section 9.3.1) verified that up-scaling the system used for the culture of *I. galbana* affected the rate of growth and this was attributed to limitations on light intensity, carbon dioxide supply or both. The light intensity received by each cell is affected by the culture density. Numerous studies have shown that the light intensity used in PBR systems have a significant effect on microalgal growth rates and eventual biomass concentrations (Wijanarko *et al*., 2008; Meireles *et al*., 2008; Yoon *et al*., 2008). The present study was aimed at determining if variations in the light intensities, during the course of algal growth in batch culture, had a positive effect on the rate of *I. galbana* growth and final biomass yield.

An initial PBR run, with an illumination intensity of 720 µmol photons/m^2/s, resulted in an extensive lag phase (approximately 12 days as compared to 4 days with decreased illumination batch PBR runs; Figure 9.4). During the early stages of growth the culture density is very low and light penetrates through the entire algal culture in the PBR ensuring that all cells receive adequate light levels. When these light levels exceed the requirements of the cells the photons of light are not completely used and get dissipated resulting in energy losses (Luo and Al-Dahhan, 2004). As the illumination levels increase further photosynthesis is inhibited due to photo-inhibition (Adir *et al.*, 2003). Thus, the extended lag phase was probably a result of photo-inhibition effects on the cells, especially since the cells had not been pre-adapted to high light intensities. However as the cell numbers increased a rapid exponential phase was observed (Figure 9.4) and the growth rate exceeded that observed in batch cultures grown under an illumination intensity of 186 µmol photons/m^2/s (Table 9.4). This implies that high cell

densities (exponential phase) require an elevated light intensity, to achieve high growth rates, as apposed to low cell densities (lag phase) where such elevated light intensities initiate photo-inhibition.

Regardless of the elevated growth rate in the culture grown under 720 µmol photons/m^2/s (in comparison to the culture grown under 186 µmol photons/m^2/s), the final cellular yield was much lower than that observed in the culture grown under 186 µmol photons/m^2/s (Figure 9.4). The reduced cellular yield could be in response to the damage of the photosynthetic apparatus of some of the cells (induced by inhibitory levels of light) preventing further growth and division. It could also be attributed to the consumption of the nutrients in the *f/2* medium by contaminating bacteria etc. (non-axenic cultures were used as inoculum) during the extended lag phase, resulting in limited nutrient levels being available for algal growth when the exponential phase was finally reached.

In an attempt to decrease the lag phase, in the culture grown under 720 µmol photons/m^2/s, but retain the rapid growth (observed during the exponential phase) two light intensities were used over two stages . The initial intensity was 215 µmol photons/m^2/s for 6 days (till the end of the lag phase and beginning of exponential phase) followed by 750 µmol photons/m^2/s for the remainder of the experiment. A decreased initial light intensity resulted in a decrease in the duration of the lag phase (in comparison to the culture grown under 720 µmol photons/m^2/s; Figure 9.4) which lasted approximately 4 days, which is beneficial. However after day 6, when the light intensity was increased, in an attempt to increase the growth rate, a slight lag was observed (Figure 9.4). This may be as a result of the time taken for the cells to adapt to the large increase in illumination intensity (750 µmol photons/m^2/s). The dual light intensities still resulted in a greater growth rate than both the single light intensities tested (Table 9.4) proving that sequential changes in light corresponding to the growth stage of *I. galbana* has an overall positive effect on growth.

To further test this proposal another set of light intensities was tested consisting of three changes or three steps in the illumination intensity (215, 361 and 750 µmol

photons/m^2/s). The gradual increase in the light intensities (3 light changes) did not result in the slow down in cell growth rate due to adaptation responses to large step increases in the light intensity as observed in the two step light intensity change experiment (Figure 9.4). The maximal cellular yield in the 186 µmol photons/m^2/s, two step and three step light intensity increases tested were all similar (Figure 9.4) implying that gradual changes in the light had no effect on the final biomass yield, but only effected the time interval required for the achievement of the final biomass. Sequential alterations in light intensities with respect to the growth stage of *I. galbana* can reduce the duration of the PBR run (due to increased growth rates) resulting in cost reductions. Furthermore, initiating PBR runs at lower light intensities would also prevent unnecessary energy losses thus optimizing light utilization and costs.

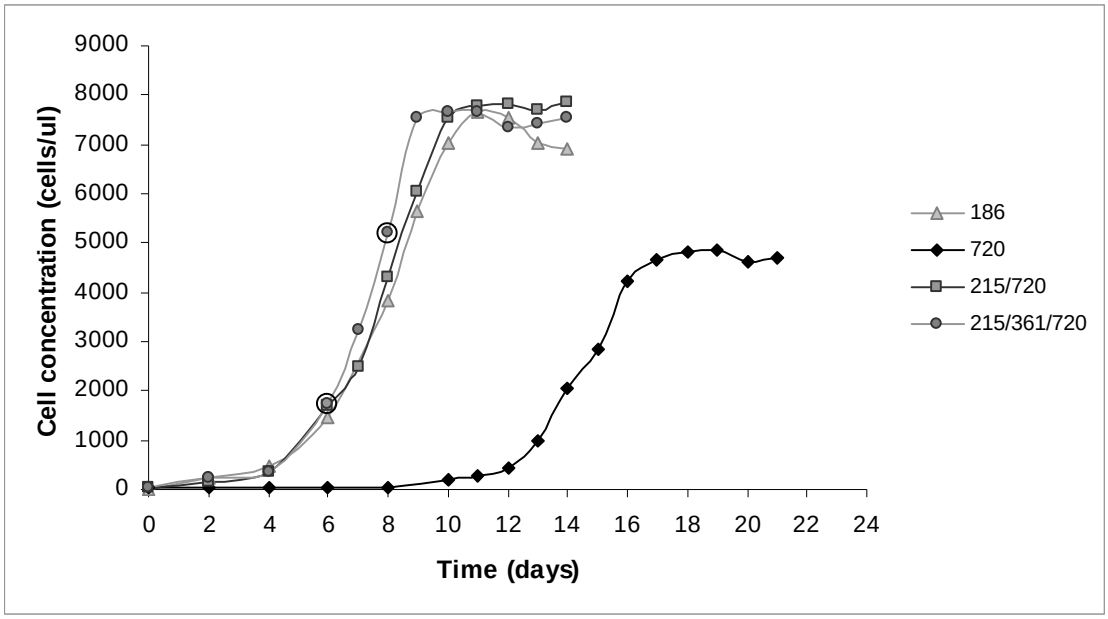

Figure 9.4: *Isochrysis galbana* growth curves showing the effect of varying light intensities on cellular concentration when the alga was grown in a 7 L PBR, under batch conditions. Circled points depict points of changes in light intensities. (Key units: µmol photons/m^2/s)

Table 9.4: The effect of varying light intensities on the rate of *I. galbana* growth and maximal cellular yields

Light Intensity (µmol photons/m^2/s)	Growth Rate (cells/µl/day)	Divisions per day (div/day)	Generation time (days)
186	0.257	0.371	2.698
720	0.278	0.401	2.494
215/720	0.301	0.423	2.354
215/361/720	0.355	0.512	1.953

9.3.3 Seven liter continuous culture with varying levels of nitrogen

The concentration of nitrogen in the culture medium has a definitive effect on *I. galbana* growth and the stationary phase was initiated by nitrogen starvation in most instances (Chapter 5). System 1 is the biomass accumulating phase of the two-phase PBR setup and System 2 is for lipid accumulation. Attempts to maximize the cellular concentration in System 1 are important because a greater cellular yield will reduce dewatering costs. Since maximal cellular yields were achieved in culture medium containing elevated nitrogen levels (Chapter 5) a continuous experiment was conducted with increasing levels of nitrogen in the medium influent to determine if the nitrogen concentration has an effect on the steady-state cell growth rate in System 1. The effluent was transferred to multiple growth vessels (System 2) to monitor lipid accumulation.

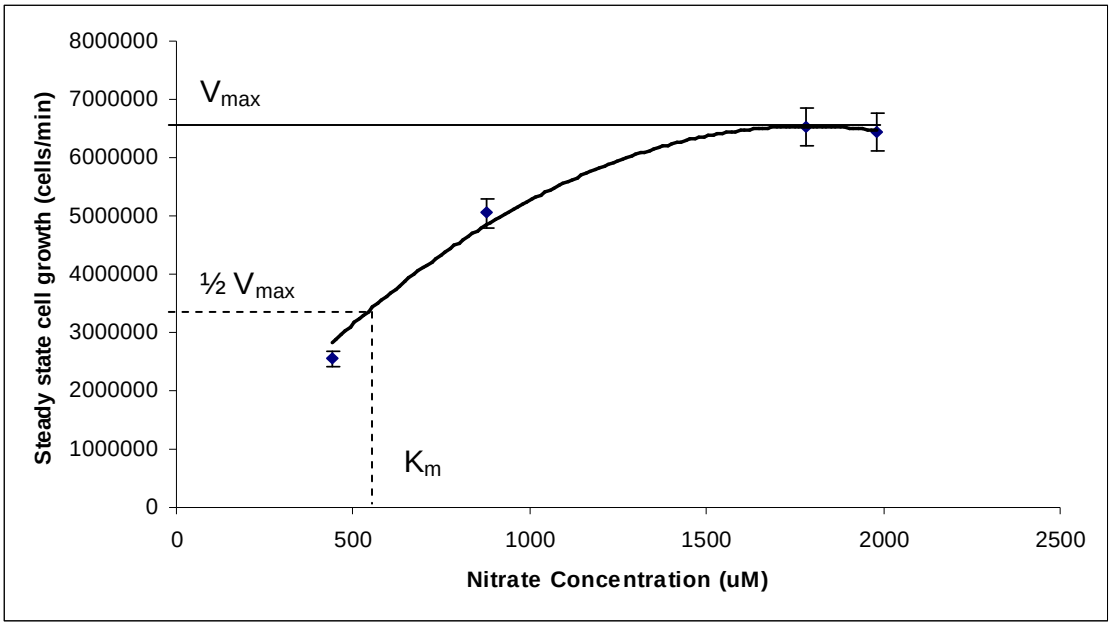

Figure 9.5: Michaelis-Menten curve showing steady state cell growth (velocity) versus nitrate concentration (substrate concentration) of *I. galbana* cells grown under continuous conditions.

The maximum steady-state cell growth rate was approximately 6500000 cells/min produced per total bioreactor volume (V_{max}; Figure 9.5). The growth rate increased as the nitrogen concentration in the influent increased until 1780 µM sodium nitrate was fed into the system (2 X the sodium nitrate level in *f/2* medium; Figure 9.5). At sodium nitrate concentrations of 1780 µM and greater a leveling out of the growth rate was observed indicating nitrogen saturation and that other parameters such as light, carbon dioxide or phosphate became limiting. Hence, such high N levels (>1780 µM sodium nitrate) are disadvantageous since it does not promote algal growth and nitrogen is merely 'washed-out' from System 1 into System 2 (cost implications). Furthermore, elevated N levels in System 2 are unfavorable since System 2 is the growth-limiting system and should promote lipid accumulation, not growth.

The effluent from System 1 was transferred to bubbled and non-bubbled vessels simulating a closed PBR and an open pond setup for System 2, respectively. Ideally, System 2 should run over a short duration and result in maximal lipid yields to ensure that the culture process is cost effective. If an opened pond setup is used as System 2 the

cost implications of the duration of the second phase run is not as high as a closed PBR would be but the run duration is still limited by evaporation of the medium, which would affect culture salinity, and contamination risks.

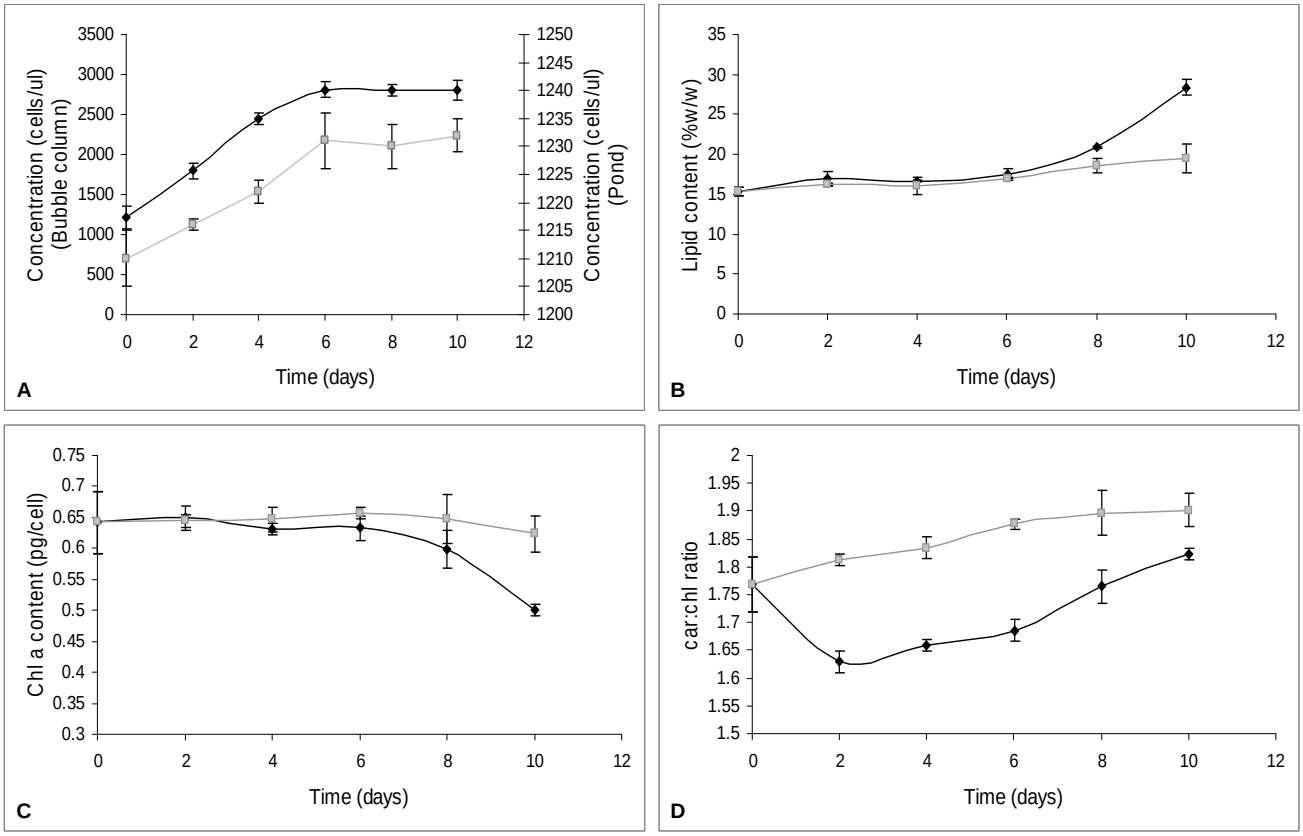

Figure 9.6: Bubbled (bubble column; ◆) and non-bubbled (pond; □) *I. galbana* batch cultures obtained from the effluent of System 1 of the continuous PBR that was supplemented with 440 µM sodium nitrate. The cell concentration (**A**), lipid content (**B**), chlorophyll a content **(C**) and carotenoid to chlorophyll ratio (**D**) were monitored. Error bars represent standard deviation (n = 3).

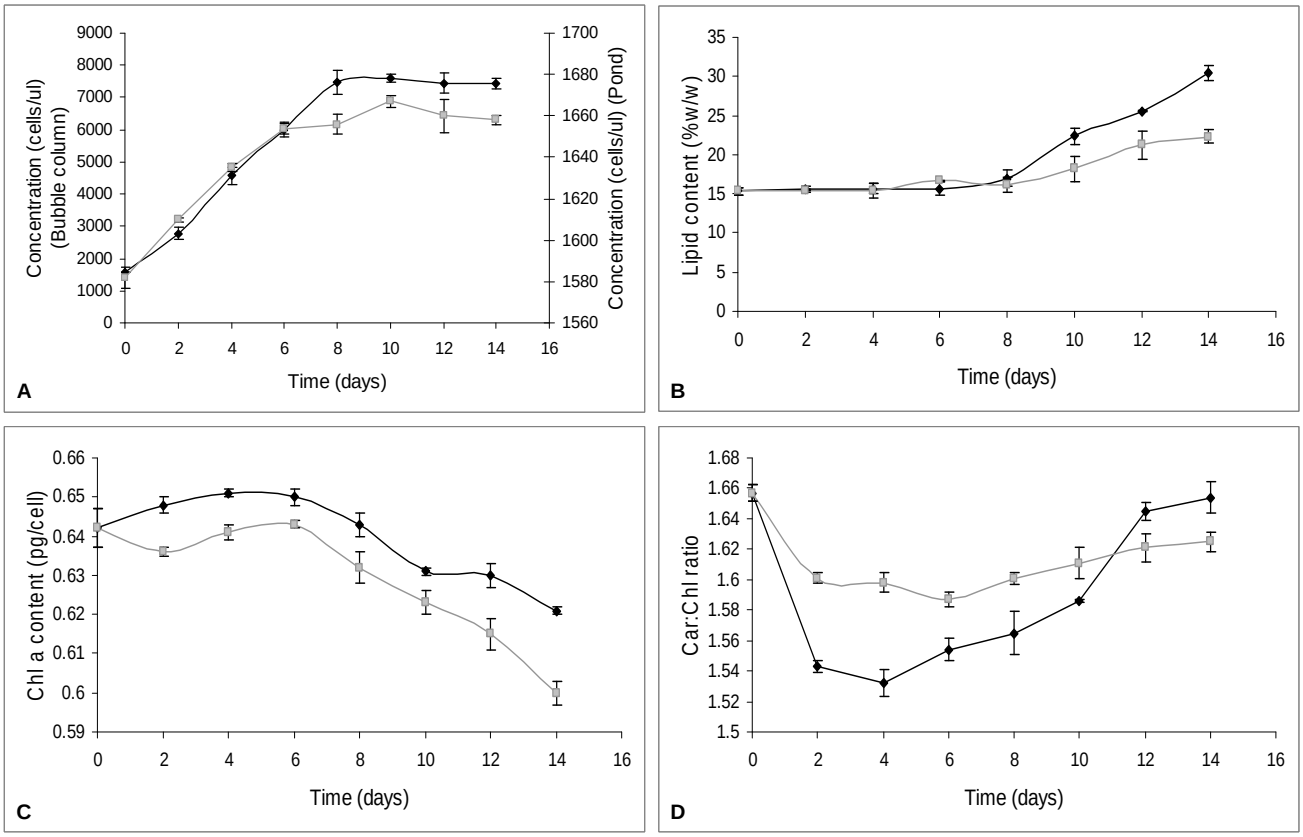

Figure 9.7: Bubbled (bubble column; ◆) and non-bubbled (pond; □) *I. galbana* batch cultures obtained from the effluent of System 1 of the continuous PBR that was supplemented with 880 µM sodium nitrate. The cell concentration (**A**), lipid content (**B**), chlorophyll a content **(C**) and carotenoid to chlorophyll ratio (**D**) were monitored. Error bars represent standard deviation (n = 3).

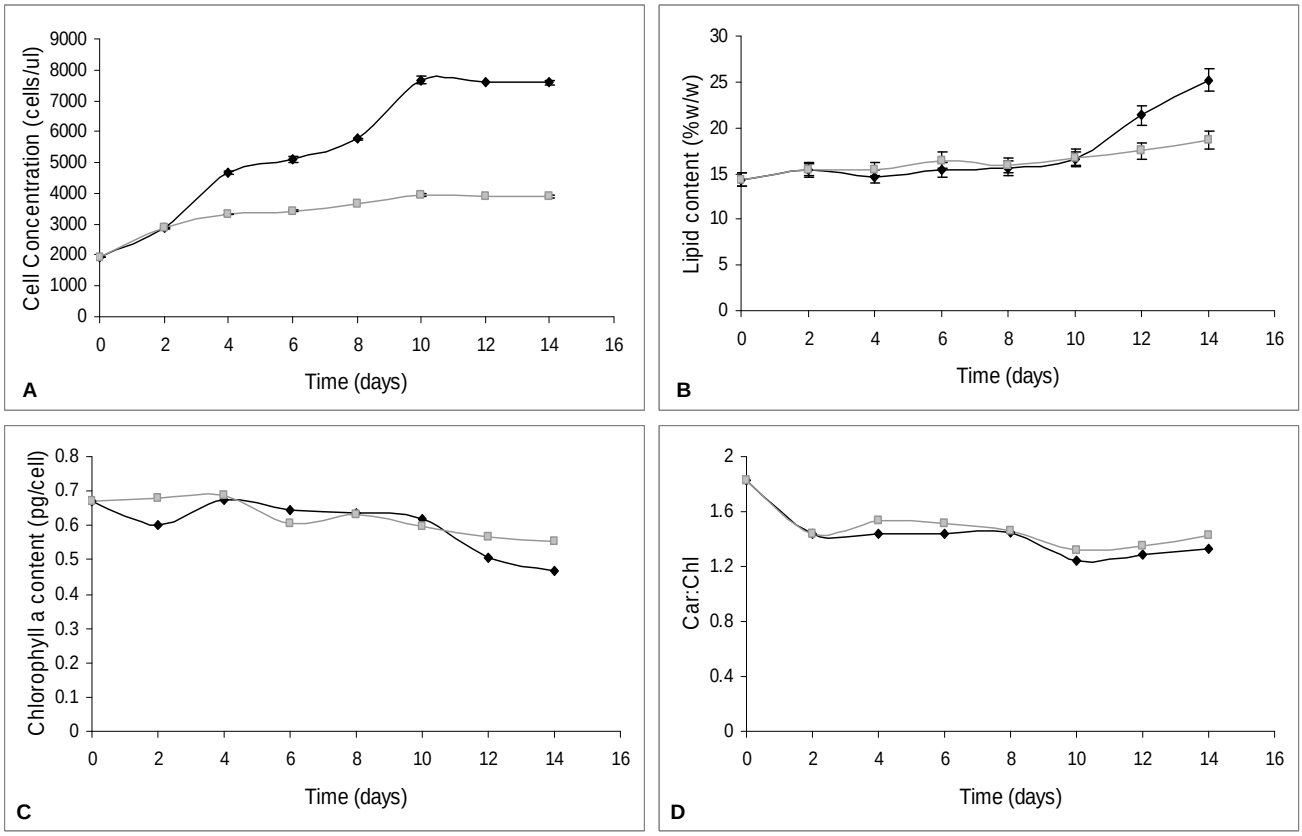

Figure 9.8: Bubbled (bubble column; ◆) and non-bubbled (pond; □) *I. galbana* batch cultures obtained from the effluent of System 1 of the continuous PBR that was supplemented with 1780 µM sodium nitrate. The cell concentration (**A**), lipid content (**B**), chlorophyll a content **(C**) and carotenoid to chlorophyll ratio (**D**) were monitored. Error bars represent standard deviation (n = 3).

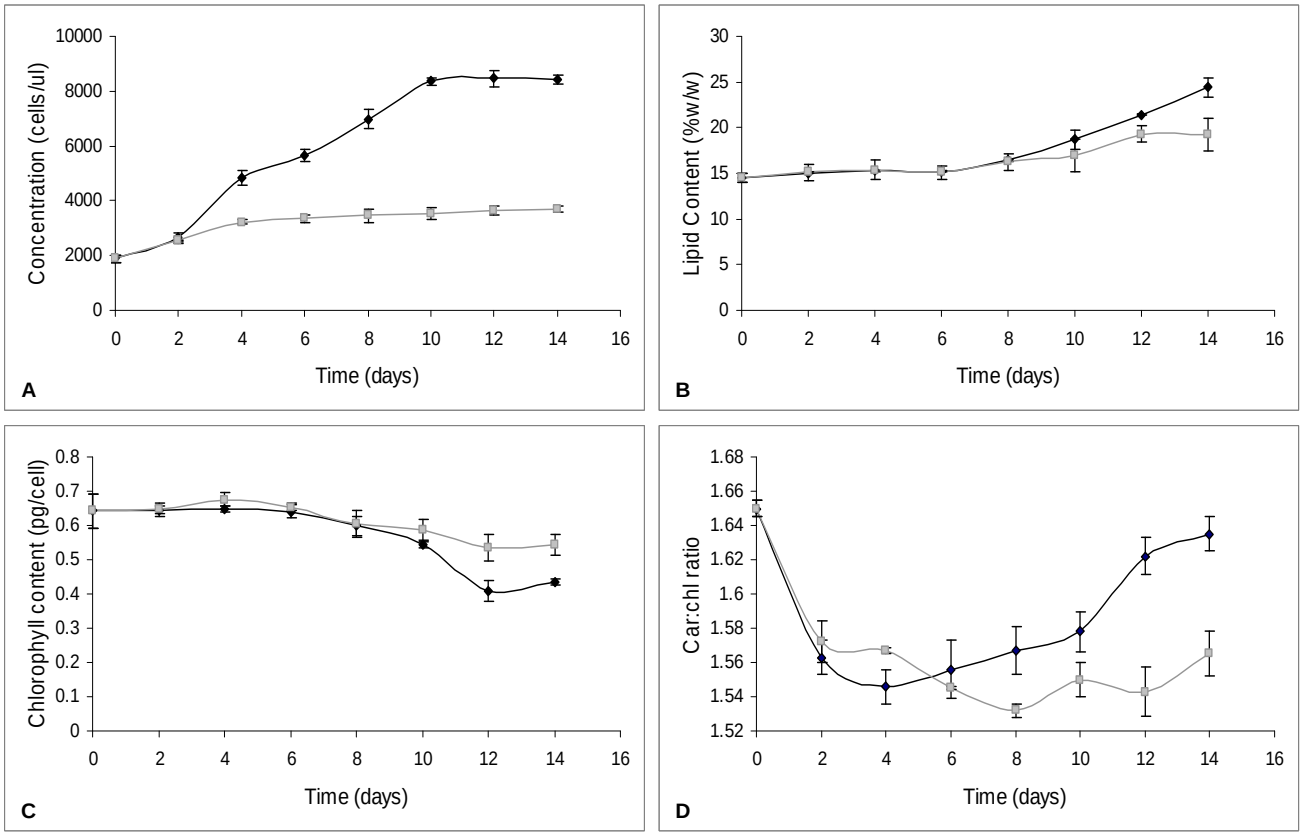

Figure 9.9: Bubbled (bubble column; ◆) and non-bubbled (pond; □) *I. galbana* batch cultures obtained from the effluent of System 1 of the continuous PBR that was supplemented with 1980 µM sodium nitrate. The cell concentration (**A**), lipid content (**B**), chlorophyll a content **(C**) and carotenoid to chlorophyll ratio (**D**) were monitored. Error bars represent standard deviation (n = 3).

The concentration of nitrogen in the medium influent was directly proportional to the time of the initiation of the stationary phase in System 2 (e.g. the second-phase culture with the least nitrogen [440µm sodium nitrate] reached the stationary phase the quickest [day 6] in comparison to all other nitrogen treatments [cf. Figures 9.6 A to 9.9 A]). Hence, the stationary phase in System 2 was most probably a direct consequence of nitrogen starvation. The maximal cell yields, in all bubbled cultures, were much greater than that observed in the non-bubbled cultures (Figures 9.6 – 9.9). This is not surprising since non-bubbled cultures would experience carbon dioxide limitation effects which include lower levels of growth and lower lipid yield which was also observed when comparing bubbled and non-bubbled cultures (Figures 9.6 B – 9.9 B).

Lipid production was only observed during the stationary phase in all the cultures (Figures 9.6 B – 9.9 B). This observation was made in numerous studies of *Isochrysis* sp. In these studies the protein content was elevated during the exponential phase and lipid content increased during the stationary phase (Brown *et al*., 1993; Zhu *et al*., 1997b; Fidalgo *et al*., 1998; Phatarpekar *et al*., 2000). Lipid production was in response to stresses induced by the depletion of internal nitrogen reserves which were only experienced from day 6 onwards (Figure 9.6). Hence, if the nitrogen concentrations that were tested (440 µm to 1980 µm sodium nitrate) are to be used, in the culture influent, an additional 6 days or more (corresponding to the initial nitrogen concentration in the influent) of the second phase of the PBR system would have to be carried out to increase growth and lead to the initiation of lipid synthesis. Furthermore, an additional number of days would be necessary to increase the lipid yield to high enough levels for maximal oil extraction. The minimum duration of the second phase (earliest initiation of the stationary phase and lipid accumulation) was experienced by the culture that was grown with 440 µm sodium nitrate (Figures 9.6 A and B) but this treatment also resulted in the lowest steady-state cell growth rate (Figure 9.5) and the final cell yield in the second phase was less than half that observe in all other nitrogen treatments tested (cf. Figures 9.6 A and 9.7 – 9.9 A). Thus, the tradeoff between cell growth and lipid accumulation is highlighted here.

The pigmentation of all the cultures followed a similar trend (Figures 9.6 C & D – 9.9 C & D). An increase in the carotenoid to chlorophyll ratio was observed during the stationary phase when the cells were nutrient stressed. A decrease in the chlorophyll content was also evident indicating that chlorophyll was either used as a nitrogen source when N levels became limiting or the chlorophyll was degraded in an attempt to decrease photosynthetic rates during growth-inhibiting conditions.

Non-bubbled cultures would be beneficial in that it would reduce energy costs however, as evident in the above graphical representations (Figure 9.6 – 9.9), the disadvantages associated with the non-bubbled system drastically outweigh the energy saving since both the cellular and lipid yield are lower in those cultures.

An increase in the nitrogen fed into System 1 has a great impact on the duration of the second phase of the bioreactor system (Figures 9.6 – 9.9). An increase in the nitrogen concentration results in an increase in the eventual biomass yield however it also results in an increase in the duration of the second phase run which has cost implications. Thus a balance between the variables needs to be achieved. The optimal range of nitrogen to be used for the continuous culture of *I. galbana* is between 880 to 1780 µm sodium nitrate. Levels below this range result in reductions in final cellular yield and levels above result in nitrogen saturation effects (Figure 9.5). Regardless of the lower stead-state cell growth when *I. galbana* was grown in medium supplemented with 880 µm sodium nitrate, in comparison to the other treatments with higher levels of nitrogen (Figure 9.5), the eventual cell yield in the second phase mirrored that of the treatments with elevated nitrogen levels (cf. Figures 9.6 A – 9.9 A). This coupled with the earlier onset of the stationary phase and the earlier initiation of lipid synthesis (cf. Figures 9.6 A & B – 9.9 A & B) makes the 880 µm sodium nitrate treatment (normal sodium nitrate concentration in *f/2* medium) ideal in terms of cost reductions (less nitrogen than the other higher treatments used) and the reduced duration of the second phase run.

9.3.4 Sixteen liter continuous culture with flow rate variations

The ideal concentration of nitrogen in the culture medium, when running the PBR in continuous mode, was shown to be 880 µm sodium nitrate (Section 9.3.3). The present experiment was aimed at determining the optimal flow rate when *I. galbana* was grown in *f/2* medium supplemented with 880 µm sodium nitrate.

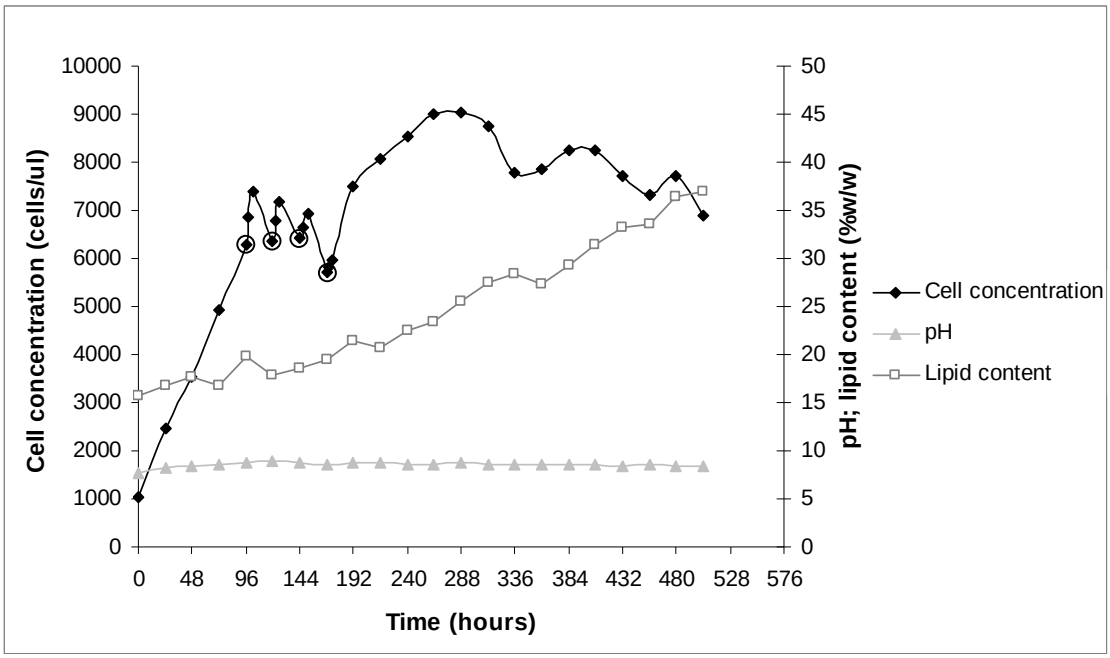

Figure 9.10: Growth curve showing *I. galbana* growth, lipid accumulation and medium pH when cultured in a 16 L PBR. Circled points indicate switches from batch to continuous mode at flow rates of 1.44, 2.16, 3.59 and 5.03 ml/min respectively. The culture was maintained in batch mode after 173 hours.

I. galbana cells grew rapidly when cultured in batch mode (Figure 9.10; 0 – 96 hours). Rapid growth continued even when continuous mode was initiated implying that cellular washout had little effect on the eventual cellular yield during day-time conditions (i.e. cell division exceeded culture washout). But, night-time drops in the cell concentration were observed (e.g. Figure 9.10; 103 – 120 hours). The absence of light at night results in up to 25% biomass losses (Chisti, 2008). Hence, the sudden drops in cellular yield during the night may be attributed to biomass losses due to the washout of cells in continuous runs. The erratic stationary phase cellular yield observed when the system was run in batch mode after 173 hours was attributed to rapid clumping and de-clumping of cells (Figure 9.10). The lipid yield increased as the batch culture aged due to the storage of lipids as an energy source under unfavorable conditions (Figure 9.10). The pH of the culture medium remained somewhat constant throughout the PBR run highlighting the buffer capacity of seawater. The culture effluent obtained after alterations in each flow rate was collected and grown in a 'second lipid-accumulating phase'.

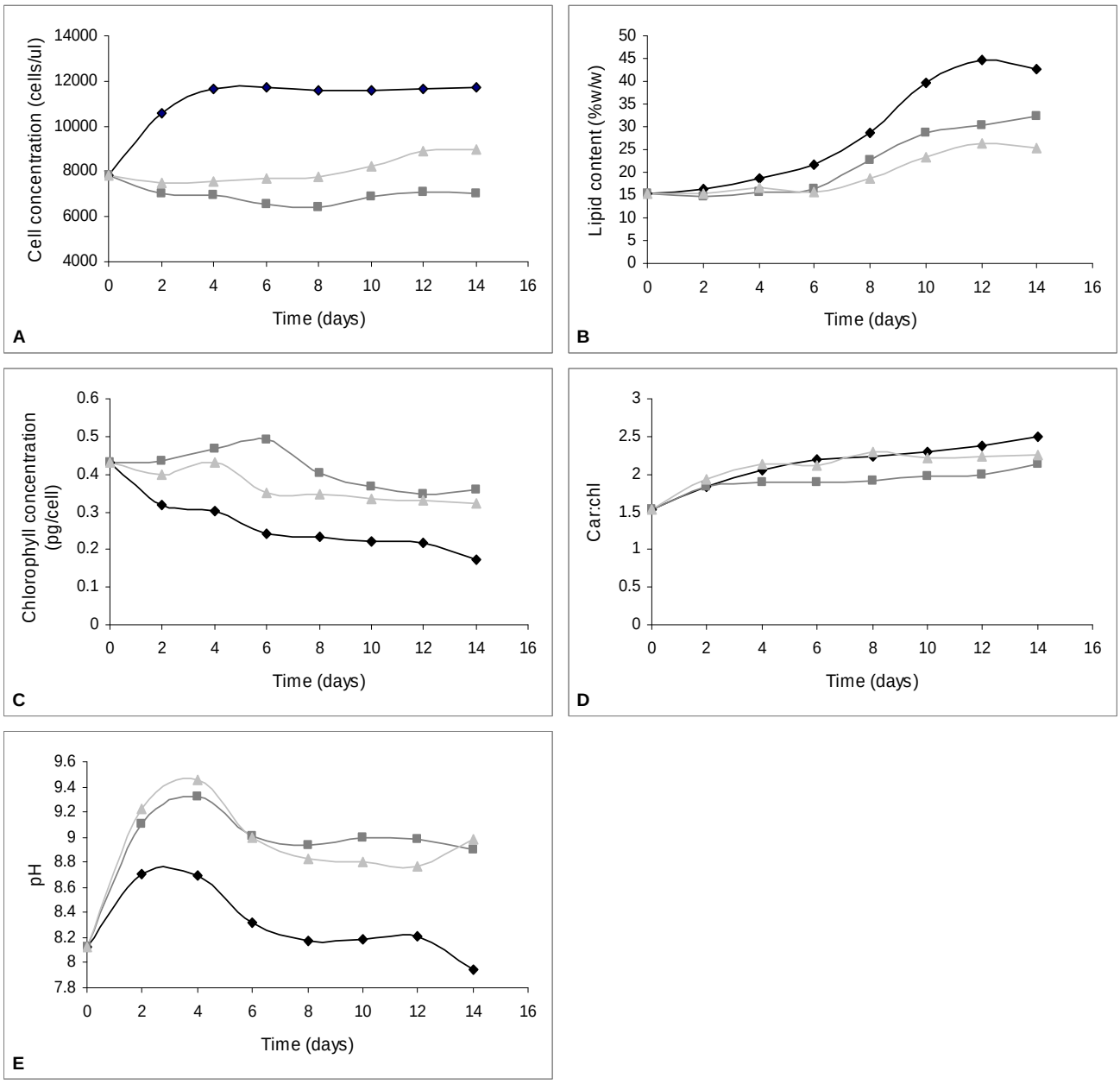

Figure 9.11: Bubbled (bubble column; ◆) and non-bubbled (raceway [shaken]; ■ and pond [still]; ▲) *I. galbana* batch cultures obtained from the effluent of System 1 of the continuous PBR with a flow rate of 1.44 ml/min. The cell concentration (**A**), lipid content (**B**), chlorophyll a content **(C**) carotenoid to chlorophyll ratio (**D**) and pH (**E**) were monitored.

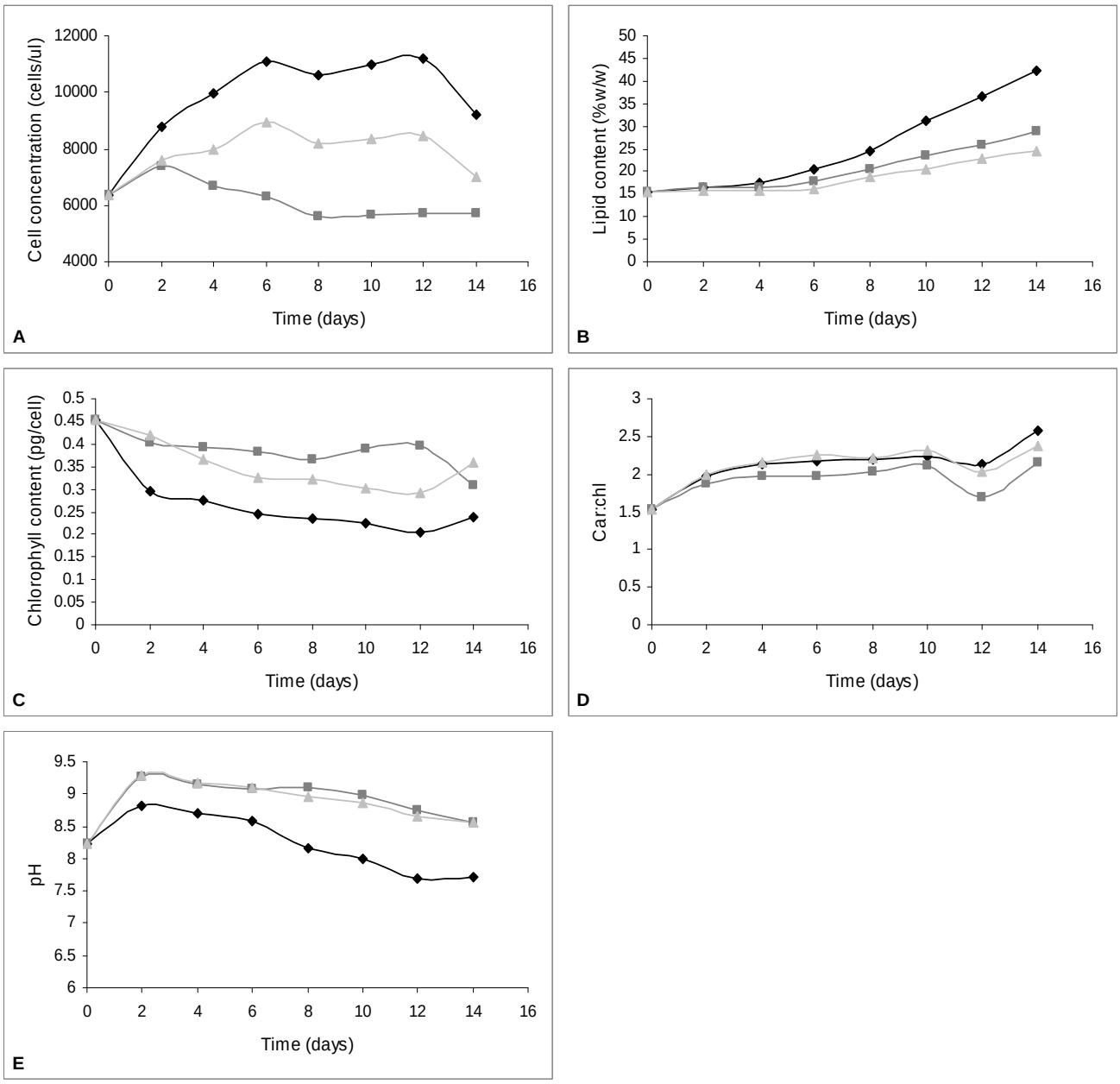

Figure 9.12: Bubbled (bubble column; ◆) and non-bubbled (raceway [shaken]; ■ and pond [still]; ▲) *I. galbana* batch cultures obtained from the effluent of System 1 of the continuous PBR with a flow rate of 2.16 ml/min. The cell concentration (**A**), lipid content (**B**), chlorophyll a content **(C**) carotenoid to chlorophyll ratio (**D**) and pH (**E**) were monitored. .

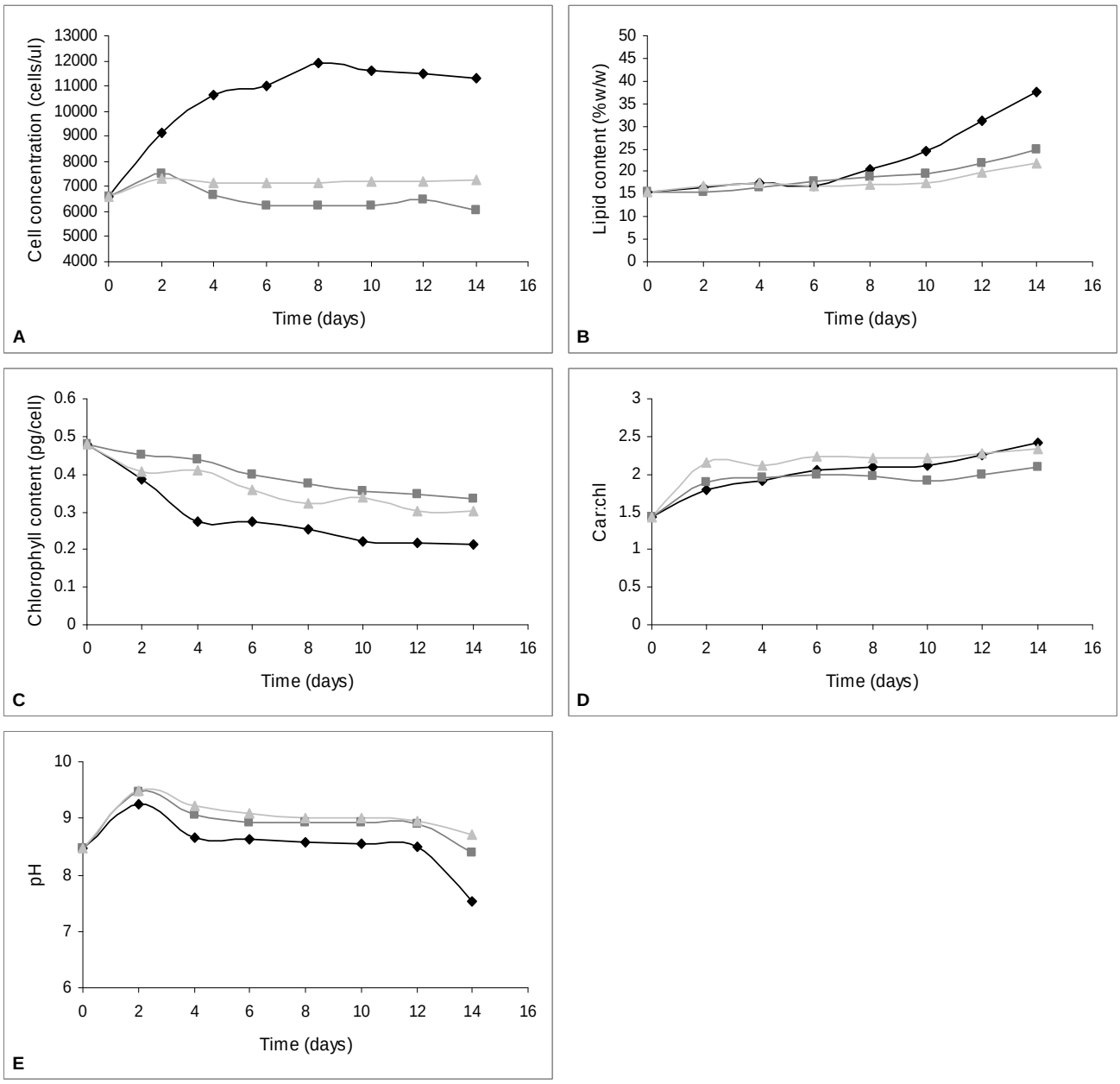

Figure 9.13: Bubbled (bubble column; ◆) and non-bubbled (raceway [shaken]; ■ and pond [still]; ▲) *I. galbana* batch cultures obtained from the effluent of System 1 of the continuous PBR with a flow rate of 3.59 ml/min. The cell concentration (**A**), lipid content (**B**), chlorophyll a content **(C**) carotenoid to chlorophyll ratio (**D**) and pH (**E**) were monitored.

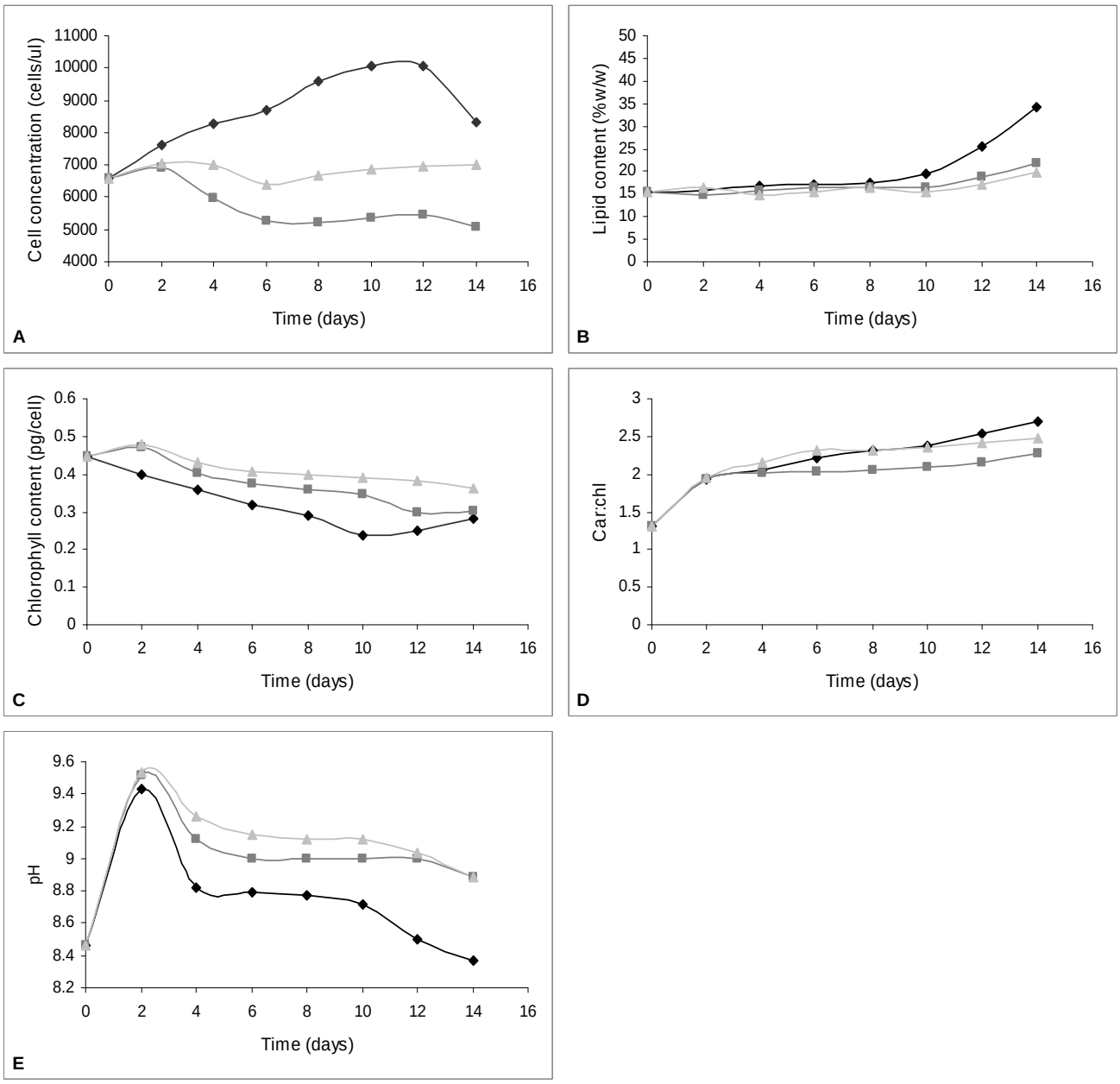

Figure 9.14: Bubbled (bubble column; ◆) and non-bubbled (raceway [shaken]; ■ and pond [still]; ▲) *I. galbana* batch cultures obtained from the effluent of System 1 of the continuous PBR with a flow rate of 5.03 ml/min. The cell concentration (**A**), lipid content (**B**), chlorophyll a content **(C**) carotenoid to chlorophyll ratio (**D**) and pH (**E**) were monitored.

The effluent from System 1 was maintained in vessels that simulated a bubble column, raceway system and pond (representing System 2). An observation of interest that was noted in the bubble column vessels was that the stationary phase was initiated earlier in the cultures with a lower dilution rate and vice versa (Figures 9.11 A – 9.14 A). As the dilution rate increases (increase in addition of fresh medium) so to does the cellular washout. This washout consists of the cells and medium containing the nutrients that have not been taken up by the cells. Hence, at high dilution rates nutrients that stimulate algal growth and division are transferred to System 2 thus prolonging the exponential phase of growth. Ideally, System 1 should be the growth chamber where nutrients are taken up and maximal biomass is produced. The continuation of growth in System 2 is undesirable since this would increase the duration of the System 2 run which has cost implications.

The biomass yield in the raceway and pond setups were much lower than that observed in the bubble columns (Figures 9.11 A – 9.14 A). This is most probably a consequence of the low levels of carbon dioxide in both the pond and raceway setup in comparison to the bubble columns. Aeration in the bubble column also allows for the mixing of the culture ensuring that all cells get exposed to the light source. Light and carbon dioxide are essential for both growth and lipid accumulation. The raceway setup is continuously agitated hence it is expected that the levels of carbon dioxide and the exposure of cells to the incident light would be greater in this system than in the pond system where the culture was kept still. If the argument substantiating the increased levels of growth in the bubble column is valid, than the levels of growth in the raceway setup should be higher than that evident in the pond setup. However, the opposite was observed when the PBR was run at all flow rates (Figure 9.11 A -9.14 A). This was merely a consequence of the rapid clumping of the cells (due to continual collisions between the cells and clumps) in the raceway setup hence only the free-swimming cells in the medium were enumerated.

The lipid levels were the highest in the bubble columns and the lowest in the pond setup. Cells cultured in the raceway setup demonstrated intermediate lipid levels (Figures 9.11 B – 9.14 B). This is not surprising since carbon dioxide and light are necessary for lipid

accumulation and, as mentioned previously, the bubble column provides the most light and carbon dioxide and the pond the least. The initiation of lipid accumulation was a direct consequence of the flow rate where it was initiated earlier in cultures with a lower flow rate and vice versa (Figure 9.11 B – 9.14 B). This observation is expected since lipid is accumulated in response to stress and this stress is imposed later in cultures with a higher flow rate.

The pigmentation of all cells showed a pattern consistent with algal growth where the chlorophyll content increases when growth is maximal and than decreases in response to stress (Figures 9.11 C – 9.14 C). An increase in the carotenoid to chlorophyll ratio was also noted in all treatments which is indicative of algal stress (Figures 9.11 D – 9.14 D). The initial increase in the culture pH in all treatments and at all flow rates was expected since rapidly growing cells fix carbon dioxide which results in the alkalization of the culture medium (Clark, 1999; Figures 9.11 E – 9.14 E). A decrease in the pH in all treatments followed but this decrease was much more pronounced in the bubbled columns than in the raceway and pond setup (Figures 9.11 E – 9.14 E). This is due to higher levels of carbon dioxide in the medium in bubbled columns and as the cells age less carbon dioxide is taken up hence the pH of the medium decreases rapidly.

This study proved that lower flow rates are preferred as these would reduce the duration of the second phase run (cost implications). Maximal cellular and lipid yield were obtained when System 2 was a bubble column as apposed to a pond or raceway.

9.4 CONCLUSION

Numerous variables need to be taken into consideration when attempting to optimize a PBR system. The effect of variations in the size of the PBR, light intensities used, nitrogen concentration and the flow rate were tested in this study. Multiple light intensities were proven to increase the rate of growth. An increase in the sodium nitrate concentration in a continuous PBR system was shown to increase the steady-state cell growth rate however it also resulted in the increase in the duration of the second lipid

accumulating phase of the bioreactor run. Similarly, an increase in the dilution rate used also resulted in concomitant increases in the duration of the second lipid-accumulating phase which has cost implications. Further optimization and scale-up of the continuous system is necessary to achieve economic viability.

CHAPTER TEN

Summarising Discussion & Conclusion

Microalgae may be used as a feedstock for numerous products including biohydrogen (Akkerman *et al*., 2002), polyunsaturated fatty acids (Apt and Behrens, 2006; Spolaore *et al*., 2006), pigments and proteins (Bermudez *et al*., 2004). Microalgae may also be used for the bioremediation of environmental pollutants (Mehta and Gaur, 2005; e.g. for carbon dioxide capture; Vunjak-Novakovic *et al*., 2005; Brown, 1996). The focus of the current work was on the synthesis of lipids by microalgae. These lipids would be used as a feed for biodiesel production.

Microalgae have been considered for biodiesel production due to the numerous desirable attributes associated with these micro-organisms. A few amongst these include their rapid growth rate, their simple cellular structure, the capability to produce large amounts of lipid and the ability of microalgae to thrive in low-cost water (e.g. wastewaters and brackish water) or seawater (Um and Kim, 2009).

In the current study a selection of microalgal species were screened and a model organism for biodiesel production was chosen and identified. Initial experiments were conducted to unravel the response of the model organism to varying growth conditions (nitrogen supply) in an attempt to better understand the biology of the selected species. Cost-reduction experiments for the mass culture of the model organism were then conducted. Cell harvesting approaches and mass algal production in various configurations of a PBR were also tested.

10.1 Screening, selection and identification

Three microalgal species were selected as candidates for the screening process (i.e. *Platychrysis* sp., *Isochrysis* sp. and *Pleurochrysis* sp.). Upon culturing of the various species it became evident that *Platychrysis* sp. has a tendency to stick to the culture vessels thus forming an obstruction to light penetration which causes an unwanted energy loss. Hence, *Platychrysis* sp. was eliminated from the screening process. When *Isochrysis* sp. and *Pleurochrysis* sp. were compared it became apparent that *Isochrysis* sp. was superior in terms of its growth rate, lipid yield and lipid productivity. Hence

Isochrysis sp. was chosen to be used as the model organism and was used in all subsequent experimentation.

A dual method of microalgal identification was used to ensure the definitive, unambiguous identification of the species (morphological and molecular methods). The morphological methods proved that the species is indeed a member of the Haptophyta division and presumably a strain of *I. galbana*. Molecular methods provided evidence that the isolate belongs to Clade C of the class Prymnesiophyceae and is certainly a strain of *Isochrysis galbana* and was henceforth termed *Isochrysis galbana* strain U4 (U4 was the title of the culture in the culture collection).

10.2 Effect of nitrogen supply on *I. galbana* U4

A better understanding of the biology of *I. galbana* U4 was imperative to develop ways to optimize the lipid production and growth capabilities of the species. An initial experiment was conducted where algal growth, pigmentation and nitrogen uptake abilities were monitored when the alga was cultured in normal *f/2* medium and *f/2* medium lacking any external nitrogen source. This experiment proved that nitrogen is essential for *I. galbana* growth and that this species was capable of luxury N uptake and storage. Hence, the intracellular nitrogen content determines the rate of growth, commencement of the stationary phase and initiation of lipid synthesis in *I. galbana* U4 when ambient N is depleted. It was also deduced that the pigment concentration (chlorophyll content and carotenoid to chlorophyll ratio) is strongly related to the nutrient status of the culture.

Observed ultrastructural changes that were initiated by nitrogen starvation included the production of numerous large cytoplasmic and plastidial lipid bodies, the reduction in the size of the pyrenoid, plastid degradation and the formation of masses in the nucleus (presumably heterochromatin). The distinct onset of lipid accumulation only in the stationary phase verified that this species was an ideal candidate to be used in a two-phase PBR system where the initial phase was nitrogen sufficient, promoting maximal biomass production and the second phase was nutrient-deplete to boost lipid synthesis.

Since nitrogen was proven to be the key nutrient involved in the initiation of the stationary phase, the effect of varying nitrogen levels on *I. galbana* lipid yield, biomass productivity and lipid productivity were tested. As expected, an inverse relationship between the lipid yield and biomass productivity was observed, however the lipid productivity was not constant throughout the culture period. This was attributed to the greater influence of lipid yield than biomass productivity on lipid productivity. The lipid productivities were observed to be maximal during the early stationary phase and declined towards the late stationary phase when lipid ceased to accumulate. Thus, it was shown that the precise timing of *I. galbana* harvesting (during the stationary phase) has a great impact on the final lipid yield.

10.3 Cost optimization for *I. galbana* mass culture

Cost reductions for algal culture are imperative for the successful commercialization of the mass culture process. In an attempt to reduce costs the growth of *I. galbana* in medium supplemented with various nitrogen sources were tested. It was concluded that *I. galbana* grew well in medium supplemented with urea which is a relatively cheap source of nitrogen in comparison to all the N sources that were tested. Hence urea is the preferred N source in the scale-up, commercial culture processes for this particular species.

Phosphorus was another essential nutrient for algal growth that has been neglected thus far. *I. galbana* growth in medium supplemented with varying phosphorous concentrations was tested. The study proved that the P deficiency threshold for *I. galbana* lies below 0.25 ppm P (quarter the P concentration in *f/2* medium). *I. galbana* was capable of growing at the same rate and producing the same amount of lipid when cultured in quarter the amount of P in *f/2* medium as it is when grown in 1.5 times the amount of P in *f/2* medium. Reducing the concentration of P in the culture medium would contribute to cost reductions and also prevent excessive P from promoting the growth of contaminating organisms. The luxury uptake of P by *I. galbana* was also noted in this study.

10.4 *Isochrysis galbana* dewatering processes and mass culture

Isochrysis galbana was successfully flocculated by increasing the culture pH but cells flocculated automatically in bubbled cultures, which is beneficial since this method does not require the addition of chemicals (cost reductions).

7 L and 16 L PBR systems were tested for the mass culture of *I. galbana*. The increase in the volume of the PBR resulted in a concomitant decrease in the algal growth rate which was attributed to limitations on the carbon dioxide and light supply upon system upscale. Sequential stepped increases in the light intensity in response to the stage of algal growth increased the growth rate of *I. galbana.* A continuous run of the PBR with varying levels of nitrogen in the influent showed that the steady-state cell growth rate increased as a function of the nitrogen input until inhibitory N levels were supplied. Greater levels of N in the influent had a positive effect on the cell concentration in System 1, of the two-phase culture, but negative effects on System 2, where greater N input levels prolonged growth in what should be the lipid-accumulating system. A comparison between the System 2 'pond' and 'bubble column' setup proved that the bubble column was the most promising in terms of *I. galbana* final cell yield and lipid accumulation abilities. Similarly, the growth of *I. galbana* in a continuous PBR system run with varying flow rates showed that increases in the flow rate prolonged the culture run in System 2 (cost implications). Here, a 'pond', 'raceway' and 'bubble column' setup for System 2 were tested. Again, the 'bubble column' setup represented the ideal System 2 configuration in terms of *I. galbana* final cell yield and lipid accumulation abilities.

10.5 Conclusion

Overall, this study proved that *I. galbana* is a promising candidate for biodiesel production. The variables that have an implication on the growth rate and lipid production tested in this study included nitrogen levels and source, phosphorus levels and the light intensities used. Numerous other variables may be analysed in future studies, including the carbon dioxide supply and temperature. Furthermore, one of the most relevant future studies should be based on the fatty acid profile of *I. galbana* U4 to determine if the lipid produced by this species is feasible for biodiesel production.

A simplified PBR system has been designed and tested. This system has much potential for further design improvement that would aid in optimizing the system. Since the growth rate of *I. galbana* was influenced by the upscale of the PBR system it is suggested that the system should not be upscaled further and multiple small units should be used in an industrial setup. If *I. galbana* is to be mass cultured, the cost of the process can be minimized by implementing the cost reduction approaches (reduced P concentrations and the use of urea as a N source) that have been discussed previously. Further optimization of the PBR would lead to more cost reductions which may result in a commercially viable system.

REFERENCES

Abalde, J., Fabregas, J. and Herrero, C. (1991) Beta carotene content of the marine microalga *Dunaliella tertiolecta* cultured with different nitrogen sources, *Bioresource Technology*, vol.38, pp. 121-125.

Adams, C., Godfrey, V., Wahlen, B., Seefeldt, L. and Bugbee, B. (2013) Understanding precision nitrogen stress to optimize the growth and lipid content tradeoff in oleaginous green microalgae, *Bioresource Technology*, vol.131, pp. 188-194.

Adir, N., Zer, H., Shochat, S. and Ohad, I. (2003) Photoinhibition – a historical perspective. *Photosynthesis Research*, vol. 76, pp. 343-370.

Ahlgren, G. and Hyenstrand, P. (2003) Nitrogen limitation effects of different nitrogen sources on nutritional quality of two freshwater organisms, *Schenedesmus quadricauda* (Chlorophyceae) and *Synechococcus* sp. (Cyanophyceae), *Journal of Phycology*, vol.19, pp. 906-917.

Akkerman, I., Jansen, M., Rocha, J. and Wijffels, R.H. (2002) Photobiological hydrogen production: Photochemical efficiency and bioreactor design. *International Journal of Hydrogen Energy*, vol. 27, pp. 1195-1208.

Akinci, B., Kassebaum, P.G., Fitch,J.V. and Thompson, R.W. (2008) The role of bio-fuels in satisfying US transportation fuel demands, *Energy Policy*, vol.38, pp. 3485-3491.

Alba, L.G., Torri, C., Samori, C., van der Spek, J., Fabbri, D., Kersten, S.R.A. and Brilman, D.W.F. (2012) Hydrothermal Treatment (HTT) of Microalgae: Evaluation of the Process As Conversion Method in an Algae Biorefinery Concept, *Energy Fuels*, vol.26, pp. 642–657.

Anderson, R.A. (2004) Biology and systematics of Heterokont and Haptophyte algae, *American Journal of Botany*, vol.91, no.10, pp. 1508–1522.

Apt, K.E., and Behrens, P.W. (1999) Commercial developments in microalgal biotechnology, *Journal of Phycology*, vol. 35, pp. 215-226.

Arumugam, M., Agarwal, A., Arya, M.C. and Ahmed, Z. (2013) Influence of nitrogen sources on biomass productivity of microalgae *Scenedesmus bijugatus*, *Bioresource Technology*, doi: http://dx.doi.org/10.1016/j.biortech.2012.12.159

Babcock Jr, W.B., Malda, J. and Radway, J.C. (2002) Hydrodynamics and mass transfer in a tubular airlift photobioreactor, *Journal of Applied Phycology*, vol. 14, pp. 169-184.

Barsanti, L. and Gualtieri, P. (2006) Algae: Anatomy, Biochemistry and Biotechnology. New York, CRC Press.

Beach, E.S., Eckelman, M.J., Cui, Z., Brentner, L. and Zimmerman, J.B. (2012) Preferential technological and life cycle environmental performance of chitosan flocculation for harvesting of the green algae *Neochloris oleoabundans*, *Bioresource Technology*, vol. 121, pp. 445-449.

Becker, E.W. (1994) Microalgae: Biotechnology and Microbiology. Cambridge University Press, Cambridge.

Beer, L.L., Boyd, E.S., Peters. J.W. and Posewitz, M.C. (2009) Engineering algae for biohydrogen and biofuel production, *Current Opinion in Biotechnology*, vol. 20, pp. 264-271.

Bellinger, B.J., Gretz, M.R., Domozych, D.S., Kiemle, S.N. and Hagerthev, S.E. (2010) Composition of extracellular polymeric substances from periphyton assemblages in the Florida Everglades, *Journal of Phycology*, vol. 46, pp. 484-496.

Ben-Amotz, A. and Avron, M. (1983) On the factors which determine massive β-carotene accumulation in halotolerant alga *Dunaliella bardawil*, *Plant Physiology*, vol. 72, pp. 593-597.

Berberoglu, H., Yin, J. and Pilon, L. (2007) Light transfer in bubble sparged photobioreactors for hydrogen production and carbon dioxide mitigation, *International Journal of Hydrogen Energy*, vol. 32, pp. 2273–2285.

Bermudez, J., Rosales, N., Loreto, C., Briceno, B. and Morales, E. (2004) Exopolysaccharide, pigment and protein production by the marine microalga *Chroomonas* sp. in semicontinuous cultures, *World Journal of Microbiology and Biotechnology*, vol. 20, pp. 179-183.

Berry, J. (2011) Marine and Freshwater Microalgae as a Potential Source of Novel Herbicides. In Herbicides and Environment, Andreas Kortekamp (Ed.), InTech, Croatia.

Blanchemain, A., Grizeau, D. and Guary, J.C. (1994) Effect of different organic buffers on the growth of Skeletonema costatum cultures: further evidence for an autoinhibitory effect, *Journal of Plankton Research,* vol. 16, pp. 1433–1440.

Blanchemain, A. and Grizeau, D. (1999) Increased production of eicosapentaenoic acid by *Skeletonema costatum* cells after decantation at low temperature, *Biotechnology Techniques,* vol. 13, pp. 497-501.

Bligh. E.G. and Dyer. W.J. (1959) A rapid method for total lipid extraction and purification, *Journal of Biochemistry and Physiology,* vol. 37, pp. 911-917.

Borowitzka, M.A. (1997) Microalgae for aquaculture: Opportunities and constraints, *Journal of Applied Phycology,* vol. 9, pp. 393–401.

Borowitzka, M.A. (1999) Commercial production of microalgae: ponds, tanks, tubes and fermenters, *Journal of Biotechnology,* vol. 70, pp. 313-321.

Bouldin, D.R., Johnson, R.L., Burda, C. and Kao, C.W. (1974) Losses of inorganic nitrogen from aquatic systems. *Journal of Environmental Quality.*, vol.3, pp. 107-114.

Brennan, L. and Owende, P. (2010) Biofuels from microalgae—a review of technologies for production, processing, and extractions of biofuels and co-products, *Renewable & Sustainable Energy Reviews*, vol. 14, pp. 557–77.

Breuer, G., Lamers, P.P., Martens, D.E., Draaisma, R.B. and Wijffels, R.H. (2012) The impact of nitrogen starvation on the dynamics of triacylglycerol accumulation in nine microalgae strains, *Bioresource Technology*, vol. 124, pp. 217-226.

Brown, L.M. (1996) Uptake of carbon dioxide from flue gas by microalgae. *Energy Conversion and Management,* vol. 37, pp. 1363-1367.

Brown, M.R., Garland, C.D., Jeffrey, S.W., Jameson, I.D. and Leroi, J.M. (1993) The gross and amino acid compositions of batch and semi-continuous cultures of *Isochrysis sp.* (clone T-ISO), *Pavlova Lutheri* and *Nannochloropsis oculata*, *Journal of Applied Phycology*, vol. 5, pp. 285-296

Burton, T., Lyons, H., Lerat, Y., Stanley, M. and Rasmussen, M.B (2009) A Review of the Potential of Marine Algae as a Source of Biofuel in Ireland, *Sustainable Energy Ireland*, www.sei.ie/**algae**report.

Cade-Menun, B.J. and Paytan, A. (2010) Nutrient temperature and light stress alter phosphorus and carbon forms in culture-grown algae, *Marine Chemistry*, vol. 121, pp. 27-36.

Carpenter, E.J., Remsen, C.C., and Watson, S.W. (1972) Utilization of urea by some marine phytoplankters, *Lymnology and Oceanography*, vol. 17, pp. 265-269.

Carvalho, A.P., Meireles, L.A. and Malcata, F.X. (2006) Microalgal Reactors: A review of enclosed system designs and performances, *Biotechnology Progress.* vol. 22, pp. 1490-1506.

Carvalho, J., Ribeiro, A., Castro, J., Vilarinho, C. and Castro, F. (2011) Biodiesel production by microalgae and macroalgae from North Littoral Portuguese Coast, *WASTES: Solutions, Treatments and Opportunities*, 1st International Conference, September 12th-14th 2011.

Cataldo, D.A., Haroon, M., Schrader, L.E. and Youngs, V.L. (1975) Rapid colorimetric determination of nitrate in plant-tissue by nitration of salicylic acid, *Communications in Soil Science and Plant Analysis*, vol. 6, pp. 71-80.

Cavalier-Smith, T. (1998) A revised six-kingdom system of life, *Biological Reviews* vol. 73, pp. 203–266.

Cembella, A.D., Antia, N.J. and Harrison, P.J. (1984) The utilization of inorganic and organic phosphorus compounds as nutrients by eukaryotic microalgae: A multidisciplinary perspective: Part 1, *Critical Reviews in Microbiology*, vol. 10, pp. 317-391.

Chen, P.S., Toribara, T.Y. and Warner, H. (1956) Microdetermination of phosphorus, *Analytical Chemistry*, vol. 28, pp. 1756-1758.

Chen, Y.C. (2003) Immobilized *Isochrysis galbana* (Haptophyta) for long-term storage and applications for feed and water quality control in clam (*Meretrix lusoria*) cultures, *Journal of Applied Phycology*, vol. 15, pp. 439-444.

Chen, C., Yeh, K., Aisyah, R., Lee, D. and Chang, J. (2011) Cultivation, photobioreactor design and harvesting of microalgae for biodiesel production: A critical review, *Bioresource Technology*, vol. 102, pp. 71-81.

Chen, J., Li, Y., Xie, M., Chiu, C., Liao, S. and Lai, W. (2012a) Factorial Design of Experiment for Biofuel Production by *Isochrysis Galbana*, *IPCBEE*, vol. 33, pp. 91-95.

Chen, S.Y., Pan, L.Y., Hong, M.J., and Lee, A.C. (2012b) The effects of temperature on the growth of and ammonia uptake by marine microalgae, *Botanical Studies*, vol. 53, pp. 125-133.

Chisti, Y. (2007) Biodiesel from Microalgae, *Biotechnology Advances*, vol. 25, pp. 294-306.

Chisti, Y. (2008) Biodiesel from microalgae beats bioethanol, *Trends in Biotechnology*, vol. 26, pp. 126-130.

Chiu, S.Y., Kao, C.Y., Tsai, M.T., Ong, S.C., Chen, C.H. and Lin, C.S. (2009) Lipid accumulation and CO2 utilization of *Nannochloropsis oculata* in response to CO^2 aeration. *Bioresource Technology*, vol. 100, pp. 833–838.

Cho, S.H. and Thompson, G.A. (1986) Properties of a fatty acid hydrolase preferentially attacking monogalactosyldiacylglycerols in *Dunaliella salina* chloroplasts, *Biochim. Biophys.*, vol. 878, pp. 353-359.

Choi, J.H., Jung, H.J., Kim, H.S. and Cho, H.G. (2000) PhyloDraw: a phylogenetic tree drawing system, *Bioinformatics*, vol. 16, pp. 1056-1058.

Clark, D.R., Merret, M.J. and Flynn, K.J. (1999) Utilization of dissolved inorganic carbon (DIC) and the response of the marine flagellate *Isochrysis galbana* to carbon or nitrogen stress, *New Phytologist,* vol. 144, pp. 463-470.

Costa, J.A.V., Cozza, K.L., Oliveira, L. and Magagnin, G. (2001) Different nitrogen sources and growth responses of *Spirulina platensis* in microenvironments, *World Journal of Microbiology and Biotechnology,* vol. 17, pp. 439-442.

Csavina, J.L. (2008) The Optimization of Growth Rate and Lipid Content from Select Algae Strains, Masters thesis (Unpublished).

Da Silva, T.L., Reis, A., Medeiros, R., Oliviera, A.C. and Gouveia, L. (2008) Oil production towards biofuel from autotrophic microalgae semicontinuous cultivations monitorized by flow cytometry, *Applied Biochemistry and Biotechnology,* vol. 159, pp. 568-578.

Danquah, M.K., Ang, L., Uduman, N., Moheimani, N. and Forde, G.M. (2009a) Dewatering of microalgae culture for biodiesel production: exploring polymer flocculation and tangential flow filtration, *Journal of Chemical Technology and Biotechnology,* vol. 84, pp. 1078-1083.

Danquah, M.K., Gladman, B., Moheimani, N. and Forde, G.M. (2009b) Microalgal growth characteristics and subsequent influence on dewatering efficiency, *Chemical Engineering Journal,* vol. 151, pp. 73-78.

Daugbjerg, N. and Anderson, R.A. (1997) Phylogenetic Analyses of the *rbc*L Sequences from Haptophytes and Heterokont Algae Suggest Their Chloroplasts are Unrelated, *Molecular Biology and Evolution,* vol. 14, no. 12, pp. 1242-l 251.

Davidson, K., Flynn, K.J. and Cunningham, A. (1991) Relationships between photopigments, cell carbon, cell nitrogen and growth rate for a marine nanoflagellate, *Journal of Experimental Marine Biology and Ecology,* vol. 153, pp. 87-96.

Davis, N.S. and Foust, O.J. (1969) Flocculation of suspensions. U.S. patent 3, 431, 200.

Dayananda, C., Saradha, R., Bhattacharya, S. and Ravishankar, G.A. (2006) Effect of media and culture conditions on growth and hydrocarbon production from *B. braunii*, *Process Biochemistry*, vol. 40, pp. 3125-3131.

de-Bashan, L.E., Bashan, Y., Moreno, M., Lebsky, V, K. and Bustillos, J.J. (2002) Increased pigment and lipid content, lipid variety, and cell and population size of the microalgae *Chlorella* spp. when co-immobilized in alginate beads with the microalgae-growth-promoting bacterium *Azospirillum brasilense*, *Canadian Journal of Microbiology*, vol. 48, no. 6, pp. 514-521.

De la Jara, A., Mandoza, H., Martel, A., Molina, C., Nordstron, L., de la Rosa, V., and Diaz, R. (2003) Flow cytometric determination of lipid content in a marine dinoflagellate, *Cryphthecodinium cohnii*, *Journal of Applied Phycology*, vol.15, pp. 433-438.

Deng, X., Li, Y. and Fei, X. (2009) Microalgae: A promising feedstock for biodiesel, *African Journal of Microbiology Research*, vol. 3, no. 13, pp. 1008-1014.

Doan, T.T.Y., Sivaloganathan, B. and Obbard, J.P. (2011) Screening of marine microalgae for biodiesel feedstock, *Biomass and Bioenergy*, vol. 35, pp. 2534-2544.

Dodge, J.D. (1973) The fine structure of algal cells, Academic Press Inc., London.

Dorich, J.A. and Nelson, D.W. (1983) Direct colorimetric measurement of ammonium in potassium chloride extracts in soil, *Soil Science Society of American Journal,* vol. 55, pp. 171-178

Dortch, Q., Clayton Jr., J.R., Thoresen, S.S. and Ahmed, S.I. (1984) Species differences in accumulation of nitrogen pools in phytoplankton, *Marine Biology*, vol. 81, pp. 237-250.

Doyle, J. J. & Doyle, J. L. (1990) Isolation of plant DNA from fresh tissue, *Focus*, vol. 12, pp. 13–15.

Droop, M.R. (1973) Some thoughts on nutrition limitation in algae. *Journal of Phycology*, vol. 9, pp. 264–272.

Droop, M.R. (1974) The nutrient status of algal cells in continuous culture, *Journal of the Marine Biological Association of the United Kingdom*, vol. 54, pp. 825-855.

Duan, J. and Gregory, J. (2003) Coagulation by hydrolysing metal salts, *Advances in Colloid and Interface Science*, vol. 100, pp. 475–502.

Duan, X., Ren, G.Y., Liu, L.L. and Zhu, W.X. (2012) Salt-induced osmotic stress for lipid overproduction in batch culture of *Chlorella vulgaris*, *African Journal of Biotechnology*, vol. 11, no. 27, pp. 7072-7078.

Dubois, M., Gilles, K.A., Hamilton, J.K., Rebers, P.A. and Smith. F. (1956) Colorimetris method of determination of sugars and related substances, *Analytical Chemistry*, vol. 18, pp. 350-356.

Dyhrman, S.T. and Palenik, B.P. (1997) The identification and purification of a cell-surface alkaline phosphatase from the dinoflagellate *Prorocentrum minimum* (Dinophyceae), *Journal of Phycology*, vol. 33, pp. 602– 612.

Edvardsen, B., Eikrem, W., Green, J.C., Anderson, R.A., Moonvan Der Staay, S.Y. and Medlin, L.K. (2000) Phylogenetic reconstructions of the Haptophyta inferred from 18S ribosomal DNA sequences and available morphological data, *Phycologia*, vol. 39, pp. 19–35.

Edzwald, J.K. (1993) Coagulation in drinking water treatment: Particles, organics and coagulants. *Water Science and Techology*, vol. 27, no. 11, pp. 21.

Edzwald, J.K. (1995) Principals and applications of dissolved air flotation, *Water Science and Technology*, vol. 31, no. 4, pp. 1-23.

Eldridge, R.J. Hill, D.R.A. and Gladman, B.R. (2012) A comparative study of coagulation behaviour of marine microalgae, *Journal of Applied Phycology*, DOI 10.1007/s10811-012-9830-4.

Elmaleh, S., Coma, J., Grasmick, A. and Bourgade, L. (1991) Magnesium induced algal flocculation in a fluidized bed, *Water Science and Technol*ogy, vol. 23, pp. 1695–1702.

Elmaleh, S., Coma, J. and Borsato, J. (1992) Algal flocculation in a magnesium exchanger fluidized bed, *Water Science and Technology*, vol. 26, pp. 1689–1696.

Elmaleh, S., Yahi, H. and Coma, J. (1998) Are flocculants required in a flocculation process? *Environmental Engineering and Policy*, vol. 1, no. 2, pp. 97–102.

Elshahed, M.S. (2010) Microbiological aspects of biofuel production: Current status and future directions, *Journal of Advanced Research*, vol. 1, pp. 103–111.

El-Sheek, M.M. and Rady, A.A. (1994) Effect of phosphorus starvation on growth, photosynthesis and some metabolic processes in the unicellular green alga *Chlorella kessleri*, *Phyton. (Horn, Austria)*, vol. 35, pp. 139-151.

Eltgroth, M.L., Watwood, R.L. and Wolfe, G.V. (2005) Production and cellular localization of neutral long-chain lipids in the haptophyte algae *Isochrysis galbana* and *Emiliana huxleyi*, *Journal of Phycology*, vol. 41, pp. 1000-1009.

Enright, C.T., Newkirk, G.F., Craigie, J.S. and Castell, J.D. (1986) Evaluation of phytoplankton as diets for juvenile *Ostrea edulis* L. J., *Experimental Marine Biology and Ecology*, vol. 96, pp. 1–13.

Eriksen, N.T., Poulsen, B.R. and Iversen, J.J.L. (1998) Dual sparging laboratory scale photbioreactor for continuous production of microalgae, *Journal of Applied Phycology*, vol. 10, pp. 377-382.

Fabregas, J., Herrero, C., Cabezas, B. and Abalde, J. (1986) Biomass production and biochemical composition in mass cultures of the marine microalga *Isochrysis galbana* Parke at varying nutrient concentrations, *Aquaculture*, vol. 53, pp. 101-113.

Falkowski, P.G., Sukenik, A. and Herzig, R. (1989) Nitrogen limitation in *Isochrysis galbana* (Haptophyceae). II Relative abundance of chloroplast proteins, *Journal of Phycology*, vol. 25, pp. 471-478.

Fawley, M.W. and Fawley, K.P. (2004) A simple and rapid technique for the isolation of DNA from microalgae, *Journal of Phycology*, vol. 40, pp. 223-225.

Feng, D., Chen, Z., Xue, S. and Zhang, W. (2011) Increased lipid production of the marine oleaginous microalgae *Isochrysis zhangjiangensis* (Chrysophyta) by nitrogen supplement, *Bioresource Technology*, vol. 102, pp. 6710–6716.

Fidalgo, J.P., Cid, A., Torres, E., Sukenik, A. and Herrero, C. (1998) Effects of nitrogen source and growth phase on proximate biochemical composition, lipid classes and fatty acid profile of the marine microalga *Isochrysis galbana*, *Aquaculture*, vol. 116, pp. 105-116

Field, C.B., Behrenfeld, M.J., Randerson, J.T. and Falkowski, P. (1998) Primary production of the biosphere: integrating terrestrial and oceanic components, *Science*, vol. 281, pp. 237–240.

Flynn, K.J., Garrido, J.L., Zapata, M., Öpik, H. and Hipkin, C.R. (1992) Changes in fatty acids, amino acids and carbon/nitrogen biomass during nitrogen starvation of ammonium and nitrate-grown *Isochrysis galbana*, *Journal of Applied Phycology*, vol. 4, pp. 95-104.

Flynn, K.J., Zapata, M., Garrido, J.L., Öpik, H. and Hipkin, C.R. (1993) Changes in carbon and nitrogen physiology during ammonium and nitrate nutrition and nitrogen starvation in *Isochrysis galbana*, *European Journal of Phycology*, vol. 28, no. 1, pp. 47-52.

Folkman, Y. and Wachs, A.M. (1973) Removal of algae from stabilization pond effluents by lime treatment, *Water Research*, vol. 7, pp. 419-435.

Fran, G., S., Lewis, M. and McCrone, P. (2006) Efficacy of ethyl-eicosapentaenoic acid in bipolar depression, *British Journal of Psychiatry*, vol. 188, pp. 46-50.

Fujiki, T. and Taguchi, S. (2002) Variability in chlorophyll a specific absorption coefficient in marine phytoplankton as a function of cell size and irradiance, *Journal of Plankton Research*, vol. 24, no. 9, pp. 859-874.

Gardner, R., Peyton, B. And Cooksey, K. (2012) Bicarbonate trigger for inducing lipid accumulation in algal systems, *World Intellectual Property Organization*, WO 2012/040698 A2.

Geider, R., Macintyre, Graziano, M.L. and McKay, R.M. (1998) Responses of the photosynthetic apparatus of *Dunaliella tertiolecta* (Chlorophyceae) to nitrogen and phosphorous limitation, *European Journal of Phycology*, vol. 33, no. 4, pp. 315-332.

Giordano, M. (1997) Adaptation of *Dunaliella salina* (Volvocales, Chlorophyceae) to growth on NH4 + as the sole nitrogen source, *Phycologia*, vol. 36, pp. 345-350.

Goldman, J.C., Dennet, M.R. and Riley, C.B. (1982) Effect of nitrogen mediated changes in alkalinity on pH control and CO2 supply in intensive microalgal cultures, *Biotechnology and Bioengineering*, vol. 24, pp. 619-631.

Golueke, C.S. and Oswald, W.J. (1965) Harvesting and Processing Sewage Grown Planktonic Algae, *Journal of Water Pollution Control Federation*, vol. 37, pp. 471-498.

Golvano, M.P., Felipe, M.R. and Cintas, A.M. (1982) Influence of nitrogen sources on chloroplast development in wheat seedlings, *Physiologia Plantarum*, vol. 56, no. 3, pp. 353-360.

Gonzalez-Gil, S., Keafer, B.A., Jovine, R.V.M., Aguilera, A., Lu, S. and Anderson, D.M. (1998) Detection and quantification of alkaline phosphatase in single cells of phosphorus-starved marine phytoplankton, *Marine Ecology Progress Series*, vol. 164, pp. 21-35.

Gouveia L. and Oliveira, A.C. (2009) Microalgae as a raw material for biofuels production, *Journal of Industrial Microbiology and Biotechnology*, vol. 36, pp. 269-274.

Green, J.C. and Leadbeater, B.S.C. (1994) The Haptophyte Algae. Clarendon Press, Oxford.

Green, J.C. and Pienaar, R.N. (1977) The taxonomy of the order Isochrysidales (Prymnesiophyceae) with special reference to the genera *Isochrysis* Parke, *Dictateria* Parke and *Imantonia* Reynolds, *Journal of the Marine Biological Association of the United Kingdom*, vol. 57, pp. 7-17.

Greenwell, H.C., Laurens, L.M.L., Shields, R.J., Lovitt, R.W. and Flynn, K.J. (2010) Placing microalgae on the biofuels priority list: a review of the technological challenges, *Journal of Royal Society Interface*, vol. 7, pp. 703-726.

Greenspan, P., Mayer, E.P., and Fowler, S.D. (1985) Nile Red – A selective fluorescent stain for intracellular lipid droplets, *The Journal of Cell Biology*, vol. 100, pp. 965-973.

Griffiths, M.J. and Harrison, S.T.L. (2009) Lipid productivity as a key characteristic for choosing algal species for biodiesel production, *Journal of Applied Phycology*, vol. 21, no. 5, pp. 493-507.

Griffiths, J., Dicks, R.G., Richardson, C. and Harrison, S.T.L. (2011) Advantages and Challenges of Microalgae as a Source of Oil for Biodiesel. In Biodiesel - Feedstocks and Processing Technologies, Stoytcheva, M. and Montero, G. (Eds.), InTech, Croatia.

Griffiths, M.J., van Hille, R.P. and Harrison, S.T.L. (2012) Lipid productivity, settling potential and fatty acid profile of 11 microalgal species grown under nitrogen replete and limited conditions, *Journal of Applied Phycology*, vol. 24, pp. 989-1001.

Grima, M.E., Belarbi, E.H., Fernandez, F.G.A., Medina, A.R. and Chisti, Y. (2003) Recovery of microalgal biomass and metabolites: process options and economics, *Biotechnology Advances*, vol. 20, pp. 491–515.

Guillard, R.R. and Ryther, J.H. (1962) Studies of marine planktonic diatoms. I. *Cyclotella nana Hustedt*, and *Detonula confervacea* (Cleve) Gran, *Canadian Journal of Microbiology*, vol. 8, pp. 229–239.

Gunaseelan, V.N. (1997) Anaerobic digestion of biomass for methane production: A review, *Biomass and Bioenergy*, vol. 1, pp. 83-114.

Haag, A.L. (2007) Algae Bloom Again, *Nature*, vol. 447, pp. 520-521.

Harris, R.C. and Kirk, J.T.O. (1969) Control of chloroplast formation in *Euglena gracilis*, *Biochemical Journal*, vol. 113, pp. 195-205.

Harrison, P. J., Thompson, P. A. and Calderwood, G. S. (1990) Effects of nutrient and light limitation on the biochemical composition of phytoplankton, *Journal of Applied Phycology*, vol. 2, pp. 45–56.

Hankamer, B., Lehr, F., Rupprecht, J., Mussgnug, J. H., Posten, C. and Kruse, O. (2007) Photosynthetic biomass and hydrogen production by green algae: from bioengineering to bioreactor scale-up, *Physiologia Plantarum*, vol. 131, pp. 10–21.

Hanlon, A.R.M., Bellinger, B., Haynes, K., Xiao, G. and Hofmann, T.A. (2006) Dynamics of extracellular polymeric substance (EPS) production and loss in an estuarine, diatom-dominated, microalgal biofilm over a tidal emersion–immersion period, *Limnology and Oceanography*, vol. 51, pp. 79-93.

Hannon, M., Gimpel, J., Tran, M., Rasala, B. and Mayfield, S. (2010) Biofuels from algae: challenges and potential, *Biofuels*, vol. 1, no. 5, pp. 763-784.

Hansmann, E. (1973) Handbook of phycological methods, Culture methods and growth measurements, Cambridge University Press, London, pp. 359 – 368.

Harith, Z.T., Yusoff, F.M., Mohamed, M.S., Shariff, M., Din, M. and Ariff, B. (2009) Effect of different flocculants on the flocculation performance of microalgae, *Chaetoceros calcitrans*, cells, *African Journal of Biotechnology*, vol. 8, no. 21, pp. 5971-5978.

Harun, R., Singh, M., Forde, G.M. and Danquah, M.K. (2010) Bioprocess engineering of microalgae to produce a variety of consumer products. *Renewable and Sustainable Energy Reviews*, vol. 14, pp. 1037–1047.

Harwood, J.L. and Guschina, I.A. (2009) The versatility of algae and their lipid metabolism, *Biochimie*, vol. 91**,** pp. 679-684.

Havaux, M. (1998) Carotenoids as membrane stabilizers in chloroplasts, *Trends in plant science*, vol. 3, pp. 147-151.

Heath, M.R., Richardson, K. and Kiorboe, T. (1990) Optical assessment of phytoplankton nutrient depletion. *Journal of Plankton Research*, vol. 12, pp. 381-396.

Helm, M.M. and Laing, I. (1987) Preliminary observations on the nutritional value of 'Tahiti *Isochrysis*' to bivalve larvae, *Aquaculture*, vol. 62, pp. 281-288.

Henderson, R.K., Parsons, S.A. and Jefferson, B. (2008) Successful removal of algae through the control of zeta potential, *Separation Science and Technology*, vol. 43, no. 7, pp. 1653-1666.

Herzig, R. and Falkowski, P.G. (1989) Nitrogen limitation in *Isochrysis galbana*. I. Photosynthetic energy conversions and growth efficiencies, *Journal of Phycology*, vol. 25, pp. 462-471.

Hori, T. and Green. J.C. (1985) The ultrastructure of mitosis in *Isochrysis galbana* Parke (Prymnesiophyceae), *Protoplasm*, vol. 125, pp. 140-151.

Hibberd, D.J. (1980). Prymnesiophytes (¼ Haptophytes). In Cox ER (ed) Phytoflagellates. Elsevier Science, Amsterdam, pp 273—31

Hori, T. and Green, J.C. (1985) The ultrastructure of mitosis in *Isochrysis galbana* Parke (Prymnesiophyceae), *Protoplasma*, vol. 125, pp. 140–151.

Hori, T. and Green. J.C. (1991) The ultrastructure of the flagellar root system of *Isochrysis galbana* (Prymnesiophyta), *Journal of the Marine Biological Association of the United Kingdom*, vol. 71, pp. 137-152.

Hu, Q., Zhang, C.W. and Sommerfeld, M. (2006) Biodiesel from algae: lessons learned over the past 60 years and future perspectives, *Journal of Phycology*, vol. 42, pp. 37.

Hu, Q. Sommerfeld, M., Jarvis, E., Ghirardi, M., Posewitz, M., Seibert, M. and Darzins, A. (2008) Microalgal triacylglycerols as feedstocks for biofuel production: perspectives and advances, *The Plant Journal*, vol. 54, pp. 621-639.

Huerlimann, R., de Nys, R. and Heimann, K. (2010) Growth, lipid content, productivity and fatty acid composition of tropical microalgae for scale-up production, *Biotechnology and Bioengineering*, vol. 107, no. 2, pp. 245-257.

Hung, M.T. and Liu, J.C. (2006) Microfiltration for separation of green algae from water, *Colloids and Surfaces B: Biointerfaces*, vol. 51, pp. 157–164.

Hunter, R.J. (1988) Zeta potential in colloid science: Principles and applications, Academic Press, London.

Hunter, R.J. (2001) Foundations of colloid science. Oxford University Press, New York.

Huntley, M. E. and Redalje, D.G. (2007) CO2 Mitigation and renewable oil from photosynthetic microbes: A new appraisal, *Mitigation and Adaptation Strategies for Global Change*, vol. 12, pp. 573-608.

Inouye, I. and Kawachi, M. (1994) The haptonema. In The haptophyte algae, Green, J.C. and Leadbeater, B.S.C. (Eds.), Clarendon Press, Oxford, UK.

Ives, K.J. (1959) The significance of surface electric charge on algae in water purification, *Journal of Biochemical and Microbiological Technology and Engineering*, vol. 1, no. 1, pp. 37-47.

Jalal, K.C.A., Shamsuddin, A.A., Rahman, M.F., Nurzatul, N.Z. and Rozihan, M. (2013) Growth and total carotenoid, chlorophyll a and chlorophyll b of tropical microalgae (*Isochrysis* sp.) in laboratory cultured conditions, *Journal of Biological Sciences*, vol. 13, pp. 10-17.

Ji, Y. and Sherrell, R.M. (2008) Differential effects of phosphorus limitation on cellular metals in *Chlorella* and *Microcystis*, *Limnology and Oceanography*, vol. 53, pp. 1790–1804.

Jones, H.L.J., Leadbeater, B.S.C. and Green, J.C. (1993) Mixotrophy in marine species of Chrysochromulina (Prymnesiophyceae): ingestion and digestion of a small green flagellate, *Journal of the Marine Biological Association of the United Kingdom*, vol. 73, pp. 283-296.

Jordan, R.W. and Chamberlain, A.H.L. (1997) Biodiversity among haptophyte algae, *Biodiversity and Conservation,* vol. 6, pp. 131-152.

Jordon, R.W. and Green, J.C. (1994) A check-list of the extant Haptophyta of the world, *Journal of the Marine Biological Association of the United Kingdom,* vol. 74, pp. 147-174.

Ju, Z., Ding, L., Zheng, F., Zhang, Q. and Li, Y. (2011) Effects of silicon, calcium or boron on cell growth and lipid accumulation in *Pinnularia gibba* var. Linearis, *IPCBEE*, vol. 22, pp. 100-104.

Juario, J.V. and Storch, V. (1984) Biological evaluation of phytoplankton (*Chlorell* sp., *Tetraselmis* sp. and *Isochrysis galbana*) as food for milkfish (*Chanos chaos*) fry. *Aquaculture*, vol. 40, pp. 193-198.

Kai, A.K.L., Cheung, Y.K and Wong, J.T.Y. (2006) Development of single-cell PCR methods for the Rapidophyceae, *Harmful Algae,* vol. 5, pp. 649-657.

Kain, J.M. and Fogg, G.E. (1958) Studies on the growth of marine phytoplankton *Isochrysis galbana* Parke, *Journal of the Marine Biological Association of the United Kingdom*, vol. 37, pp. 781-788.

Kawachi,M., Inouye, I., Maeda, O., and Chihara, M. (1991) The haptonema as a food-capturing device: observations on *Chrysochromulina hirta* (Prymnesiophyceae), *Phycologia,* vol. 30, pp. 563–573.

Kawasaki, L.Y., Tarifeno-Silva, E., Yu, D.P., Gordon, M.S. and Chapman, D.J. (1981) Aquacultural approaches to recycling of dissolved nutrients in secondarily treated domestic wastewaters – 1. Nutrient uptake and release by artificial food chains, *Water Research,* vol. 16, pp. 37-49.

Kazakis, N.A., Papadopoulos, I.D. and Mouza, A.A. (2007) Bubble columns with fine-pore sparger operating in the pseudo-homogeneous regime: Gas hold up prediction and a criterion for the transition to the heterogeneous regime, *Chemical Engineering Science,* vol. 62, no. 12, pp. 3092-3103.

Kennedy, E.P. (1961) Biosynthesis of Complex Lipids, *Federation Proceedings of the American Society of Experimental Biology*, vol. 20, no. 4, pp. 934-940.

Kester, D.R., Duedall, I.W., Connors, D.N. and Pykowics, R.M. (1967) Preparation of artificial seawater. *Limnology and Oceanography*, vol. 12, no. 1, pp. 176-179.

Khan, S.A., Hussain, M.Z., Prasad, S. and Banerjee, U.C. (2009) Prospects of biodiesel production from microalgae in India, *Renewable and Sustainable Energy Reviews*, vol. 13, pp. 2361-2372.

Kiorboe, T. and Hansen, J.L.S. (1993) Phytoplankton aggregate formation: observations of patterns and mechanisms of cell sticking and the significance of exopolymeric material, *Journal of Plankton Research*, vol. 15, no. 9, pp. 993-1018.

Klass, D.L. (2004) Biomass for renewable energy and fuels. In: Cleveland, C.J., Ayres, R.U. (Eds.), Encyclopedia of Energy. Elsevier Academic Press, Amsterdam, pp. 193–212.

Knuckey, R., Brown, M., Robert, R., and Frampton, D.M. (2006) Production of microalgae concentration by flocculation and their assessment as aquaculture feeds, *Aquaculture engineering*, vol. 35, pp. 300-313.

Koller, M., Salerno, A., Tuffner, P., Koinigg, M., Bochzelt, H., Schober, S., Pieber, S., Schnitzer, H., Mittelbach, M. and Braunegg, G. (2012) Characteristics and potential of micro algal cultivation strategies: a review, *Journal of Cleaner Production*, vol. 37, pp. 377-388.

Koo, A.J.K., Ohlrogge, J.B., and Pollard, M. (2004) On the export of fatty acids from the chloroplast. *Journal of Biological Chemistry*, vol. 279, no. 16, pp. 16101-16110.

Kruse, O., Rupprecht, J., Mussgnug, J.H., Dismukes, G.C. and Hankamer. (2005) Photosynthesis: a blueprint for solar energy capture and biohydrogen production technologies. *Photochemistry and Photobiological Sciences*, vol. 4, pp. 957–969.

Kurat, C.F., Natter, K., Petshnigg, J., Wolinski, H., Scheuringer, K., Scholz, H., Zimmermann, R., Leber, R., Zechner, R. and Kohlwein, S.D. (2006) Obese yeast: triglyceride lipolysis is functionally conserved from mammals to yeast, *Journal of Biolical Chemistry*, vol. 281, pp. 491-500.

Lacour, T., Sciandra, A., Talec, A., Mayzaud, A. and Bernard, O. (2012a) Neutral lipid and carbohydrate productivities as a response to nitrogen status in *Isochrysis* sp. (T-ISO; Haptophyceae): Starvation versus Limitation, *Journal of Phycology*, vol. 48, pp. 647-656.

Lacour, T., Sciandra, A., Talec, A., Mayzaud, A. and Bernard, O. (2012b) Diel variations of carbohydrates and neutral lipids in nitrogen-sufficient and nitrogen-starved cyclostat cultures of *Isochrysis* sp., *Journal of Phycology*, vol. 48, pp. 966-975.

Landry, D.M., Gaasterland, T. and Palenik, B.P. (2006) Molecular characterization of a phosphate-regulated cell-surface protein from the coccolithophorid, *Emiliania huxleyi* (Prymnesiophyceae), *Journal of Phycology*, vol. 42, pp. 814–821.

Larson, T.E. and Buswell, A.M. (1940) Theoretical limits of the lime-soda method of water softening, *Industrial and Engineering Chemistry*, vol. 32, pp. 132- 134.

Lavin, P.L. and Lourenco, S.O. (2005) An evaluation of the accumulation of intracellular inorganic nitrogen pools by marine microalgae in batch cultures. *Brazilian Journal of Oceanography*, vol. 53, pp. 55-68.

Lee, S.J., Kim, S., Kim, J., Kwon, G., Yoon, B. and Oh, H. (1998) Effects of Harvesting Method and Growth Stage on the Flocculation of the Green Alga *Botryococcus braunii*, *Letters in Applied Microbiology*, vol. 27, no. 1, pp. 14-18.

Lee, Y.K. (2001) Microalgal mass culture systems and methods: Their limitation and potential. *Journal of Applied Phycology*, vol. 13, pp. 307–315.

Lee, A.K., Lewis, D.M. and Ashman, P.J. (2009) Microbial flocculation, a potentially low-cost harvesting technique for marine microalgae for the production of biodiesel, *Journal of Applied Phycology*, vol. 21, pp. 559–567.

Leentvar, J. and Rebhun, M. (1982) Effect of magnesium and calcium precipitation on coagulation – flocculation with lime, *Water Research,* vol. 16, pp. 655-662.

Leon-Banares, R., Gonzalez-Ballester, D., Galvan, A. and Fernandez, E. (2004) Transgenic microalgae as green cell-factories, *TRENDS in biotechnology*, vol. 22, pp. 45-52.

Levasseur, M.E., Harrison, P.J., Heimdal, B.R. and Therriault, J.C. (1990) Simultaneous nitrogen and silicate deficiency of a phytoplankton community in a coastal jet-front, *Mar. Biol.(Berl.)*, vol. 104, pp. 329-338.

Levasseur, M.E., Thompson, P.A. and Harrison, P.J. (1993) Physiological acclimation of marine phytoplankton to different nitrogen sources, *Journal of Phycology*, vol. 29, pp. 587-595.

Li, R., Wilhelm, S.W., Carmichael, W.W. and Watanabe, M.M. (2008a) Polyphasic characterization of water bloom forming *Raphidiopsis* species (cyanobacteria) from central China, *Harmful algae*, vol. 7, pp. 146-153.

Li, Y., Horsman, M., Wang, B., Wu, N. and Lan, C.Q. (2008b) Effects of nitrogen sources on cell growth and lipid accumulation of green alga *Neochloris oleoabundans*, *Applied Microbiology and Biotechnology,* vol. 81, pp. 629-636.

Li, Y., Han, D., Sommerfeld, M. and Hu, Q. (2011) Photosynthetic carbon partitioning and lipid production in the oleaginous microalga *Pseudochlorococcum* sp. (Chlorophyceae) under nitrogen-limited conditions, *Bioresource Technology*, vol. 102, pp. 123–129.

Li, Y., Fei, X. and Deng, X. (2012) Novel molecular insights into nitrogen starvation-induced triacylglycerols accumulation revealed by differential gene expression analysis in green algae *Micractinium pusillum*, *Biomass and Bioenergy*, vol. 42, pp. 199-211.

Liang, Y., Beardall, J. and Heraud, P. (2006) Effects of nitrogen source and UV radiation on the growth, chlorophyll fluorescence and fatty acid composition of *Phaeodactylum tricornutum* and *Chaetoceros muelleri* (Bacillariophyceae), *Journal of Photochemistry and Photobiology B: Biology*, vol. 82, pp. 161–172.

Liang, K., Zhang,Q., Gu, M. And Cong, W. (2012) Effect of phosphorous on lipid accumulation in freshwater microalga *Chlorella* sp., *Journal of Applied Phycology*, DOI 10.1007/s10811-012-9865-6.

Lin, S. and Carpenter, E.J. (1997a) Pyrenoid localization of rubisco in relation to the cell cycle and growth phase of *Dunaliella tertiolecta* (Chlorophyceae), *Phycologia*, vol. 36, no. 1, pp. 24-31.

Lin, S. and Carpenter, E.J. (1997b) Rubisco of *Dunaliella tertiolecta* is redistributed between the pyrenoid and the stroma as a light/shade response, *Marine Biology*, vol. 127, pp. 521-529.

Lindner, R.C. and Harley, C.P. (1942) A rapid method for the determination of nitrogen in plant tissue, *Science n.s.*, vol. 96, pp. 565-566.

Liu, C.P. and Lin, L.P. (2001) Ultrastructural study and lipid formation of *Isochrysis* sp. CCMP 1324, *Botanical Bulletin of Academia Sinica*, vol. 42, pp. 207-214.

Liu, Z.Y., Wang, G.C. and Zhou, B.C. (2007) Effect of iron on growth and lipid accumulation in *Chlorella vulgaris*, *Bioresource Technology*, doi:10.1016/j.biortech.2007.09.073

Liu, J., Yuan, C., Hu, G. and Li, F. (2012) Effects of light intensity on the growth and lipid accumulation of microalga *Scenedesmus* sp. 11-1 under nitrogen limitation, *Applied Biochemistry and Biotechnology*, vol. 166, no. 8, pp. 2127-2137.

Livne, A. and Sukenik, A. (1990) Acetyl coenzyme A carboxylase from the marine Prymnesiophyte *Isochrysis galbana*, *Plant Cell Physiology*, vol. 31, pp. 851-858.

Livne, A. and Sukenik, A. (1992) Lipid Synthesis and Abundance of Acetyl CoA Carboxylase in *Isochrysis galbana* (Prymnesiophyceae) Following Nitrogen Starvation, *Plant and Cell Physiology*, vol. 33, no. 8, pp. 1175-1181.

Loubiere, K., Olivo, E., Bougaran, G., Pruvost, J., Robert, R. and Legrand, J. (2008) A new photobioreactor for continuous microalgal production in hatcheries based on external loop airlift and swirling flow, *Biotechnology and Bioengineering*, vol. 102, pp. 132-147.

Lourenco, S.O., Marquez, U.M.L., Mancini-Filho, J., Barbarino, E. and Aidar, E. (1997) Changes in biochemical profile of *Tetraselmis gracilis* I. Comparison of two culture media, *Aquaculture*, vol. 148, pp. 153-168.

Lourenco, S.O., Barbarino, E., Mancini-Filho J., Schinke, K.P. and Aidar, E. (2002) Effects of different nitrogen sources on the growth and biochemical profile of 10 marine microalgae in batch culture: an evaluation for aquaculture, *Phycologia*, vol. 41, no. 2, pp. 158-168.

Luo, H.P. and Al-Dahhan, M.H. (2003) Analyzing and modeling of photobioreactors by combining first principles of physiology and hydrodynamics. *Biotechnology and Bioengineering*, vol. 85, pp. 382-393.

Lynn, S.G., Kilham, S.S., Kreeger, D.A. and Interlandi, S.J. (2000) Effect of nutrient availability on the biochemical and elemental stoichiometry in the freshwater diatom *Stephanodiscus minutulus* (Bacillariophyceae), *Journal of Phycology*, vol. 36, pp. 510–522.

Mason, P.L., Vogelbein, W.K., Haas, J.W. and Shields, J.D. (2003) An improved stripping technique for lightly armored dinoflaggelates. *Journal of Phycology*, vol. 39, pp. 253-258.

Mata, T.M., Martins, A.A. and Caetano, N.S. (2010) Microalgae for biodiesel production and other applications: A review, *Renewable and Sustainable Energy Reviews*, vol. 14, pp. 217–232.

Matsumoto, M., Sugiyama, H., Maeda, Y., Sato, R., Tanaka, T. and Matsunaga, T. (2010) Marine diatom, *Navicula* sp. strain JPCC DA0580 and marine green alga, *Chlorella* sp.Strain NKG400014 as a potential source for biodiesel production, *Applied Biochemistry and Biotechnology*, vol. 161, pp. 483-490.

Matsunaga, T., Matsumoto, M., Maeda, Y., Sugiyama, H., Sato, R. and Tanaka, T. (2009) Characterization of marine microalga, *Scenedesmus* sp. strain JPCC GA0024 toward biofuel production, *Biotechnology Letters*, vol. 31, pp. 1367–1372.

McKay, R.M.L., Gibbs, S.P. and Vaughn, K.C. (1991) Rubisco activase is present in the pyrenoid of green algae, *Protoplasta*, vol. 162, pp. 38-45.

McKendry, P. (2002) Energy production from biomass (part 1): overview of biomass. *Bioresource Technology*, vol. 83, pp. 37–46.

Mehta, S.K. and Gaur, J.P. (2005) Use of alge for removing heavy metal ions from wastewater: Progress and prospects, *Critical Reviews in Biotechnology*, vol. 25, pp. 113-152.

Meier, R.L. (1955) Biological cycles in the transformation of solar energy into useful fuels. In Solar Energy Research (Daniels, F. and Duffie, J.A., eds). Madison, WI: University of Wisconsin Press, pp. 179–183.

Meireles, L.A., Guedes, A.C., Barbosa, C.R., Azevedo, J.L., Cunha, J.P. and Malcata, F.X. (2008) On-line control of light intensity in microalgal bioreactor using a novel automatic system, *Enzyme and Microbial Technology*, vol. 42, pp. 554-559.

Merzlyak, M.N., Chivkunova, O.B., Gorelova, O.A., Reshetnikova, I.V. and Solovchenko, E. (2007) Effect of nitrogen starvation on optical properties, pigments and arachidonic acid content of the unicellular alga *Parietochloris incisa* (Trebouxiophyceae, Chlorophyta), *Journal of Phycology*, vol. 43, pp. 833-843.

Metting Jr. F.B. Biodiversity and Application of Microalgae. (1996) *Journal of Industrial Microbiology*, vol. 17, pp. 477-489.

Meyerhof, O., Shatas, R. and Kaplan, A. (1953) Heat of hydrolysis of trimetaphosphate, *Biochem. biophys. Acta*, vol. 12, pp. 121-127.

Michinaka, Y., Shimauchi, T., Aki, T., Nakajima, T., Kawamoto, S., Shigeta, S., Suzuki, O. and Ono. K. (2003) Extracellular secretion of free fatty acids by disruption of a fatty acyl-CoA synthetase gene in *Saccharomyces cerevisiae*. *J. Biosci. Bioeng*. vol. 95, pp. 435–440.

Millamena, O.M., Aajero, E.J. and Borlonganm I.G. (1990) Techniques on algae harvesting and preservation for use in culture and as larval food, *Aquacultural engineering*, vol. 9, pp. 295-304.

Mishra, A. and Jha, B. (2009) Isolation and characterization of extracellular polymeric substances from micro-algae *Dunaliella salina* under salt stress, *Bioresource Technology*, vol. 100, pp. 3382-3386.

Miyachi, S. Kanai, R. Mihara, S. Miyachi, S. and Aoki, S. (1964) Metabolic roles of inorganic polyphosphates in *Chlorella* cells, *Biochim. Biophys. Acta*, vol. 93, no. 3, pp. 625–634.

Mock, T. and Kroon, B.M.A. (2002) Photosynthetic energy conversion under extreme conditions-I: important role of lipids as structural modulators and energy sink under N-limited growth in Antarctic sea ice diatoms, *Phytochemistry*, vol. 61, pp. 41-51.

Moheimani, N. and Borowitzka, M.A. (2006) The long-term culture of the coccolithophore *Pleurochrysis carterae* (Haptophyta) in outdoor raceway ponds, *Journal of Applied Phycology*, vol. 18, pp. 703–712.

Molina, E.M., Fernandez, F.G., Camacho, F.G., Rubio, F.C. and Chisti, Y. (2000) Scale-up of tubular photobioreactors, *Journal of Applied Phycology*, vol. 12, pp. 355-368.

Molina, E., Fernandez, J., Acien, F.G. and Chisti, Y. (2001) Tubular photobioreactor design for algal cultures, *Journal of Biotechnology*, vol. 92, pp. 113-131.

Moraine, R., Shelef, G., Sandbank, E., Bar-Morshe, Z. and Shvartzbard, L. (1980) Algae Biomass. Elsevier, Amsterdam.

Msanne, J., Xu, D., Konda, A.R., Casas-Mollano, J.A., Awada, T., Cahoon, E.B. and Cerutti, H. (2012) Metabolic and gene expression changes triggered by nitrogen deprivation in the photoautotrophically grown microalgae *Chlamydomonas reinhardtii* and *Coccomyxa* sp. C-169, *Phytochemistry*, vol. 75, pp. 50–59.

Mulholland, M.R. and Lomas, M.W. (2008) Nitrogen Uptake and Assimilation. In Nitrogen in the Marine Environment (Capone, D.G., Bronk, D.A., Mulholland, M.R. and Carpenter, E.J., eds.). Academic Press. San Diego, pp 303-384.

Murphy, D.J. (2005) Plant Lipids: Biology, Utilisation and Manipulation. Blackwell Publishing Ltd, Oxford, UK.

Murray M. G, and Thompson W.F. (1980) Rapid isolation of high molecular weight plant DNA, *Nucl Acids Res*, vol. 8, pp. 4321-4325.

Mussgnug, J.H., Klassen, V., Shluter, A. and Kruse, O. (2010) Microalgae as substrates for fermentative biogas production in a combined biorefinery concept, *Journal of Biotechnology*, vol. 150, no. 1, pp. 51-56.

Msanne, J., Xu, D., Konda, A.R., Casas-Mollano, J.A, Awada, T, Cahoon, E.B. and Cerutti, H. (2012) Metabolic and gene expression changes triggered by nitrogen deprivation in the photoautotrophically grown microalgae *Clamydomonas reinhardtii* and *Coccomyxa* sp. C-169, *Phytochemistry*, vol. 75, pp. 50-59.

Myklestad, S. and Haug, A. (1972) Production of carbohydrates by the marine diatom *Chaetoceros affinis* var. *Willei* (Gran) Hustedt. I. Effect of the concentration of nutrients in the culture medium, *J. exp. Biol. Ecol.*, vol. 9, pp. 125-136.

Nagasato, C., Yoshikawa, S., Yamashita, M., Kawai, H. and Motomura, T. (2003) Pyrenoid formation associated with cell cycle in the brown alga, *Scytosiphon lomentaria* (Scytosiphonales, Phaeophyceae), *Journal of Phycology*, vol. 39, pp. 1172-1180.

Nojima, Y., Kibayashi, A., Matsuzaki, H., Hatano, T. and Fukui, S. (1999) Isolation and characterization of triacylglycerol-secreting mutant strain from yeast, *Saccharomyces cerevisiae*, *J. Gen. Appl. Microbiol.* vol. 45, pp. 1–6.

Nozaki, H., Ito, M., Watannabe, M.M., Takano, H. and Kuroiwa, T. (1997) Phylogenetic analysis of morphological species of *Carteha* (Volvocales, Chlorophyta) based on rbcL gene sequences. *Journal of Phycology*, vol. 33, pp. 864-867.

Nurdogan, Y. and Oswald, W.J. (1995) Enhanced nutrient removal in high rate ponds, *Water Sci. Technol.*, vol. 31, pp. 33-43.

Oh, H.M., Lee, S., Park, M.H., Kim, H.S., Kim, H.C., Yoon, J.H., Kwon, G.S. and Yoon, B.D. (2001) Harvesting of *Chlorella vulgaris* using a bioflocculant from *Paenibacillus* sp., AM49. *Biotechnol. Lett.*, vol. 23, pp. 1229-1234.

Ohlrogge, J. and Browse, J. (1995) Lipid biosynthesis. *The Plant Cell*, vol. 7, pp. 957-970.

Omland, T. H. (2009) Particle settling in non-newtonian drilling fluids. PhD Thesis (unpublished).

Oswald, W.J. and Golueke, C. (1960) Biological transformation of solar energy, *Advanced Applied Microbiology*, vol. 2, pp. 223-262.

Paasche, E. (1971), Effect of ammonia and nitrate on growth, photosynthesis, and ribulosediphosphate carboxylase content of *Dunaliella tertiolecta. Physiol. Plant.*, vol. 25, pp. 294-299.

Park, J.B.K., Craggs, R.J. and Shilton, A.N. (2011) Recycling algae to improve species control and harvest efficiency from a high rate algal pond, *Water Research*, vol. 45, pp. 6637–6649.

Park, T.K., Bolch, C.J.S. and Hallegraeff, G.M. (2007) Morphological and molecular genetic characterization of *Cryptoperidiniopsis brodyi* (Dinophyceae) from Australia-wide isolates, *Harmful Algae*, vol. 6, pp. 718-733.

Patil, V. (2007) The relevance of biofuels, *Current Science*, vol. 92, pp. 707.

Walker, T.L., Purton, S., Becker, D.K. and Collet.C. (2005) Microalgae as bioreactors, *Plant Cell Rep*, vol. 24, pp. 629-641.

Phatarpekar, P.V., Sreepada, R.A., Pednekar. C. and Achuthankutty, C.T. (2000) A comparative study of growth performance and biochemical composition of mixed cultures of *Isochrysis galbana* and *Chaetoceraos calcitrans* with monocultures, *Aquaculture*, vol. 181, pp. 141-155.

Piccolo, A. (2009) Algae oil production and its potential in the Mediterranean region. 1st EMUNI Research Souk 2009 (EMUNI ReS 2009). The Euro-Mediterranean Student Research Multi-conference. Unity and Diversity of Euro-Mediterranean Identities.

Plant Biochemistry. (2013) Nitrogen metabolism – Essential and non-protein amino acid biosynthesis. [online]. (updated 5 February 2013).
Available at: http://www.uky.edu/~dhild/biochem/24

Posten, C. and Schaub, G. (2009) Microalgae and terrestrial biomass as source for fuels: a process view, *Journal of Biotechnology*, vol. 142, pp. 64–69.

Powell, N., Shilton, A., Chisti, Y. and Pratt, S. (2009) Towards a luxury uptake process via microalgae – Defining the polyphosphate dynamics, *Water Research*, vol. 43, pp. 4207-4213.

Pulz, O. and Gross, W. (2004) Valuable products for biotechnology of microalgae, *Applied Microbiology and Biotechnology*, vol. 65, no. 6, pp. 635-648.

Radakovits, R., Jinkerson, R.E., Darzins, A. and Posewitz, M.C. (2010) Genetic Engineering of Algae for Enhanced Biofuel Production, *Eukaryotic Cell*, vol. 9, no. 4, pp. 486-501.

Ratledge, C. and Cohen, Z. (2008) Microbial and algal oils: do they have a future for biodiesel or as commodity oils? *Lipid Technology*, vol. 20, no. 7, pp. 155-160.

Ravi, D. and Sivasankara, P. (2002) Flocculation of algae using chitosan, *Journal of Applied Phycology*, vol. 14, pp. 419-422.

Raven, J.A. (2011) Effects on marine algae of changed seawater chemistry with increasing atmospheric CO_2. *Biology and Environment: Proceeding of the Royal Irish Academy*, vol. 111B, pp. 1-17.

Redfield, A.C. (1934) On the proportions of organic derivatives in sea water and their relation to the composition of plankton. In Daniel, R.J. (ed.). James Johnstone Memorial Volume, University Press of Liverpool, pp. 177-192.

Reitan, K.I., Rainuzzo, J.R. and Olsen, Y. (1994) Effect of nutrient limitation on fatty acid and lipid content of marine microalgae, *Journal of Phycolology*, vol. 30, no. 6, pp. 972-979.

Renaud, S.M., Parry, D.L, Luong-Van, Thinh, Kuo, C., Padovan, A. and Sammy, N. (1991) Effect of light intensity on the proximate biochemical and fatty acid composition of *Isochrysis* sp. and *Nannochloropsis oculata* for use in tropical aquaculture. *Journal of Applied Phycology*, vol. 3, pp. 43-53.

Reynolds, E.C. (1963) The use of lead citrate at high pH as an electron opaque stain in electron microscopy, *Journal of Cell Biology*, vol. 17, pp. 208–212.

Richmond, A. (2004) Microalgal Culture. In Dowstream processing of cell mass and products, Molina, E., Fernandez, F.G.A. and Medina, A.R. (Eds.), Blackwell Science Ltd., Oxford, UK.

Roche, J.L., Geider, R.J., Graziano, L.M., Murray, H. and Lewis, K. (1993) Induction of specific proteins in eukaryotic algae grown under iron, phosphorus and nitrogen deficient conditions, *Journal of Phycology*, vol. 29, pp. 767-777.

Rodolfi, L., Zittela, G.C., Bassi, N., Padovani, G., Biondi, N., Bonini, G. and Tredici, M.R. (2009) Microalgae for oil: Strain selection, induction of lipid synthesis and outdoor mass cultivation in a low-cost photobioreactor, *Biotechnology and Bioengineering*, vol. 102, pp. 100-112.

Roessler , P.G. (1990) Environmental control of glycerolipid metabolism in microalgae: Commercial implications and future research directions. *Journal of Phycology*, vol. 26, pp. 393–399.

Roessler, P.G. and Ohlrogge, J.B. (1993) Cloning and characterization of the gene that encodes acetyl-coenzyme A carboxylase in the alga *Cyclotella cryptica, J. Biol. Chem.*, vol. 268, pp. 19254-19259.

Roessler, P.G., Bleibaum, J.L., Thompson, G.A. and Ohlrogge, J.B. (1994) Characteristics of the gene that encodes acetyl-CoA carboxylase in the diatom *Cyclotella cryptica, Ann. N. Y. Acad. Sci,* vol. 721, pp. 250-256.

Sanchez, A., Maceiras, R., Cancela, A. And Perez, A. (2012) Culture aspects of *Isochrysis galbana* for biodiesel production, *Applied Energy,* http://dx.doi.org/ 10.1016/j.apenergy.2012.03.027. (Article in press).

Sanyano, N., Chetpattananodh, P. and Chongkhong, S. (2011) Optimization of Flocculation of Marine *Chlorella* sp. by Response Surface Methodology. *TIChE International Conference.*

Sayegh, F.A.Q. and Montagnes, D.J.S. (2011) Temperature shifts induce intraspecific variation in microalgal production and biochemical composition, *Bioresource Technology*, vol. 102, pp. 3007-3013.

Scheiner, D. (1976) Determination of ammonia and kjeldahl nitrogen by indophenol method. *Water Research*, vol. 10, pp. 31-36.

Scott, S.A., Davey, M.P., Dennis, J.S., Horst, I., Howe, C.J., Lea-Smith, D.J. and Smith, A.G. (2010) Biodiesel from algae: challenges and prospects. *Current Opinion in Biotechnology*, vol. 21, pp. 277–286

Schenk, P.M., Thomas-Hall, S.R., Stephens, E., Marx, U.C., Mussgnug, J.H., Posten, C., Kruse, O. and Hankamer, B. (2008) Second generation biofuels: high-efficiency microalgae for biodiesel production, *Bioenergy Research*, vol. 1, pp. 20-43.

Schlesinger, A., Eisenstadt, D., Bar-Gil, A., Carmely, H., Einbinder, S. and Gressel, J. (2012) Inexpensive non-toxic flocculation of microalgae contradicts theories; overcoming a major hurdle to bulk algal production, *Biotechnology Advances,* doi:10.1016/j.biotechadv.2012.01.011.

Schluter, L., Henrikson, P., Nielson, T.G. and Jakobsen, H.H. (2011) Phytoplankton composition and biomass across the southern Indian Ocean, *Deep-Sea Research I*, vol. 58, pp. 546-556.

Sciandra, A., Gostan, J., Collos, Y., Descolas-Gros, C., Leboulanger, C., Martin-Jezequel, V., Denis, M., Lefevre, D., Copin-Montegut, C. and Avril, B. (1997) Growth-compensating phenomena in continuous cultures of *Dunaliella tertiolecta* limited simultaneously by light and nitrate, *Limnology and Oceanography*, vol. 42, no. 6, pp. 1325-1339.

Seoane, S., Eikrem, W., Pienaar, R. and Edvarsen, B. (2009) *Chrysochromulina palpebralis* sp. nov. (Prymnesiophyceae): a haptophyte, possessing two alternative morphologies, *Phycologia*. vol. 48, pp. 165-176.

Seshadri, C.V., Umesh, B.V. and Manoharan, R. (1991) Beta-carotene studies in Spirulina. *Bioresource Technology*, vol. 38, pp. 111-113.

Sharma, K.K., Schuhmann, H. and Schenk, P.M. (2012a) High lipid content in microalgae for biodiesel production. *Energies*, vol. 5, pp. 1532-1553.

Sharma, P., Jha, A.B., Dubey, R.S. and Pessarakli, M. (2012b) Reactive oxygen species, oxidative damage, and antioxidative defence mechanisms in plants under stressful conditions, *Journal of Botany*, doi:10.1155/2012/217037

Sheehan, J., Dunahay, T., Benemann, J. and Roessler, P. (1998) A Look Back at the U.S. Department of Energy's Aquatic Species Program: Biodiesel from Algae. Close-Out report. National Renewable Energy Lab, Department of Energy, Golden, Colorado, U.S.A. Report number NREL/TP-580-24190, dated July 1998.

Shelef, G. and Soeder, C.J. (1980) Algal biomass. Elsevier/North Holland, Biomedical. Press, Amsterdam.

Shelef, G., Sukenik, A. and Green, M. (1984) Microalgae harvesting and processng: A literature review. *Solar Energy Research Institute*, www.nrel.gov/docs/legosti/old/2396.

Shifrin, N.S. and Chisholm, S.W. (1981) Phytoplankton lipids: interspecific differences and effects of nitrate, silicate and light–dark cycles, *Journal of Phycology*, vol. 17, pp. 374–384.

Show, K.Y., Lee, D.J. and Chang, J.S. (2012) Algal biomass dehydration. *Bioresource Technology*, http://dx.doi.org/10.1016/j.biortech.2012.08.021.

Sigee, D.C., Bahrami, F., Estrada, B., Webster, R.E. and Dean, A.P. (2007) The influence of phosphorus availability on carbon allocation and P quota in *Scenedesmus subspicatus*: a synchrotron-based FTIR study, *Phycologia*, vol. 46, pp. 583–592.

Singh, J. and Gu, S. (2010) Commercialization potential of microalgae for biofuels production, *Renewable and Sustainable Energy Reviews*, vol. 14, pp. 2596–2610.

Skovgaard, A. and Hansen, P.J. (2003) Food uptake in the harmful alga Prymnesium parvum mediated by excreted toxins, *Limnology & Oceanography*, vol. 48, no. 3, pp. 1161-1166.

Smith, B.T. and Davis, R.H. (2012) Sedimentation of algae flocculated using naturally-available magnesium-based flocculants, Doi:10.1016/j.algal.2011.12.002.

Solomon. J.A., Hand, Jr., R.E. and Mann, R.C. (1986) Ultrastructural and flow cytometric analysis of lipid accumulation in microalgae. A Subcontract Report. pp. 1-55.

South, G.R. and Whittick, A. (1987) Introduction to Phycology. Balckwell Science Publishing, Oxford, London.

Spilling, K., Seppala, J. and Tamminen, T. (2011) Inducing autoflocculation in the diatom *Phaeodactylum tricornutum* through CO_2 regulation, *Journal of Applied Phycology*, vol. 23, pp. 959-966.

Spoehr, H.A. and Milner, H.W. (1948) The chemical composition of *Chlorella*; effect of environmental conditions, *Plant Physiology*, vol. 24, pp. 120-148.

Spolaore, P., Joannis-Cassan, C., Duran, E. and Isambert, A. (2006) Commercial applications of microalgae, *Journal of Bioscience and Bioengineering*, vol. 101, pp. 87-96.

Spurr, A.R. (1969) A low viscosity epoxy resin embedding medium for electron microscopy, *J. Ultrastruct. Res.*, vol. 26, pp. 31–43.

Stephenson, P.G., Moore, C.M., Terry, M.J., Zubkov, M.V. and Bibby, T.S. (2011) Improving photosynthesis for algal biofuels: toward a green revolution, *Trends in Biotechnology*, vol. 29, no. 12, pp. 615-623.

Stevenson, J.G. and Stoermer, E.F. (1982) Luxury consumption of phosphorus by five *Cladorphora* epiphytes in Lake Huron, *Trans. Am. Microsc. Soc.*, vol. 101, pp. 151–161.

Stewart, W.D.P. (1984) Algal Physiology and Biochemistry. University of California Press, Berkeley, California.

Sukenik, A., Bilanovic, D. and Shelef, G. (1988) Flocculation of microalgae in brackish and sea waters, *Biomass*, vol. 15, pp. 187-199.

Sukenik, A. and Shelef, G. (1984) Algal autoflocculation – Verification and proposed mechanism, *Biotechnology and Bioengineering*, vol. 26, pp. 142-147.

Sukenik, A. and Wahnon, R. (1991) Biochemical quality of marine unicellular algae with special emphasis on lipid composition. I. *Isochrysis galbana*, *Aquaculture*, vol. 97, pp. 61-72.

Sun, M.M., Sun, J., Qiu, J.W., Jing, H. and Liu, H. (2012) Characterization of the Proteomic Profiles of the Brown Tide Alga *Aureoumbra lagunensis* under Phosphate- and Nitrogen-Limiting Conditions and of Its Phosphate Limitation-Specific Protein with Alkaline Phosphatase Activity, *Appl. Environ. Microbiol.*, vol. 78, no. 6, pp. 2025. DOI: 10.1128/AEM.05755-11.

Sym, S.D., Pienaar, R.N., Edvardsen, B. and Egge, E.S. (2011) Fine structure and systematics of *Prymnesium radiatum* sp. nov. (Prymnesiophyceae) from False Bay and Franskraal, South Africa., *European Journal of Phycology*, vol. 46, pp. 229-243.

Syrett, P.J. (1988) Uptake and utilization of nitrpgen compounds, *Proceedings of the Phytochemical Society of Europe*, vol. 28, pp. 22-39.

Tamura, K., Peterson, D., Peterson, N., Stecher, G., Nei, M. and Kumar, S. (2011) MEGA5: Molecular evolutionary genetics analysis using maximum likelihood, evolutionary distance, and maximum parsimony methods, *Molecular Biology and Evolution*, doi: 10.1093/molbev/msr121.

Tedesco, M. & Duerr, E.O. (1989) Light, temperature and nitrogen starvation effects on the total lipid and fatty acid content and composition of *Spirulina platensis* UTEX 1928, *Journal of Applied Phycology*, vol. 1, pp. 201-209.

Thinh, L.V. (1994) Potential use of ageing cultures of *Isochrysis* aff. *Galbana* (*Isochrysis* Tahitan, T.Iso) as starter cultures for live algal food production in tropical aquaculture, *J. Appl. Phycol.*, vol. 6, pp. 357-358.

Thompson, P.A., Levasseur, M.E. and Harrison, P.J. (1989) Light-limited growth on ammonium vs. nitrate: What is the advantage of marine phytoplankton, *Limnology and Oceanography*, vol. 34, pp. 1014-1024.

Thompson, G.A. (1996) Lipids and membrane function in green algae, *Biochim. Biophys. Acta*, vol. 1302, pp. 17–45.

Tomas, C.R. (1997) Identifying marine phytoplankton. Academic Press, London.

Uduman, N., Qi, Y., Danquah, M.K. and Hoadley., F.A. (2010a) Marine microalgae flocculation and focused beam reflectance measurement, *Chemical Engineering Journal*, vol. 162, pp. 935 – 940.

Uduman, N., Qi, Y., Danquah, M.K., Forde, G.M. and Hoadley, A. (2010b) Dewatering of microalgal cultures: A major bottleneck to algae-based fuels, *Journal of renewable and sustainable energy*, vol. 2, pp. 012701.

Um, B.H. and Kim, Y.S. (2009) Review: A chance for Korea to advance algal-biodiesel technology, *Journal of Industrial and Engineering Chemistry*, vol. 15, pp. 1-7.

Vandamme, D., Foubert, I., Fraeye, I., Meesschaert, B. and Muylaert, K. (2012) Flocculation of *Chlorella vulgaris* induced by high pH: Role of magnesium and calcium and practical implications, *Bioresource Technology*, vol. 105, pp. 114–119.

Van Mooy, B.A.S., Fredericks, H.F., Pedler, B.E., Dyhrman, S.T., Karl, D.M., Koblizek, M., Lomas, M.W., Mincer, T.J., Moore, L.R., Moutin, T., Rappe, M.S. and Webb, E.A. (2009) Phytoplankton in the ocean use non-phosphorus lipids in response to phosphorus scarcity. *Nature*, vol. 458, pp. 69-72.

Verma, N.M., Mehrotra, S., Shukla, A. and Mishra, B.N. (2010) Prospective of biodiesel production utilizing microalgae as the cell factories: A comprehensive discussion, *African Journal of Biotechnology*, vol. 9, no. 10, pp. 1402-1411.

Vunjak-Novakovic, G., Kim, Y., Wu, X., Berzin, I. and Merchhu, J.C. (2005) Air-lifg bioreactors for algal growth on flue gas: Mathematical modeling and pilot-plant studies. *Industrial and Engineering Chemistry Research*, vol 44, pp. 6154-6163.

Wakil, S.J., Stoops, J.K. and Joshi, V.C. (1983) Fatty acid synthesis and its regulation, *Annu. Rev. Biochem.*, vol 52, pp. 537-579.

Widjaja, A. (2009) Lipid production from microalgae as a promising candidate for biodiesel production, *Makara Teknologi*, vol. 13, pp. 47-51.

Wijanarko, A., Dianursanti, Sendjaya, A.Y., Haermansyah, H., Witarto, A.B. and Gozan, M. (2008) Enhanced *Chlorella vulgaris* Buitenzorg growth by photon flux density alteration in serial photobioreactors, *Biotechnology and Bioprocessing Engineering*, vol. 13, pp. 476–482.

Wijffels, R.N. (2007) Potential of sponges and microalgae for marine biotechnology, *Trends in Biotechnology*, vol. 26, pp 26-31.

Wikfors, G.H. and Patterson, G.W. (1994) Differences in strains of *Isochrysis* of importance to mariculture, *Aquaculture*, vol. 123, pp. 127-135.

Williams, P.J.B. and Laurens, L.M.L. (2010) Microalgae as biodiesel & biomass feedstocks: Review & analysis of the biochemistry, energetics and economics, *Energy Environmental Science*, vol. 3, pp. 554–590.

Wu, X. and Merchuk, J.C. (2004) Simulation of algae growth in a bench scale internal loop airlift reactor, *Chemical Engineering Science*, vol. 59, pp. 2899-2912.

Wu, Z., Zhu, Y., Huang, W., Zhang, C., Li, T., Zhang, Y. and Li, A. (2012) Evaluation of flocculation induced by pH increase for harvesting microalgae and reuse of flocculated medium, *Bioresource Technology*, vol. 110, pp. 496-502.

Xin, L., Hong-ying, H., Ke, G. and Ying-xue, S. (2010) Effects of different nitrogen and phosphorus concentrations on the growth, nutrient uptake and lipid accumulation of a freshwater microalga *Scenedesmus* sp., *Bioresource Technology*, vol. 101, pp. 5494-5500.

Xin, L., Hong-ying, H. and Yu-ping, Z. (2011) Growth and lipid accumulation properties of a freshwater microalga *Scenedesmus* sp. under different cultivation temperature. *Bioresource Technology*, vol. 102, pp. 3098-3102.

Xu, N., Zhang, X., Fan, X., Han, L. and Zeng, C. (2001) Effects of nitrogen source and concentration on growth rate and fatty acid composition of *Ellipsoidion* sp. (Eustigmatophyta), *Journal of Applied Phycology*, vol. 13, pp. 463-469.

Xu, Y., Wahlund, T.M., Feng, L., Shaked, Y. and Morel, F.M.M. (2006) A novel alkaline phosphatase in the coccolithophore *Emiliania huxleyi* (Prymnesiophyceae) and its regulation by phosphorus, *Journal of Phycology*, vol. 42, pp. 835– 844.

Xu, L., Weathers, P.J., Xiong, X., Liu, C. (2009) Microalgal bioreactors: Challenges and opportunities, *Eng. Life Sci.*, vol. 3:, pp. 178-189.

Yahi, H., Elmaleh, S. and Coma, J. (1994) Algal flocculation-sedimentation by pH increase in a continuous reactor, *Water Sci. Technol.*, vol. 30, pp. 259–267.

Yeang, K. (2008) Biofuel from Algae. John Wiley & Sons Ltd.

Yoon, J.H., Shin, J.H., Ahn, E.K., and Park, T.H. (2008) High cell density culture of *Anabaena variabilis* with controlled light intensity and nutrient supply, *Journal of Microbiology and Biotechnology*, vol. 18, pp. 918-925.

Yoshida, M., Noel, M.H., Nakayama, T., Naganuma, T. and Inouye, I. (2006) A haptophyte bearing siliceous scales: Ultrastructure and phylogenetic position of *Hyalolithus neolepis* gen. et sp. nov. (Prymneciophyceae, Haptophyta), *Protist*, vol. 157, pp. 213–234.

Young, A.J. (1991) The protective role of carotenoids in higher plants. *Physiologia Plantarum*, vol. 83, pp. 702-708.

Yu, W.L., Ansari, W., Schoepp, N.G., Hannon, M. J., Mayfield, S.P. and Burkart, M.D. (2011) Modifications of the metabolic pathways of lipid and triacylglycerol production in microalgae, *Microbial Cell Factories*, vol. 10, pp. 91.

Zebib, T. (2008) Microalgae grown in photobioreactors for mass production of biofuel, (unpublished)

Zhang, Y., Tian, J.Y., Nan, J., Gao, S.S., Liang, H., Wang, M.L. and Li, G.B. (2010a) Effect of PAC addition on immersed ultrafiltration for the treatment of algae-rich water, *J. Hazard. Mater.*, vol. 186, pp. 1415-1424.

Zhang, X.Z., Hu, Q., Sommerfeld, M., Puruhito, E., and Chen, Y.S. (2010b) Harvesting algal biomass for biofuels using ultrafiltration membranes, *Bioresource Technology*, vol. 101, pp. 5297-5304.

Zhila, N.O., Kalacheva, G.S and Volova, T.G. (2005) Effect of Nitrogen Limitation on the Growth and Lipid Composition of the Green Alga *Botryococcus braunii* Kütz IPPAS H-252, *Russian Journal of Plant Physiology*, vol. 52, pp. 311-319.

Zhu, C.J. and Lee, Y.K. (1997) Determination of biomass dry weight of marine microalgae, *Journal of Applied Phycology*, vol. 9, pp. 189-194.

Zhu, C.J., Lee, Y.K. and Chao, T.M. (1997b) Effects of temperature and growth phase on lipid and biochemical composition of *Isochrysis galbana* TK1, *J. Appl. Phycol.*, vol. 9, pp. 451 – 457.

Zhukova, N.V. and Aizdaicher, N.A. (1995) Fatty acid composition of 15 species of marine microalgae, *Phytochemistry*, vol. 39, no. 2, pp. 351-356.

APPENDIX

Preparation of *f/2* enriched seawater medium (Guillard and Ryther, 1962)

The following was added to 1L seawater:

$NaNO_3$	0.08g
NaH_2PO_4 * 2H2O	0.005g
Microelement Solution	1ml
Vitamin Solution	1ml

Stock solutions were made as follows:

Microelement Solution

The following was added to 1L seawater:

3.150g	$FeCl_2$ * 6H2O
4.160g	Na_2EDTA
0.180g	$MnCl_2$ * 4H2O
0.010g	$CoCl_2$ * 6H2O
0.010g	$CuSO_4$ * 5H2O
0.022g	$ZnSO_4$ * H2O
0.006g	Na2MoO_4 * 2H2O

Vitamin Solution

The following was added to 1L seawater:

0.5mg	Biotin (Vitamin H)
100mg	Thiamine HCl (Vitamin B1)
0.5mg	Cyanocobalamin (Vitamin B12)

Then the pH was adjusted to 8 with 1*M* NaOH or HCl

DNA Extraction

- Seven day old culture was centrifuged at 1000 rpm for 19 minutes to obtain a significant amount of pellet.
- The pellet was then transferred to a 2 ml eppendorf and fresh media was added to the 2 ml mark to wash off the excess polysaccharides and centrifuged at 7000 rpm for five minutes. The supernatant was than decanted.
- Glass beads were added to cover the cells and fresh media was added to the 0.5 ml mark. The eppendorf was than immersed in liquid nitrogen until the liquid was frozen.
- 1ml of CTAB buffer (consisting of 1 g 2% CTAB, 4.091 g 1.4 M NaCl, 0.7305 g 50 mM EDTA and 0.788 g 100 mM Tris dissolved in 50 ml distilled water) and 2 µl mercaptoethanol was preheated in a 60 ºC water bath and a 1:1 ratio of the above mixture was added to the frozen sample.
- The sample was than placed in a 60 ºC water bath and vortexed intermittently for 30 minutes.
- 1 ml of chloroform:isoamyl alcohol (24:1) was added.
- The eppendorf was than agitated for 20 minutes followed by centrifugation at 18 000 rpm for 5 minutes. The top phase was than transferred to a new eppendorf.
- The chloroform:isoamyl alcohol extraction step was repeated with the top phase however the tube was only agitated for ten minutes this time. The tube was centrifuged for five minutes at 15 300 rpm and the top phase was placed into a third eppendorf. This sample was than placed on crushed ice to cool.
- -20 ºC isopropanol was added to the sample to achieve a 2:3 isopropanol:sample ratio.
- The sample was than placed in a -20 ºC freezer for 20 minutes.
- Centrifugation followed at 15 300 rpm and the isopropanol was removed.
- 1 ml -20 ºC 80% ethanol was then added to the eppendorf and the sample was left in a -20ºC freezer for 30 minutes.
- Centrifugation followed at 13 000 rpm for ten minutes and the supernatant was decanted.

- The remaining pellet in the eppendorf was left overnight in a dessicator with silica crystals to dehydrate.
- The following day the pellet was resuspended in 50 ul TE buffer and placed on ice. Deionised Milli-Q water was than added to make up the volume to 200 ul.
- This DNA was stored at 4 ºC until it was used for PCR.

Gel Electrophoresis

Agarose Gel (50 ml)
Agarose (0.4 g for 0.8% and 0.5 g for 1%)
10 ml 5X TBE
40 ml Distilled water
Heat until agarose has completely dissolved and add 1.5 µl Ethidium Bromide

5X TBE
54 g Tris base
27.5 g Boric acid
20 ml 0.5M EDTA pH 8.0

Mix with 1 L distilled water and autoclave at 121 C at 15 psi for 20 minutes

Electrophoresis Buffer
100 ml 5X TBE
900 ml sterile distilled water
2.5 µl Ethidium Bromide

Tracking dye
40% (W/V) Sucrose in water
0.25% Bromothymol blue

Loading instructions

5 µl DNA sample

1.5 µl tracking dye

5 µl molecular ladder

TE buffer

A 10 mM Tris-Cl (pH 7.5) and 1 mM EDTA was made by adding 10ml 1 M Tris-Cl (pH 7.5) per L and 2 ml 500 mM EDTA (pH 8.0).

The stock solutions were made as follows:

- 1 M Tris (crystallized free base) was made by adding 60.57 g to 0.5 L Milli-Q water. The pH was decreased to 7.5 using HCl.

- 0.5 M EDTA was made by adding 18.6 g in 100 ml Milli-Q water. The pH was increased to 8.0 using NaOH and the solution was heated to dissolve all the EDTA.

Lugol's solution

10 g potassium iodide was dissolved in 100 ml of distilled water.
5 g iodine crystals was slowly added to the solution above, while shaking.
The mixture was than filtered and stored in a tightly stoppered brown bottle.

Spurr's Resin

10 g	Vinylcyclohexane dioxide (VCD or ERL 4206)
6 g	Diglycidyl ether of polypropylene glycol (DER 736)
26 g	Nonenyl succinic anhydride (NSA)
0.4 g	Dimethylaminoethanol (DMAE or S1)

The first three ingredients were added first and stirred with a magnetic stirrer followed by the addition of the S1 accelerator. The resin was continually stirred with minimal exposure to atmospheric moisture until it was used.